CORA Cork Open Research Archive
Cartlann Taighde Oscailte Chorcaí

Title	Investigating the role of interleukin-6 in neuronal dysfunction in the mdx mouse model of Duchenne muscular dystrophy
Authors	Stephenson, Kimberley Alix
Publication date	2022-01-07
Original Citation	Stephenson, K. A. 2022. Investigating the role of interleukin-6 in neuronal dysfunction in the mdx mouse model of Duchenne muscular dystrophy. PhD Thesis, University College Cork.
Type of publication	Doctoral thesis
Rights	© 2022, Kimberley Alix Stephenson. - https://creativecommons.org/licenses/by-nc-nd/4.0/
Download date	2026-11-16 13:26:13
Item downloaded from	https://hdl.handle.net/10468/14118

UCC
University College Cork, Ireland
Coláiste na hOllscoile Corcaigh

Ollscoil na hÉireann, Corcaigh

National University of Ireland, Cork



Investigating the role of interleukin-6 in neuronal dysfunction in the *mdx* mouse model of Duchenne Muscular Dystrophy

Thesis presented by

Kimberley Alix Stephenson, BHSc (Hons)

Department of Physiology, University College Cork

Under the supervision of

Dr. Dervla O'Malley

Dr. Mark Rae

Head of department

Professor Ken D. O'Halloran

For the degree of

Doctor of Philosophy

2022

Table of Contents

Table of Contents I

Table of Figures V

List of Tables X

Declaration XI

Acknowledgements XII

List of Abbreviations XIII

Abstract XV

Chapter 1: Introduction 1

1.1. Duchenne Muscular Dystrophy 2

1.1. Pathology of loss of dystrophin from muscle 3

1.2. Cognitive dysfunction in individuals with DMD 4

1.3. Dystrophin Gene 6

1.4. Dystrophin-Associated Protein Complex (DAPC) in myocytes and brain tissue 8

1.5. The role of Dystrophin in the brain 10

1.6. *Mdx* mouse model of DMD 12

1.7. The role of the hippocampus in memory formation 14

1.8. Hippocampal dysfunction in the *mdx* mouse 19

1.9. Intracellular Ca^{2+} handling in dystrophic hippocampal neurons 21

1.10. Interleukin-6 is a pleiotropic cytokine with modulatory actions in the central nervous system (CNS). 23

1.10.1. Classical signalling mechanism of IL-6 and its receptor 23

1.10.2 Trans-signalling mechanism of IL-6 and its receptor 24

1.11. IL-6 modifies long-term potentiation 26

1.12. IL-6 modifies hippocampal adult neurogenesis and cognitive function 28

1.13. Perspectives 30

Aims 31

Objectives 31

Chapter 2: Methods 32

2.1. Animals 33

2.2. Tissue preparation for immunocytochemistry and immunohistochemistry 34

2.2.1. Hippocampal neuron culture 34

2.2.2. Poly-D-lysine coating of coverslips 36

2.2.3 Preparation of Hippocampal tissue for Immunohisto/cytochemistry 38
2.3. Immunocytochemistry techniques 40
2.3.1 Immunofluorescent labelling of cultured hippocampal neurons 40
2.3.2. Immunofluorescent labelling of whole brain sections 41
2.3.3 Confocal microscopy 43
2.3.4 Image Analysis 43
2.4. Calcium imaging with cultured hippocampal neurons 45
2.4.1. Fluorescent calcium dye loading protocol. 45
2.4.2 Experimental design 46
2.4.3 Analysis of calcium imaging data 47
2.5. Gene Expression 48
2.5.1. RNA Extraction and Preparation 48
2.5.2. Reverse Transcription of RNA 50
2.5.3. qRT-PCR 51
2.6. Immunoassay for protein quantification 53
2.6.1. Animals 53
2.6.2. Protein Extraction and Quantification 53
2.6.3. Bradford Protein Assay 53
2.6.4. Enzyme Linked Immunosorbent Assay (ELISA) 54
2.7. Behavioural tests 56
2.7.1. Animals 56
2.7.2. Novel Object Recognition (NOR) Test 56
2.7.3. Open field behavioural test 59
2.8. Slice Electrophysiology 60
2.8.1. Preparing hippocampal slices 60
2.8.2. Extracellular electrophysiological recording 62
2.8.3. Induction of LTP 63
2.8.4. Analysis of electrophysiological recordings. 65
2.9. Intervention Study 66
2.9.1. Intrathecal Injection 66
2.10. Statistical Analysis 68
2.11. Materials 68
Chapter 3: Dystrophin-deficient *mdx* mice exhibit deficits in molecular correlates of learning and memory. 69
3.1. Introduction 70
3.1.1. Study objectives 72

3.1.2. Animals....72
3.1.3. Techniques used....72
3.2. Dystrophin is absent in all regions of the hippocampus in gthe *mdx* mouse.....73
3.3. Hippocampal long-term potentiation (LTP) is reduced in dystrophin-deficient *mdx* mice....74
3.4. Recognition memory is not deficient in *mdx* mice.....78
3.5. Behavioural characteristics are altered in *mdx* mice relative to WT.....79
3.6. $GABA_A$ receptor expression in neurons in the dentate gyrus of *mdx* mice is similar to that in WT mice.....82
3.7. Loss of dystrophin increases neuronal excitability in cultured hippocampal neurons 85
3.8. Neuronal density in the dentate gyrus decreases with age in *mdx* mice.....88
3.9. The number of DCX-positive cells in the dentate gyrus of *mdx* mice decreases with age....92
3.10. Glial filamentary acidic protein is significantly decreased in the *mdx* mouse.....98
3.11. Discussion....101
3.12. Conclusions....105
Chapter 4....107
Interleukin-6: its potential as a neuromodulatory factor underpinning aberrant hippocampal activity in dystrophin-deficient *mdx* mice....107
4.1. Introduction....108
4.1.1. Study objectives....111
4.1.2. Techniques used....111
4.2. Dystrophin isoform is co-localised at synaptophysin-labelled hippocampal synapses. 112
4.3. IL-6Rs are clustered at synaptophysin-labelled hippocampal synapses.....114
4.4. IL-6 exposure increases IL-6R clustering in dystrophin containing hippocampal neuronal processes.....115
4.4. Hippocampal interleukin-6 (IL-6) expression is comparable between WT and *mdx* mice....117
4.5. Hippocampal IL-6 receptor expression and intracellular signalling is not altered in the absence of dystrophin....118
4.6. Regional differences in hippocampal IL-6 expression were detected in *mdx* mice..121
4.7. Regional differences in hippocampal IL-6 receptor expression were detected in *mdx* mice....124
4.8. IL-6 supresses spontaneous calcium activity in dystrophin-deficient hippocampal neurons.....127
4.9. Exposure to IL-6 modifies LTP in WT but not *mdx* hippocampal slices....129

4.10. Discussion 136
4.11. Conclusions 139
Chapter 5 141
Intervention study: Neutralisation of IL-6 receptor-mediated signalling improves cellular correlates of learning and memory. 141
5.1. Introduction 142
5.1.1. Study objectives 145
5.1.2. Techniques used 145
5.2. Study design for intervention 146
5.3. Intrathecal administration of xIL-6R antibodies normalises hippocampal LTP in *mdx* mice 147
5.4. xIL-6R administration did not modify NOR recognition memory in WT or *mdx* mice. 154
5.5. Anxiety-like behaviours in *mdx* mice. 155
5.6. Discussion 159
5.7. Conclusions 162
Chapter 6: 164
Summary and Conclusions 164
6.1. Overview of research findings 165
6.2. Conclusion ..... - 175 -
6.3. Limitations ..... - 176 -
6.4. Future directions ..... - 177 -
Chapter 7: References ..... - 179 -
Appendix ..... - 206 -

Table of Figures

Chapter 1: Introduction

Figure 1.1: Dystrophin protein isoforms present in DMD

Figure 1.2: Organisation of the Dystrophin-Associated Protein Complex (DAPC) in muscle

Figure 1.3: The molecular organization of dystrophin and the DAPC in neurons

Figure 1.4: Schematic representation of the hippocampal formation, which is comprised of the dentate gyrus, CA1, CA2 and CA3 regions.

Figure 1.5: A visual representation of the induction of LTP in the post synaptic cell.

Figure 1.6: A representation of IL-6/ IL-6Rα classic and trans-signalling mechanisms.

Chapter 2: Methods

Figure 2.1: Flow diagram displaying the process of primary hippocampal neuron dissociation and culture.

Figure 2.2: Brightfield image of the 3 regions of the hippocampus.

Figure 2.3: Representative image of analysis of whole brain sections for cell counting using Image J.

Figure 2.4: Flow diagram displaying the steps involved in RNA extraction from hippocampal tissue.

Figure 2.5: RNA analysis using agarose gel electrophoresis.

Figure 2.6: Template used for all qRT-PCR reactions.

Figure 2.7: ELISA protocol followed using the LEGEND MAX™ Mouse IL-6 ELISA Kit.

Figure 2.8: Novel Object Recognition test setup.

Figure 2.9: Representative images showing behaviours in the open field arena.

Figure 2.10: Recording chamber set up.

Figure 2.11: A schematic of the placement of the stimulation-recording path (Schaffer collateral-CA1 synapses) in the mouse hippocampus.

Figure 2.12: A representative trace of how the fEPSP slope (mV/ms) is analysed on each sweep and normalised to 100%.

Figure 2.13: The schematic and photograph illustrate the procedure whereby an intrathecal injection was administered between the L5 and L6 vertebrates.

Chapter 3: Dystrophin-deficient mdx mice exhibit deficits in molecular correlates of learning and memory.

Figure 3.1: Immunofluorescent labelling of dystrophin in CA1, CA3 and DG regions of the hippocampus of WT mice.

Figure 3.2: Immunofluorescent labelling of dystrophin in CA1, CA3 and DG regions of the hippocampus of *mdx* mice.

Figure 3.3: Input/output curves constructed during baseline recordings.

Figure 3.5: Recognition memory is not significantly different between WT and *mdx* mice.

Figure 3.6: Behaviours of *mdx* and WT mice in an open field.

Figure 3.7: The number of GABAAR positive neurons in the granule cell layer and hilus of the dentate gyrus of WT and mdx *mice* at two different ages (4 months and 8 months) is similar.

Figure 3.8: Brightfield images of mdx and WT neurons, 4-5 days after primary culture.

Figure 3.9: Baseline activity in cultured mdx hippocampal neurons in increased.

Figure 3.10: Neuronal density in the dentate gyrus decreases with age in mdx mice (4 and 8 months).

Figure 3.11: Immunofluorescence images looking at NeuN staining for neurons in the dentate gyrus.

Figure 3.12: Immunofluorescence and brightfield images looking at NeuN staining for neurons in the dentate gyrus.

Figure 3.13: The number of DCX-positive cells in the granule cell layer of the dentate gyrus is decreased 8-week-old mdx mice.

Figure 3.14: The number of DCX-positive cells in the granule cell layer of the dentate gyrus is decreased in 4-month-old mdx mice.

Figure 3.15: The number of DCX positive cells in the granule cell layer of the dentate gyrus is decreased in in 8-month-old mdx mice.

Figure 3.16: The number of DCX-positive cells in the cell layer of the dentate gyrus is decreased in mdx mice across 3 ages.

Figure 3.17: The number of astrocytes was significantly decreased in mdx mice and significantly increased in WT mice in 8-week-old, 4-month-old and 8-month-old mice.

Figure 3.18 The number of astrocytes is significantly decreased in mdx mice with age and significantly increases in WT mice at 8-weeks-old, 4-months-old and 8-months-old.

Chapter 4: Interleukin-6: its potential as a neuromodulatory factor underpinning aberrant hippocampal activity in dystrophin-deficient mdx mice.

Figure 4.1: Dystrophin is expressed at hippocampal synapses.

Figure 4.2: IL-6 receptors are expressed at hippocampal synapses.

Figure 4.3: Hippocampal IL-6 gene expression is not different in mdx mice.

Figure 4.4: Hippocampal protein expression of IL-6 did not differ significantly between WT and mdx mice.

Figure 4.5: Hippocampal IL-6R gene expression is not different in mdx mice.

Figure 4.6: Hippocampal gp130 gene expression does not differ significantly in mdx mice.

Figure 4.7: Hippocampal STAT3 gene expression is not different in mdx mice.

Figure 4.8: Regional hippocampal immunofluorescent expression of IL-6 is increased in dystrophin-deficient mdx mice.

Figure 4.9: Representative images of regional hippocampal immunofluorescent illustrate that the expression of IL-6 is increased in dystrophin-deficient mdx mice.

Figure 4.10: Regional hippocampal immunofluorescent expression of IL-6R is increased in dystrophin-deficient mdx mice.

Figure 4.11: Representative images of regional hippocampal immunofluorescent illustrate that the expression of IL-6R is increased in dystrophin-deficient mdx mice.

Figure 4.12: Spontaneous calcium activity in mdx hippocampal neurons is suppressed by exogenous IL-6.

Figure 4.13: LTP in WT hippocampal Schaeffer collaterals-CA1 synapses was suppressed by IL-6.

Figure 4.14: LTP in mdx hippocampal Schaeffer collaterals-CA1 synapses was not changed by IL-6.

Figure 4.15: LTP in WT+IL-6 hippocampal Schaeffer collaterals-CA1 synapses mirror mdx controls.

Figure 4.16: LTP in WT+IL-6 hippocampal Schaeffer collaterals-CA1 synapses also mirror mdx+IL-6.

Chapter 5: Intervention study: Neutralisation of IL-6 receptor-mediated signalling improves cellular correlates of learning and memory.

Figure 5.1: Long-term potentiation in the SC-CA1 pathway of the hippocampus in mdx mice intrathecally-injected with xIL-6R is enhanced compared to untreated mdx controls.

Figure 5.2: Long-term potentiation in the SC-CA1 pathway of the hippocampus in WT mice intrathecally-injected with xIL-6R is enhanced compared to untreated WT controls.

Figure 5.3: Intrathecal injection of saline had no impact on LTP induction and/or maintenance in WT mice.

Figure 5.4: Intrathecal injection of saline had no impact on LTP induction and/or maintenance in mdx mice.

Figure 5.5: The NOR recognition index values for mdx and WT mice injected intrathecally injected with either saline or xIL-6R did not differ significantly from each other.

Figure 5.6: Behaviours of saline-treated and xIL-6R treated mdx and WT mice in an open field.

Chapter 6: Summary and Conclusions

Figure 6.1: Loss of hippocampal dystrophin results in progressive pathophysiological changes.

Figure 6.2: The figure illustrates the potential mechanisms of how IL-6Rs could be involved in hippocampal dysfunction associated with a loss of dystrophin.

List of Tables

Chapter 2: Methods

Table 2.1: Reagent setup for primary hippocampal neuron culture.

Table 2.2: Primary hippocampal neuron culture medium composition.

Table 2.3: Reagent set up for immunocytochemistry/immunohistochemistry.

Table 2.4: Antibodies used in this thesis.

Table 2.5: Lysis Buffer Recipe.

Table 2.6: Electrophysiology reagents – cutting solution recipe.

Table 2.7: Electrophysiology reagents – aCSF recipe.

Declaration

"This is to certify that the work I am submitting is my own and has not been submitted for another degree, either at University College Cork or elsewhere. All external references and sources are clearly acknowledged and identified within the contents. Calcium experiments were conducted by Michael Vaughan and data analysis by Claire Denley. I have read and understood the regulations of University College Cork concerning plagiarism and intellectual property."

Signed by Kimberley Stephenson, January 2022

Acknowledgements

Although my PhD journey has not been an easy one, especially the end, due to Covid-19, I will forever be grateful for the opportunity to undertake my PhD, in the Physiology Department at UCC and in Ireland as well as everything I learned about myself in the process.

Firstly, to my supervisors, Dervla O'Malley and Mark Rae, thank you both for all your patience, guidance and continual support throughout my studies. Without you both, I would not have made it this far.

To the HRB and UCC, thank you for the funding and support throughout this project.

To Jay Radford, thank you for your support with 'my' mice and making me laugh when I wanted to cry during intrathecal injections on those early mornings as well as Noelle and the rest of the BSU staff for facilitating my project and making me smile when I was in the SPF for hours on end! I appreciate you all so much.

To Greg, Miriam and Marcella, thank you all for your help in my PhD, whether it was technical help or just a chat. You made my PhD experience so much easier.

To Jackie, Nicola and Nora, thank you all for helping me settle into Ireland when I first got here and helping with any visa related business after that and anything really.

To the PhD students (and Eric!) in Physiology, even though some of you have gotten your PhDs already, thank you for the laughs, cups of tea and the best lunches in the breakroom, before Covid that is.

To Mike, thank you for always being there for me, especially at the times when I really needed it. I truly cherish our friendship.

To Anja and Maura, I am so grateful for demonstrating in Pharmacology, because without it, we would not be friends! Here's to all the beautiful walks we will go on and all the cups of hot chocolate to come.

To the rest of my friends, here in Ireland and back home in South Africa, thank you for checking in on me, travelling so very far (or not!) to see me, and for all the video chats to make me feel like I was right there at home. I love you all.

To my family, Dad – thank you for always supporting my dreams, no matter how big, Willemien – thank you for always encouraging me and Reece and Connor – thank you for being the best 'big' little brothers. I love you all.

Lastly, to my Mom, thank you for all the support you have always given me, especially this last year. You are the light that taught me how to shine and I love you so much.

List of Abbreviations

ACSF	Artificial cerebrospinal fluid
ADHD	Attention Deficit Hyperactivity Disorder
AMPAR	Alpha-amino-3-hydroxy-5-methyl-4-isoxazolepropionate receptor
ASD	Autism Spectrum Disorder
BMD	Becker Muscular Dystrophy
Ca^{2+}	Calcium
$CaCl_2$	Calcium chloride
CaMKII	Ca2+/calmodulin-dependent protein kinase
CNS	Central nervous system
CS	Cutting solution
DAPC	Dystrophin associated protein complex
DAPI	4',6-diamidino-2-phenylindole
DEPC	Diethyl pyrocarbonate
DG	Dentate gyrus
dH_2O	Deionized water
DMD	Duchenne Muscular Dystrophy
DMEM	Dulbecco's modified eagle's medium
EPSP	Excitatory post synaptic potential
FBS	Foetal bovine serum
GABA	γ-aminobutyric acid
H&E	Haematoxylin and Eosin
HBSS	HEPES-buffered saline solution
HPRA	Health Products Regulatory Authority
HPRT	Hypoxanthine-guanine phosphoribosyltransferase
IL	Interleukin
IL-6	Interleukin 6
IL-6Rα	Interleukin-6 Receptor alpha
IL-6st	Interleukin-6 signal transducer

IQ	Intelligence quotient
IVCs	Individually ventilated cage
K^+	Potassium
KCl	Potassium chloride
LPS	Lipopolysaccharide
LTP	Long Term Potentiation
mAb	Monoclonal antibody
MAPK	Mitogen-activated protein kinase
$MgCl_2$	Magnesium chloride
NaCl	Sodium chloride
NaH_2PO_4	Monosodium phosphate
$NaHCO_3$	Sodium bicarbonate
NMDA	N-methyl-D-aspartate
NOR	Novel object recognition
O.C.T	Optimal cutting temperature embedding medium
OCD	Obsessive compulsive disorder
OsMom	Osmolarity
pAb	Polyclonal antibody
PBS	Phosphate buffered saline
PFA	Paraformaldehyde
PI 3-K	Phosphoinositide 3-kinase
P-S	Penicillin-Streptomycin
ROS	Reactive oxygen species
SC	Schaffer Collaterals
SPF	Specific pathogen-free
SR2	Serum Replacement 2
STAT 3	Signal transducer and activator of transcription 3
TNF	Tumour necrosis factor
WT	Wild type

Abstract

Duchenne Muscular Dystrophy (DMD) is a fatal musculoskeletal disorder that results in a loss of dystrophin in muscle fibres, leading to progressive immobility, chronic inflammation and premature death. Inflammation is characterised by increased circulating levels of pro-inflammatory cytokines such as IL-6. However, it is apparent that dystrophin not only functions in skeletal muscle, but in the CNS as well, with an increased incidence of cognitive impairment and deficits in verbal, short-term and working memory in individuals with DMD. The hippocampus is critical for learning and the formation and consolidation of memories and can be modified by neuroimmune cytokines, such as IL-6. The aim of this programme of research was to investigate the possible contribution of the neuroimmune molecule, IL-6 in cognitive impairment associated with loss of the structural protein, dystrophin.

Initially, we used the dystrophic *mdx* mouse to investigate what impact loss of dystrophin had on normal hippocampal function. Significantly, LTP, the molecular correlate of learning and memory was shown to be decreased in *mdx* mice, which has been linked to memory dysfunction. Moreover, changes in the density and structure of *mdx* hippocampal neurons and glia was observed over time.

Subsequently, we examined the possible effects of IL-6 on hippocampal function in *mdx* mice. IL-6 and IL-6R expression were altered in specific regions in the hippocampus, which underpins function relating to learning and memory. Indeed, *in vivo* blockade of IL-6-mediated signalling in the CNS of *mdx* mice restored LTP, although at this age, it did not impact on learning behaviours.

These studies have elucidated previously unknown cellular and molecular changes in the hippocampus of dystrophin-deficient mice. Moreover, we have linked the neuromodulatory cytokine, IL-6, with the observed pathophysiology.

Chapter 1: Introduction

1.1. Duchenne Muscular Dystrophy

Duchenne Muscular Dystrophy (DMD) is a heritable X-linked recessive disorder which affects approximately 1 in 3,500 live male births and subsequently has one of the highest incidences of all inherited disorders (Emery, 1991). DMD results in the loss of the structural protein, dystrophin (Bulfield *et al.*, 1984), due to mutations in the *DMD* gene (Hoffman & Kunkel, 1989). In DMD-affected boys, the loss of dystrophin becomes apparent from an early age, with muscle weakness progressively leading to physical disability and eventual immobility. DMD patients are usually wheelchair-bound by the age of 12 (Wagner, 2008) and suffer a premature death in their early twenties, often through respiratory failure, due to loss of function in the diaphragm muscle, or cardiac failure (Perloff, 1984).

There is currently no cure for DMD with the most effective treatment being corticosteroids that have strong anti-inflammatory effects and which delay the onset and progression of the disease (Simpson *et al.*, 2016). However, there has been an improvement in the efficacy of other interventions (Reinig *et al.*, 2017) including nocturnal ventilation, routine flu vaccinations, early delivery of antibiotics and physiotherapy (Eagle *et al.*, 2002) which, combined with corticosteroids such as deflazacort, has increased the lifespan of individuals with DMD (Biggar *et al.*, 2006). As such, the life expectancy of patients with DMD has increased to approximately 28.1 years (Landfeldt *et al.*, 2020; Broomfield *et al.*, 2021). More recent therapeutic strategies have targeted the genetic origins of the disease, namely, eteplirsen, an oligonucleotide that facilitates skipping of exon 51 mutations in the

dystrophin gene, which slows but does not halt disease progression (Mendell & Rodino-Klapac, 2016).

1.1. Pathology of loss of dystrophin from muscle

In the absence of the protective function served by dystrophin, skeletal muscle fibres in DMD patients are more susceptible to contraction-induced damage. This ultimately results in an increased efflux of calcium (Ca^{2+}) from the sarcolemma into the sarcoplasm, which in turn, triggers an inflammatory response during the repair of the damaged tissue resulting in muscle fibre phagocytosis and necrosis as muscle fibres lose the ability to regenerate and recover (Anderson *et al.*, 1987; Blake *et al.*, 2002; Davies & Nowak, 2006; Zhou & Lu, 2010).

A sustained increase in intracellular Ca^{2+} results in the activation of apoptotic (Tidball *et al.*, 1995) and necrotic cell death pathways in DMD (Morgan *et al.*, 2018). Cytoplasmic Ca^{2+} levels also influence mitochondrial Ca^{2+} uptake which, in turn, leads to altered metabolism and increased production of reactive oxygen species (ROS). The failure to moderate physiological levels of oxygen radicals results in sustained membrane depolarisation leading to cell death (Feno *et al.*, 2019). Following an increase in cytosolic Ca^{2+}, pro-inflammatory immune mediators are secreted from the contraction-induced damaged muscle fibres (De Paepe & De Bleecker, 2013) resulting in chronic inflammation.

Macrophages are the most abundant of the infiltrating immune cells, although T cells, particularly CD4+ lymphocytes, also predominate (McDouall *et al.*, 1990). Elevated concentrations of pro-inflammatory cytokines such as tumour necrosis factor (TNF) (Abdel-Salam *et al.*, 2009), interleukin (IL)-1 (Evans *et al.*, 2009) and IL-6 (Messina *et al.*, 2011) are also detected at early stages of the disease, with the inflammatory response worsening as DMD progresses. Specifically with regard to IL-6, which is considered to be both pro- and anti-inflammatory, plasma levels of this cytokine are consistently raised in DMD patients (Rufo *et al.*, 2011). In fact, chronic stimulation of an immune response and altered immune mediator profiles, are characteristic features of the progressive DMD muscular phenotype. While DMD has been studied extensively primarily with regard to its effects upon skeletal muscle function/physiology, it is important to note that dystrophin is also expressed in cardiac and smooth muscle, endocrine glands and notably, in neurons, in the peripheral and central nervous systems (Knuesel *et al.*, 2000) and such cognitive dysfunction is another aspect of DMD that needs to be considered.

1.2. Cognitive dysfunction in individuals with DMD

In addition to skeletal muscle pathology discussed above, DMD is characterised by significant cognitive and behavioural problems which include; having lower intelligence quotients (IQs) (Felisari *et al.*, 2000; Nardes *et al.*, 2012), significant cognitive impairment (Bresolin *et al.*, 1994; Anderson *et al.*, 2002), communication difficulties and poor affect recognition (Hinton *et al.*, 2006; Hinton *et al.*, 2007), and

specific deficits in verbal, short-term and working memory (Hinton *et al.*, 2000, 2001; Snow *et al.*, 2013) as well as reading deficits similar to those observed in patients with phonological dyslexia (Dorman *et al.*, 1988; Billard *et al.*, 1992; Castles & Coltheart, 1993). Additionally, there is a higher incidence of attention-deficit/hyperactivity disorder (ADHD), obsessive-compulsive disorder (OCD), autism spectrum disorders (ASD), anxiety disorders (Hendriksen & Vles, 2008; Pane *et al.*, 2013a; Banihani *et al.*, 2015) and epilepsy (Pane *et al.*, 2013a) in individuals with DMD.

Although the aetiology of the cognitive impairment and memory deficits seen in patients with DMD is not well understood, neurons in the hippocampus, cerebral cortex, amygdala and cerebellum all express the full-length isoform of dystrophin (Lidov *et al.*, 1990; Bies *et al.*, 1992; Lidov *et al.*, 1993; Knuesel *et al.*, 2000; Sekiguchi *et al.*, 2009). With a loss of dystrophin linked to neuronal loss, neurofibrillary tangles, alterations to dendritic branching, cortical atrophy as well as metabolic abnormalities in the brains of individuals with DMD (Rosman, 1970; Yoshioka *et al.*, 1980; Jagadha & Becker, 1988; Tracey *et al.*, 1995; Lv *et al.*, 2011).

Further, while a hallmark feature of the muscle pathology in DMD is its progressive nature, there are no longitudinal studies that have shown whether the cognitive pathology in humans with DMD is progressive due to the shortened life expectancy of the disease. Interestingly however, while developmental delay was reported in younger boys, more cerebral atrophy was seen in men with DMD, compared to boys, which may indicate a progression in cognitive dysfunction with age (Yoshioka *et al.*, 1980; Pane *et al.*, 2013b; Doorenweerd *et al.*, 2018).

1.3. Dystrophin Gene

The *DMD* gene is large and complex, comprising of at least five promoters. Three independent promoters located on the 5'-end of the *DMD* gene, namely the B(brain) - M(muscle) - and P- (Purkinje cell) promoters, regulate the expression of three full-length isoforms of dystrophin (Dp427) as well as numerous smaller dystrophin proteins, namely, Dp260, Dp140, and Dp116, Dp71, Dp40 (Gorecki *et al.*, 1992; Ahn & Kunkel, 1993), which is illustrated in Figure 1.1 below. Most of these smaller proteins are present in both the central and peripheral nervous systems.

In skeletal muscle, the full-length dystrophin protein has a unique N-terminal amino acid sequence and referred to as Dp427m (muscle) (Howard *et al.*, 1999). In neurons, the start sequence of Dp427m is replaced by a unique N-terminal amino acid sequence, and called Dp427c (cortex) (Nudel *et al.*, 1989). In Purkinje cells of the cerebellum, a unique N-terminal amino acid sequence is expressed, named Dp427p (Purkinje) (Gorecki *et al.*, 1992). All of these full-length dystrophin proteins comprise a central rod domain containing 24 spectrin-like repeats.

Importantly, all isoforms of dystrophin have different locations of expression. Dp260 is a C-terminal isoform of dystrophin, the formation of which is induced by an alternative promoter located on intron 29 of the *DMD* gene (D'Souza *et al.*, 1995), containing 15 spectrin-like rod repeats in the rod domain, is mainly expressed in retinal tissue. Dp140 is another C-terminal dystrophin isoform formed by the action of another alternative promoter on intron 44 of the *DMD* gene,

contains six spectrin-like rod repeats, and is mainly expressed during foetal brain development and thus is associated with a higher risk of cognitive impairment in DMD and Becker Muscular Dystrophy (BMD) (Chamova *et al.*, 2013). Dp116 is an alternative C-terminal dystrophin short isoform, specific to Schwann cells in peripheral nervous system (Byers *et al.*, 1993). Dp71 is a ubiquitous isoform of dystrophin expressed with an alternative promoter located in intron 62 and is expressed in the brain, namely the hippocampus and is associated with cognitive deficits, specifically learning and memory (Rapaport *et al.*, 1992; Waite *et al.*, 2012). Lastly, Dp40 is the shortest known isoform of dystrophin expressed in hippocampal neurons and is known to interact with various presynaptic proteins (Tozawa *et al.*, 2012; Fujimoto *et al.*, 2014).

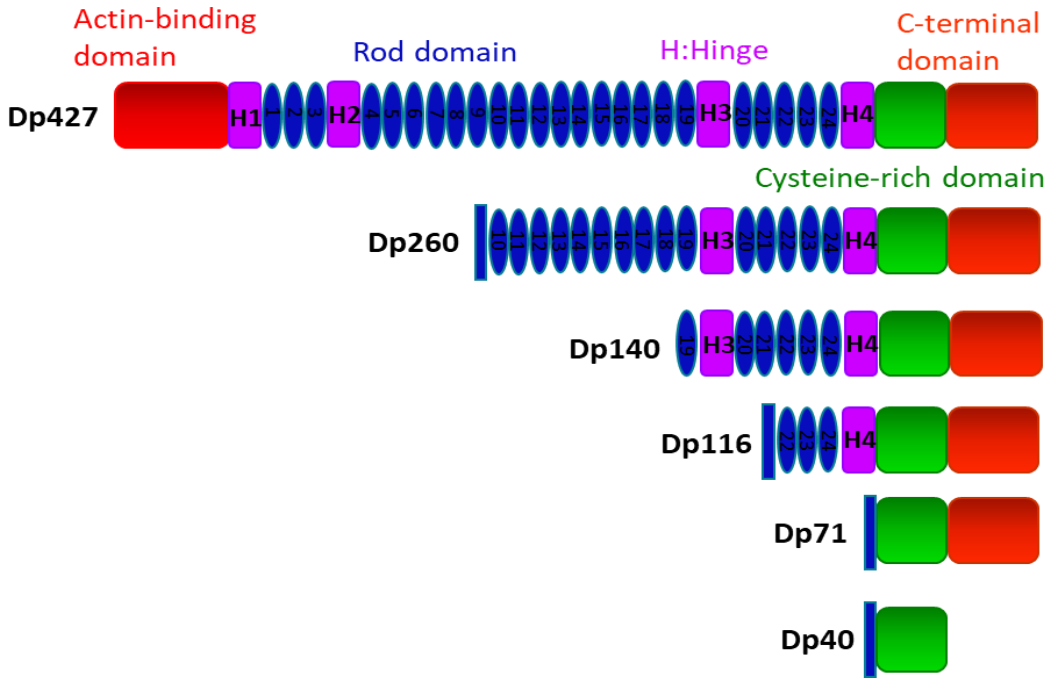


Figure 1.1: Dystrophin protein isoforms present in DMD (adapted from (Nichols et al., 2015). This figure illustrates the different isoforms of the dystrophin protein that are present in different regions of the body. Specifically, Dp427 in muscle and the brain, Dp260 in the retina, Dp116 in Schwann cells in the peripheral nervous system, Dp140, Dp71 and Dp40 in the brain.

1.4. Dystrophin-Associated Protein Complex (DAPC) in myocytes and brain tissue

In muscle, dystrophin forms part of the dystrophin-associated protein complex (DAPC) that functions as an essential link connecting the sarcolemmal cytoskeletal actin to the extracellular matrix (Ervasti & Campbell, 1993; Blake *et al.*, 2002; Davies & Nowak, 2006). This structural function of dystrophin seems to stabilize the sarcolemma and subsequently protect it from any disruption during muscle contraction (Zubrzycka-Gaarn *et al.*, 1988). The DAPC has a dual function in that it supplies mechanical support to the sarcolemma as well as communicating contractile force between muscle fibres, suggesting that the DAPC is also involved in transmembrane signalling (Lapidos *et al.*, 2004). The DAPC maintains physiological handling of Ca^{2+} in muscle fibres as the DAPC acts as an anchor for numerous signalling proteins (Constantin, 2014). The DAPC also provides a strong mechanical link between the sarcolemmal cytoskeleton and the extracellular matrix (thereby mediating interactions between them) in skeletal muscle as it consists of cytoplasmic, transmembrane and extracellular proteins (Rando, 2001). The DAPC is made up of three distinct components: (i) α- and β-dystroglycan, (ii) the sarcoglycan complex (SGC), and (iii) the cytoplasmic subcomplex which is composed of dystrophin, the dystrobrevins and the syntrophin protein family (Blake *et al.*, 2002), as illustrated in Figure 1.2 below.

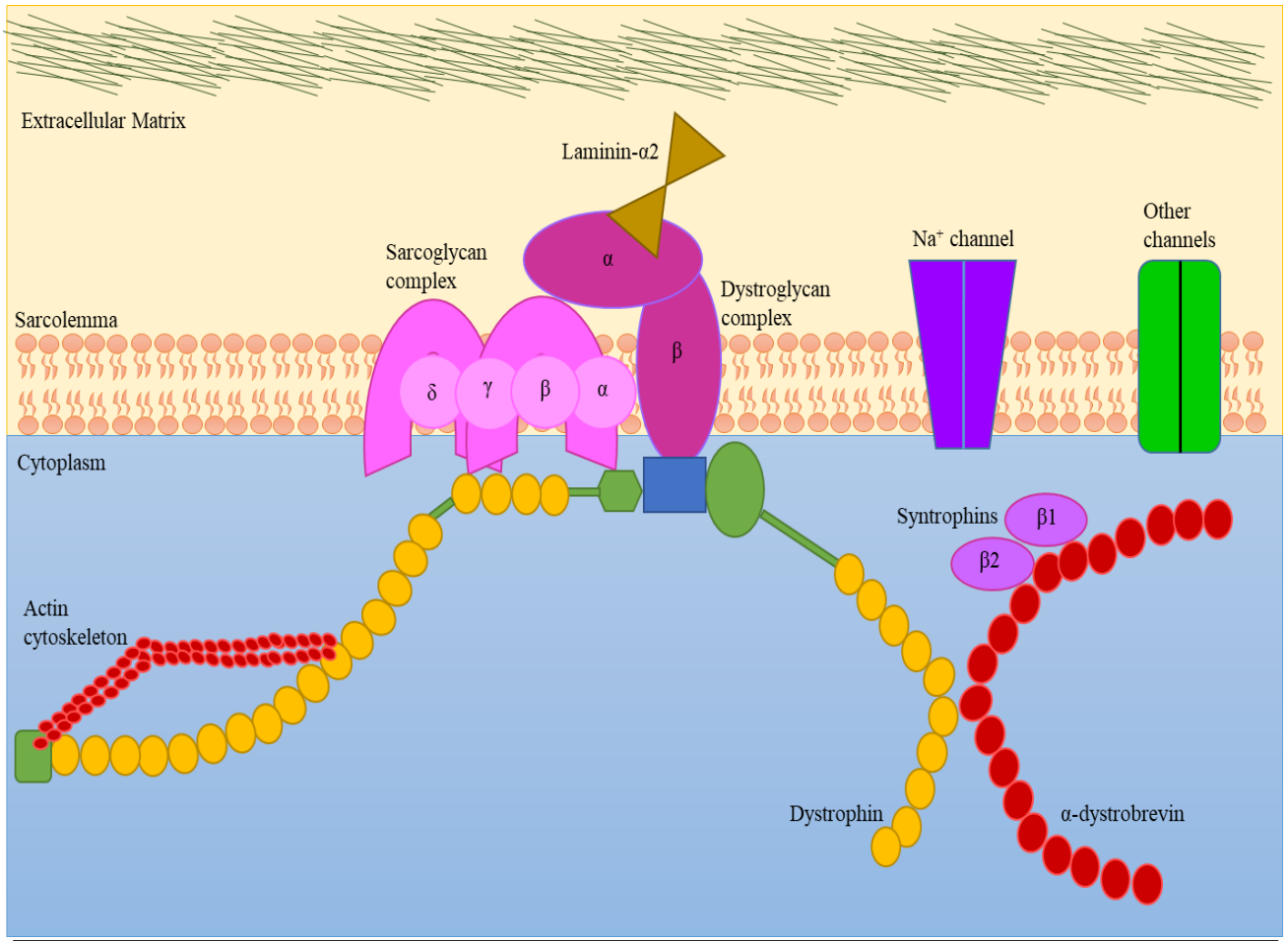


Figure 1.2: Organisation of the Dystrophin-Associated Protein Complex (DAPC) in muscle (adapted from (Fairclough et al., 2013). There are the three distinct components that make up the DAPC: (i) α- and β-dystroglycan, (ii) the sarcoglycan complex (SGC), and (iii) the cytoplasmic subcomplex, which is composed of dystrophin, the dystrobrevins and the syntrophin protein family. Dystrophin provides a crucial structural link between the sarcolemmal cytoskeleton and the extracellular matrix in muscle.

1.5. The role of Dystrophin in the brain

In cells of the central nervous system (CNS), dystrophin and other members of the DAPC partake in macromolecular assemblies that play a role in anchoring receptors to dedicated sites within the membrane (Waite *et al.*, 2009). Furthermore, full length dystrophin, Dp427, co-localizes with γ-aminobutyric acid type A $(GABA)_A$ receptors and is involved in the postsynaptic clustering and stability of inhibitory GABAergic synapses (Knuesel *et al.*, 1999; Anderson *et al.*, 2002) in the postsynaptic membrane of cortical and cerebellar Purkinje neurons (Lidov *et al.*, 1990; Kim *et al.*, 1992; Brunig *et al.*, 2002; Waite *et al.*, 2009). This type of clustering and stabilisation of GABAergic synapses is necessary for effective synaptic signal transduction (Vaillend & Billard, 2002; Kueh *et al.*, 2008).

Importantly, there is evidence that distinct and heterogeneous complexes of the DAPC are present in neurons (Blake et al., 1999; Moukhles & Carbonetto, 2001). Meaningfully, the DAPC in neurons differs from that in muscle in that laminin is replaced by neurexin-α and $GABA_A$ receptors, which are stabilised in the cellular membrane by the DAPC. Further, dystrophin associates with β-dystrobrevin, which plays a role in postsynaptic densities (PSDs) rather than α-dystrobrevin as in skeletal muscle (Blake *et al.*, 1999). These differences in structure of the DAPC in neurons is illustrated in Figure 1.3. Interestingly, defects in the processing and assembly of the DAPC have been associated with brain abnormalities such as mild cognitive impairment and neuronal migration disorders (Blake et al., 1999; Waite et al., 2012), further highlighting the possible impact that a loss of dystrophin, or its

associated proteins, might have on the brain and its normal function. Importantly, in patients with DMD, neuronal loss, neurofibrillary tangles, abnormalities in dendritic development, as well as alterations in the morphology of the presynaptic neuronal cytoskeleton, have been reported (Yoshioka *et al.*, 1980; Jagadha & Becker, 1988; Sogos *et al.*, 1997; Anderson *et al.*, 2002; Lv *et al.*, 2011), which could be the result of altered DAPC function.

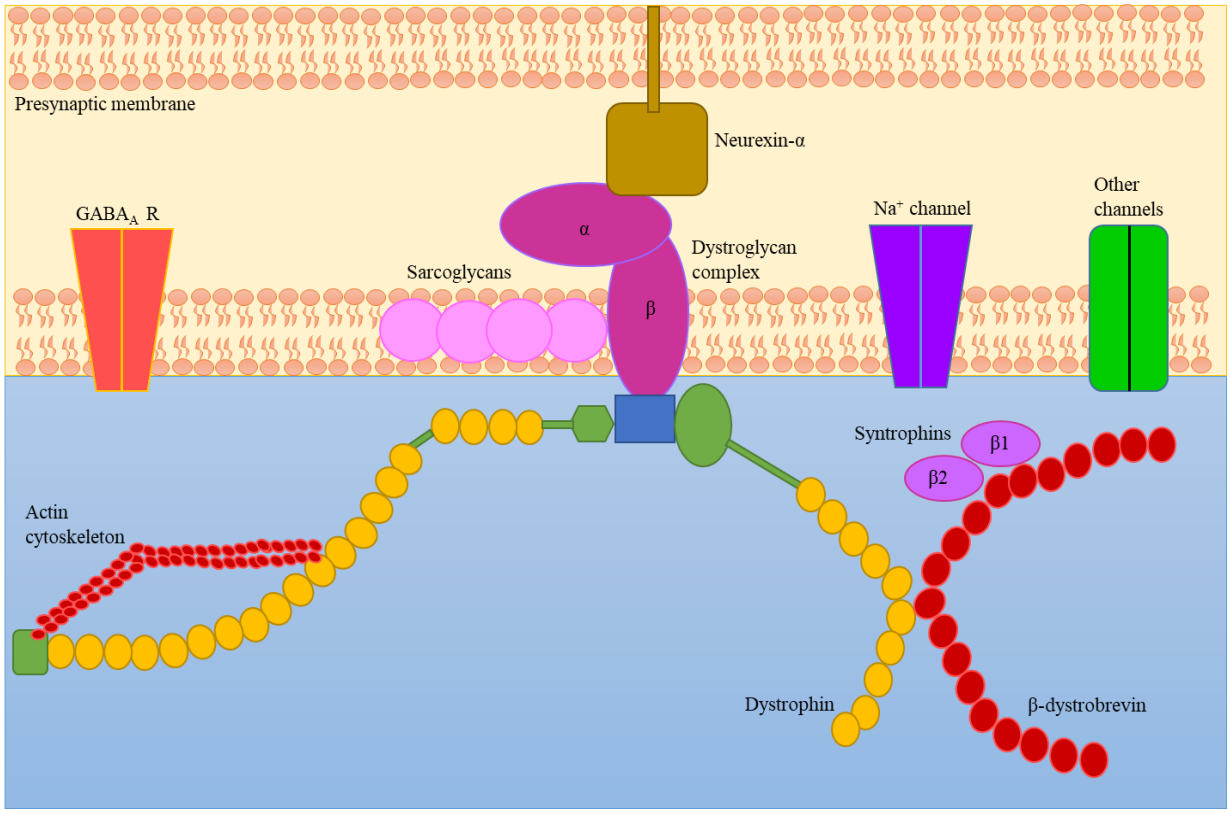


Figure 1.3: The molecular organization of dystrophin and the DAPC in neurons (adapted from (Waite et al., 2009). The DAPC in neurons differs from that in muscle in that laminin is replaced by neurexin-α and GABAA receptors which are stabilised in the cellular membrane by the DAPC.

1.6. *Mdx* mouse model of DMD

The *mdx* mouse has been used as a pre-clinical model of DMD for more than 30 years, since it arose due to a spontaneous mutation in the premature stop codon of exon 23 in the *DMD* gene (Arechavala-Gomeza *et al.*, 2010) of the C57BL/10ScSnJ mouse (Bulfield *et al.*, 1984). The *mdx* mouse is genetically equivalent to DMD in humans and has proven to be advantageous for the investigation of the consequences of the loss of dystrophin on multiple physiological systems. However, despite certain similarities, there are differences between the pathophysiology of DMD in humans compared to that seen in *mdx* mice.

For example, whilst loss of dystrophin in humans and *mdx* mice both result in contraction-induced damage and loss of sarcolemmal integrity in skeletal muscle, the severity in pathology is dependent upon age in *mdx* mice (Moens *et al.*, 1993). This difference in the mouse model is due to the presence of another protein, utrophin, which shares some structural and functional traits with dystrophin such as the fact that it can bind and interact with the same proteins within the cytoskeleton as dystrophin (Matsumura *et al.*, 2011), resulting in a less severe phenotype than in the human disease.

Normally, utrophin is down-regulated in muscle when dystrophin is present (Blake *et al.*, 1996). However, in the absence of dystrophin, utrophin is able to carry out the same function(s) that dystrophin normally would (Keep, 2000). Consequently, in *mdx* mice, the upregulation of utrophin results in the regeneration of sarcolemmal

and plasma membrane integrity, thus saving muscle from deterioration, resulting in a less severe DMD phenotype with regard to skeletal muscle function (Gilbert *et al.*, 1999). In human DMD muscle however, despite there being an upregulation of utrophin relative to unaffected individuals, the levels present in the sarcolemma are not sufficient to prevent the progression of the disease and the subsequent degradation of muscle (Love *et al.*, 1989). Interestingly, the progressive deterioration of the diaphragm of *mdx* mice is similar to that of humans with DMD, with widespread fibrosis present in *mdx* mice from 12 weeks of age until death (Stedman *et al.*, 1991).

While the *mdx* mouse shows differences in skeletal muscle to the DMD profile in humans, there are similarities between humans with DMD and *mdx* mice with regard to dystrophin in the brain. Although no major alterations in gross brain structure have been identified in *mdx* mice relative to controls (Miranda *et al.*, 2009), *mdx* mice do possess fewer neurons, as well as neural shrinkage, in the cerebral cortex and brainstem (Sbriccoli *et al.*, 1995; Carretta *et al.*, 2001). Other architectural changes, as well as reductions in dendritic branching and condensed spinal density in corticospinal neurons of *mdx* mice have also been described (Sbriccoli *et al.*, 1995; Carretta *et al.*, 2003; Carretta *et al.*, 2004). Furthermore, loss of Dp427 appears to be associated with both an increase in the number of inhibitory synapses between axons and dendrites, and alterations in the arrangement of PSDs, in the CA1 region of the hippocampus in *mdx* mice (Miranda *et al.*, 2009). Further, in the *mdx* mouse model of DMD, a study by Bagdatlioglu *et al*., 2020, showed that hippocampal spatial learning and memory was decreased in

mdx mice, particularly long-term memory, which progressively worsened with age (Bagdatlioglu *et al.*, 2020).

1.7. The role of the hippocampus in memory formation

In the brain, the hippocampus is a paired structure present within the limbic system. The hippocampus forms part of the hippocampal formation, which is comprised of the entorhinal cortex, dentate gyrus (DG) and cornu ammonis (CA) regions (CA1–CA3). The hippocampus facilitates the formation of new memories, mainly declarative memory (Vargha-Khadem *et al.*, 1997; Tulving & Markowitsch, 1998) and has also been shown to play a role in spatial navigation and spatial memory (Snow *et al.*, 2013). The main cell type present in the hippocampus are pyramidal cells, which reside in regions CA1-CA3, whereas within the DG, granule cells are most abundant.

One way in which memory formation and consolidation have been described experimentally is through the phenomenon of synaptic long-term potentiation (LTP) that can be induced in excitatory tri-synaptic circuit that characterises the hippocampal formation (see Figure 1.4). There is evidence that LTP is the molecular mechanism underlying memory formation (Morris *et al.*, 1986; Bliss & Collingridge, 1993; Izquierdo *et al.*, 2007) and, more specifically, that it plays a role in hippocampal spatial learning in rodents (Morris *et al.*, 1986; Martin *et al.*, 2000; Morris *et al.*, 2003). The induction of LTP results in a long-lasting enhancement of

synaptically-evoked potentials (Bliss & Lomo, 1973; Bliss & Collingridge, 1993). The majority of LTP experimentation has been conducted upon circuits within the hippocampus, with the first LTP studies focussed upon the dentate gyrus (Bliss & Lomo, 1973) (although it is now clear that LTP can be elicited within many difference areas of the brain, including the amygdala and cerebellum (Artola *et al.*, 1990; Bliss & Collingridge, 1993)).

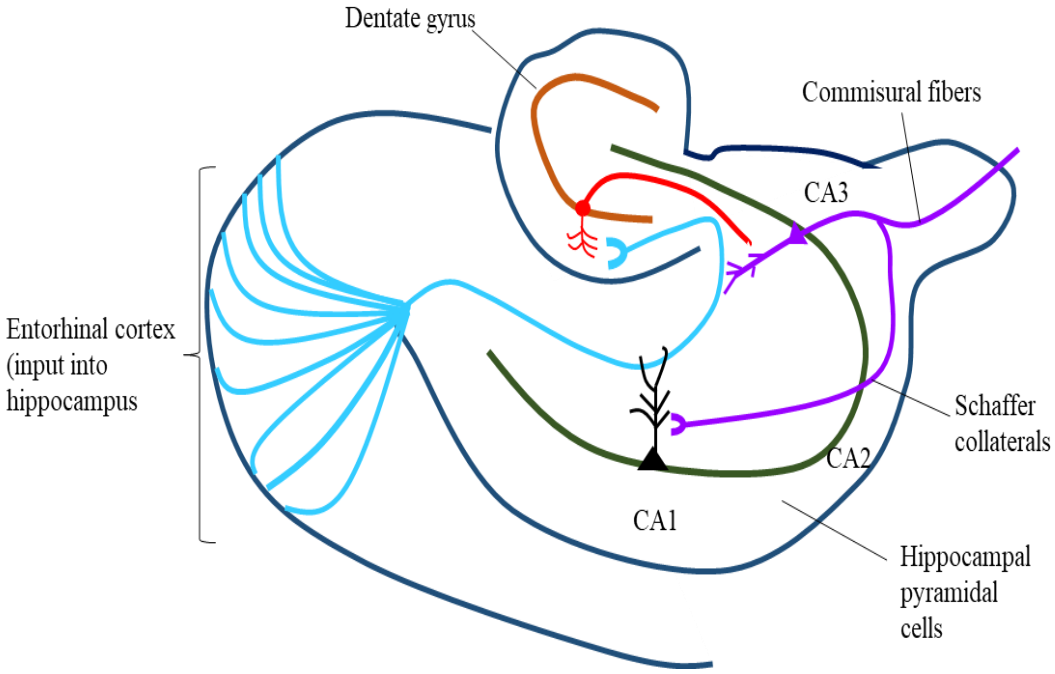


Figure 1.4: Schematic representation of the hippocampal formation, which is comprised of the dentate gyrus, CA1, CA2 and CA3 regions. Most LTP experiments have investigated synaptic plasticity processes that occur between the Schaffer collaterals (purple) and dendrites of CA1 pyramidal cells. Adapted from (Hitti & Siegelbaum, 2014).

In the hippocampus, most experiments investigating LTP have focussed upon the synapses connecting the Schaffer Collaterals (SC) (running from area CA3) to the dendrites of CA1 pyramidal cells, which reside within the *stratum radiatum* above

the hippocampal fissure (Malenka & Nicoll, 1999). When SC axons are electrically stimulated at a basal frequency (*e.g.,* 1 pulse every 20 seconds), this induces the release of the primary excitatory neurotransmitter within the CNS, glutamate, from pre-synaptic terminals of the CA3 axons. The released glutamate then binds to, and opens, a type of ionotropic glutamatergic receptor, known as an AMPA receptor (AMPAR), on CA1 dendrites, evoking excitatory post-synaptic potentials (EPSPs) (Collingridge *et al.*, 1983; Muller *et al.*, 1988; Bliss & Collingridge, 1993). Following the induction of LTP at these same synapses using a high frequency stimulus (*e.g.* "theta-burst stimulation" (Larson *et al.*, 1986), several bursts of 4 pulses at 100Hz), when normal basal stimulation is resumed, EPSP amplitude is significantly enhanced for a prolonged period after application of the LTP stimulus (Bliss & Collingridge, 1993). LTP at the SC-CA1 synapses is induced due to the activation of glutamatergic N-methyl-D-aspartate (NMDA) receptors, which are activated by the release of glutamate (Bliss & Collingridge, 1993). The activation of these NMDA receptors are required for LTP to occur (Collingridge *et al.*, 1983) and this is likely due to an increase in the permeability of the NMDA receptors to calcium, after a release of a magnesium ion and the subsequent influx of calcium during LTP (Ascher & Nowak, 1988). After the subsequent elevated Ca^{2+} influx through activated NMDARs, this results in calmodulin-dependent activation of Ca2+/calmodulin-dependent protein kinase (CaMKII) (Lisman *et al.*, 2002), where its function is to phosphorylates the GluR1 subunit in the AMPA receptor which results in increased AMPA conductance and potentiates synaptic transmission (Lisman *et al.*, 2002). As such, LTP results in changes to the post-synaptic synapse and increased synaptic transmission. Importantly, this potentiation is input-specific. That is, the increase in

EPSP amplitude is only observed at the synapses subjected to the LTP stimulus but not at other SC-CA1 synapses (untouched by the LTP stimulus).

The maintenance of LTP beyond 1 to 3 hours in the hippocampus requires de novo protein synthesis (Frey & Morris, 1997). When solely posttranslational modifications are reflected, this is termed early LTP (E-LTP). The duration of E-LTP varies considerably across studies, mainly because conditioning protocols differ in their abilities to produce the relevant posttranslational changes, such as the phosphorylation of synaptic proteins. The stable, protein synthesis-dependent phase is called late LTP (L-LTP); however, this phase can occur relatively early in LTP, newly synthesized proteins to LTP can be detected as early as 20 min after high frequency stimulation with the use of protein synthesis inhibitors (Osten et al., 1996).

Through the ability to experimentally induce LTP in the hippocampus (and several other brain regions), we now have some understanding as to how the hippocampus functions in relation to memory formation and consolidation (Morris *et al.*, 1986; Teyler & DiScenna, 1987; Bliss & Collingridge, 1993; Izquierdo *et al.*, 2007). LTP induction at the post-synaptic neuron can be seen in figure 1.5 below.

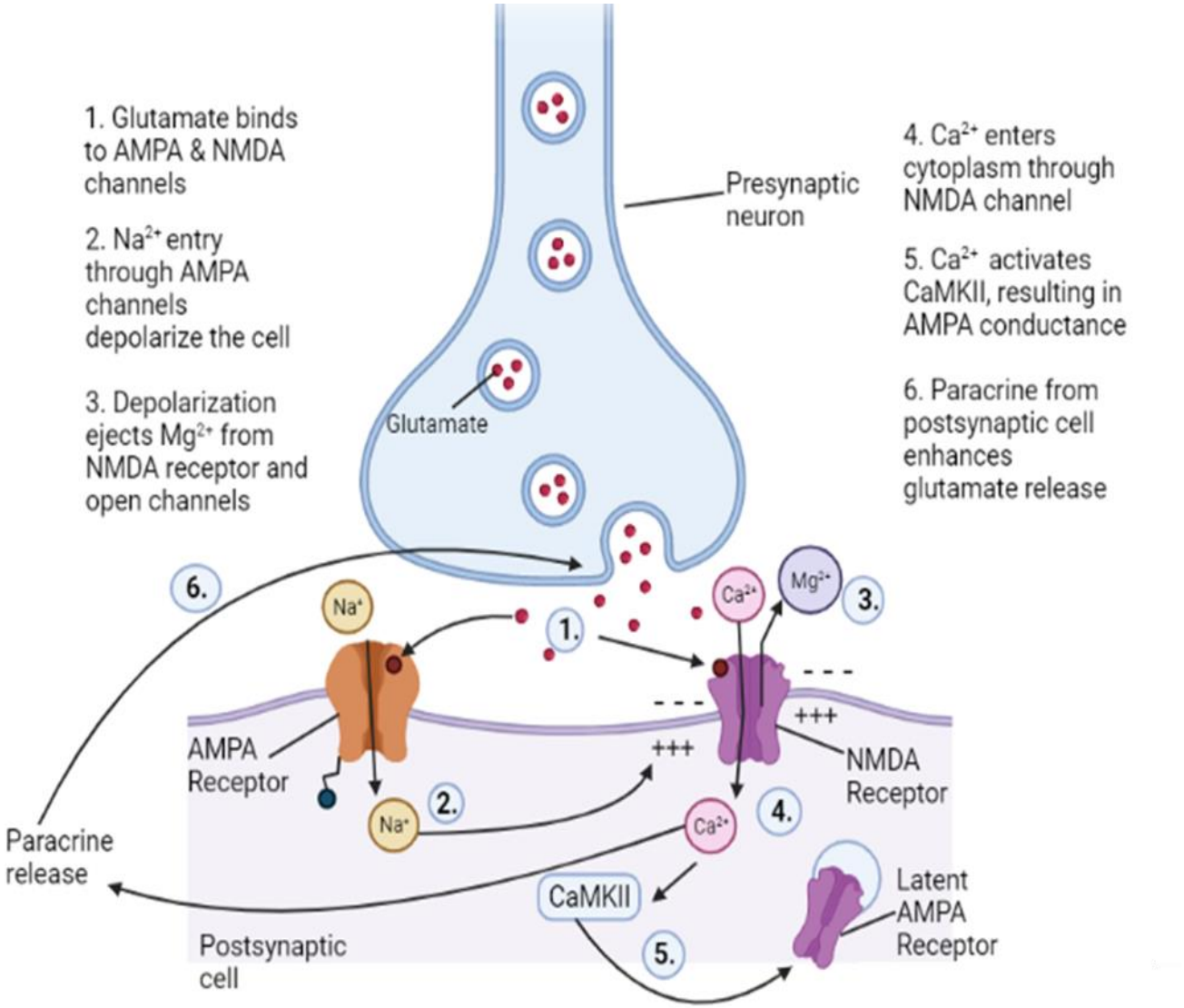


Figure 1.5: A visual representation of the induction of LTP in the post synaptic cell – adapted from (Unglaub Silverthorn, 2013). During normal synaptic transmission, glutamate is released from the presynaptic bouton and acts on both AMPARs and NMDARs. However, Na^+ flows only through the AMPA receptor, but not the NMDA receptor, because Mg^{2+} blocks the channel of the NMDA receptor. Depolarization of the postsynaptic cell relieves the Mg^{2+} block of the NMDA receptor channel, allowing Na^+ and Ca^{2+} to flow into the dendritic spine by means of the NMDA receptor. The resultant rise in Ca^{2+} within the dendritic spine is the critical trigger for LTP.

1.8. Hippocampal dysfunction in the *mdx* mouse

Dystrophic *mdx* mice display a neurological and behavioural profile that is similar to DMD patients (Muntoni *et al.*, 1991; Chaussenot *et al.*, 2015) as mentioned in section 1.6. Further, they display a poor capacity to learn new tasks, and deficits in spatial memories (Vaillend *et al.*, 1995; Vaillend *et al.*, 2004; Chaussenot *et al.*, 2015) which are consistent with dysfunctions of the hippocampus. They also display deficits in associative learning and in the general processes involved in memory formation and consolidation which are both dependent upon optimal functioning of the hippocampus (Chaussenot *et al.*, 2015).

Changes in short- and long-term memory formation and consolidation may be linked with altered synapse morphology and plasticity associated with a loss of Dp427 (Miranda *et al.*, 2009). However, electrophysiological studies conducted on *mdx* mouse brain slices in order to elucidate the role dystrophin might play in synaptic function have generated contradictory findings. For example, initial studies found no obvious deficit in hippocampal NMDA-dependent LTP in *mdx* mice that lacked Dp427 relative to controls (Sesay *et al.*, 1996). Furthermore, no differences in hippocampal-dependent spatial learning tasks were found between *mdx* mice and wild-type controls (Sesay *et al.*, 1996), implying that hippocampal synaptic processes remained intact in *mdx* mice. However, subsequent studies have described deficits in long-term hippocampal spatial memory (Vaillend *et al.*, 2004; Bagdatlioglu *et al.*, 2020), which progressively worsened with age (Bagdatlioglu *et al.*, 2020), as well as deficits in object recognition (Vaillend *et al.*, 2004) in *mdx* mice

relative to controls. Further, hippocampal LTP in *mdx* mice was also abnormally enhanced relative to controls (Vaillend *et al.*, 2004). Although the reason(s) for these contrasting findings remain unclear, one possibility is that the particular training procedures mice were subjected to by the Sesay group may at least partially account for them as the tasks might have helped to alleviate any subtle memory deficits that may have been present before training. Vaillend *et al.* (2004) proposed that the abnormally enhanced hippocampal LTP observed in the *mdx* brain slices could at least, in part, be responsible for the memory deficits seen in the *mdx* mouse. Thus, somewhat counterintuitively, an abnormal enhancement of synaptic plasticity and neuronal excitability might actually inhibit normal cognitive functioning (Vaillend *et al.*, 2004).

Later studies found that the *mdx* brain dysfunction was associated with a loss of Dp427 that resulted in defective synaptic inhibition (Perronnet & Vaillend, 2010) possibly due to Dp427-dependent reduction in the number of $GABA_A$ receptor clusters, which are essential for normal neuronal excitability and synaptic transmission (Dallerac *et al.*, 2011), in the hippocampus (as well as in other brains regions such as the cerebellum and amygdala (Vaillend *et al.*, 2010)). A reduction in $GABA_A$ receptor clusters was also seen in cerebellar Purkinje and hippocampal CA1 neurons of the *mdx* mouse (Knuesel *et al.*, 1999).

It is notable that when Vaillend *et al.* (2010) restored expression of a dystrophin-like protein to 15–25% of normal dystrophin levels in area CA1 of the hippocampus of *mdx* mice (using an AAV vector expressing antisense sequences to modulate

splicing of the dystrophin pre-mRNA), this facilitated a complete recovery of α2 subunit-containing $GABA_A$-receptor clustering in this brain region of *mdx* mice (Vaillend *et al.*, 2010). This highlights the importance of the role of Dp427 and its association with $GABA_A$ receptors in modulating hippocampal synaptic plasticity. Additionally, using the same treatment, NMDA-dependent LTP was also restored (Vaillend *et al.*, 2010).

1.9. Intracellular Ca^{2+} handling in dystrophic hippocampal neurons

Calcium (Ca^{2+}) has a significant role in cell signalling such that many cellular functions are directly or indirectly controlled by the intracellular concentration of Ca^{2+} (Missiaen *et al.*, 2000).

Similarly, in the brain, Ca^{2+} plays an important role in the regulation of numerous neuronal processes such as neuronal plasticity and survival, as well as transcription factor regulation (Brini *et al.*, 2014) and is tightly regulated by complex regulatory mechanisms which balance the influx of Ca^{2+} into the cell and release from intracellular stores (Brini *et al.*, 2014). Intracellular free Ca^{2+} concentration is involved in the control of many physiological functions in all cell types, including neurons. An influx of Ca^{2+} through voltage-dependent and ligand-gated channels in the plasma membrane is a critical signal for the release of neurotransmitters from presynaptic terminals and for responses of the postsynaptic neuron (Yuste *et al.*, 2000; Burnashev & Rozov, 2005; Hartmann & Konnerth, 2005). Ca^{2+} can also play a role in synaptic plasticity which depends on NMDAR activation (Mattson, 2007).

Any disturbance of the normal regulation of intracellular Ca^{2+} (such as an increase in Ca^{2+} from intracellular stores) can result in pathology (Missiaen *et al.*, 2000). Interestingly, in DMD, there is evidence that a lack of dystrophin is associated with irregular intracellular Ca^{2+} homeostasis. For example, an absence of dystrophin in neurons has been associated with an increase in the open time of Ca^{2+} permeable ion channels in cerebellar neurons in *mdx* mice (Haws & Lansman, 1991), which could ultimately trigger a neuronal cytotoxic cascade resulting in neuronal death.

Most recently, a study by Lopez *et al*. (2018), found that intracellular Ca^{2+} was elevated in cortical and hippocampal pyramidal neurons of adult *mdx* mice compared to WT animals and this increase in Ca^{2+} progressed with age (Lopez *et al.*, 2018). It is notable that the cognitive deficits shown by these *mdx* mice were partially reversed with the injection of GsMTx-4 which blocks stretch-activated channels that are involved in Ca^{2+} regulation (Suchyna *et al.*, 2000; Lopez *et al.*, 2018). Thus, with an injection of GsMTx-4 into *mdx* mice, this resulted in a decrease of intracellular Ca^{2+} in cortical and hippocampal neurons and improvement in spatial learning memory compared to WT mice (Lopez *et al.*, 2018). Interestingly, dystrophin deficiency dysregulated hippocampal intracellular calcium levels to a greater extent in cortical neurons in an age-dependent manner (Lopez *et al.*, 2018). While dystrophin-deficiency undoubtedly impacts upon cognitive function, with regards to intracellular Ca^{2+} (Lopez *et al.*, 2018) and $GABA_A$-receptor clustering (Vaillend *et al.*, 2010), this may be due entirely to its role as a structural protein. However, another consideration, following with the pathogenesis of DMD, could be to investigate inflammation. DMD is known to result in altered cytokine profiles, thus, we may speculate that this altered cytokine profile may also mediate some of

the negative cognitive effects observed in human DMD patients, for the reasons I will discuss in the next section(s).

1.10. Interleukin-6 is a pleiotropic cytokine with modulatory actions in the central nervous system (CNS).

Cytokines are traditionally described as being immune molecules that are critical for pro- or anti-inflammatory signalling. Of these, IL-6 has pleiotropic effects, on many cells. In health, plasma levels of IL-6 range from ~1–10 pg/ml (Akira *et al.*, 1993) but this can rise to the lower nanogram/ml range during infection or inflammation (Jones, 2005). IL-6 can be secreted by both immune and non-immune cells (Marz *et al.*, 1998), and has a key role in regulating immune cell function (Hirano *et al.*, 1985), although this 26kDa protein can also modify functions in other cells, including neurons.

IL-6 evokes its biological effects by binding to IL-6 receptors, which can either be soluble or membrane bound. However, membrane-bound IL-6 receptors (IL-6Rα) are only expressed in a restricted subset of cells (Rothaug *et al.*, 2016). Whereas soluble IL-6 receptors may form a complex with IL-6 and stimulate distant cells including neurons (Rose-John & Heinrich, 1994; Erta *et al.*, 2012).

1.10.1. Classical signalling mechanism of IL-6 and its receptor

The classical signalling mechanism of IL-6 entails the binding of IL-6 to membrane bound IL-6Rα in a complex with glycoprotein (gp)130. This binding results in the homodimerization of the signal transducing protein gp130 and subsequent

phosphorylation of Janus kinase/signal transducer and activator of transcription (JAK/STAT) (Darnell *et al.*, 1994). Not only does the complex of IL-6/ IL-6Rα activate STATs, it also activates the mitogen-activated protein (MAPK) and phosphoinositide 3-kinase (PI 3-K) cascades (Eulenfeld *et al.*, 2012). IL-6 can, however, also evoke signalling in cells which don't express IL-6Rα on their cell membranes.

1.10.2 Trans-signalling mechanism of IL-6 and its receptor

IL-6Rα can be proteolytically cleaved from the cell membrane to generate a soluble IL-6Rα (sIL-6Rα), which is still able to bind to its ligand, IL-6, as seen in classical signalling (Müllberg *et al.*, 1993). And similar to the classical signalling pathway, sIL-6Rα/IL-6 complex binds to gp130 expressed on the cell membrane of neurons (Rose-John & Heinrich, 1994; Scheller *et al.*, 2011b) to evoke this trans-signalling mechanism. In humans, sIL-6Rα can also be generated by translation of an alternatively spliced mRNA (Lust *et al.*, 1992), although this has not been seen in mice (Scheller *et al.*, 2011a).

Even though a membrane bound receptor for IL-6 is limited to a subset of cells, gp130 is ubiquitously expressed on the cellular membrane of most cell types including neural cells in the CNS (Watanabe *et al.*, 1996). Expression of gp130 is not changed during inflammation but concentrations of sIL-6Rα can increase between two and five-fold (Rose-John, 2012; Schaper & Rose-John, 2015), inferring the importance of sIL-6R in the activation of IL-6. Importantly, downstream activation of JAK/STAT or PI 3-kinase occurs in cells that don't express membrane-bound IL-

6Rα in a similar manner to classical IL-6Rα signalling (Ernst & Jenkins, 2004; Campbell *et al.*, 2014). Thus, as many cells respond to IL-6 during inflammation, which do not express membrane-bound IL-6Rs, the importance of sIl-6R for the activation of IL-6 is evident. See Figure 1.5 below for a visual representation of classical and trans-signalling mechanisms of IL-6.

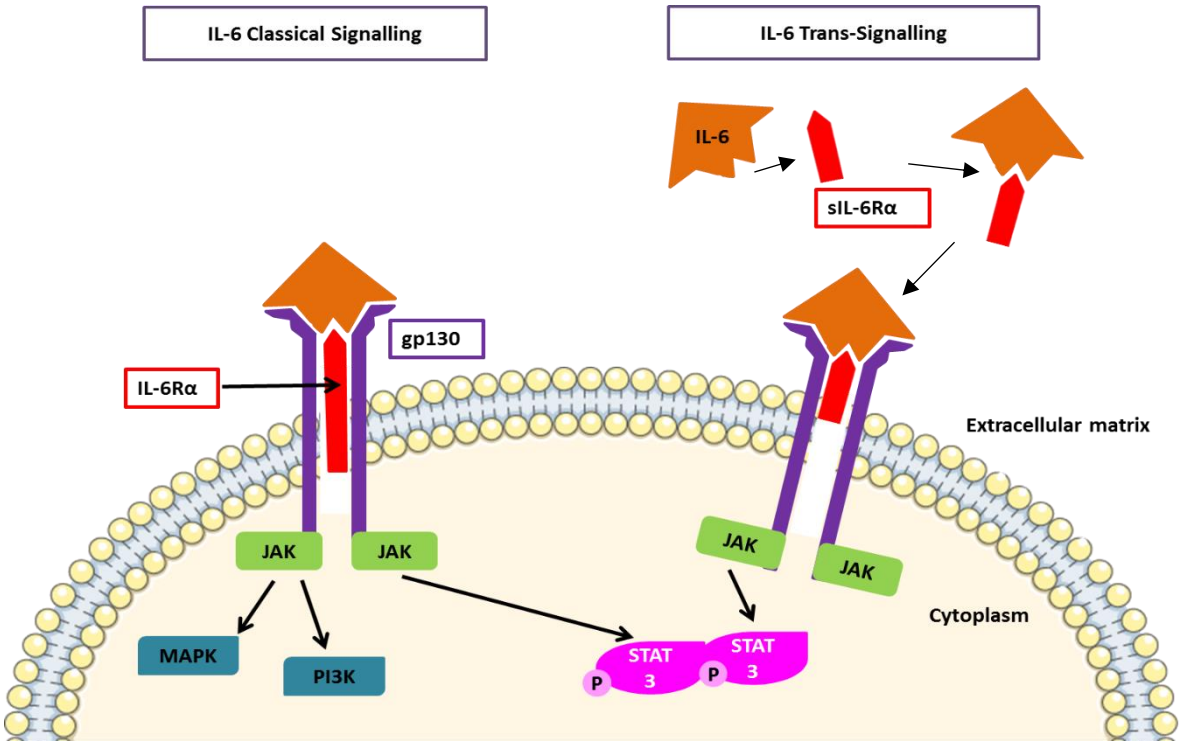


Figure 1.6: A representation of IL-6/ IL-6Rα classic and trans-signalling mechanisms – adapted from (Schaper & Rose-John, 2015). Classical signalling involves IL-6 binding to a membrane bound IL-6Rα, with this complex subsequently binding to, and activating, the signal transduction of gp130 for downstream activity of JAK/STAT, MAPK and PI3K. Trans-signalling involves IL-6 binding to a soluble IL-6Rα in the extracellular matrix and only then binding to gp130 for activation of downstream signalling.

Importantly, differences in the evoked cellular response between classic receptor-mediated IL-6 signalling and trans-signalling can be detected by the cellular outcomes. Classical IL-6 signalling evokes anti-inflammatory signals, in contrast to the pro-inflammatory, and potentially deleterious, actions of IL-6/sIL-6R-evoked trans-signalling (Garbers *et al.*, 2015).

The signalling kinetics of these two distinct mechanisms also differ, leading to fundamentally different cellular responses (Rothaug *et al.*, 2016). In the CNS, neuronal degeneration evoked by IL-6 is mediated by trans-signalling, whereas membrane receptor-mediated IL-6 signalling plays a role in neural tissue regeneration (Campbell *et al.*, 2014) and neuronal protection (Garbers *et al.*, 2015). Understanding the specific signalling mechanisms is particularly relevant when therapeutically targeting this signalling pathway in neurological disorders.

1.11. IL-6 modifies long-term potentiation

Ex vivo hippocampal slices retain the hippocampal architecture and intact neural pathways of the dentate gyrus, CA1 and CA3 areas (Malenka & Nicoll, 1999). As explained in an earlier section, hippocampal LTP is believed to recapitulate the molecular mechanisms underlying the coding of new memories in the brain by modifying the strength of synaptic transmission (Collingridge *et al.*, 1983; Muller *et al.*, 1988; Bliss & Collingridge, 1993).

IL-6 gene expression in the CA1 region of the hippocampus is increased after induction of LTP, although it is important to note that expression of IL-6 mRNA was

specific to nearby astrocytes, not neurons (Jankowsky *et al.*, 2000). Significant increases in the levels of IL-6 mRNA one hour post-stimulation were also noted in *ex vivo* experiments, but only when LTP had been successfully induced (Balschun *et al.*, 2004). Interestingly, blockade of the effects of endogenous IL-6 production using a neutralizing antibody after 90 minutes resulted in a remarkable prolongation of LTP, as well as improved performance in spatial memory tests in mice, further emphasising the pleiotropic actions of this cytokine in the CNS (Balschun *et al.*, 2004). However, it appears that either too little or too much IL-6 may impair memory formation, as IL-6 knock-out mice performed less well in hippocampus-dependent memory tests (Baier *et al.*, 2009) and are more susceptible to hippocampal damage following induced convulsions relative to controls (Penkowa *et al.*, 2001; De Sarro *et al.*, 2004), whereas transgenic mice with cerebral over-expression of IL-6 were characterised by suppressed LTP in the dentate gyrus region (Bellinger *et al.*, 1995).

Although it is recognised that exogenous application of IL-6 may not mimic endogenously released IL-6 during LTP (Balschun *et al.*, 2004), application of IL-6 still inhibited hippocampal LTP using a mechanism that was dependent upon IL-6R activation (Tancredi *et al.*, 2000). Moreover, IL-6-induced LTP inhibition was attenuated by administration of monoclonal antibodies, used to block IL-6 receptors (Li *et al.*, 1997). Thus, IL-6 may fine-tune memory consolidation by acting as a molecular filter, limiting the long-term storage of some types of information.

1.12. IL-6 modifies hippocampal adult neurogenesis and cognitive function

The posterior or dorsal portion of the hippocampus participates in contextual learning, declarative memory and spatial navigation {Kheirbek, 2013, Moser & Moser, 1998) . Whereas the ventral portion of the hippocampus is thought to be involved in emotional processing, such as anxiety (Bannerman et al., 2003, (Bannerman et al., 2004, Bannerman et al., 2014). The dentate gyrus is one of the few brain regions where neurogenesis occurs and adult-born neurons are integrated into pre-existing neuronal circuits (Gage, 2000). The process of hippocampal adult neurogenesis is initiated when neuronal progenitor cells from the subgranular zone of the hippocampal dentate gyrus migrate into the granule cell layer and subsequently differentiate into neuronal or glial cells (Gage, 2000). Newly generated neurons then extend their axons into the CA3 region of the hippocampus and eventually form synapses with adjacent cells (Gould *et al.*, 2000; van Praag *et al.*, 2002). Integration of new cells into neuronal circuits is proposed to contribute to hippocampal-dependent learning and memory processes (Wu & Hen, 2014). The dentate gyrus is positioned as the input zone of the hippocampus and has low neuronal activity with upstream cortical areas. Interestingly, IL-6 has been shown to influence neural stem cells in neurogenesis (Islam *et al.*, 2009), with proliferation, survival and differentiation of hippocampal progenitor cells being compromised in the dentate gyrus when IL-6 concentrations are elevated (Vallieres *et al.*, 2002).

In a study by Kong *et al*. (2019), IL-6 concentration-dependently reduced neural stem cell proliferation, decreased neuronal differentiation and ultimately impacted upon hippocampal adult neurogenesis through activation of the JAK2/STAT3 signalling pathway. The importance of JAK2/STAT3 signalling in memory consolidation was further highlighted when cognitive deficits in a mouse model of neuroinflammation (APP/PS1) were rescued by inhibiting this signalling cascade (Kong *et al.*, 2019).

In humans, a deterioration in cognitive function is a hallmark feature of 'sickness behaviour' which is linked to high circulating levels of pro-inflammatory cytokines including IL-6 and IL-1β (Gibertini, 1998). IL-6 has also been implicated in lipopolysaccharide (LPS) -evoked cognitive dysfunction (Sparkman *et al.*, 2006). Moreover, transgenic mice over-expressing IL-6 exhibit broad memory impairment (Heyser *et al.*, 1997; Wei *et al.*, 2012; Wei *et al.*, 2013) and severe neurological pathologies (Campbell *et al.*, 1993). The explicit effect of this cytokine on learning and memory function is further supported by the finding that transgenic mice deficient in IL-6 possess enhanced spatial learning capabilities in the radial arm maze (Braida *et al.*, 2004) and the Morris water maze (Bialuk & Winnicka, 2018) behavioural task-learning assessments.

In early studies, transgenic mice overexpressing IL-6, developed severe neurological pathologies such as tremor, ataxia, and seizure, concomitant with neurodegeneration, astrocytosis and angiogenesis (Campbell *et al.*, 1993). Further studies using the same transgenic mouse model found a significant reduction in

overall neurogenesis in the dentate gyrus of the hippocampus with neural progenitor cells also reduced in the granule cell layer (Vallieres *et al.*, 2002). These studies suggested that overexpression of IL-6 is detrimental to adult neurogenesis and can have a direct pathogenic role not only in inflammation and infections, but also neurodegenerative CNS disease (Campbell *et al.*, 1993; Vallieres *et al.*, 2002).

1.13. Perspectives

Most research on DMD has focussed on the loss of dystrophin from skeletal muscle. As new therapies have improved life expectancy in patients with DMD, greater attention to other aspects of DMD, such as cognitive impairment, is warranted. DMD patients can have communication difficulties and poor affect recognition (Hinton *et al.*, 2006; Hinton *et al.*, 2007) and specific deficits in verbal, short-term and working memory (Hinton *et al.*, 2000, 2001; Snow *et al.*, 2013). In healthy individuals, dystrophin is expressed in the hippocampus, cerebral cortex, amygdala and cerebellum (Lidov *et al.*, 1990; Bies *et al.*, 1992; Lidov *et al.*, 1993; Knuesel *et al.*, 2000; Sekiguchi *et al.*, 2009) and loss of dystrophin has been linked to neuronal loss, neurofibrillary tangles, alterations to dendritic branching, cortical atrophy as well as metabolic abnormalities (Rosman, 1970; Yoshioka *et al.*, 1980; Jagadha & Becker, 1988; Tracey *et al.*, 1995; Lv *et al.*, 2011).

In parallel, contraction-induced damage to muscle fibres (De Paepe & De Bleecker, 2013) results in chronic inflammation, and elevated circulating levels of IL-6, a pro-inflammatory cytokine which has the capacity to modulate brain function, is raised in DMD patients (Rufo *et al.*, 2011) and *mdx* mice (Pelosi *et al.*, 2015) alike. Further,

IL-6 has also been shown to influence long term potentiation (Li *et al.*, 1997; Tancredi *et al.*, 2000; Stampanoni Bassi *et al.*, 2019), neurogenesis (Islam *et al.*, 2009) and astrogliogenesis (Nakanishi *et al.*, 2007).

Aims

To investigate the physiological mechanisms underpinning the neuromodulatory effects of IL-6 in hippocampal-dependent cognitive deficits in the dystrophin-deficient *mdx* mouse model.

Objectives

1. To investigate the impact of loss of dystrophin on hippocampal function in *mdx* mice.
2. To investigate the importance of IL-6 in hippocampal function in dystrophic hippocampal function.
3. To determine if *in vivo* administration of neutralising monoclonal anti-IL-6 receptor antibodies (xIL-6R) improves cognitive dysfunction in *mdx* mice.

Chapter 2: Methods

2.1. Animals

All animal experiments were approved and performed following guidelines set out by the Health Products Regulatory Authority (HPRA) and following project authorisation (AEI9130/P088), as well as individual authorisation (AEI9130/I303). Animals were euthanized in accordance with European Directive 2010/63/EU. Animals aged under P14 (postnatal age) were decapitated with sharp scissors. Animals older than P21 were anaesthetised with Isoflurane (5% Isoflurane in oxygen, Harvard Apparatus) before decapitation with sharp scissors.

Dystrophin-deficient C57BL/10ScSn-Dmd^{mdx}/J (*mdx*) and wild type C57BL/10ScSnJ (WT) controls were purchased from The Jackson Laboratory (Bar Harbor, Maine, USA). Breeding colonies of both *mdx* and WT mice were established and maintained in the Specific Pathogen Free (SPF) unit of the Biological Services Unit, University College Cork, Ireland. To generate *mdx* mice, homozygous females were bred with hemizygous males. Animals were housed with littermates before being weaned at P21. After sexing, given that boys express the DMD phenotype, only males were housed in individually ventilated cages (IVCs) with no more than 4 male littermates in each cage. IVCs were kept under a 12-hour light/dark cycle between 06:00 and 18:00, with water and standard chow provided *ad libitum*. Further, IVCs contained sawdust made from aspen wood chip, sizzlenest (bedding) and cardboard tubes as play tunnels for environment enrichment.

2.2. Tissue preparation for immunocytochemistry and immunohistochemistry

2.2.1. Hippocampal neuron culture

Primary hippocampal neuronal cultures were prepared using neonatal male *mdx* and WT mice pups (3-5 days old).

In order to minimise the risk of contamination of cultured neurons, the initial hippocampal dissection and subsequent cell culture preparation were carried out in a laminar flow cabinet (OSN Horizontal Laminar Airflow Cabinet, Nicotra), with all equipment sterilized with 70% ethanol (prepared from 99.9% ethanol (Brenntag, Essen, Germany)) solution prior to use. All solutions used in the preparation of cultured hippocampal neurons were syringe filtered (0.2µm pore size; Corning Inc., New York, USA) again, to minimise infection, with strict aseptic technique adhered to throughout for the same purpose.

Primary hippocampal neuron cultures were prepared as described previously in our lab (Kaar *et al.*, 2017). The brain was removed and bisected into two hemispheres. Hippocampi were then isolated and placed into a dissection solution made up with HEPES-buffered saline solution (HBSS) (see Table 2.1 for reagent setup and Table 2.1 for culture medium composition).

Following dissection and isolation of the hippocampi, the tissue was transferred to a papain (Worthington, Ohio, USA) solution (2mg/ml; Table 2.2 for culture medium composition) for 45 minutes at 37˚C in order to facilitate the dissociation of individual hippocampal neurons from the hippocampal tissue. Papain has previously

been shown to be the most suitable protease for cell dissociation (Brewer, 1997). Dissociated neurons were then rinsed three times with a trituration solution (see Table 2.2: culture medium composition) and then mechanically dissociated three times with a plastic Pasteur pipette (with a diameter of 2mm, Sarstedt, North Carolina, USA) leaving a suspension of cells in the trituration solution. This cellular supernatant was then transferred to another tube with the plastic Pasteur pipette and centrifuged at 1200rpm for two minutes. After centrifugation, the trituration solution was gently poured out of the tube without dissociating the pelleted hippocampal neurons. Approximately 600-700µl plating solution was then added (Table 2.2: culture medium composition) and the pellet gently detached from the bottom of the tube prior to 'finger' vortexing the cells until they were completely resuspended in the plating solution. Dissociated cells were seeded onto poly-D-lysine hydrobromide (Sigma-Aldrich, Missouri, USA) – coated coverslips (see section 2.2.2 Poly-D-lysine coating of coverslips) in 35mm plastic petri dishes (Corning Inc., New York, USA) and incubated (Galaxy S CO_2 Incubator, New Brunswick Scientific, New Jersey, USA) at 37˚C with gas levels maintained at 95% O_2 and 5% CO_2. Culture medium was added after 45 minutes (Table 2.2: culture medium composition). Coverslips were then inverted after a further 2 hours in the incubator. Cultures were routinely maintained in the incubator at 37˚C, 95% O_2 and 5% CO_2 for 10-12 days. See Figure 2.1 for an overview of the technique.

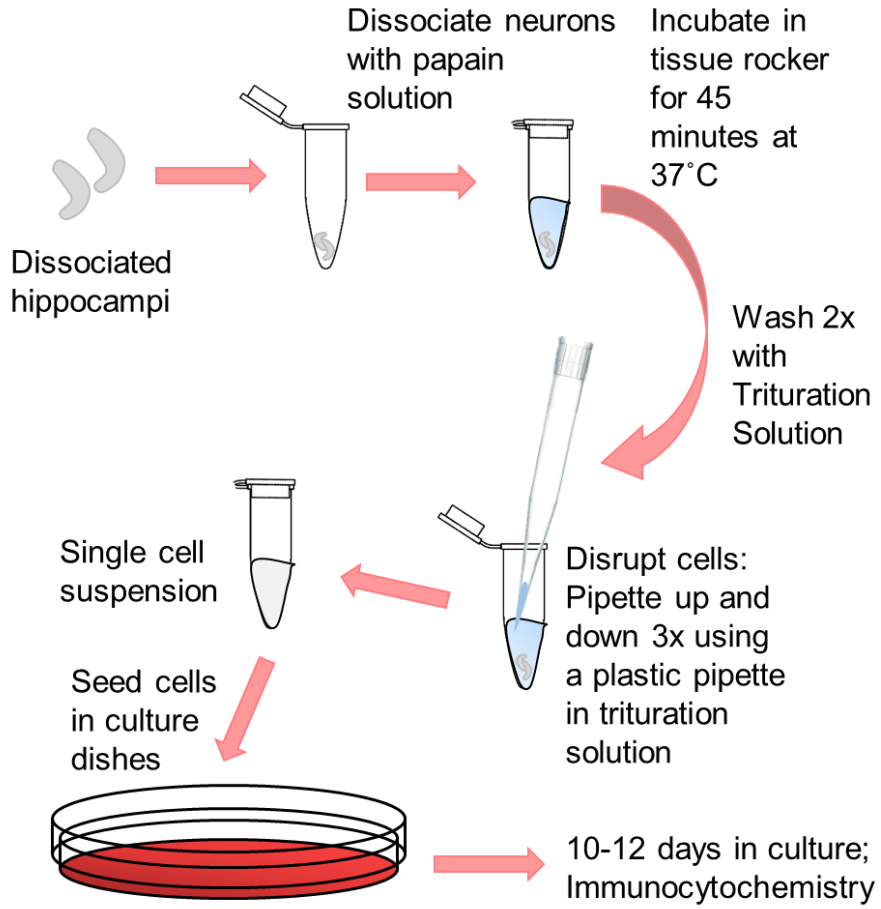


Figure 2.1: Flow diagram displaying the process of primary hippocampal neuron dissociation and culture.

2.2.2. Poly-D-lysine coating of coverslips

In order to minimise the risk of contamination, coverslips were prepared for the culture process in a laminar flow cabinet. Coverslips (13mm - TAAB Laboratories Equipment Ltd., UK) were sterilised in 70% ethanol before being transferred to 35mm dishes (Corning, New York, USA). Poly-D-lysine hydrobromide (35 µl - 55 µl, 0.1mg/ml, Sigma-Aldrich, Missouri, USA) was filter-syringed onto each coverslip,

aspirated after 1 hour and the coverslips then washed twice with dH_2O. Coverslips were coated with Poly-D-lysine hydrobromide up to 3 days before a culture.

Table 2.1: Reagent setup for primary hippocampal neuron culture.

Dissection HEPES-buffered saline solution (HBSS), osMom 310, pH 7.35-7.45	**Composition (mM)**	**Source**
NaCl	130	Sigma-Aldrich
HEPES	10	Sigma-Aldrich
KCl	5.4	Sigma-Aldrich
$MgCl_2$	2	Fisher Scientific
D-Glucose	2	Fisher Scientific
$CaCl_2$	0.5	Sigma-Aldrich

Table 2.2: Primary hippocampal neuron culture medium composition.

Reagents	**Components**		**Source**
Dissection solution	HBSS	8ml	See reagent setup
containing	Glutamax™ supplement	0.5mM	ThermoFisher Scientific
	L-Glutamic acid	0.025mM	Sigma-Aldrich
	Penicillin–Streptomycin (P-S)	1%	Sigma-Aldrich
Papain solution	Dissection solution (as	2ml	See reagent set up
containing	above)	2mg/ml	Worthington

	Papain		
Trituration	HBSS	15ml	See reagent set up
solution	Foetal Bovine Serum (FBS)	10%	Sigma-Aldrich
containing	Glutamax™ supplement	0.5mM	ThermoFisher Scientific
	L-Glutamic acid	0.025mM	Sigma-Aldrich
	P-S	1%	Sigma-Aldrich
Plating solution	DMEM	3ml	Sigma-Aldrich
containing	FBS	10%	Sigma-Aldrich
	Glutamax™ supplement	0.5mM	ThermoFisher Scientific
	L-Glutamic acid	0.025mM	Sigma-Aldrich
	P-S	1%	Sigma-Aldrich
Culture medium	DMEM – low glucose		Sigma-Aldrich
containing	Serum Replacement 2 (SR2)	2%	Sigma-Aldrich
	Glutamax™ supplement	0.5mM	ThermoFisher Scientific
	L-Glutamic acid	0.025mM	Sigma-Aldrich
	P-S	1%	Sigma-Aldrich

2.2.3 Preparation of Hippocampal tissue for Immunohisto/cytochemistry

Mice (8–12-week-old WT and *mdx*) were anaesthetised with isoflurane (5% in oxygen) and then immediately euthanized by decapitation using sharp scissors. The whole brain was excised from the skull and submerged in 4% PFA (Sigma-Aldrich,

Missouri, USA) for 72 hours, then cryo-protected by immersing in a 30% sucrose solution (Sigma-Aldrich, Missouri, USA) made up in 0.1mM Phosphate Buffered Saline (PBS, See Table 2.3: reagent setup) for 24 hours. Tissue was then flash frozen in liquid nitrogen and stored at -80°C until cryo-sectioned (CM1850, Leica, Germany) in Optimal Cutting Temperature (OCT) embedding medium (Thermofisher Scientific, Massachusetts, USA) in 20µm sections for subsequent immunohistochemistry and immunofluorescence procedures. Cryo-sectioned tissue was mounted onto positively charged glass slides (SuperFrost© Plus, VWR International, Pennsylvania, USA).

Importantly, in later immunofluorescence experiments, on hippocampal adult neurogenesis specifically, tissue was collected and processed using a different technique. Mice (8–12-week-old WT and *mdx*) were anaesthetised with isoflurane (5% in oxygen) and then were perfused with approximately 15ml intracardiac saline (Sigma-Aldrich, Missouri, USA), followed by approximately 15ml formalin (Sigma-Aldrich, Missouri, USA). Whole brains were excised from the skull and post fixed in formalin (Sigma-Aldrich, Missouri, USA) for 72 hours then cryo-protected by immersing in a 30% sucrose solution (Sigma-Aldrich, Missouri, USA) made up in 0.1mM Phosphate Buffered Saline (PBS, See Table 2.3: reagent setup). Samples were frozen in isopentane and stored at -80°C until cryo-sectioned (CM1850, Leica, Germany) in OCT embedding medium (Thermofisher Scientific, Massachusetts, USA) in 20µm sections for subsequent immunohistochemistry and immunofluorescence procedures. Cryo-sectioned tissue was again mounted onto positively charged glass slides (SuperFrost© Plus, VWR International, Pennsylvania, USA).

Table 2.3: Reagent set up for immunocytochemistry/immunohistochemistry

Phosphate Buffered Saline (PBS)	**Composition (mM)**	**Source**
NaCl	137	Sigma-Aldrich
KCl	2.7	Sigma-Aldrich
NA_2HPO_4	10	Sigma-Aldrich
KH_2PO_4	1.8	Sigma-Aldrich

2.3. Immunocytochemistry techniques

2.3.1 Immunofluorescent labelling of cultured hippocampal neurons

After 10-12 days in culture, culture medium was removed from the culture dish, and hippocampal cell cultures were washed with PBS and fixed in 4% paraformaldehyde (PFA – Sigma-Aldrich, Missouri, USA) for 90 min at 4°C. Subsequently, fixed samples were permeabilized with 0.1% Triton X-100 (Sigma-Aldrich, Missouri, USA) at room temperature for 5 min. Samples were then washed three times with PBS and blocked with 1% Donkey Serum (Sigma, Missouri, USA) for 1 hour at room temperature, which is essential for preventing non-specific binding of antibodies to tissue. Primary antibodies were diluted in PBS (see Table 2.4 for antibodies used in this thesis), and preparations were incubated with them for 2 hours at room temperature. After washing three times with PBS (5 mins per wash),

preparations were incubated with the appropriate secondary antibody (see Table 2.4) for 2 hours at room temperature. Finally, samples were washed with PBS three times (5 mins per wash) and the coverslips containing the fixed neurons were mounted onto a microscope glass slide (VWR International, Pennsylvania, USA) using Fluoroshield mounting medium with 4',6-diamidino-2-phenylindole (DAPI - Abcam, Cambridge, UK) which binds to adenine-thymine rich regions in the DNA in order to visualise nuclei of cells.

2.3.2. Immunofluorescent labelling of whole brain sections

After whole brain tissue cryo-sectioning, the tissue was permeabilized with 0.1% Triton X-100 (Sigma-Aldrich, Missouri, USA) at room temperature for 1 hour. Samples were then washed three times in PBS (3x 10 minutes) and blocked with 1% Donkey Serum (Sigma-Aldrich, Missouri, USA) for 2 hours at room temperature. Primary antibodies (Table 2.4) were diluted in PBS, and tissue incubated with them overnight at 4°C. After washing three times with PBS (3x 10 minutes), preparations were incubated with the appropriate secondary antibody (Table 2.4) for 2 hours at room temperature. Finally, samples were washed with PBS (3 x 10 minutes) and a glass coverslip (VWR, Pennsylvania, USA) mounted onto the slide with Fluoroshield mounting medium with DAPI (Abcam, Cambridge, UK). Donkey serum blocking was used for the following primary antibodies: Dystrophin, Synaptophysin, Dystrophin (MANDRA-1), IL-6 and IL-6Rα.

Alternatively, after whole brain tissue cryo-sectioning, a Blocking-Permeabilization Buffer, composed of 10% Foetal Bovine Serum (FBS), 1% BSA and 0.1% Triton X-100

(Sigma-Aldrich, Missouri, USA) in PBS, was used. Sectioned tissue was permeabilized and blocked with this Blocking-Permeabilisation Buffer for 1 hour at room temperature. Samples were then washed in PBS (3x 10 minutes). Primary antibodies (Table 2.4) were diluted in PBS, and tissue incubated with them overnight at 4°C. After washing once more with PBS (3x 10 minutes), preparations were incubated with the appropriate secondary antibody (Table 2.4) for 2 hours at room temperature. After a final wash with PBS (3 x 10 minutes), the tissue was mounted onto a glass slide with Fluoroshield mounting medium with DAPI (Abcam, Cambridge, UK) and coversliped (VWR, Pennsylvania, USA). FBS blocking was used on the following antibodies: doublecortin, $GABA_AR$, NeuN and GFAP.

Table 2.4: Antibodies used in this thesis

Primary Antibody	**Host**	**Dilution**	**Source**
pAb to Dystrophin	Rabbit	1:250	Abcam
mAb to Synaptophysin	Rabbit	1:100	Abcam
mAb to Dystrophin (MANDRA-1)	Mouse	1:100	Abcam
mAb to IL-6 (1)	Mouse	1:250	Santa Cruz Biotechnology
mAb to IL-6Rα (D-8)	Mouse	1:250	Santa Cruz Biotechnology
pAb to Doublecortin (DCX)	Rabbit	1:100	Invitrogen
mAb to $GABA_AR$	Mouse	1:100	Abcam

pAb to NeuN	Rabbit	1:100	Invitrogen
mAb to GFAP	Rabbit	1:100	Invitrogen
Secondary Antibody			
Rhodamine (TRITC)	Donkey anti-rabbit	1:250	Jackson Immuno-Research
Fluoroscein (FITC)	Goat anti-mouse	1:250	Jackson Immuno-Research
Alexa Flour AP 488	Goat anti-rabbit	1:250	Abcam

2.3.3 Confocal microscopy

Imaging of fluorescently-labelled proteins was carried out using a confocal microscope (Olympus Fluoview, FV10i). Laser and saturation settings were set for each immunofluorescently-labelled protein and kept consistent for all samples within a group.

2.3.4 Image Analysis

When imaging cultured hippocampal neurons, 3 individual fields were imaged at random across the coverslip of cultured hippocampal neurons. Hippocampal neurons from at least three different cultures from each group (*e.g.,* WT and *mdx*) were compared for each experiment.

When imaging the different regions of the hippocampus, namely CA1, CA3 and DG (Figure below 2.2), three individual fields were imaged in each region for an appropriate overview. Hippocampal tissue from at least three different animals from each group (*e.g.,* WT and *mdx*) were compared for each experiment.

Depending on the staining being visualised and assessed, different techniques were applied using Image J. Mean fluorescence intensity (minus background) was assessed in a region of a specified area for the expression of dystrophin, IL-6 and IL-6R. For other antibodies, such as doublecortin (DCX), Neuronal nuclear protein (NeuN), Glial fibrillary acidic protein (GFAP) and γ-aminobutyric acid type A receptors ($GABA_AR$), the number of cells in the granule cell layer and/or hilus in the DG expressing each protein was counted (see Figure 2.3 below). Further explanation on analysis of each antibody is provided in the results.

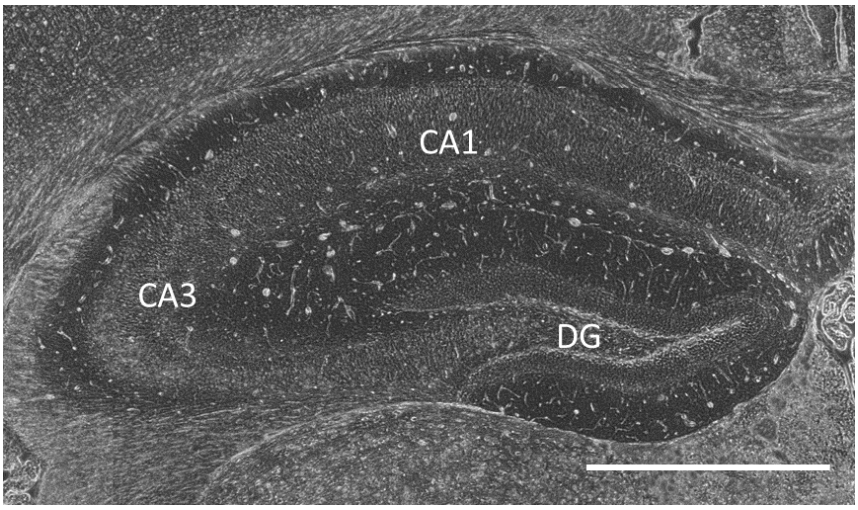


Figure 2.2: Brightfield image of the 3 regions of the hippocampus.

Confocal images were taken from 3 different regions of the hippocampus, namely CA1, CA3 and DG. Scalebars are 1mm.

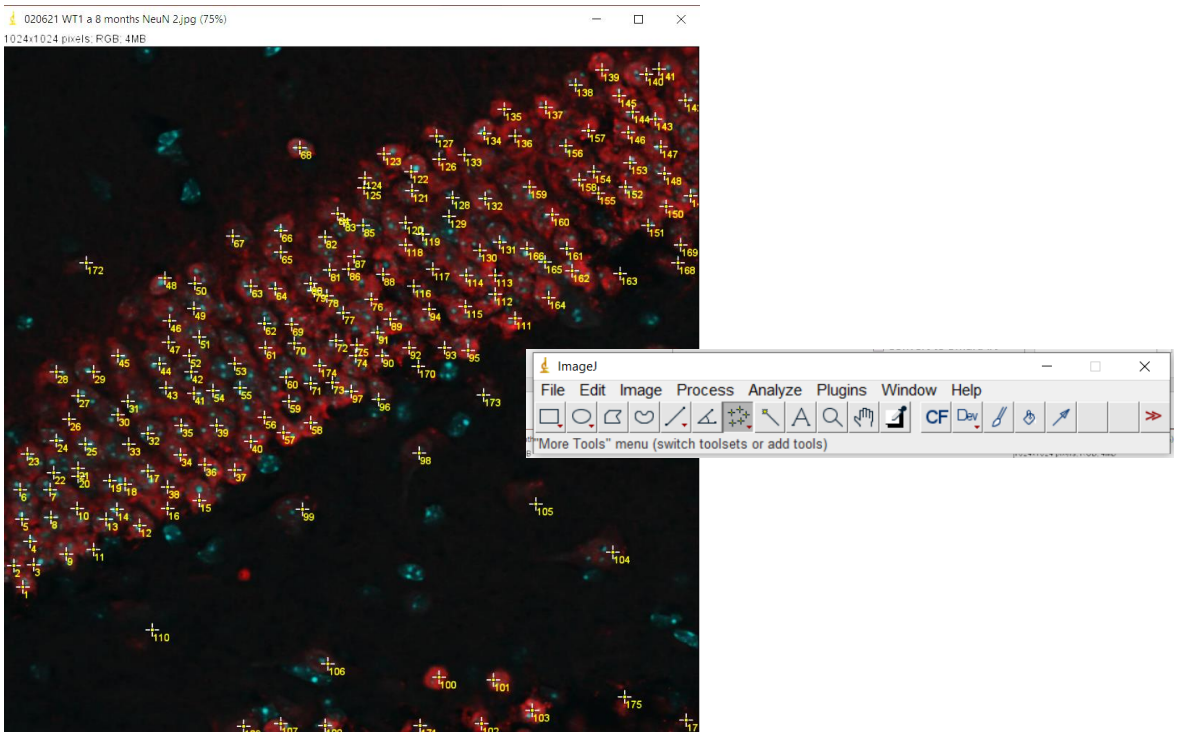


Figure 2.3: Representative image of analysis of whole brain sections for cell counting using Image J.

Image J was used as a tool for marking (white crosses) each neuron (NeuN, red stain) in order to count the number present in both the granule cell layer and hilus in the DG. DAPI (blue stain) showed nuclei of each cell.

2.4. Calcium imaging with cultured hippocampal neurons

2.4.1. Fluorescent calcium dye loading protocol.

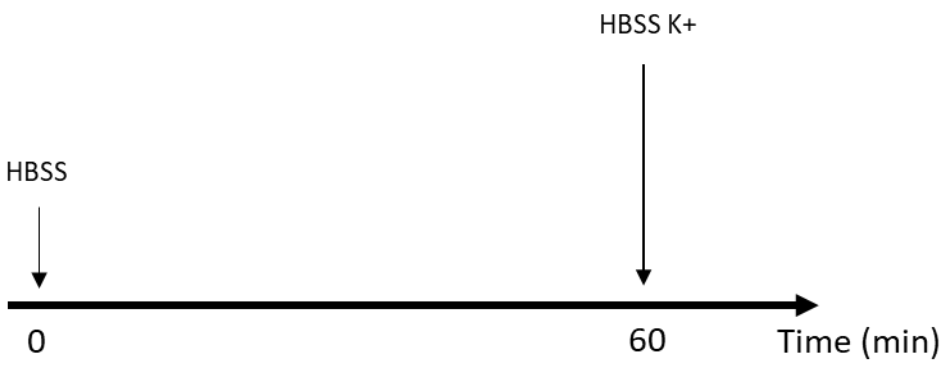
After 3-4 days incubation, intracellular calcium measurements from neuronal somata were conducted as previously described (Rae et al., 2000). Cultured

hippocampal neurons were preloaded with a single wavelength, intensity modulating calcium indicator, Fluo-2 AM (8µM dissolved in HBSS, Sigma-Aldrich, Missouri, USA), for 1 hour at room temperature in the dark. After that time, and prior to imaging the dye was washed off the neurons with HBSS.

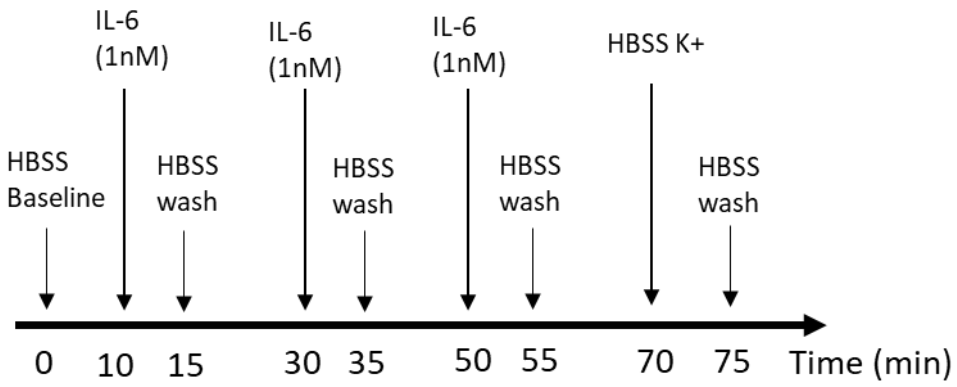
Coverslips upon which the neurons had been plated were then placed into a recording chamber and placed in the light path of an upright microscope (Olympus BX50 WI) in a dark room and superfused with HBSS alone or in the presence of drugs as appropriate (see section 2.4.2 below for experimental design). Initially, normal white light was used to find the appropriate field of view of neurons on the coverslips with a bright light source (Olympus TH4-200). At that point, the neurons were illuminated by a fluorescent light source monochromator (excitation at 488 nm, emission at 550 nm), generated by a monochromator (Cairn Technologies) and visualised with an integrating camera (Hamamatsu ORCA-ER), DAQ device (USB6229) and frame grabber, under both 20x and 40x magnification, as appropriate.

2.4.2 Experimental design

1. HBSS Spontaneous activity



2. IL-6 (1nM)



Images were acquired at one-second intervals using the open-source imaging software, Winfluor (John Dempster, University of Strathclyde, Scotland). Data files with time (seconds) *vs* fluorescence values (arbitrary units) for each region of interest (ROI) were exported from Winfluor as standard text files. GraphPad Prism was then used to produce XY line graphs to analyse changes in intracellular calcium for each cell indicated by a ROI.

2.4.3 Analysis of calcium imaging data

For each identified neuron (identified by high K+ response after experiments), the frequency of peaks (number of peaks per minute) was determined in non-stimulated WT and *mdx* cultures.

In experiments where neurons were exposed to IL-6 (1nM, 5 minutes), the frequency of peaks during the stimulated period were compared to the frequency of peaks during baseline (HBSS only). WT cultures were compared to *mdx* cultured neurons.

2.5. Gene Expression

Hippocampi from *mdx* and WT (8-12 week) whole brains were bisected from each hemisphere and stored in RNALater (Thermofisher Scientific, Massachusetts, USA) for 24-48 hours. Hippocampi were then flash frozen in liquid nitrogen and stored at -80°C.

2.5.1. RNA Extraction and Preparation

Total RNA was extracted from hippocampi (10 WT and 10 *mdx*) by homogenization using a glass tissue grinder (Dounce tissue grinder, 1ml) in the presence of Tripure Isolation Reagent (Roche Diagnostics Ltd., UK). This was followed by a series of chloroform (Sigma-Aldrich, Missouri, USA) and iso-propanol (Sigma-Aldrich, Missouri, USA) steps, as well as 3 centrifugation steps (Figure 2.4 below). The quantity as well as purity of the RNA was then assessed by spectrophotometry using a Nanodrop 1000 (Thermofisher Scientific, Massachusetts, USA). The quality of the RNA was assessed using an agarose gel electrophoresis system (E-Gel© X, Invitrogen, California, USA), with the subsequent visualisation of clear 18S and 28S ribosomal RNA bands used to confirm that there was no degradation of the sample during the extraction process (Figure 2.5). For mammalian RNA, a 28S:18S RNA ratio of 2:1 is generally representative of good-quality RNA.

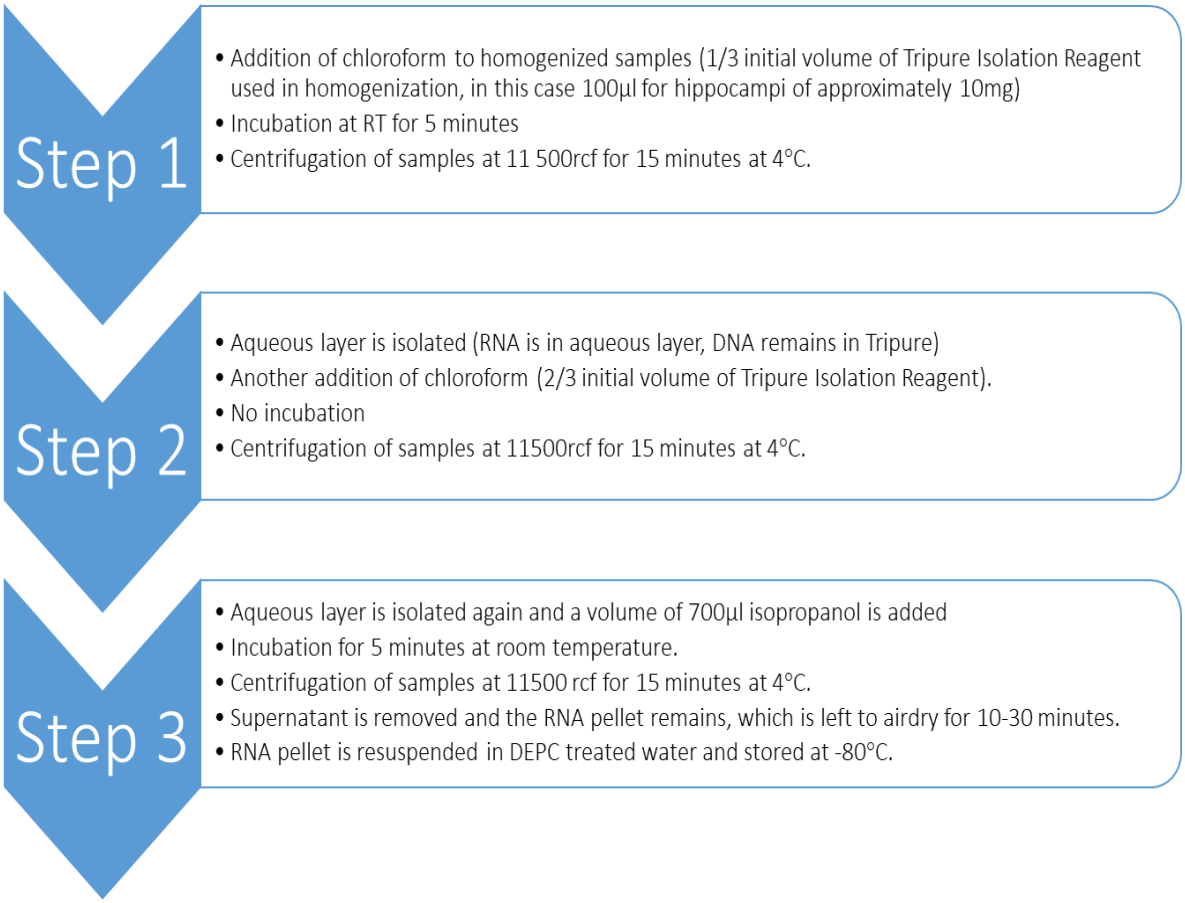


Figure 2.4: Flow diagram displaying the steps involved in RNA extraction from hippocampal tissue.

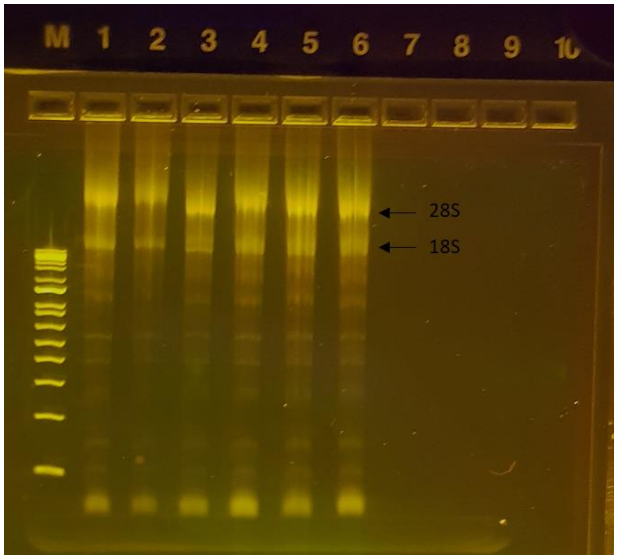


Figure 2.5: RNA analysis using agarose gel electrophoresis.

The bands indicated on the gel show distinct 28S and 18S bands which indicates that there was no degradation of the sample.

2.5.2. Reverse Transcription of RNA

RNA from hippocampal tissue was reverse transcribed using Transcriptor First Strand cDNA Synthesis Kit (Roche Diagnostics Ltd., UK). The following steps were followed:

- After the total mRNA was determined from the Nanodrop 1000 (Thermofisher Scientific, Massachusetts, USA), the sample was diluted in Diethyl pyrocarbonate (DEPC) treated water to a final concentration of 200ng.
- A template-primer mix was made up of 1µg total RNA, anchored-oligo$(dT)_{18}$ primer (50pmol/µl – with a final concentration of 2.5µM), random hexamer

primer (600 pmol/µl – with a final concentration of 60µM) and DEPC-treated water.

- The remaining components of the reverse transcription (RT) mix are added which contained Transcriptor Reverse Transcriptase Reaction Buffer (8mM $MgCl_2$), protector RNAse inhibitor (20U/µl), a deoxynucleotide mix (10mM – with a final conc. 1mM) and a Transcriptor Reverse Transcriptase (20 U/µl – final concentration of 10 U).
- The RT reaction was then incubated for 10min at 25°C, followed by 30min at 55°C and 5min at 85°C.

2.5.3. qRT-PCR

cDNA was amplified using Realtime ready Catalog or Designer Assays (Roche Diagnostics Ltd., UK) (as described above) and Fast Start Essential DNA Probe Master (Roche Diagnostics Ltd., UK) in 20 µl reactions (5 µl cDNA and 15 µl master mix) using the LightCycler 96 (Roche Diagnostics Ltd., UK) on 96-well plates. All reactions were performed in duplicate and reverse transcriptase negatives, RNA negatives, and cDNA negatives (with no template), and plate calibrator controls were used on every plate (an example of this template is shown in figure 2.6 below). Hippocampal gene expression was normalized to a reference gene, HPRT1, to compensate for variations in input amounts of RNA/cDNA and the efficiency of reverse transcription. The relative expression of genes was calculated using the ΔΔCT method, i.e., normalized expression of the gene of interest to that of the

reference gene, with changes in expression displayed as a fold change relative to the control group.

LightCycler® 96

Experiment: kim stephenson il6st 060421.lc96p Plate Id: <None>

*	1	2	3	4	5	6	7	8	9	10	11	12
A	U mdx 1 gp130	U mdx 2 gp130	U mdx 3 gp130	U mdx 4 gp130	U mdx 5 gp130	U mdx 7 gp130	U mdx 10 gp130	U mdx 11 gp130	U mdx 12 gp130	U mdx 13 gp130	- NTC None	- NTC None
B	U mdx 1 gp130	U mdx 2 gp130	U mdx 3 gp130	U mdx 4 gp130	U mdx 5 gp130	U mdx 7 gp130	U mdx 10 gp130	U mdx 11 gp130	U mdx 12 gp130	U mdx 13 gp130	- RNA NEG None	- RNA NEG None
C	U WT 1 gp130	U WT 3 gp130	U WT 5 gp130	U WT 7 gp130	U WT 9 gp130	U WT 12 gp130	U WT 13 gp130	U WT 16 gp130	U WT 15 gp130	U WT 14 gp130	-- RT NEG HPRT	-- RT NEG HPRT
D	U WT 1 gp130	U WT 3 gp130	U WT 5 gp130	U WT 7 gp130	U WT 9 gp130	U WT 12 gp130	U WT 13 gp130	U WT 16 gp130	U WT 15 gp130	U WT 14 gp130	+ Cal HPRT	+ Cal HPRT
E	U mdx 1 HPRT	U mdx 2 HPRT	U mdx 3 HPRT	U mdx 4 HPRT	U mdx 5 HPRT	U mdx 7 HPRT	U mdx 10 HPRT	U mdx 11 HPRT	U mdx 12 HPRT	U mdx 13 HPRT	-- RT NEG gp130	-- RT NEG gp130
F	U mdx 1 HPRT	U mdx 2 HPRT	U mdx 3 HPRT	U mdx 4 HPRT	U mdx 5 HPRT	U mdx 7 HPRT	U mdx 10 HPRT	U mdx 11 HPRT	U mdx 12 HPRT	U mdx 13 HPRT		
G	U WT 1 HPRT	U WT 3 HPRT	U WT 5 HPRT	U WT 7 HPRT	U WT 9 HPRT	U WT 12 HPRT	U WT 13 HPRT	U WT 16 HPRT	U WT 15 HPRT	U WT 14 HPRT		
H	U WT 1 HPRT	U WT 3 HPRT	U WT 5 HPRT	U WT 7 HPRT	U WT 9 HPRT	U WT 12 HPRT	U WT 13 HPRT	U WT 16 HPRT	U WT 15 HPRT	U WT 14 HPRT		

Figure 2.6: Template used for all qRT-PCR reactions. Half the plate (Rows A to D, column 1 to 10) are dedicated to samples and the probe of interest (in this case, IL-6st) and the other half is dedicated to the reference housekeeping gene (which was HPRT, and was included in all probe runs). Column 11 and 12 are dedicated to reverse transcriptase negatives for both the reference gene and target gene, RNA negatives, and cDNA negatives (with no template), and plate calibrator controls.

2.6. Immunoassay for protein quantification

2.6.1. Animals

WT and *mdx* mice were euthanised by cervical dislocation and decapitation at 8-12 weeks, with whole brains removed from the skull. Hippocampi were then excised from each hemisphere and immediately flash frozen in liquid nitrogen and stored at -80°C.

2.6.2. Protein Extraction and Quantification

Protein was extracted from one hippocampi from each sample (10 WT and 10 *mdx*) by homogenisation using a glass tissue grinder (Dounce, 1ml tissue grinder) in 500 µl lysis buffer (Table 2.5 below) made up with Tris-HCL (10mM, pH7.0), 0.5% Triton X-100 (Sigma-Aldrich, Missouri, USA) as well as cOmplete™, Mini, EDTA-free Protease Inhibitor Cocktail (Roche Diagnostics Ltd., UK). Samples were then centrifuged at 10,000 rpm for 10 minutes at 4˚C. Aliquots of the supernatant were then stored at -80˚C to limit freeze thaw cycles.

2.6.3. Bradford Protein Assay

Bradford reagent (Sigma-Aldrich, Missouri, USA) was used to quantify the concentration of protein in each sample. Bradford protein quantification is a colorimetric assay which measures the shift in absorbance of Commasie Brilliant Blue G-250 (Bradford 1976). Using a standard curve of known protein concentration of bovine serum albumin (BSA, Sigma-Aldrich, Missouri, USA), with concentration

standards ranging from 0mg/ml to 1.5mg/ml, the concentration of the unknown samples was determined. Samples were diluted with Tris-HCL (10mM, pH7.0, Sigma-Aldrich, Missouri, USA) in a 1:4 dilution. Absorbance was read at 595nm on a spectrophotometer (Molecular Devices, SpectraMax M3, USA) and the concentration of protein was determined using SoftMax Pro 6 software package.

Table 2.5: Lysis Buffer Recipe.

Reagent	Composition	Source
Tris- HCL (10 mM, pH7.0)	1M Tris-HCL	Sigma
Triton X-100	0.5%	Sigma
cOmplete™, Mini, EDTA-free Protease Inhibitor Cocktail	1 tablet per 10ml	Roche Diagnostics Ltd., UK

2.6.4. Enzyme Linked Immunosorbent Assay (ELISA)

An ELISA was performed using the LEGEND MAX™ Mouse IL-6 ELISA Kit (BioLegend, San Diego, USA) (see Figure 2.7 below), on WT and *mdx* hippocampi samples of known total protein concentration after completion of a Bradford protein assay (as described above). A standard curve was prepared using serial dilutions of standard IL-6 protein supplied with the kit (0 pg/ml, assay diluent as blank, to 500pg/ml).

The ELISA plate was read at 570nm and 450nm using a multi well spectrophotometer (Molecular Devices, SpectraMax M3, USA). The standard curve

was generated using GraphPad Prism software and each sample concentration was calculated from it.

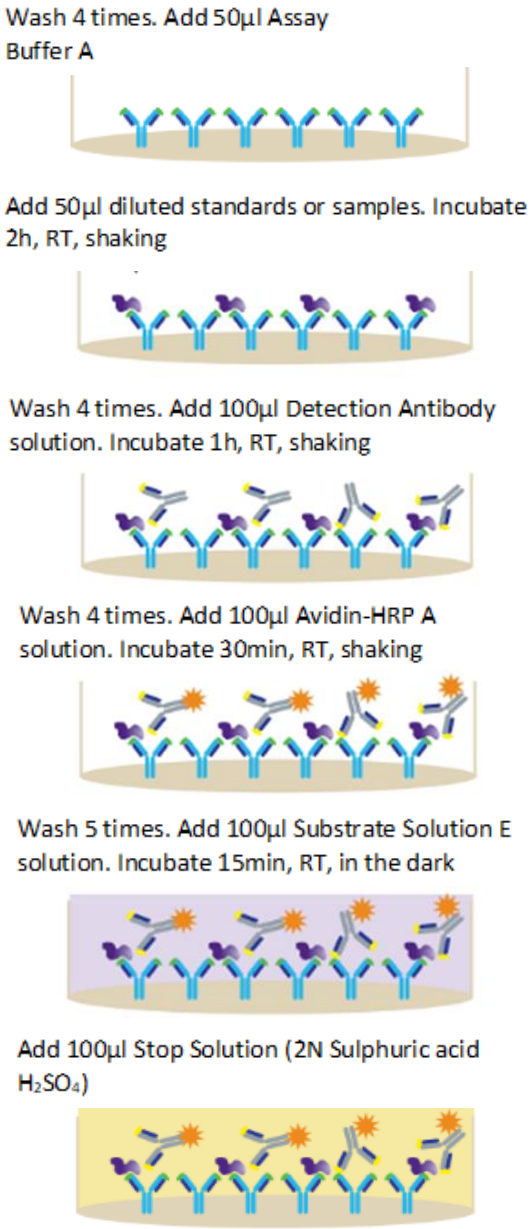


Figure 2.7: ELISA protocol followed using the LEGEND MAX™ Mouse IL-6 ELISA Kit.

2.7. Behavioural tests

2.7.1. Animals

Behavioural experiments were carried out on 8–12-week-old WT and *mdx* mice.

All behavioural experiments were carried out between 8:30-14:00 and room temperature and humidity were maintained at 22±1°C and 57±2%, respectively, throughout.

Mice were handled for 4 days prior to the start of trials in order to habituate them to any handling that may have occurred during the behavioural test phase. This type of handling involved picking up the mice 10 times on each day of handling and letting them walk along the experimenter's sleeve each time. Mice were also moved from the holding room to the testing room an hour before the start of each trial in order to habituate them to the room.

2.7.2. Novel Object Recognition (NOR) Test

NOR tests are used to test a rodent's ability to recognise a previously presented object or stimulus (Ennaceur & Delacour, 1988) and as such, are used to assess recognition memory. NOR tests were carried out in an open field arena (30cm x 30cm x 30cm) under a light intensity of approximately 15 Lux. Firstly, mice were allowed to habituate to the open field arena without any objects for 10 minutes. The arena was then wiped down with 70% ethanol after each mouse to remove any olfactory cues. Trial 1 (training phase) took place 24 hours after the open field habituation, where mice were exposed to two identical objects (200ml purple plastic bottles filled with

water; figure 2.8 below) for 10 minutes. Trial 2 took place 24 hours later, where one object was exchanged for a novel object (a 200ml flat bottomed rectangular flask partially filled with blue dye; figure 2.7 below). Exploration of an object included directing the snout at a distance less than 1cm to the object, sniffing or touching it with the snout, plus leaning on the object while sniffing or touching it with the snout. In contrast, turning or running around the object, or climbing or sitting on the object was not considered as exploration. Mouse activity was recorded on a camera (Akaso EK7000, 4K camera) placed 50cm directly above the open field area and behaviour was analysed at a later time point by two researchers, blinded to the groups. The objects were unable to be displaced by the mouse and were wiped down thoroughly with 70% ethanol after each trial to ensure that no olfactory cues remained.

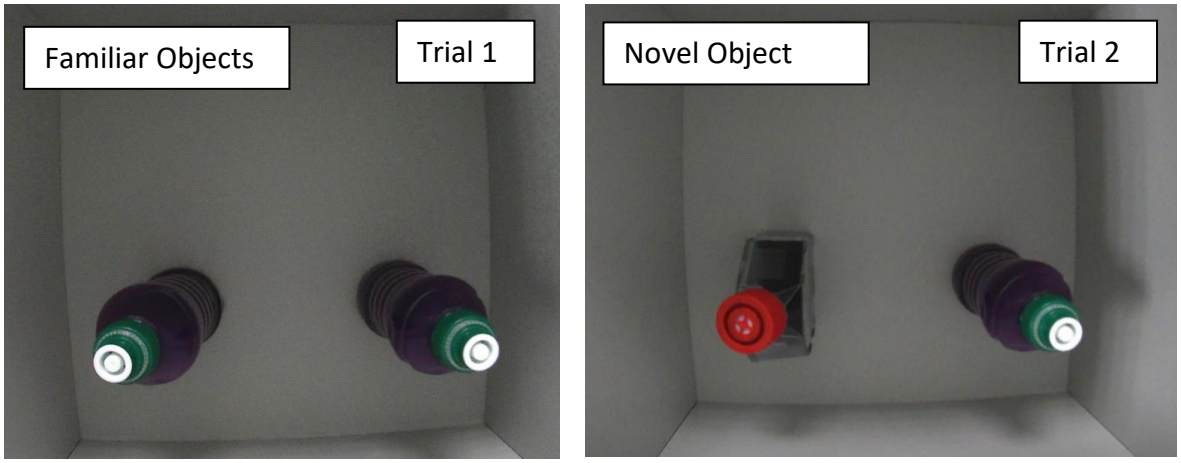


Figure 2.8: Novel Object Recognition test setup. The familiar objects used were two purple plastic bottles, filled with water (left image). The novel object, used in trial 2, was a 200ml flat bottomed rectangular flask partially filled with blue dye (right image)

The percent of time spent exploring the novel object relative to the total time spent exploring both objects can be a measure of novel object recognition (Benice *et al.*, 2006; Sarkisyan & Hedlund, 2009; Broadbent *et al.*, 2010; Oliveira *et al.*, 2010).

Thus, *Recognition Index* (RI), i.e., the time spent investigating the novel object relative to the novel object and the familiar object investigation [RI = T_N/ (T_N + T_F)] was used (Mumby *et al.*, 2002; Piterkin *et al.*, 2008; Botton *et al.*, 2010; Gaskin *et al.*, 2010; Schindler *et al.*, 2010). Overall, an exploration ratio of greater than 50% indicated that the mouse investigated the novel object more than the familiar object, which suggests a memory recall for the for the familiar object (Gareau et al., 2011).

Exclusion criteria (Lueptow, 2017):

- Mice were excluded from the study if the total exploration time (sum of both objects) was less than 20 seconds either on trial 1 or trial 2.
- During trial 1 (training phase), if mice had a less than 40%, or greater than 60%, exploration ratio (suggesting a bias towards one object) they were excluded from further analyses.

For these experiments, 5 *mdx* mice and 3 WT mice were excluded.

	Left Object Time Exploring (seconds)	Right Object Time Exploring (seconds)
***mdx* 19/034**	10,02	6,5
***mdx* 19/039**	5,17	9,42
***mdx* 19/040**	11,16	17,63
***mdx* 19/004**	3,89	6,16
***mdx* 19/022**	5,14	1,11
BL10 19/011	3,25	2,14
BL10 19/021	5,47	12,84
BL10 19/013	1,84	0,72

For the intervention experiments, 1 WT mouse was excluded.

BL10	8,7	8,4

2.7.3. Open field behavioural test

Mice were allowed to habituate to the open field arena for 10 minutes prior to NOR testing, with the mouse activity recorded (Akaso EK7000, 4K camera) placed 50cm directly above the open field area and behaviour was analysed at a later time point by two researchers, blinded to the groups. Between mice, the arena was wiped down with 70% ethanol after each mouse to remove any olfactory cues.

Importantly, this open field behavioural test was not set out as a separate experimental protocol, rather as an additional analysis to the data acquired in habituation in the NOR test.

The behaviours assessed were the following and can be visualised in figure 2.9 below:

a) Faecal output (number of boli)
b) Grooming (number of times the mouse scratched its face and fur with its forepaws)
c) Central area frequency (number of times the mouse had 4 paws in central area)
d) Freezing (number of times the mouse did not move for more than 2 seconds).
e) Rearing (number of times the mouse reared its front paws, against the wall or mid-air)
f) Jumping (number of times the mouse jumped against the wall, with all 4 paws in the air).

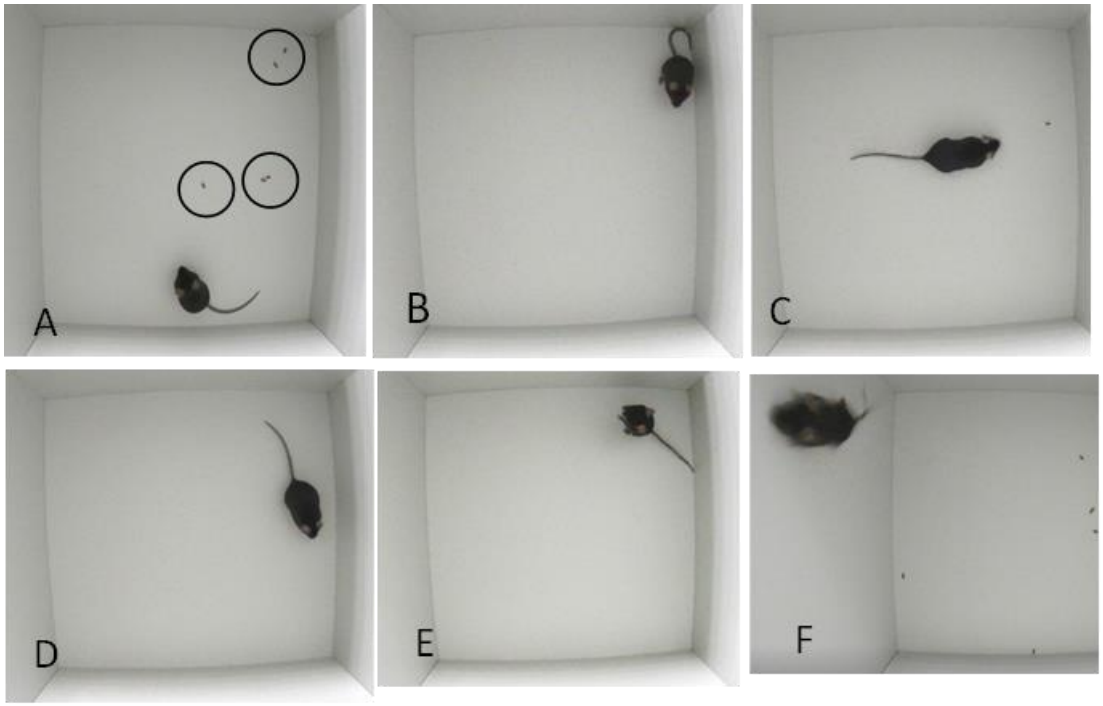


Figure 2.9: Representative images showing behaviours in the open field arena.

Number of boli, shown by black circles (A), grooming (B), central area frequency (C), freezing (D), rearing (E) and jumping (F).

2.8. Slice Electrophysiology

2.8.1. Preparing hippocampal slices

Male WT and *mdx* mice (8–12-week-old) were used for *ex vivo* extracellular electrophysiological studies.

Following decapitation, the brain was quickly removed from the skull and placed in a slush of frozen, carbogenated (95% O_2, 5% CO_2) cutting solution (CS – Table 2.6). Transverse slices of 300 µm thickness were sectioned using a vibrotome (5100mz, Campden Instruments Ltd., UK) in the same CS slush. Slices were then transferred

to a solution made up of 50:50 CS and artificial cerebrospinal fluid (ACSF – Table 2.7). After 30 minutes in this solution, slices were then transferred to 100% aCSF for at least 1 hour before recording, in order for the slices to stabilise in the artificial media. Throughout the slicing and recovery periods, the slices were constantly carbogenated (95% O_2, 5% CO_2) and maintained at room temperature (23-25°C). Importantly, the hippocampus was sliced in an orientation to display the dorsal portion of the hippocampus.

Table 2.6: Electrophysiology reagents – cutting solution recipe.

Cutting Solution	**Composition (mM)**	**Source**
Sucrose	100	Sigma-Aldrich
HEPES	20	Sigma-Aldrich
NaCl	50	Sigma-Aldrich
KCl	3	Sigma-Aldrich
NaH_2PO_4	1.25	Sigma-Aldrich
$NaHCO_3$	28	Sigma-Aldrich
$CaCl_2$	0.5	Sigma-Aldrich
$MgCl_2$	7	Fisher Scientific
D- Glucose	5	Fisher Scientific

Table 2.7: Electrophysiology reagents – aCSF recipe.

aCSF	**Composition (mM)**	**Source**
HEPES	20	Sigma-Aldrich
NaCl	125	Sigma-Aldrich

KCl	2.5	Sigma-Aldrich
NaH_2PO_4	1.25	Sigma-Aldrich
$NaHCO_3$	25	Sigma-Aldrich
$CaCl_2$	2	Sigma-Aldrich
$MgCl_2$	1	Fisher Scientific
D-Glucose	25	Fisher Scientific

2.8.2. Extracellular electrophysiological recording

After at least a 1-hour recovery period following slicing, hippocampal slices were transferred to a recording chamber, and secured in placed under a slice holder consisting of a grid of nylon threads within a circular metal frame (ALA Scientific Instruments, United States, see figure 2.10 below). The slices were continually superfused with oxygenated aCSF (2ml/min) through a feedback-controlled temperature regulator (ThermoClamp-1, Digitimer, UK) and kept at a constant 28°C for the duration of all experiments. Keeping the temperature stable at 28°C resulted in stability of recordings as well as the temperature in which we saw the largest EPSPs, whereas higher or lower temperatures resulted in fluctuation.

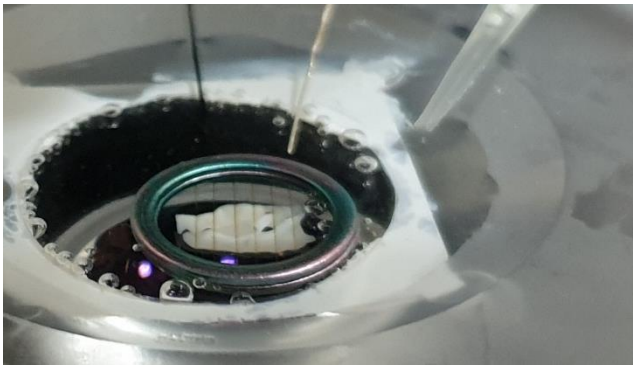


Figure 2.10: Recording chamber set up. Brain slices were secured in the recording bath by a slice holder.

2.8.3. Induction of LTP

An advantage of using the hippocampus for experimental procedures, is that is anatomically distinctive in that the cell layers in individual regions are conserved throughout. Thus, signalling pathways between the regions can be investigated in in a systematic manner between different slices. A bipolar stimulating electrode was used to stimulate axons of the Schaffer-collateral pathway (located between the CA3 region and CA1 region of the hippocampus; see figure 2.11) in order to evoke field excitatory postsynaptic potentials (fEPSPs) in the stratum radiatum of the CA1 region, which were recorded using an aCSF-filled, low resistance (2–5 MΩ), monopolar borosilicate glass electrode (premium thin wall borosilicate capillary glass with filament, Model G150TF-4, Multichannel systems, Germany). Once the evoked fEPSP amplitude had stabilised, a process that usually took approximately 1 hour, an input/output curve was generated by evoking fEPSPs at a frequency of 0.05Hz, whilst steadily increasing the stimulation current from a minimum of 0.11mA up to a maximum of 2mA. Three fEPSPs were recorded at each current, with the average slope value (mV/ms) of the three recordings used for analysis. Current stimulation intensity was then adjusted to evoke 50% of the maximal fEPSP response (as determined by the input/output curve) and a control 20-minute recording period initiated, with fEPSPs again evoked at 0.05Hz.

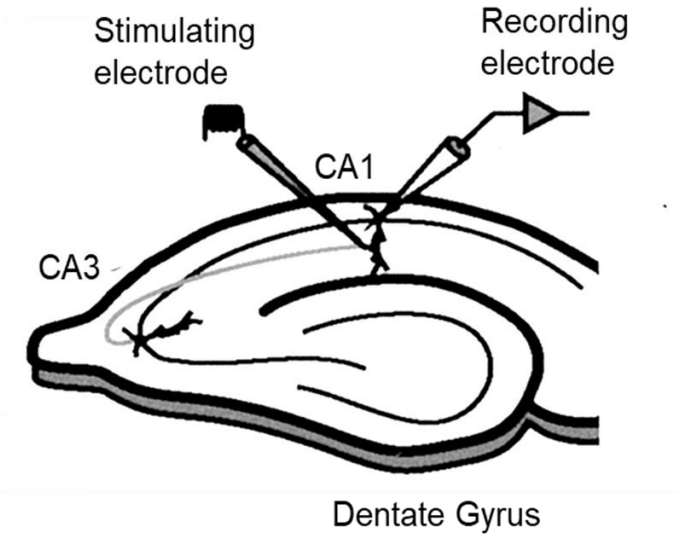


Figure 2.11: A schematic of the placement of the stimulation-recording path (Schaffer collateral-CA1 synapses) in the mouse hippocampus. A bipolar stimulation electrode (stimulating electrode) is placed in the Schaffer-collateral pathway, with responses recorded from the stratum radiatum of the CA1 region, using an aCSF-filled, low resistance (2–5 MΩ), monopolar borosilicate glass electrode (recording electrode).

After this control period, stimulation intensity was adjusted to evoke 30% of the maximal fEPSP response, and then four high frequency trains of stimuli (100Hz for 1 second, 60 second intervals) were applied to the slice. Stimulation intensity was then again returned to that required to evoke 50% of the maximal fEPSP response and evoked fEPSPs (0.05Hz) were recorded for at least a further hour. Each experiment was completed with the generation of a final input/output curve in an identical manner to that generated at the beginning of the protocol. Experiments were excluded from further analysis if the maximum fEPSP slope at the end of the experiment deviated by more than 0.5mV/ms of the control value, that experiment was excluded.

2.8.4. Analysis of electrophysiological recordings.

For analysis, fEPSP slopes were normalised to 100% with respect to the mean slope of the fEPSPs recorded during the 20-minute control period preceding induction of LTP. Post-high frequency stimulation, fEPSPs were normalised to the same baseline. (Figure 2.12: shows the manner in which fEPSP slopes were analysed).

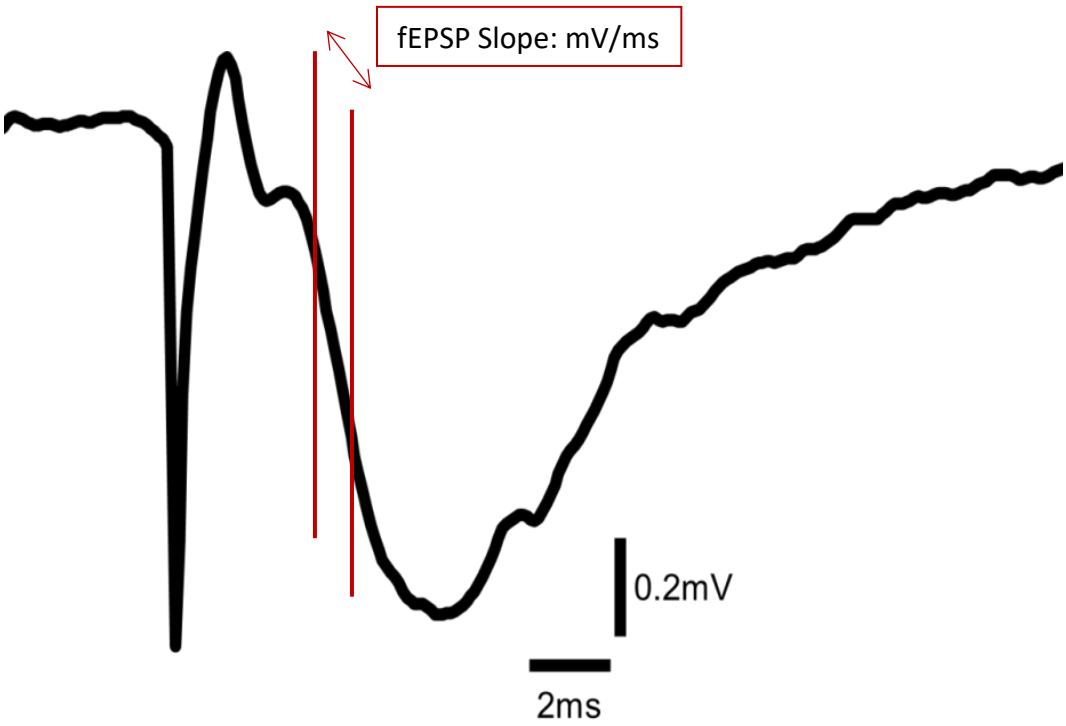


Figure 2.12: A representative trace of how the fEPSP slope (mV/ms) is analysed on each sweep and normalised to 100%.

2.9. Intervention Study

The intervention study included an intrathecal injection of xIL-6R or saline, NOR as well as LTP. The NOR and LTP protocols used were the same as those outlined in the control experiments described above.

2.9.1. Intrathecal Injection

Following the protocol described in Hylden *et al.* (1980), intrathecal injections were administered to male WT and *mdx* mice (8 – 12 weeks old) using disposable 30-gauge sterile BD Microlance™ Stainless Steel Needles (Becton Dickinson, New Jersey, USA) attached to a Hamilton™ 700 Microliter™ Syringe: Luer tip (Hamilton, Reno, USA).

Mice were anaesthetised with isoflurane (5% Isoflurane in oxygen, Harvard Apparatus), and the hair from the lower lumbar region removed. Each mouse was placed over a 50ml tube in order to expose the space between vertebrate. 70% ethanol and surgical Povidone-iodine were used to prepare the exposed area for injection. The mouse was then injected intrathecally into the subarachnoid space between L5 and L6 (Figure 2.13 below). The success of accurate spatial insertion of the needle into the subarachnoid space was confirmed by the observation of a tail flick from the anesthetised animal caused by the insertion of the needle into the correct area. A volume of 8µl of either xIL-6R antibody (made up in saline to 0.2mg/kg) or saline was injected. After injection, mice were placed into an animal holding chamber, where warm air was circulated (Thermacage, Datesand limited,

United Kingdom) at an even temperature (30°C) until they woke up from anaesthesia as providing thermal support to rodents following anaesthesia or a surgical procedure is an important intervention and is emphasised in the Guide for the Care and Use of Laboratory Animals *(National Research Council Committee for the Update of the Guide for the Care and Use of Laboratory, 2011)*. Mice were observed in order to confirm normal ambulation as incorrect injection into the spine can cause paralysis (which was an immediate humane endpoint following injection) and then placed back into their home cage for 24 hours before further experimentation (NOR and LTP).

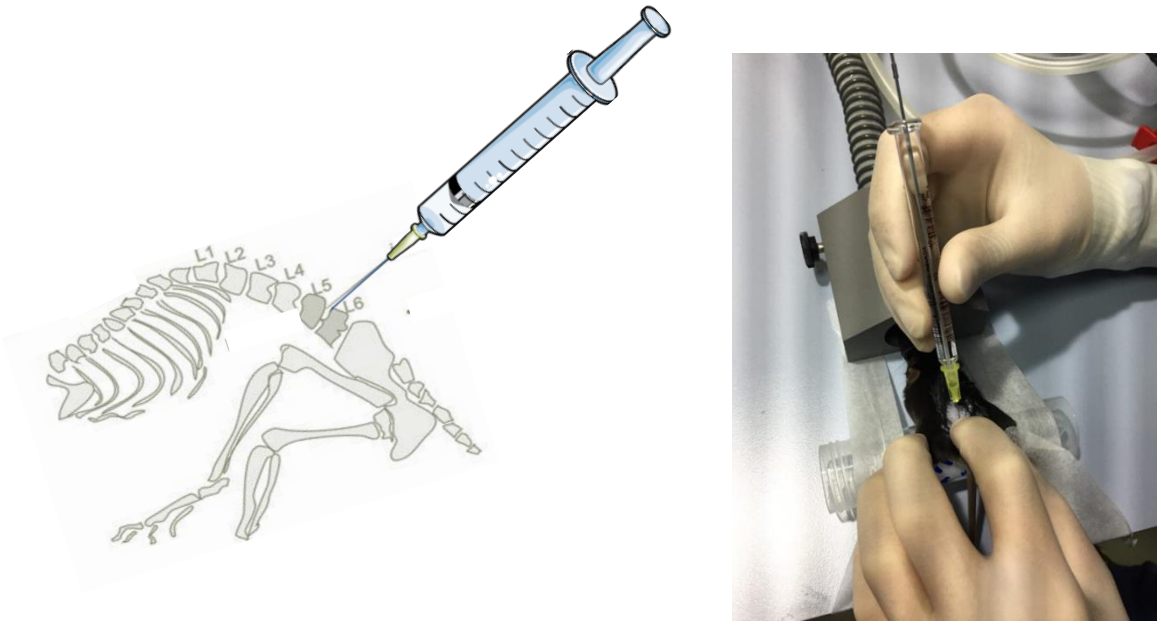


Figure 2.13: The schematic and photograph illustrate the procedure whereby an intrathecal injection was administered between the L5 and L6 vertebrates.

2.10. Statistical Analysis

Unless stated otherwise, GraphPad Prism Version 8.4.2 (GraphPad Software Inc., USA) was used for all statistical analyses. In addition, to test for normality and variance (Shapiro-Wilk test), unpaired or paired Student's t- tests were performed for comparisons between two groups with Welch's Correction or Mann-Whitney corrections, with one-way ANOVA or two-way ANOVA being performed for comparisons between multiple groups, unless stated otherwise. Appropriate *post-hoc* tests (*e.g.,* Bonferroni's test) were used for multiple comparisons. Statistical significance was accepted with p values < 0.05. Statistical significance is illustrated as $*p<0.05$, $**p<0.01$, $***p<0.001$, on graphs throughout. Data are expressed as mean ± SD.

2.11. Materials

Anti-IL-6 receptor antibody (MR16-1) used throughout this study was a kind gift from Chugai Pharmaceuticals Ltd., Tokyo, Japan. This monoclonal anti-IL-6 receptor antibody is referred to as xIL-6R through this thesis. All other reagents were purchased commercially from Sigma Aldrich, Fischer Scientific or as stated in the text.

Chapter 3: Dystrophin-deficient *mdx* mice exhibit deficits in molecular correlates of learning and memory.

3.1. Introduction

The *mdx* mouse is an animal model of DMD that mimics some aspects of the neurological and behavioural profile exhibited by individuals with the condition (Muntoni *et al.*, 1991; Chaussenot *et al.*, 2015), that are consistent with dysfunctions of the hippocampus and amygdala, such as a poor capacity to learn new tasks, and deficits in storing spatial memories as well as the processes generally involved in memory formation and consolidation (Vaillend *et al.*, 1995; Vaillend *et al.*, 2004; Chaussenot *et al.*, 2015). The hippocampus plays a central role in learning and memory (Anand & Dhikav, 2012) and is one of the regions where long term potentiation (LTP), proposed to be the molecular corelate of learning and memory (Bliss & Collingridge, 1993), occurs.

Interestingly, the literature has reported contradictory findings relating to LTP in *mdx* mice. For example, initial studies found no obvious deficits in hippocampal NMDA-dependent LTP or hippocampal-dependent spatial learning tasks in *mdx* mice that lacked Dp427 relative to controls (Sesay *et al.*, 1996), implying that hippocampal synaptic processes were intact within the *mdx* mouse. However, a later study by Vaillend *et al.* (2004) found that hippocampal-dependent LTP in *mdx* mice was in fact abnormally enhanced. This study also revealed deficits in long-term spatial memory and object recognition in *mdx* mice (Vaillend *et al.*, 2004). It has been suggested that one possible reason for the contrasting findings of Sesay *et al.* (1996) and Vaillend *et al*. (2004) may have been the particular training procedures utilised by Sesay *et al.* (1996) as they may have helped to alleviate any subtle memory deficits that were possibly present before training. Furthermore, Vaillend

et al. (2004) proposed that the abnormally enhanced hippocampal LTP observed in *mdx* mouse brain slices could, at least in part, be responsible for the memory deficits seen in these mice. Thus, somewhat counterintuitively, abnormally-enhanced synaptic potentiation and neuronal excitability might actually inhibit normal cognitive functioning (Vaillend *et al.*, 2004). Interestingly, a recent study by Bagdatlioglu *et al*., 2020, showed that hippocampal-dependent spatial learning and memory was decreased in *mdx* mice, particularly long-term memory, which progressively worsened with age (Bagdatlioglu *et al.*, 2020).

Neurogenesis, where progenitor cells differentiate into neurons, occurs in the dentate gyrus, with adult-born neurons being integrated into pre-existing neuronal circuits (Gage, 2000). Such integration of new cells into neuronal circuits is proposed to contribute to hippocampal-dependent learning and memory processes (Wu & Hen, 2014). The dentate gyrus is positioned as the input zone of the hippocampus and normally has low neuronal activity compared to upstream cortical areas (Treves & Rolls, 1994). One study has shown that a soluble mediator released from the muscle of *mdx* mice (nitrous oxide) can have an effect on hippocampal neurogenesis (Deng *et al.*, 2009). Also, this study found that the cognitive defects in DMD could result from the pathologically high number of immature neurons in the circuitry of the DG, which could disrupt the established circuitry (Deng *et al.*, 2009). Given the contradictory reports in the literature about the effect of loss of dystrophin on behaviour and the processes of learning and memory consolidation, it is apparent that further studies need to be conducted to establish the role of dystrophin in the dysfunction of hippocampal neural circuitry.

3.1.1. Study objectives

- To determine if cellular pathways involved in cognitive function are altered in the absence of dystrophin.
- To characterise behaviours in the *mdx* mouse model of DMD.
- To assess hippocampal adult neurogenesis in *mdx* mice aged 8 weeks, 4 months and 8 months compared to age-matched WT mice.

3.1.2. Animals

- *Mdx* mice aged 8-12 weeks were used in this study for electrophysiological and behavioural experiments with age-matched WT comparators.
- *Mdx* mice aged 8-weeks-old, 4 months and 8-months-old were used for immunofluorescence with age-matched WT comparators.

3.1.3. Techniques used

- Extracellular electrophysiology (more detail in methods section 2.8, pg. 74).
- Immunofluorescence on whole brain sections (see methods section 2.3.2, pg. 54).
- Novel Object Recognition test (see methods section 2.7.2, pg. 70)
- Open field behaviour (see methods section 2.7.3, pg. 73).
- Calcium imaging (see methods section 2.4. pg. 59).

3.2. Dystrophin is absent in all regions of the hippocampus in gthe *mdx* mouse.

Immunofluorescence labelling of the hippocampus of 8–12-week WT and *mdx* mice was carried out as described (see Methods section 2.3.2, pg. 39). A dystrophin polyclonal antibody was used for immunofluorescent labelling of this structural protein. Dystrophin is present in all 3 regions of the hippocampus investigated, namely CA1, CA3 and the dentate gyrus (DG) in WT mice with dystrophin present in the pyramidal cell layer of the CA1 and CA3 regions, the granule cell layer of the DG and in interneurons (indicated by white arrows in Figure 3.1). In contrast however, there was a complete absence of dystrophin labelling in any of the same regions in *mdx* mice (Figure 3.2). The appropriate positive controls and negative controls were also conducted to ensure that no random binding of either the primary or secondary antibody was occurring.

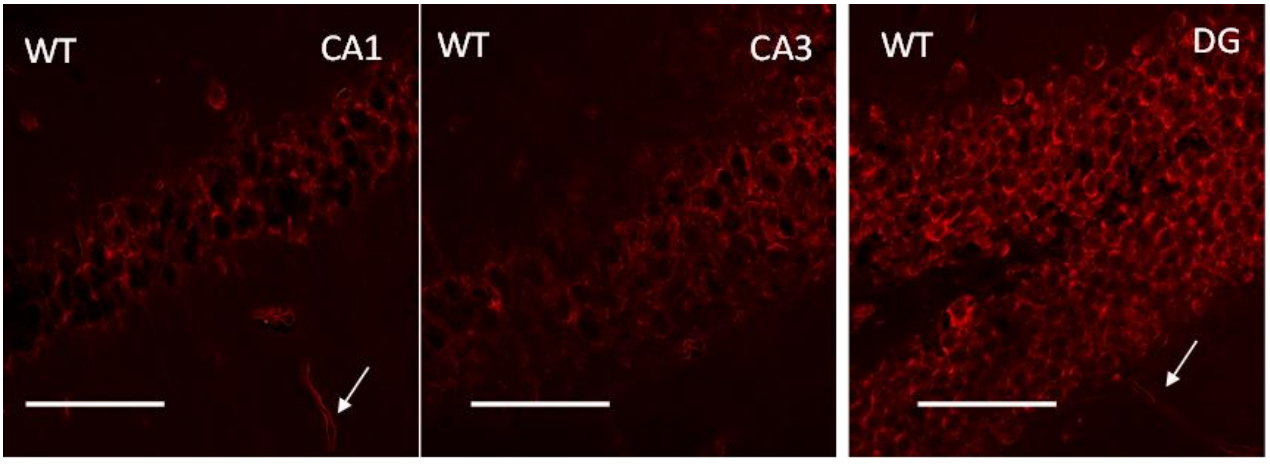


Figure 3.1: Immunofluorescent labelling of dystrophin in CA1, CA3 and DG regions of the hippocampus of WT mice. White arrows indicate interneurons. Scalebars = 70µm.

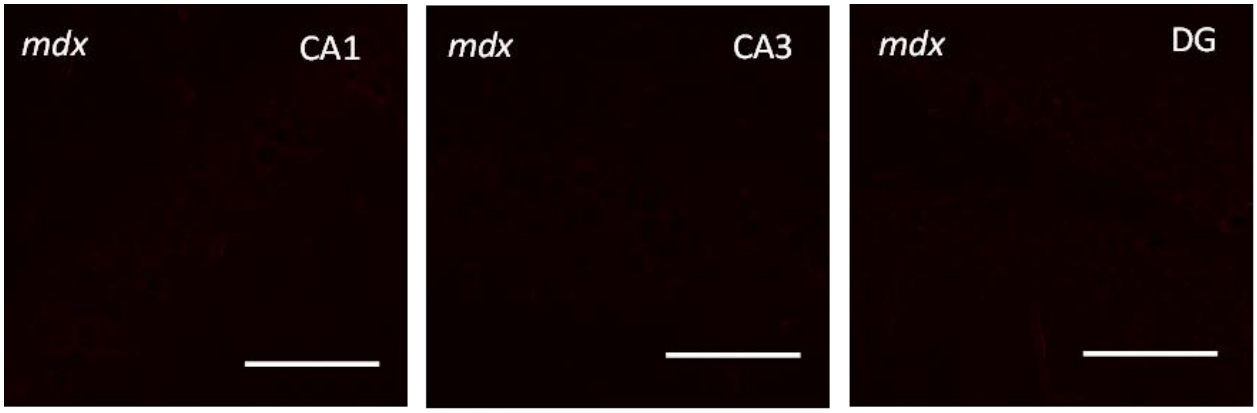


Figure 3.2: Immunofluorescent labelling of dystrophin in CA1, CA3 and DG regions of the hippocampus of mdx mice. Scalebars = 70µm

3.3. Hippocampal long-term potentiation (LTP) is reduced in dystrophin-deficient *mdx* mice.

Given the contradictory findings regarding the induction of LTP, the proposed molecular correlate of learning and memory formation, in *mdx* mice (Sesay *et al.*, 1996; Vaillend *et al.*, 2004), we investigated LTP induction in *mdx* mice and compared it to that induced in WT slices.

Field excitatory post-synaptic potentials (fEPSPs) generated by stimulating the Schäffer Collaterals (SC) running from area CA3 to synpases which terminate on the dendrites of CA1 neurons, which reside within the *stratum radiatum* above the hippocampal fissure (Malenka & Nicoll, 1999), were recorded from the CA1 region of the hippocampus.

Monopolar stimulation of SC fibres was performed by placing a stimulating electrode on the border between areas CA1 and CA3. First, input/output curves

were constructed from a range of stimulus intensities before the induction of LTP, to assess synaptic transmission and the relationship between excitatory input and firing efficiency (Figure 3.3). No significant difference was detected between the two genotypes (Two-way ANOVA, fEPSP slope: F (1, 8) = 0.2327, p=0.6425) under these basal conditions.

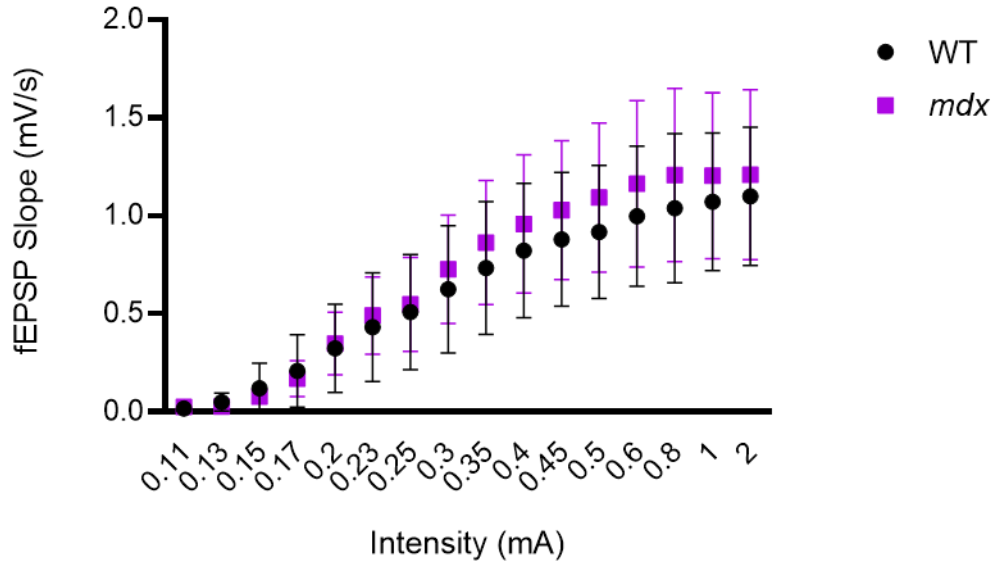


Figure 3.3: *Input/output curves constructed during baseline recordings. There is no difference between pooled baseline recordings in WT (n=6) and mdx mice (n=6). Mixed-effect analysis (p>0.05)*

Following stabilisation of the electrical recordings, which could take up to an hour, and generation of the baseline input/output curve, fEPSP baseline recordings were made for 20 minutes, stimulating every 30 seconds, using a current that induced fEPSPs that were 50% of the maximal size that could be generated. This recording period was followed by the application of four trains of high-frequency stimuli (HFS – 4 x 100 pulses, 100Hz for 1s/60s), with a current that induced fEPSPs that were 30% of the maximal size that could be generated. Immediately following the HFS

protocol, stimulation frequency and intensity was returned to baseline parameters, where we saw a dramatic increase in the slope (mV/ms) of the fEPSP for 5 minutes after HFS application. This increase in slope was observed in both WT (n=9) and *mdx* (n=6) mice. However, the mean size of the fEPSP slope was decreased in *mdx* mice compared to WT (WT 231 ± 34.63%*vs mdx* 167.8 ± 37.61%; *p*= 0.0052, figure 3.4b). Furthermore, for the entire duration of recording, 80 minutes, following HFS, LTP was significantly decreased in dystrophin-deficient *mdx* hippocampal slices (n=6) compared to that in slices from WT mice (n=9) (Genotype factor, F (1, 13) = 8,517, p= 0.0120, Interaction of time and genotype factors, F (179, 2327) = 1.370, p=0.0012, two-way repeated-measures ANOVA starting at 1 min after stimulation).

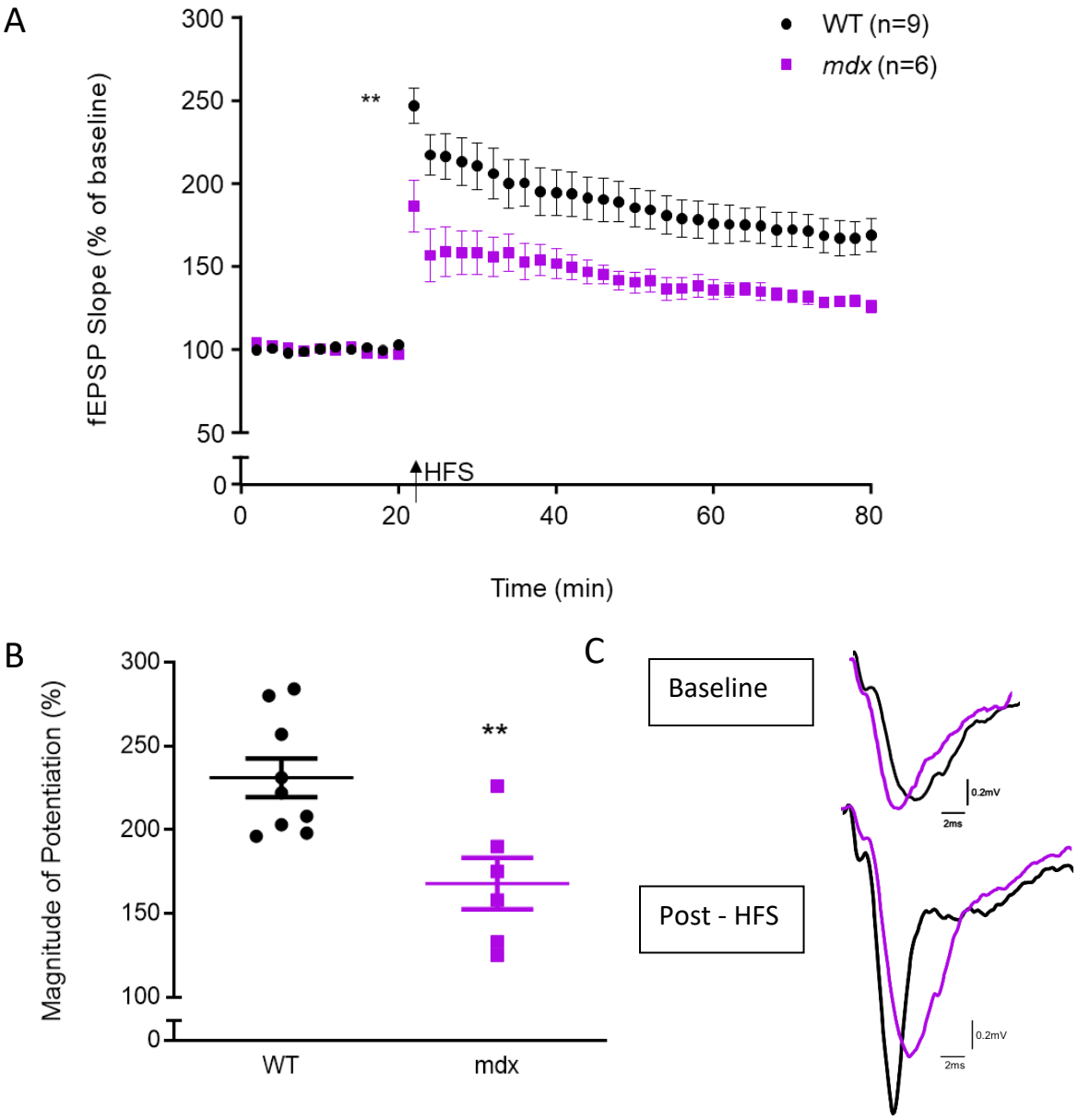


Figure 3.4: Long-term potentiation in the SC-CA1 pathway of the hippocampus is significantly decreased in mdx mice relative to WT mice.

- *A) Graph showing averaged time course of Schaffer collateral-evoked synaptic responses from WT (black circles) and mdx (purple squares) in the hippocampal region using extracellular field potential recordings in CA1 stratum radiatum (WT n=9, mdx n=6). Two-way ANOVA, p<0.01***
- *B) After high-frequency stimulation (HFS – 4 x 100 pulses, 100Hz for 1s/60s), the fEPSP slope in the mdx slices was significantly reduced compared to WT p=0.0012). Unpaired t test, p<0.01***
- *C) Representative traces show fEPSPs before and after high frequency stimulation to induce LTP in WT and mdx mice. At baseline, WT (black) and mdx (purple) fEPSP slopes (mV/ms) are similar, whereas, post-HFS, fEPSP slopes are significantly decreased in treated mdx mice.*

3.4. Recognition memory is not deficient in *mdx* mice.

To determine if the suppression of hippocampal LTP resulted in changes in memory formation in the *mdx* mice, we assessed WT and *mdx* mice using Novel Object Recognition (NOR) testing. NOR tests are used to assess recognition memory by testing a rodent's ability to recognize a previously presented object or stimulus (Ennaceur & Delacour, 1988). NOR uses two similar objects on a first testing day, and the mouse is left to explore for 10 minutes. 24 hours later, one of the similar objects is replaced with a novel object and once again the mouse is left to explore the area for 10 minutes. A percent of time spent exploring the novel object relative to the total time spent exploring both objects can be a measure of novel object recognition (Benice *et al.*, 2006; Sarkisyan & Hedlund, 2009; Broadbent *et al.*, 2010; Oliveira *et al.*, 2010). This concept can be represented by *Recognition Index* (RI), i.e., the time spent investigating the novel object relative to the total object investigation [RI = T_N/ (T_N + T_F)], and it is the main index of retention (Mumby *et al.*, 2002; Piterkin *et al.*, 2008; Botton *et al.*, 2010; Gaskin *et al.*, 2010; Schindler *et al.*, 2010). In our study however the RI was not significantly altered between WT (0.75 ± 0.02; n=14) and *mdx* (0.76 ± 0.01, n=14; p=0.7628) mice (figure 3.5).

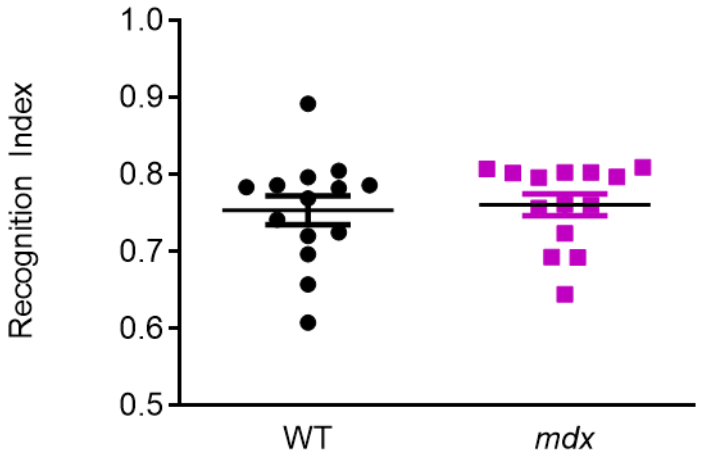


Figure 3.5: Recognition memory is not significantly different between WT and mdx mice.

The ratio of time spent exploring a novel object versus a familiar object (recognition index) was comparable in mdx mice and WT mice. Unpaired t test, p>0.05

3.5. Behavioural characteristics are altered in *mdx* mice relative to WT.

Even though recognition memory was not altered in *mdx* mice compared to controls, other behavioural and cognitive issues are also prevalent in individuals with DMD. For example, boys with DMD are commonly diagnosed with behavioural problems such as Attention-Deficit/Hyperactivity Disorder (ADHD), anxiety, depression, or other mood disorders (Hendriksen & Vles, 2008; Pane *et al.*, 2013a; Banihani *et al.*, 2015). We examined the *mdx* mouse model to determine if any behaviours related to these disorders were presented as part of the phenotype. Using a behavioural assay in an open field arena, we assessed *mdx* mice for central area frequency, freezing frequency, rearing frequency, jumping frequency, grooming frequency and faecal output (methods section 2.7.3, pg. 43).

Central area frequency is often used as a measure of anxiety in mice, such that the more time spent on the periphery of an open field, close to the walls, the more anxious the mouse (Holmes *et al.*, 2003). The central area frequency (number of times the mouse had 4 paws in central area) of *mdx* mice was comparable to WT (figure 3.6a, n=19, p=0.8186, WT 23.94 ± 6.847 vs *mdx* 23.37 ± 8.214).

Increased faecal output is also linked to increased anxiety (Hall, 1934), however, the faecal output (number of boli) in this study was comparable in *mdx* and WT mice (figure 3.6b, n=19, p=0.3431, WT 3.300 ± 2.536 vs *mdx* 2.632 ± 1.707).

Another measure of anxiety is freezing, which has been linked to fear conditioning (Blanchard & Blanchard, 1988). Interestingly, *mdx* mice displayed a significant increase in freezing frequency (number of times the mouse did not move for more than 2 seconds) in comparison to WT (figure 3.6c, WT 10.95 ± 4.839 vs *mdx* 13.89 ± 5.098; n=18, p=0.0383).

Rearing frequency (number of times the mouse reared its front paws, against the wall or mid-air) and jumping frequency (number of times the mouse jumped against the wall, with all 4 paws in the air) are related to exploratory and escape behaviours and was shown to be comparable between *mdx* and WT mice, - rearing frequency (figure 3.6d, n=17, p=0.2607, WT 88.56 ± 18.63 vs *mdx* 96.65 ± 23.08) and jumping frequency (figure 3.6e, n=18, p=0.1687, WT 0.8235 ± 1.334 vs *mdx* 1.722 ± 2.321).

Lastly, grooming frequency has been linked to autism spectrum disorder (ASD) as it is regarded as a repetitive behaviour (Silverman *et al.*, 2010), in *mdx* mice, the grooming frequency was comparable to WT mice (figure 3.6f, n=19, p=0.9108, WT 2.947 ± 1.224 vs *mdx* 2.889 ± 1.844)

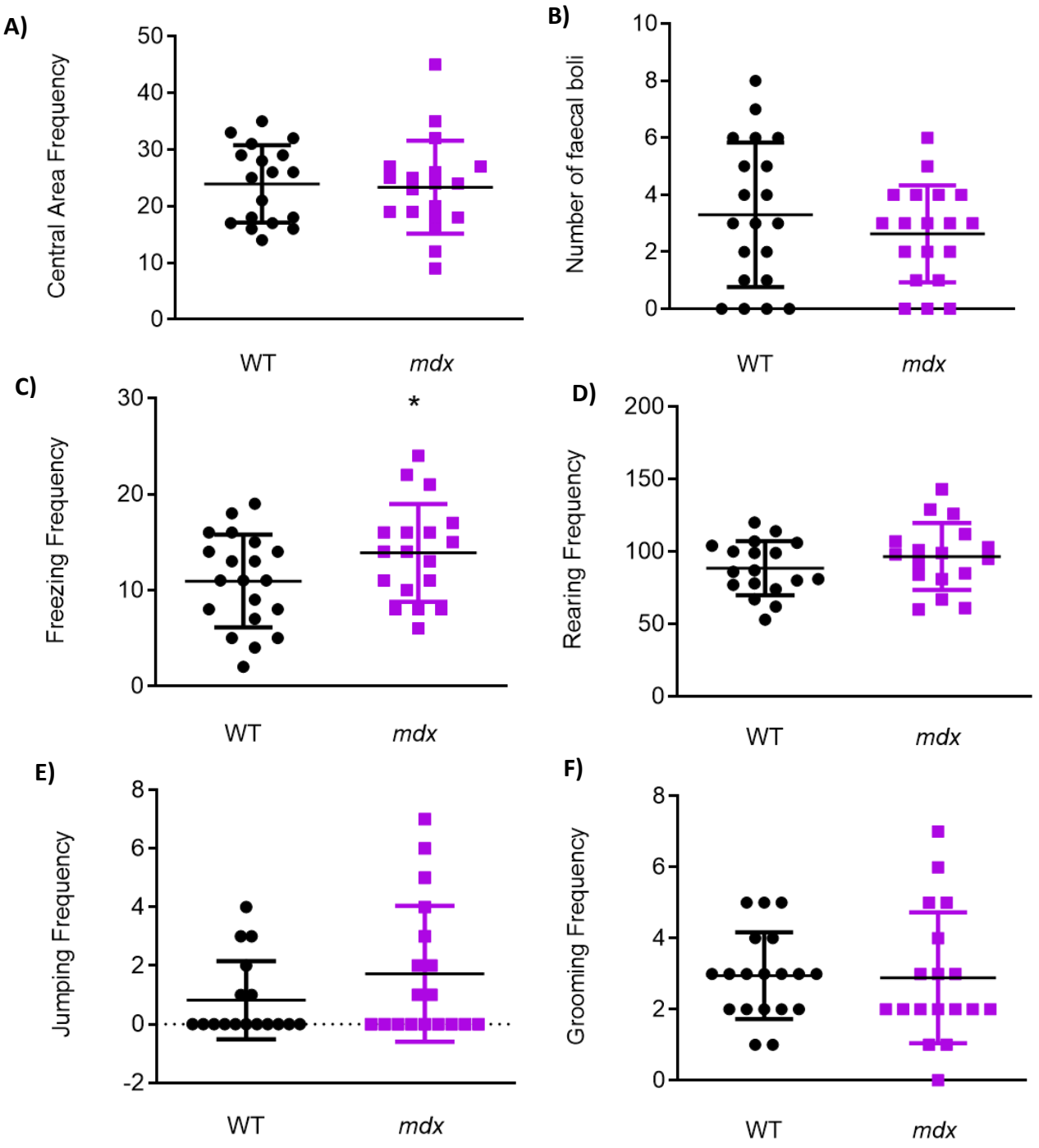


Figure 3.6: Behaviours of mdx and WT mice in an open field.

*The data plot illustrates that A) Central area frequency, where all four paws were in the central area of the open field arena, in mdx mice was similar to WT. B) Faecal output (number of boli) in mdx mice was similar to WT. C) Freezing frequency was significantly higher in mdx mice in comparison to WT. D) Rearing frequency in mdx mice was similar to WT. E) Jumping frequency was similar in mdx mice to WT. F) Frequency of grooming in mdx mice was similar to WT. Unpaired t test, $p<0.05$**

3.6. $GABA_A$ receptor expression in neurons in the dentate gyrus of *mdx* mice is similar to that in WT mice.

GABA has long been associated with mood disorders such as anxiety spectrum disorders (Nutt & Malizia, 2001; Lydiard, 2003; Hasler *et al.*, 2008) and depression (Gold *et al.*, 1980; Krystal *et al.*, 2002; Chang *et al.*, 2003).

Previous research has indicated that $GABA_A$ receptor clustering is aberrant in the absence of dystrophin (Vaillend *et al.*, 2010). The dentate gyrus in the hippocampus is one of two regions in the brain where neurogenesis occurs (Gage, 2000) and GABA is known to have a depolarizing effect on neural progenitor cells and immature neurons, both during developmental and adult neurogenesis (Ge *et al.*, 2006). As such, the dentate gyrus is a region of interest for any possible aberrant changes that could impact cognition. Using immunofluorescence, we examined $GABA_A$ receptor expression in whole brain sections, looking specifically at the dentate gyrus in the hippocampus of WT and *mdx* mice at 4 and 8 months of age (we chose these two different time points in order to determine if there are any progressive changes with age).

The number of $GABA_A$ receptor-positive neurons was counted in three different regions of the dentate gyrus in WT and *mdx* mice (n=3-4 animals), specifically within two random regions of the granule cell layer and hilus, which were then pooled for a total number of $GABA_A$ receptor-positive neurons in the dentate gyrus as a whole. The numbers of $GABA_A$ receptor positive neurons did not differ significantly between WT and *mdx* dentate gyrus in either of the two age groups (figure 3.7, Two-way ANOVA, n=3-5 animals per group, 2-3 whole brain sections per animal, 3

regions in the dentate gyrus, of the granule cell layer, $F(1, 10) = 0.08065$, $p=0.7822$), although this does not discount the fact that these neurons may be dysfunctional.

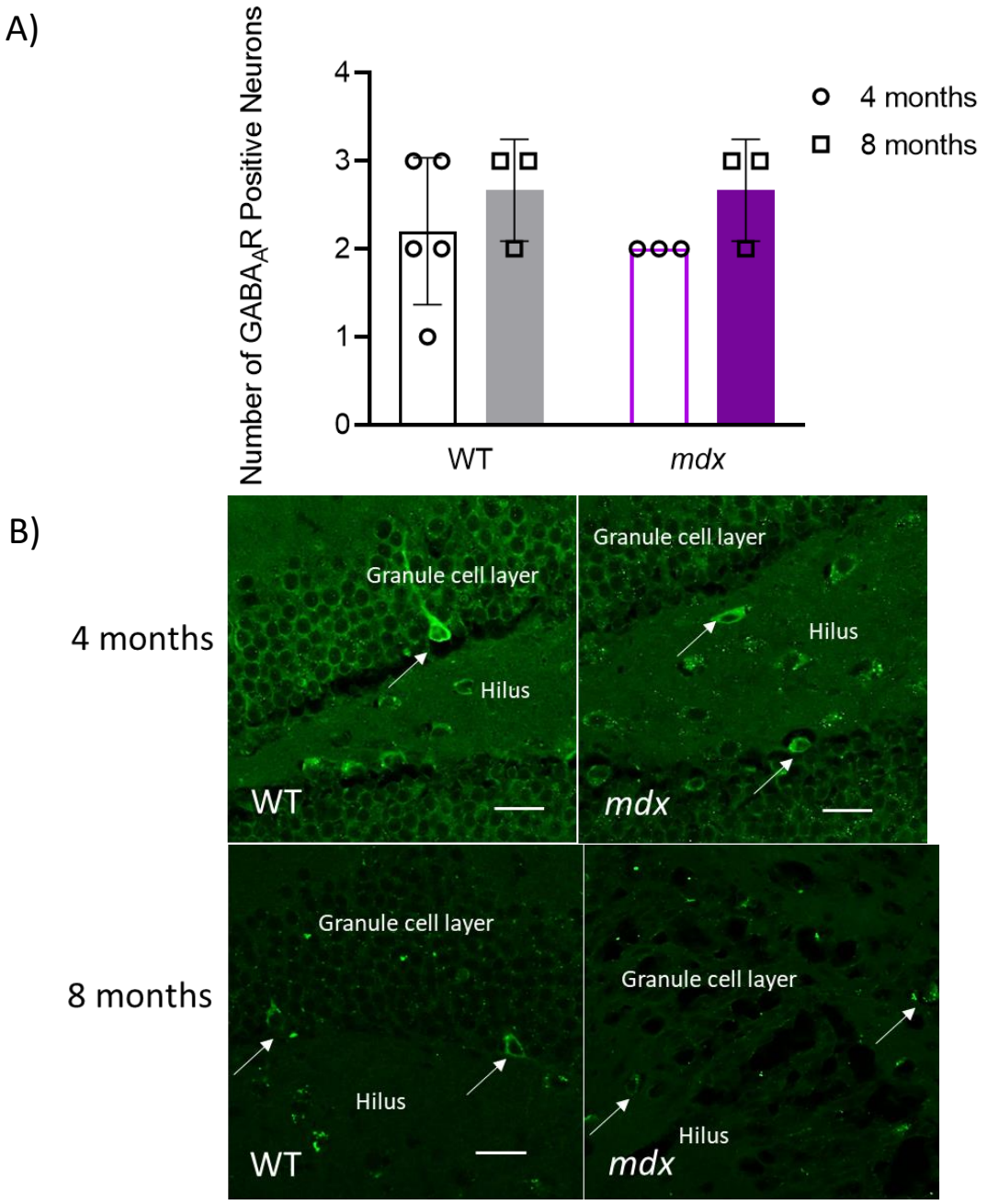


Figure 3.7: The number of GABA$_A$R positive neurons in the granule cell layer and hilus of the dentate gyrus of WT and mdx mice at two different ages (4 months and 8 months) is similar.

The number of GABA$_A$R-positive neurons did not differ significantly in the dentate gyrus of WT and mdx mice between the two age groups.

Representative immunofluorescence images of the number of GABA$_A$R positive neurons in WT and mdx mice at 4 and 8 months. GABA$_A$R-positive immunostaining is similar in WT and mdx mice at 4 and 8 months. Tissue was stained with a mouse GABA$_A$R primary antibody and a FITC (goat anti-mouse) secondary antibody. White arrows indicate GABA$_A$R-positive neurons in the granule cell layer and hilus in both WT and mdx. Scale bars are 30µm. Two-way ANOVA, p>0.05

3.7. Loss of dystrophin increases neuronal excitability in cultured hippocampal neurons

* *Experiments completed by Kimberley Stephenson and Michael Vaughan and data analysed by Claire Denley.*

Although we did not observe changes in the absolute number of GABA-expressing hippocampal interneurons in dystrophic tissue, aberrant $GABA_A$ receptor clustering (Vaillend *et al.*, 2010) could nonetheless have an impact on the neuroregulatory actions of GABAergic neurons (McCormick & Contreras, 2001; Saxena & Caroni, 2011). Using hippocampal neurons cultured (4-5 days) from neonatal mice (aged 3-5 days old), we next sought to examine basal neuronal activity by monitoring intracellular neuronal calcium levels. No apparent differences were observed in cell survival or network formation of hippocampal neurons cultured from WT and *mdx* mice (Figure 3.8). However, when we examined baseline cellular calcium levels, unstimulated *mdx* hippocampal neurons exhibited a significantly greater frequency of calcium peaks than observed in WT controls (Figure 3.9c, unpaired t test, WT 0.3234±0.1635; n=16 neurons vs *mdx* 0.7443±0.1797; n=19 neurons, $p<0.001$) over a period of 60 minutes (4000 seconds). This can be observed from the representative traces in figure 3.9, intracellular calcium activity in WT neurons (figure 3.9a) is almost non-existent in comparison to that observed in *mdx* neurons (figure 3.9b) indicating neuronal hyperexcitability in *mdx* neuronal cells.

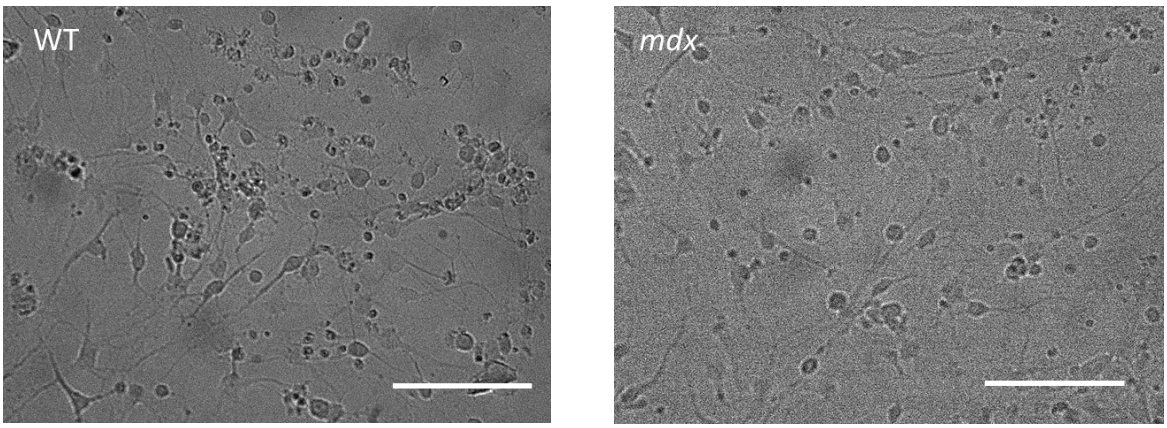


Figure 3.8: Brightfield images of mdx and WT neurons, 4-5 days after primary culture. *The morphology of WT and mdx neurons is similar. Scalebars are 35µm*

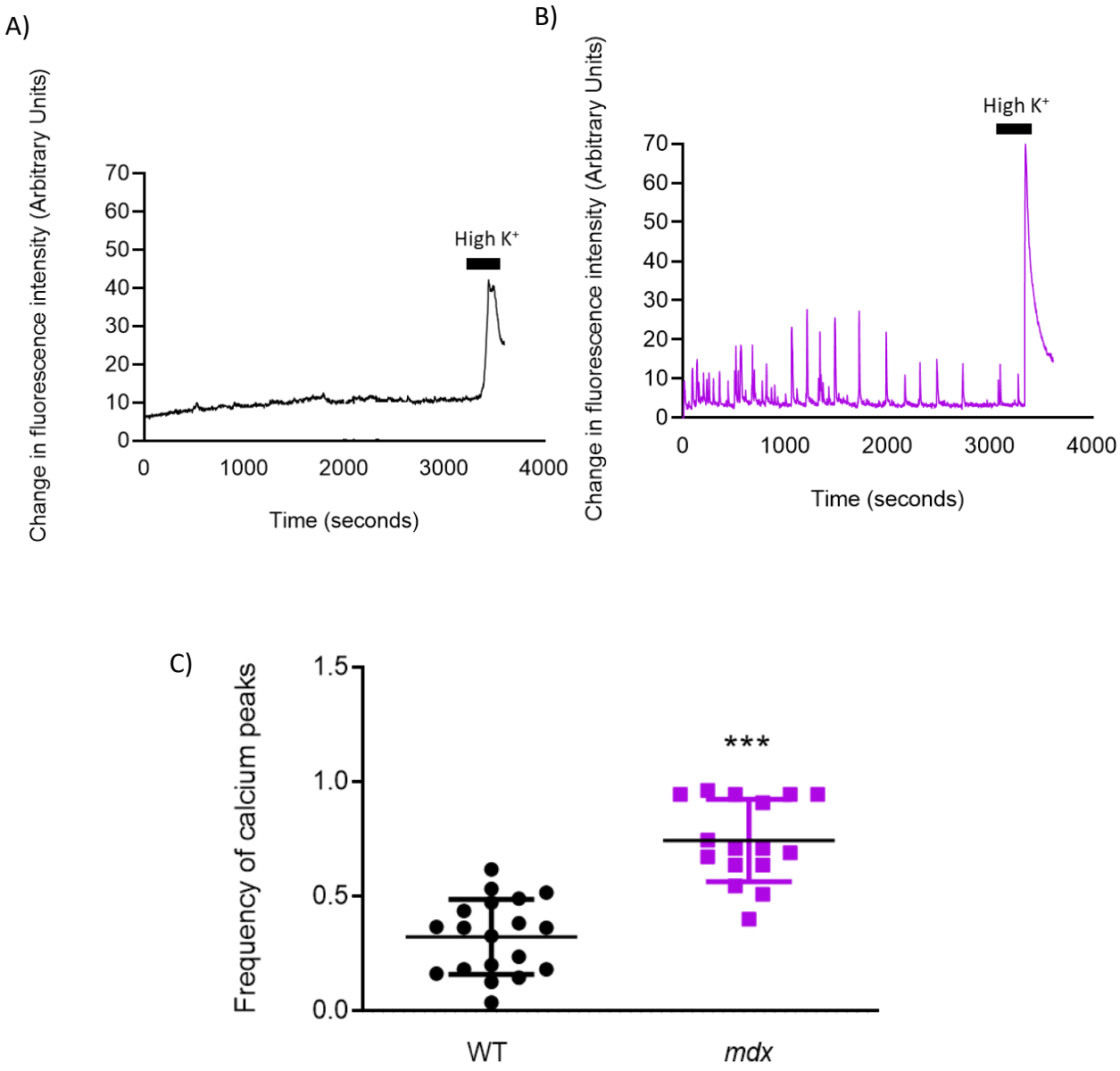


Figure 3.9: Baseline activity in cultured mdx hippocampal neurons in increased.

*Representative traces of cellular activity and frequency of peaks under basal conditions (HBSS) in A) WT mice are different to the cellular activity in B) mdx mice (purple). C) This difference is significantly different. Unpaired t test, p<0.001****

3.8. Neuronal density in the dentate gyrus decreases with age in *mdx* mice.

Using a pan-neuronal biomarker, NeuN (neuronal nuclear protein) to identify postmitotic neurons, we counted the number of neurons in the granule cell layer of the dentate gyrus. In dystrophin-expressing WT mice, neither neuronal density nor neuronal number in the granule cell layer of the dentate gyrus was changed between 4 months (adult mouse) and 8 months (aged mouse). However, we found that there was a significant decrease in neuronal number in the 8-month-old *mdx* mice relative to age-matched WT controls (Two-way ANOVA, n=3-4 animals per group, 2-3 whole brain sections per animal, 3 regions in the dentate gyrus, of the granule cell layer). The interaction between the WT and *mdx* (strain vs age) at 8 months was significantly different (figure 3.10a, $F(1, 9) = 136.8$, $p<0.0001$) and the age effect of 4 months vs 8 months in the *mdx* mice was also significantly different (figure 3.10, $F(1, 9) = 121.6$, $p<0.0001$).

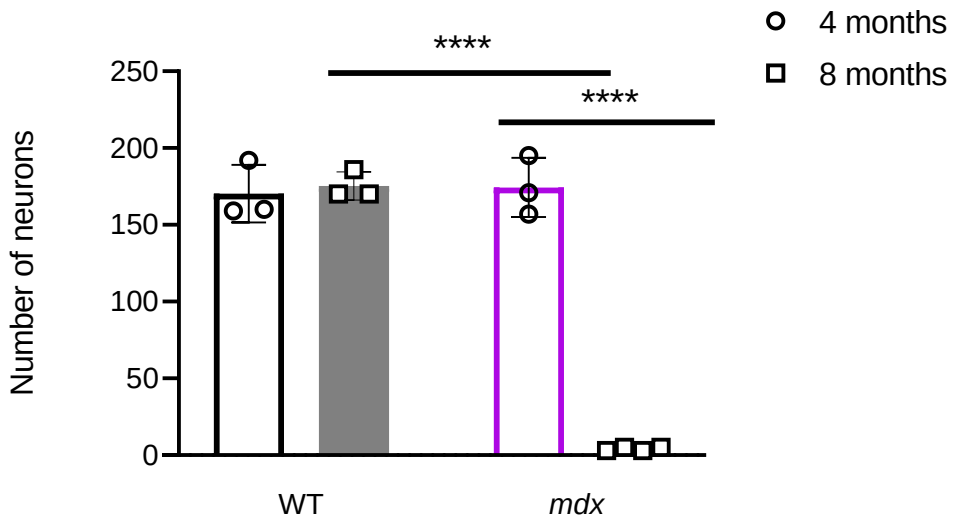


Figure 3.10: Neuronal density in the dentate gyrus decreases with age in mdx mice (4 and 8 months).

*Mean neuronal number in WT slices was the same in the two age groups studied whereas there was a significant decrease in neuronal number in the 8-month-old mdx slices compared to 4-month-old mdx and WT. Two-way ANOVA, p<0.001*****

Representative immunofluorescence images (figure 3.11a) show that there was no difference in the number of neurons in WT and *mdx* mice at 4 months old. DAPI, a nuclear marker, was used as a control stain to determine the number of cells per region. However, in the representative images (figure 3.11b), the significant decrease in the number of neurons in the granule cell layer of the dentate gyrus in 8-month-old *mdx* can be seen as an absence of neurons. However, there are other cell types present as evidenced by the DAPI staining. It is also clear that there is a change in gross cell morphology within the 8-month-old *mdx* mice in that the cells within the granule cell layer are disorganised and less densely packed relative to either the WT or 4-month-old *mdx* mice.

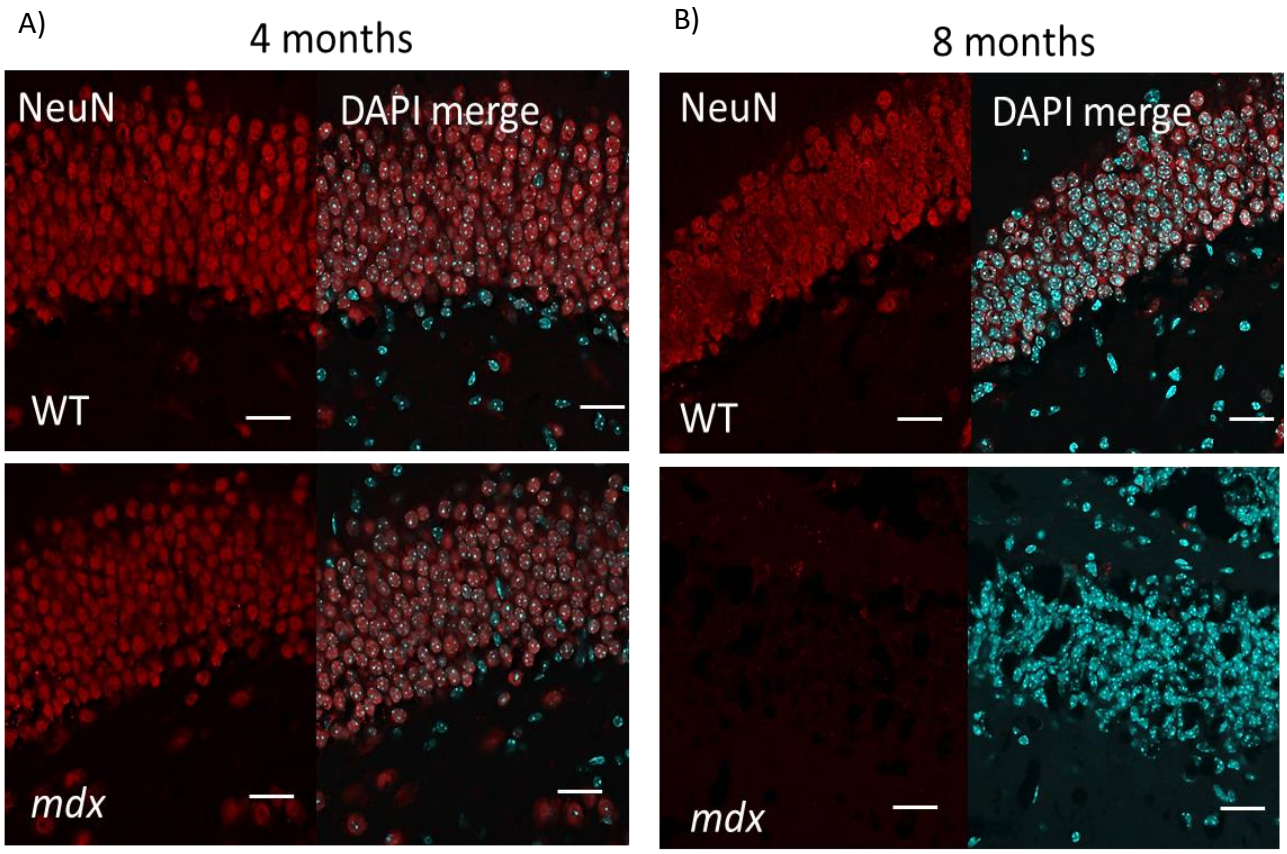


Figure 3.11: Immunofluorescence images looking at NeuN staining for neurons in the dentate gyrus. A) There is no difference between the number of neurons in WT and mdx mice at 4 months old. However, B) there is a significant decrease in the number of neurons in mdx mice at 8 months relative to age-matched WT comparators and 4-month-old mdx mice. DAPI is used as a nuclei marker for all cells. Scalebars are 30µm.

That said, there is a difference in the gross cell morphology in 8-month-old WT mice in that the neurons are more densely packed, which could be an age-related change. Further, in 8-month-old *mdx* mice, there appear to be large fluid filled structures disrupting the cell layer in the granule cell layer (figure 3.12b and c), that are not present in the 4-month-old WT and *mdx* mice (figure 3.12a). This large fluid filled structure may have displaced the neurons, resulting in a significant decrease in 8-month-old *mdx* mice.

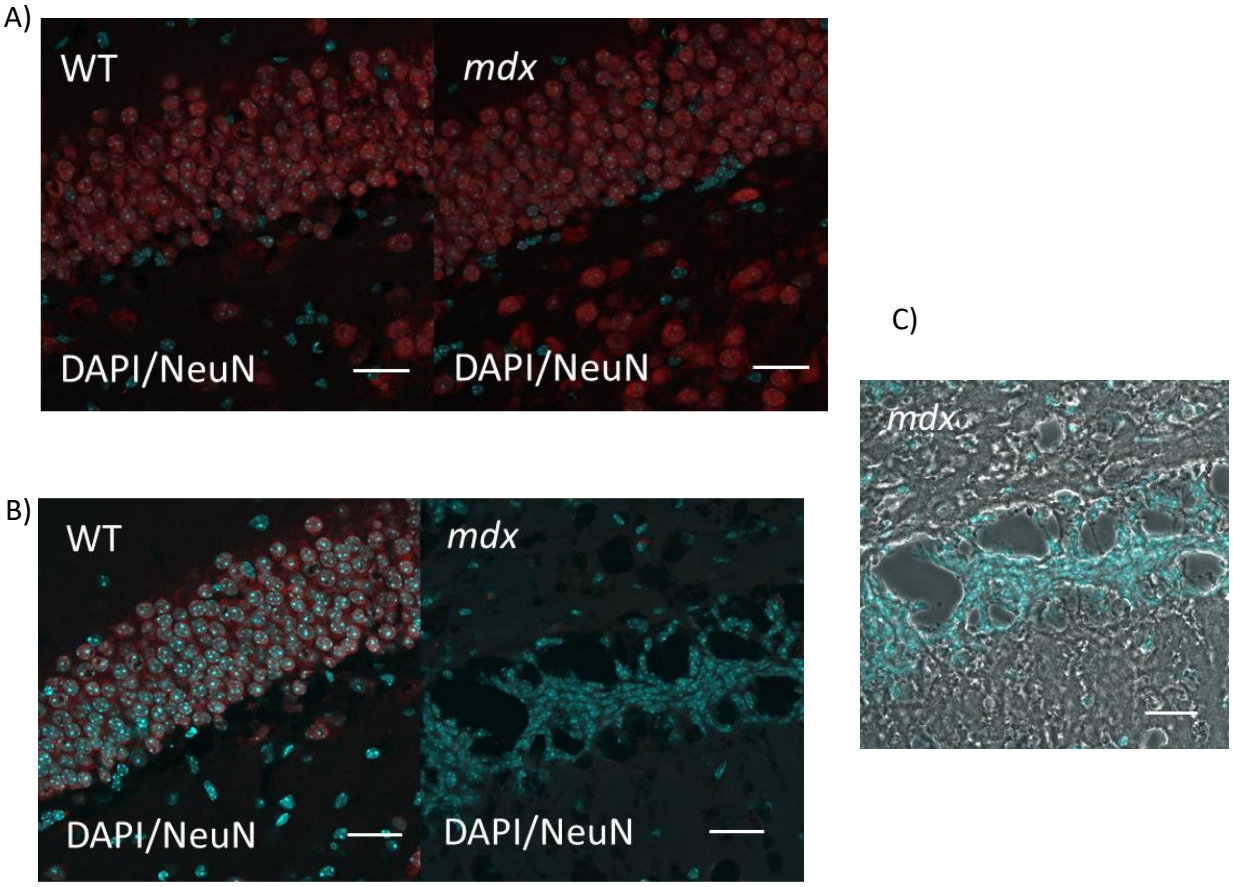


Figure 3.12: Immunofluorescence and brightfield images looking at NeuN staining for neurons in the dentate gyrus. Brightfield and DAPI/NeuN stained images of A) 4-month-old and B) 8-month-old WT and mdx mice. C) Brightfield image of the fluid filled structures that were present in the granule cell layer of 8-month-old mdx mice. Scalebars are 30µm.

3.9. The number of DCX-positive cells in the dentate gyrus of *mdx* mice decreases with age.

Doublecortin (DCX) is a microtubule-associated protein that is required for normal neocortical and hippocampal development and which has also been associated with hippocampal adult neurogenesis. As such, it is a suitable marker for neurogenesis (Couillard-Despres *et al.*, 2005).

For this part of the investigation, the number of DCX-positive cells in 8-week-old, 4-month-old and 8-month WT and *mdx* mice was counted. Three different age groups were chosen for study as hippocampal adult neurogenesis and synaptic plasticity are both greatly affected by the aging process (Rao *et al.*, 2005). For our analysis, three regions of the granule cell layer in the dentate gyrus were investigated. These regions were determined as an area where there was the greatest accumulation of cells in a 3cm x 3cm area (indicated by a white box on representative images).

In WT mice, the number of DCX-positive cells decreased between 8-week-old and 4-month-old mice, but this decrease was not statistically significant (unpaired t test, n= 5 animals, 8-week-old 5±1 vs 4-month-old 3.8± 0.8367, p= 0.0736). Further, there was no change in the number of positive DCX cells between 4-month-old and 8-month-old WT mice (n= 4-5 animals, unpaired t test, 4-month-old 3.8±0.8367 vs 8-month-old 3.750± 0.9574, p>0.05). On the other hand, the number of DCX-positive cells was significantly decreased in *mdx* mice in comparison to WT mice as such an age-effect was noted in *mdx* mice only.

When comparing the number of DCX-positive cells at each of the three ages between WT and *mdx* mice, there are significant differences in the number of cells in each group. Fewer cells were positively stained for DCX in 2-month-old *mdx* mice as compared to WT mice (figure 3.13, unpaired t test, n=5 animals, WT 5±1 vs *mdx* 2.2±1.095, p=0.0029). At 4-months-old, the number of DCX-positive cells was also significantly decreased in *mdx* mice in comparison to WT (figure 3.14, unpaired t test, n=3-5 animals, WT 3.8±0.8367 vs *mdx* 2.667±0.5774, p= 0.0436). At 8-months of age, the number of DCX-positive cells was also significantly decreased in *mdx* mice in comparison to WT (figure 3.15, unpaired t test with Welch's correction, n=4 animals, WT 3.75± 0.9574 vs *mdx* 1.75±0.5, p= 0.0167).

Representative immunofluorescence images for each age group showed a decrease of DCX-positive cells (red stain) in the granule cell layer of *mdx* mice in comparison to WT. In all analysis, DAPI, a marker of nuclei, was used as a cellular marker. Decreased neurogenesis in aging (Mathews *et al.*, 2017), was exacerbated in *mdx* mice with a clear difference between strains ($F(1, 20) = 31.6$, $p<0.0001$). No interaction between strain and age was noted.

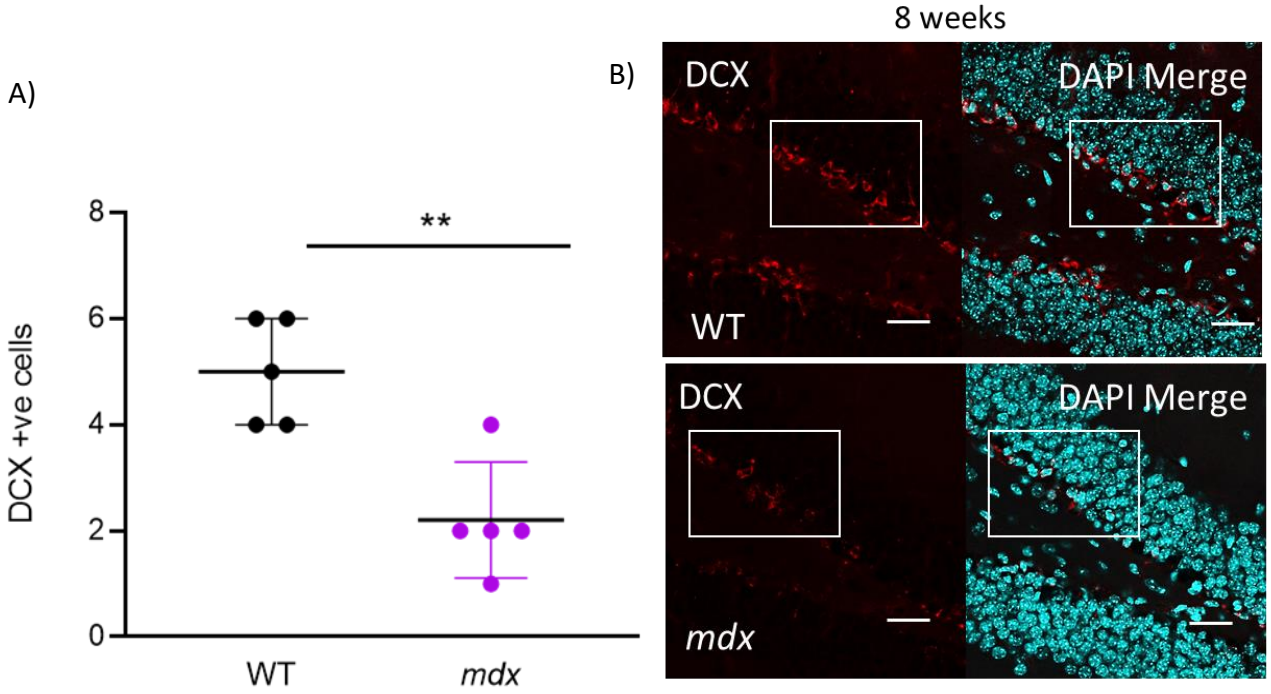


Figure 3.13: The number of DCX-positive cells in the granule cell layer of the dentate gyrus is decreased 8-week-old mdx mice.

The number of positive DCX cells is significantly reduced in mdx mice in comparison to WT.

*Immunofluorescence images of DCX-positive cells (red) counted in the white box is decreased in mdx compared to WT. Scalebars are 30µm. Unpaired t test, p<0.01***

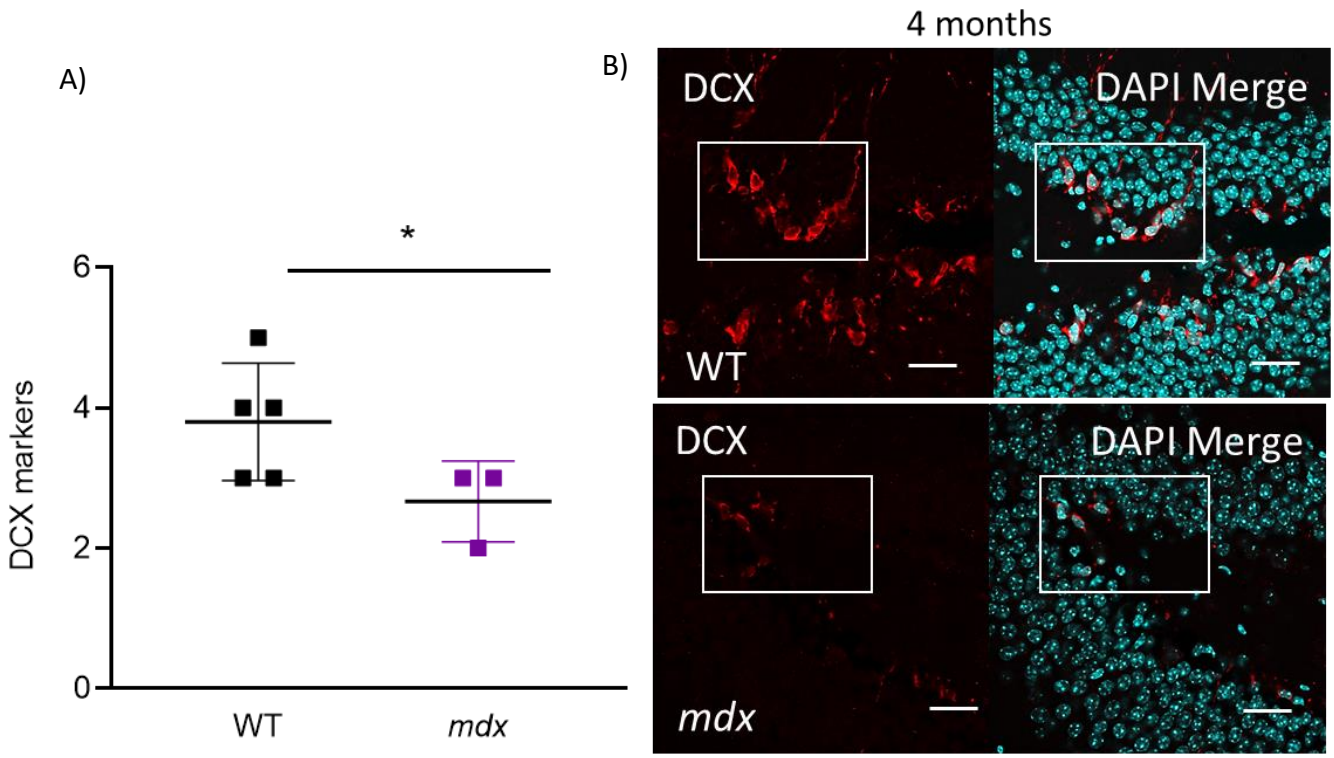


Figure 3.14: The number of DCX-positive cells in the granule cell layer of the dentate gyrus is decreased in 4-month-old mdx mice.

The number of positive DCX cells is significantly reduced in mdx mice in comparison to WT.

*Immunofluorescence images of DCX-positive cells (red) counted in the white box is decreased in mdx compared to WT. Scalebars are 30µm. Unpaired t test, $p<0.05$**

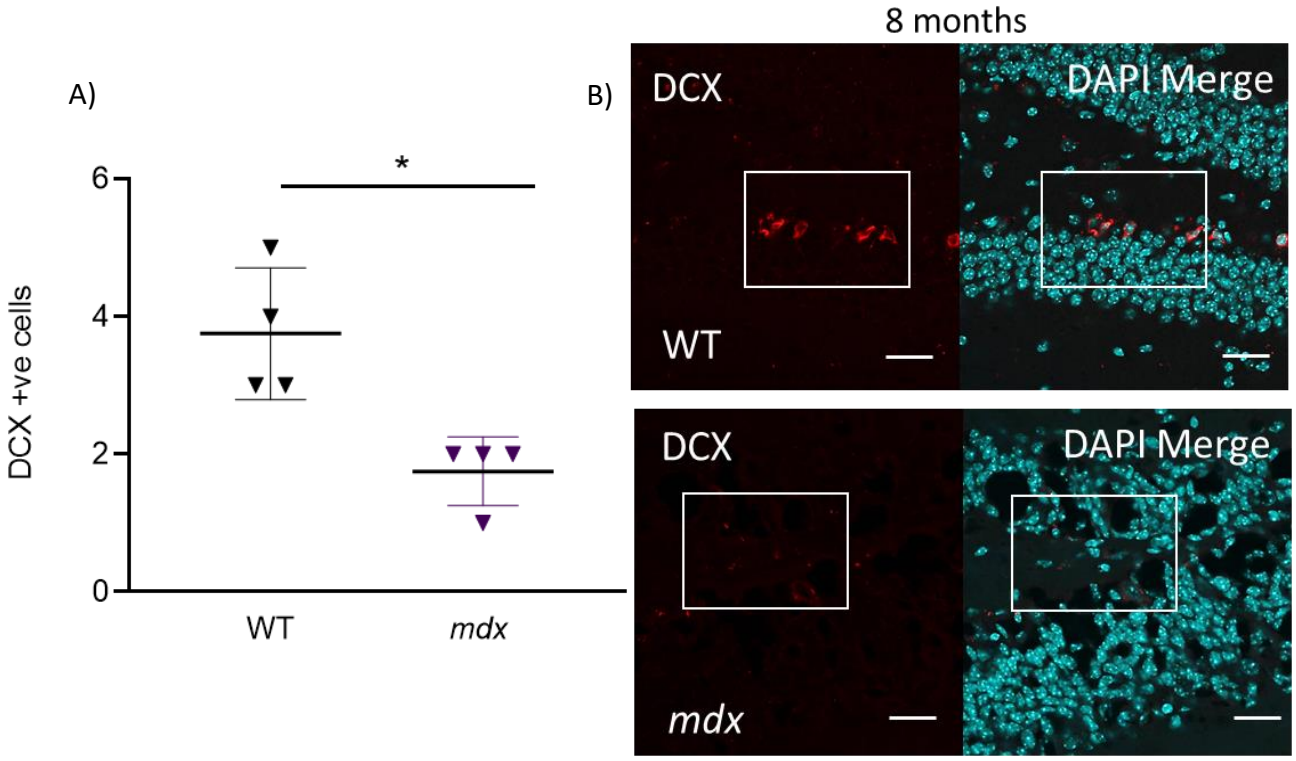


Figure 3.15: The number of DCX positive cells in the granule cell layer of the dentate gyrus is decreased in in 8-month-old mdx mice.

The number of positive DCX cells is significantly reduced in mdx mice in comparison to WT

*Immunofluorescence images of DCX positive cells (red) counted in the white box is decreased in mdx compared to WT. Scalebars are 30µm. Unpaired t test, p<0.05**

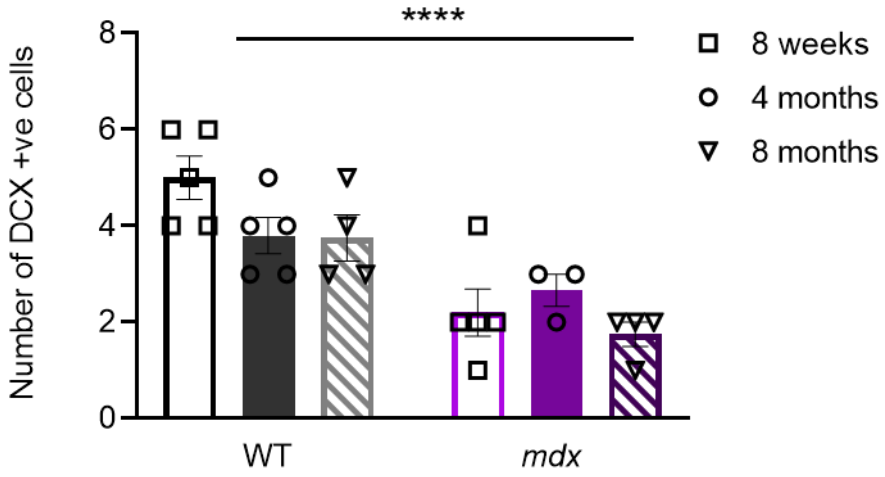


Figure 3.16: The number of DCX-positive cells in the cell layer of the dentate gyrus is decreased in mdx mice across 3 ages.

*The number of positive DCX cells decreases with age in WT mice and is significantly decreased in mdx mice with no change across age groups. Two-way ANOVA, p<0.001*****

3.10. Glial filamentary acidic protein is significantly decreased in the *mdx* mouse.

Glial filamentary acidic protein (GFAP) is an intermediate filament protein which is expressed primarily by astrocytes in the CNS (Eng *et al.*, 2000). Its main function is to maintain astrocyte structural integrity and aid in cell movement and shape change (Eng *et al.*, 2000). As such, GFAP is widely accepted as the marker for astrocytes in neurological studies (Yang & Wang, 2015). Astrocytes serve an important supportive role for neurons, providing a favourable ionic environment, modulating extracellular levels of neurotransmitters, aiding the organization of neurons (Hatten & Mason, 1990) and being actively involved in the modulation of neuronal signalling (Araque *et al.*, 2014). As astrocytes are likely to modulate neuronal signalling, they have shown to subsequently regulate glutamate transmission between neurons (Angulo *et al.*, 2004; Amiri *et al.*, 2012; Amiri *et al.*, 2013) and such are involved in long term potentiation (Henneberger *et al.*, 2010). For instance, astrocytic glutamate release has been shown to activate presynaptic NMDA receptors and promote an increase in excitatory communication between neurons (Jourdain *et al.*, 2007). As we have already demonstrated that neuronal calcium activity as well as long term potentiation is altered in *mdx* mice in comparison to WT, we wanted to determine if GFAP and thus, astrocytes, may play a role in mediating these effects.

Using a GFAP primary antibody (labelled with a AP488 secondary antibody) in the hilus and granule cell layer of the dentate gyrus, we found that the number of astrocytes significantly increased with age in WT mice, from 8-weeks to 8-months

(figure 3.17, n=3-5 animals, two-way ANOVA, F (2, 17) = 6.844, p=0.0066). We also found that although there was a significant decrease in the number of astrocytes in *mdx* mice in comparison to WT (n=3-5 animals, two-way ANOVA, F (1, 17) = 44.35, p<0.0001), there was no significant differences in the numbers of astrocytes between the 2-, 4- and 8-month-old *mdx* mice. There was an overall interaction between strain and age in the two-way ANOVA with n=3-5 animals, F (2, 17) = 9.858, p=0.0014.

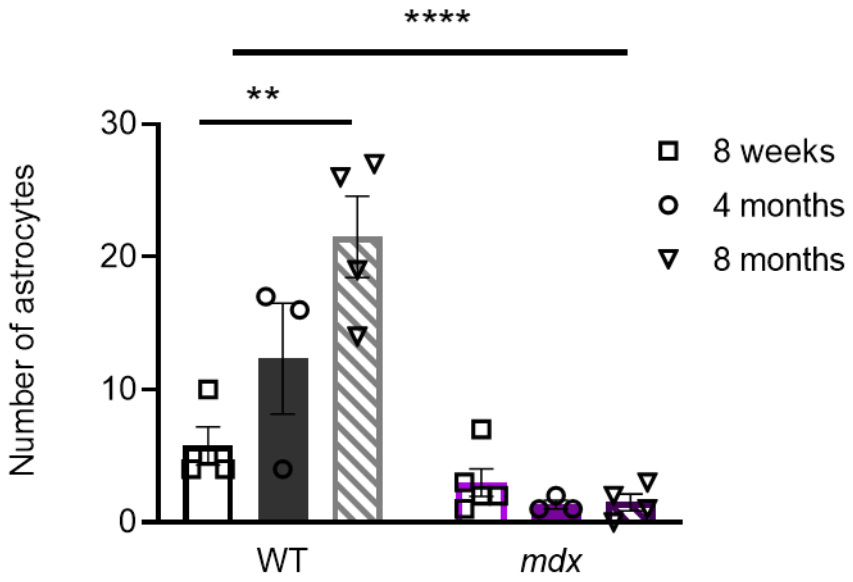


Figure 3.17: The number of astrocytes was significantly decreased in mdx mice and significantly increased in WT mice in 8-week-old, 4-month-old and 8-month-old mice.

*The number of astrocytes was significantly decreased in mdx mice relative to WT in 8-week-old, 4-month-old and 8-month-old mice. Two-way ANOVA, p<0.01** and p<0.001****

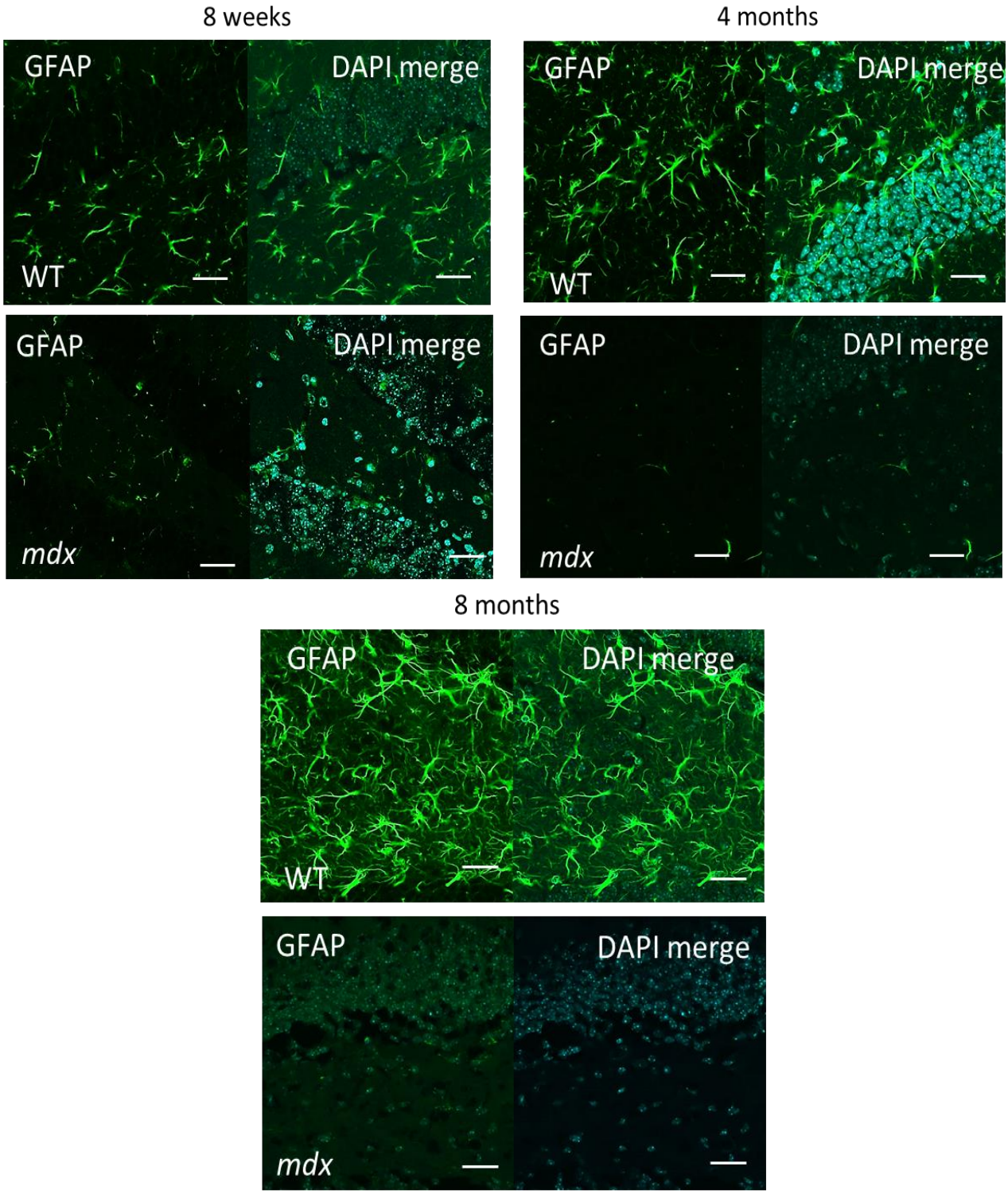


Figure 3.18: Immunofluorescence images looking at GFAP staining of astrocytes in the dentate gyrus

The number of astrocytes increases with age in WT mice compared to a significant reduction in astrocytes at all ages in mdx mice. DAPI was used as a nuclei marker for all cells. Scalebars are 30µm.

3.11. Discussion

Duchenne Muscular Dystrophy is an X-linked recessive disorder resulting in the loss of the structural protein dystrophin. Boys with DMD usually present with muscle weakness from an early age, which progresses to physical disability and eventual immobility. While most research on DMD has focused on the effect the condition has on muscle, as treatment has increased life expectancy in those affected, greater attention is now being paid to another aspect of DMD pathology: cognitive impairment. In this respect, boys with DMD have a higher incidence of mild-to-moderate cognitive impairment, with deficits in verbal, short-term and working memory (Snow *et al.*, 2013).

In our studies, LTP, proposed to be the molecular correlate of learning and memory, was decreased in *mdx* mice in comparison to WT mice, which is a novel finding as results of previous studies investigating LTP in *mdx* mice differed. In a study by Sesay and colleagues, no obvious deficit in hippocampal NMDA-dependent LTP was found in *mdx* mice (Sesay *et al*., 1996). One explanation for the difference in our results from the study by Sesay *et al.* (1996) could be that the study was carried out on animals that were 10-12 weeks old, which is similar to our study (we used 8–12-week-old mice), but the LTP experimentation took place *in vivo* on anesthetised animals held in a semi-stereotaxic apparatus. This methodology differs significantly to that used by us and may be one explanation for our differing results. In contrast, Vaillend *et al*. (2004), found that *ex vivo* LTP was enhanced. Although they did justify that enhanced LTP could underpin cognitive dysfunction, it is counterintuitive as increased LTP is normally associated with improved memory

consolidation. Our findings of supressed LTP are more consistent with the cognitive deficits in learning and memory processes in *mdx* mice (Vaillend *et al.*, 2004). Moreover, a significant decrease in LTP could impact memory in *mdx* mice leading to deficits in LTP which were associated with memory dysfunction in the spatial navigation task, the Morris water maze (Goussakov *et al.*, 2019).

Recognition memory was also investigated using the novel object recognition test, but this failed to reveal any significant differences in this study between *mdx* and WT mice. However, a recent study using NOR has shown that cognitive deficits were only observed in 4 month and older *mdx* mice, and that these cognitive deficits progressed with age (Bagdatlioglu *et al.*, 2020). As such, when we examined the *mdx* hippocampus over time, we found striking changes in the cellular structure.

We found that the total number of neurons in the hippocampal dentate gyrus, where neural progenitor cells migrate into the granule cell layer and differentiate into neuronal or glial cells (Ming & Song, 2011), were substantially reduced in *mdx* mice across all ages in comparison to WT. However, we did not see this change in adult *mdx* mice. In parallel with the observed decrease in neuronal density in aged *mdx* mice, fluid-filled structures were evident in the cell layer. These fluid-filled structures may be displacing neurons present in the cell layer and such, are likely to impact on processes that are intricately dependent on the neuronal circuitry of the hippocampus.

Another marker that has been associated with hippocampal adult neurogenesis is DCX (Couillard-Despres *et al.*, 2005). The expression of DCX is decreased with

ageing in accordance with an overall decrease in hippocampal adult neurogenesis (Kuhn *et al.*, 1996; Brown *et al.*, 2003), and as expected from previous studies in this area, we found that the number of DCX-positive cells decreased in WT mice as they aged, whereas there was a significant decrease in the number of DCX-positive cells in *mdx* mice relative to WT, which persisted up to 8 months. Decreased DCX in *mdx* mice from an early age and a reduction in hippocampal adult neurogenesis could result in a reduction in neuronal migration and proliferation (Pramparo *et al.*, 2010) resulting in disruption to the hippocampal cellular circuitry in the hippocampus. Such a disruption could result in aberrant synaptic plasticity and thus the mechanisms surrounding learning and memory would be affected, ultimately contributing to the deficits observed in individuals with DMD.

For many years the role of astrocytes within the CNS was thought to only support neurons, it is now clear that they have several diverse functions such as being actively involved in the control of neuronal functions, communication pathways, and synaptic plasticity, as they are able to receive signals from neurons and release neuroactive substances (Kirchhoff *et al.*, 2001). Astrocytes in the CNS release and regulate several neuroactive molecules that can affect neuronal activity and modulate plasticity and LTP (Theodosis *et al.*, 2008) and, as such, are involved in synaptogenesis and in regulating communication between already formed connections (Bains & Oliet, 2007). Additionally, adult neural stem cells in the subgranular zone of the dentate gyrus are both positively and negatively regulated by contact with astrocytes (Cassé et al., 2018). Any change to astrocytic function or number could alter neuronal and/or overall cognitive function. In our study, we report that the number of astrocytes expressing the GFAP marker is significantly

reduced in *mdx* mice across three age groups; 2,4 and 8 months old whereas in WT mice, there is a significant increase across the same three age groups. A decrease in astrocytes expressing GFAP, in *mdx* mice, could also be a contributory factor in the age-related changes in hippocampal structure in these mice. Thus, a loss of astrocytes and altered neurogenesis on a whole could contribute to the loss of cells in the aged hippocampus which would have a deleterious effect on brain function in these animals as normal neuronal activity and plasticity are likely to be affected by this loss.

While we were primarily focussed on hippocampally-mediated learning and memory consolidation, we also took a look at other centrally-regulated behaviours that might be affected by loss of dystrophin. When we investigated the behaviour of *mdx* mice, we found that they displayed increased freezing time in an open field compared to WT mice. Freezing behaviour is a known fear response in rodents, with studies linking this behaviour to projections from the amygdala to the brainstem (LeDoux *et al.*, 1988). In fact, an increase in freezing has previously been seen in *mdx* mice with a reduction of GABA receptors in the amygdala (Sekiguchi *et al.*, 2009). While we did not find any difference in the number of $GABA_A$-receptor expressing interneurons in the hippocampal dentate gyrus in either of the two ages investigated, in *mdx* and WT mice, this does not necessarily imply that receptor expression or function in these cells is normal. In *mdx* mice, dystrophin has been linked to clustering of $GABA_A$ receptors (Knuesel *et al.*, 1999; Miranda *et al.*, 2009; Vaillend *et al.*, 2010). Disruption in $GABA_A$ receptors has also been identified in the brain of patients of DMD (Suzuki *et al.*, 2017), and interestingly, the decline in

$GABA_A$ receptors was more evident in older adults, suggesting that there is an age-related progression of DMD on the brain.

Our studies also revealed that under basal conditions there was an increase in intracellular calcium activity in cultured hippocampal neurons of *mdx* mice resulting in neuronal hyperexcitability. Such calcium dysregulation has also been noted in other diseases characterised by cognitive impairment. For example, in Alzheimer's disease (Toescu & Verkhratsky, 2007). Dysregulated calcium can be cytotoxic and thereby contribute to premature brain aging, neuronal dysfunction and cell death (Orrenius & Nicotera, 1994) as well as neurodegeneration (Khachaturian, 1987; Landfield, 1987). At a cellular level, calcium disruption may be key to hippocampal dysfunction in *mdx* mice however, further studies are needed to elucidate this.

3.12. Conclusions

Although in early adulthood (8-12 weeks) we did not detect behavioural deficits in memory in *mdx* mice, a striking suppression of LTP, the molecular correlate of learning and memory, was apparent. Moreover, at a cellular level, calcium dyshomeostasis was evident, resulting in spontaneous neuronal hyperexcitability, which if left unregulated can lead to cellular cytotoxicity. This could be due to defective inhibitory regulation by GABAergic neurons. Although no change in the absolute number of GABAergic interneurons was detected in *mdx* hippocampal tissue, $GABA_A$ receptor post-synaptic clustering is dependent upon the presence of neuronal dystrophin (Vaillend *et al.*, 2010) thus function in these neurons could be impacted. In longitudinal studies, we also noted a loss of neurons and astrocytes

and the pathophysiological changes in the cellular structure of the hippocampus in aged *mdx* mice. Impaired hippocampal adult neurogenesis is likely to impact acutely on the formation of new memories, but may also contribute to the long-term loss of neuronal cells. The density of astrocytes, which are critical to normal neuronal function, was suppressed to an even greater extent across all age-points in *mdx* mice. Several of the cellular changes are evident even in early adulthood when the behavioural expression of these changes is not yet evident. However, compensatory mechanisms may exist to preserve these critical cognitive functions.

This research has revealed an array of structural and functional changes in the hippocampi of dystrophin-deficient *mdx* mice, which begins to elucidate the role of dystrophin in non-contractile tissue, such as hippocampal neurons.

Chapter 4

Interleukin-6: its potential as a neuromodulatory factor underpinning aberrant hippocampal activity in dystrophin-deficient *mdx* mice.

4.1. Introduction

IL-6 is a pleiotropic cytokine which plays a key role in the immune system and also in CNS physiology and pathophysiology.

IL-6 signalling occurs through two mechanisms, classical and trans-signalling. Classical IL-6 signalling occurs through the binding of IL-6 to its membrane bound receptor, IL-6Rα. Whereas trans-signalling, which is often occurs when Il-6 binds to the soluble form of the receptor. This results in homodimerization of a glycoprotein, gp130, resulting in phosphorylation of JAK/STAT (Darnell *et al.*, 1994) and further downstream activation of MAPK and PI 3-K cascades (Eulenfeld *et al.*, 2012).

In the CNS, neuronal degeneration induced by IL-6 is mediated by trans-signalling. IL-6 can also be produced locally within the CNS, mainly by astrocytes (Dong & Benveniste, 2001; Farina *et al.*, 2007) and microglia (Ye & Johnson, 1999) but may also cross the blood brain barrier *via* saturable transport systems (Banks *et al.*, 1994). Thus, acute increases in circulating levels of this pro-inflammatory cytokine as are seen in DMD patients (Rufo *et al.*, 2011)and *mdx* mice (Pelosi *et al.*, 2015), could also raise levels within the CNS.

The effects of IL-6 on the brain have been studied with regards to cognitive function. In humans, deterioration of cognitive function, a hallmark of 'sickness behaviour', is linked to high circulating levels of pro-inflammatory cytokines such as IL-1β (Gibertini, 1998) and IL-6, which has also been implicated in lipopolysaccharide (LPS) -evoked cognitive dysfunction (Sparkman *et al.*, 2006).

Moreover, transgenic mice over-expressing IL-6 exhibit broad memory impairments (Heyser *et al.*, 1997; Wei *et al.*, 2012; Wei *et al.*, 2013) and severe neurological pathologies such as tremor, ataxia, and seizure, with neurodegeneration, astrocytosis and angiogenesis also being reported (Campbell *et al.*, 1993). The explicit effect of this cytokine on learning and memory function is further supported by transgenic mice deficient in IL-6, which possess enhanced spatial learning capabilities in the radial arm maze (Braida *et al.*, 2004) and the Morris water maze (Bialuk & Winnicka, 2018) behavioural task-learning assessments.

IL-6 may also be involved directly in synaptic plasticity and the hippocampus. Application of IL-6 was shown to inhibit hippocampal LTP using a mechanism that was dependent upon IL-6R activation (Tancredi *et al.*, 2000). Moreover, IL-6-induced LTP inhibition was attenuated by administration of monoclonal antibodies, used to block IL-6 receptors (Li *et al.*, 1997).

Anatomical and biochemical abnormalities, such as a loss of neurons, the appearance of neurofibrillary tangles, alterations in dendritic branching, cortical atrophy and metabolic defects (Rosman, 1970; Jagadha & Becker, 1988; Tracey *et al.*, 1995; Lv *et al.*, 2011) are observed in both DMD patients and *mdx* mice (Miranda *et al.*, 2009). This is paired with an increased incidence of mild to moderate cognitive impairment (Bresolin *et al.*, 1994; Anderson *et al.*, 2002; Cotton *et al.*, 2005) and deficits in verbal, short-term and working memory (Snow *et al.*, 2013) in DMD patients. Cognitive deficits are also present in the *mdx* mouse. In the *mdx* mouse, there is evidence of cognitive dysfunction such as a poor capacity to learn new tasks as well as deficits in storing spatial memories, relative to controls

(Vaillend *et al.*, 1995; Vaillend *et al.*, 2004; Chaussenot *et al.*, 2015). They also display deficits in associative learning and in the general processes involved in memory formation and consolidation which are both dependent upon optimal functioning of the hippocampus and amygdala (Chaussenot *et al.*, 2015).

Given that loss of dystrophin from skeletal muscle is associated with chronic inflammation, which is characterised by elevated circulating levels of *IL-6 in humans (Rufo et al., 2011)* and the *mdx* mouse (Pelosi *et al.*, 2015), IL-6 may act as an immune mediator leading to cognitive dysfunction in the absence of dystrophin.

4.1.1. Study objectives

- To determine if IL-6, which is elevated in DMD and *mdx* plasma, is increased in dystrophic hippocampal tissue.
- To investigate if IL-6 contributes to aberrant hippocampal activity in *mdx* mice.

4.1.2. Techniques used

- Neuronal cell culture (see methods section 2.2.1, pg. 33).
- Immunocytochemistry (see methods section 2.3.1, pg. 39)
- Gene expression - qRT-PCR (see methods section 2.5, pg. 47).
- Immunoassay - ELISA (see methods section 2.6, pg.52).
- Calcium imaging (see methods section 2.4, pg. 44).
- Immunofluorescence of whole hippocampal sections (see methods section 2.3.2, pg. 40).
- Extracellular electrophysiology (see methods section 2.8, pg.59).

4.2. Dystrophin isoform is co-localised at synaptophysin-labelled hippocampal synapses.

As dystrophin expression has been reported in the postsynaptic density (PSD) of cortical and cerebellar neurons (Lidov *et al.*, 1990), we examined immunofluorescent expression of dystrophin in hippocampal neurons (10 to 12 days in culture) cultured from dystrophin-expressing C57BL/6 mice (n= 15 fields of view from 3 different cultures). Immunofluorescent staining to the monoclonal mouse MANDRA-1 antibody which identifies full length dystrophin, Dp427 as well as dystrophin variants including Dp71, the most prevalent form of dystrophin in the CNS (Hugnot *et al.*, 1992; Lederfein *et al.*, 1992; Jung *et al.*, 1993) was used. Our results demonstrate that both forms were present in both cultured neurons and non-neuronal cells. In the neuronal cell body, diffuse dystrophin staining was evident in the cytosol, whereas immunolabelling in the processes was clustered into distinct puncta. Co-labelling with a rabbit monoclonal antibody against synaptophysin, an integral membrane protein localised to synaptic terminals, further indicated localisation of dystrophin at hippocampal synapses. This pattern of staining was consistent across several cultures and all neurons imaged (Figure 4.1).

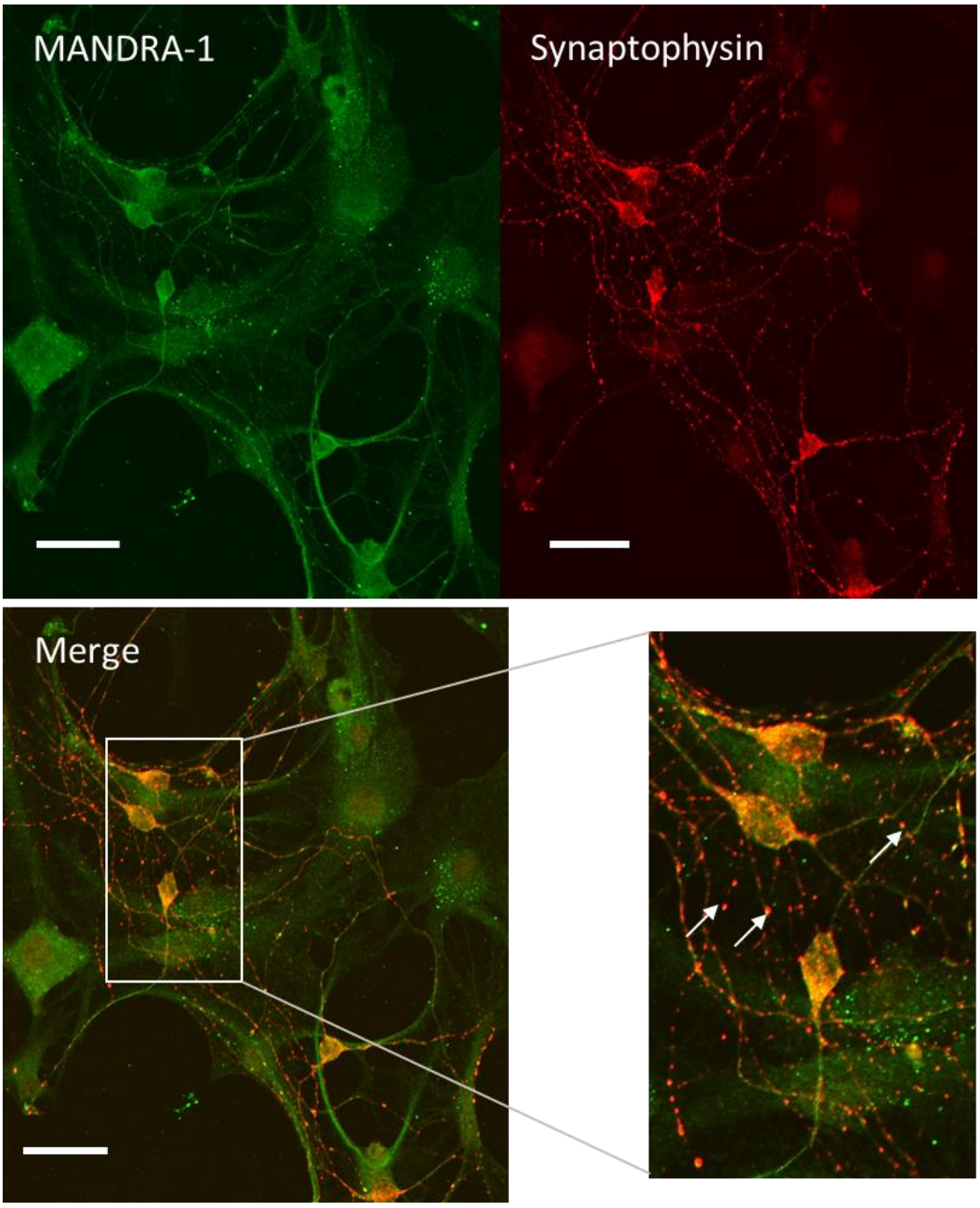


Figure 4.1: Dystrophin is expressed at hippocampal synapses.

Representative images of cultured hippocampal neurons co-stained with the MANDRA-1 antibody for several isoforms of dystrophin (green stain), and synaptophysin (red stain), a specific marker of synapses, indicate that dystrophin is expressed on synapses on neuronal cell bodies and neuronal processes (indicated by white arrows). Scalebar: 35µm.

4.3. IL-6Rs are clustered at synaptophysin-labelled hippocampal synapses.

Hippocampal neurons cultured from dystrophin-expressing C57BL/6 mice, labelled with a monoclonal mouse antibody against IL-6Rα (n= 15 fields of view from 3 different cultures), showed a similar pattern of staining to that of dystrophin. Specifically, cytosolic IL-6R was diffusely expressed in neurons, with punctate patterns of expression in dendritic processes (figure 4.2), and IL-6R expression was shown to cluster and co-localise with synaptophysin.

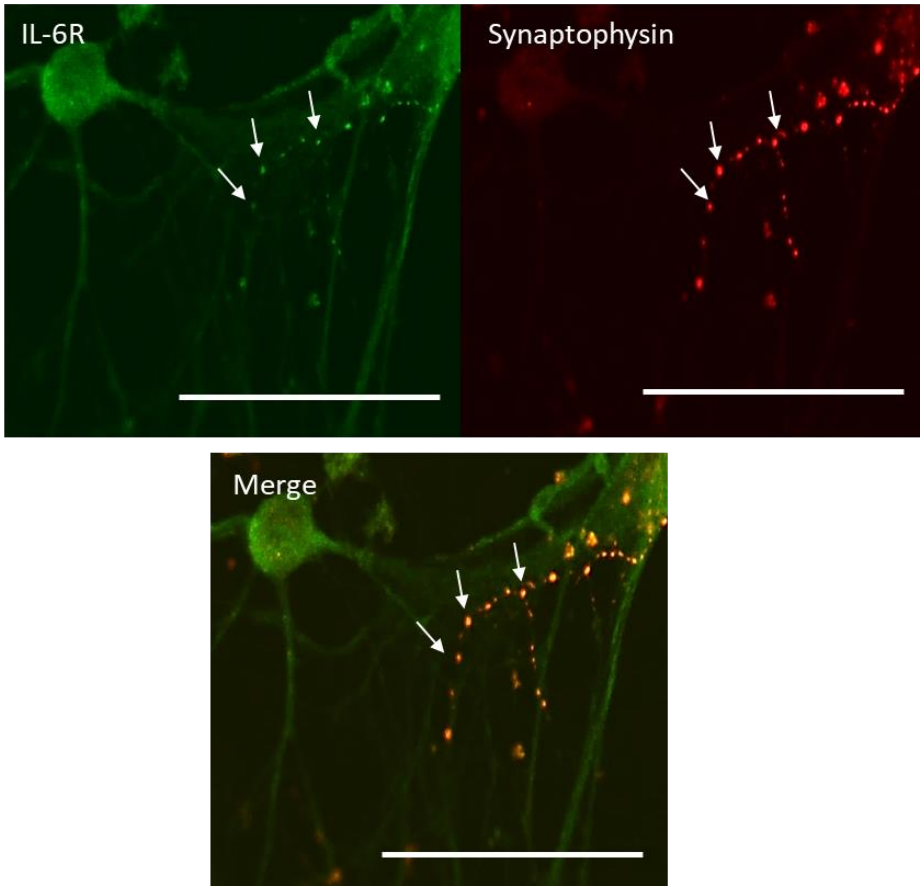


Figure 4.2: IL-6 receptors are expressed at hippocampal synapses.

Representative images of cultured hippocampal neurons illustrate that IL-6R (green staining) co-localises (yellow staining in merged image) with the pre-synaptic marker, synaptophysin (red staining, illustrated with white arrows) in cultured hippocampal neurons. Scalebar: 35µm.

4.4. IL-6 exposure increases IL-6R clustering in dystrophin containing hippocampal neuronal processes.

Given that neuronally-expressed dystrophin isoforms and IL-6Rs are both located in hippocampal synapses, we next sought to investigate possible if IL-6 stimulated synaptogenesis in control dystrophin-expressing hippocampal neurons. Neurons grown in the presence of recombinant IL-6 (1nM) were compared to control neurons without exogenous IL-6. The IL-6R-labelled immunofluorescent images generated from these neurons indicated that exposure to IL-6 induced an increase in the density of IL-6R clustering in the neuronal processes compared to untreated neurons (n=19 neurons/3 different cultures, 20mm of process from cell body, p=0.0137, figure 4.3).

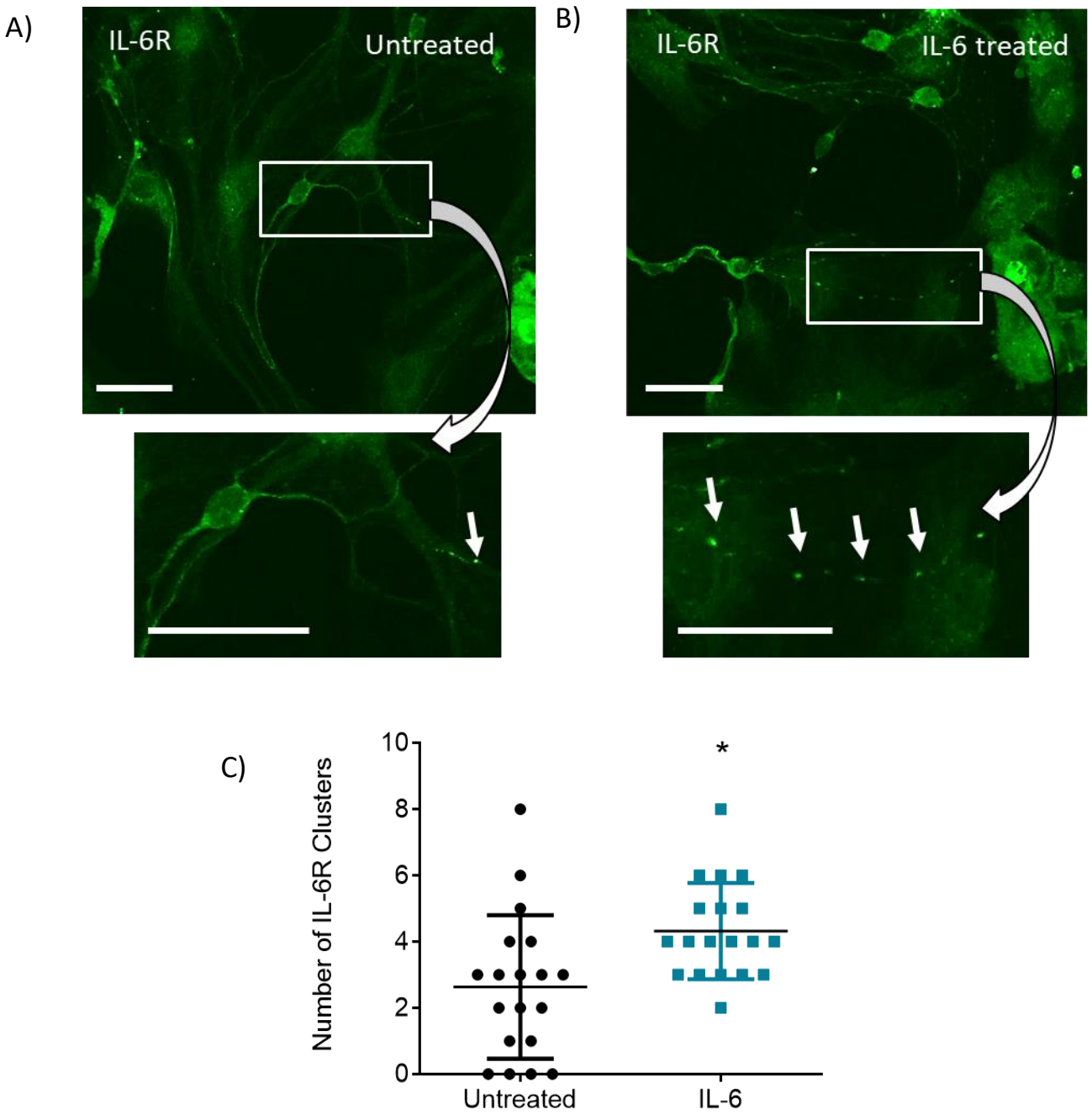


Figure 4.3: Exposure to IL-6 stimulates increased IL-6-positive puncta on hippocampal processes.

*C) The dot plot illustrates the number of IL-6R clusters per 20mm of process in dystrophin-containing C57BL/6 mice in untreated neuronal cell cultures and in neurons treated with 1nM recombinant IL-6 in culture media over 10-12 days, n=19 neurons/3 cultures. This can be seen in the representative images A) and B). The arrows indicate IL-6R clusters along the process. Scalebar: 35µm. Unpaired t test, p<0.05**

4.4. Hippocampal interleukin-6 (IL-6) expression is comparable between WT and *mdx* mice.

Given the elevations in circulating IL-6 in *mdx* mice (Pelosi *et al.*, 2015) we sought to determine if IL-6 was elevated in the hippocampus of *mdx* mice. qRT-PCR (where quantification of amplified DNA is achieved using fluorescence measurements) was conducted to determine the gene levels of IL-6 in the whole hippocampus of 8–12-week-old WT (n=10) and *mdx* mice (n=10). The hippocampal gene expression of IL-6 was not significantly different between WT (n=10, 2±2.662) and *mdx* (n=10, 2.367±3.156) mice *(p>0.9999, figure 4.3). However, as gene expression does not always correlate with protein expression (Liu et al., 2016), we also compared hippocampal IL-6 protein levels between WT and mdx mice. Using an ELISA assay, we found that* IL-6 protein in hippocampal homogenates was similar between WT (n=10, 5.059±0.8282) and *mdx* (n=10, 4.977±0.6414) mice *(p=0.8070, figure 4.4).*

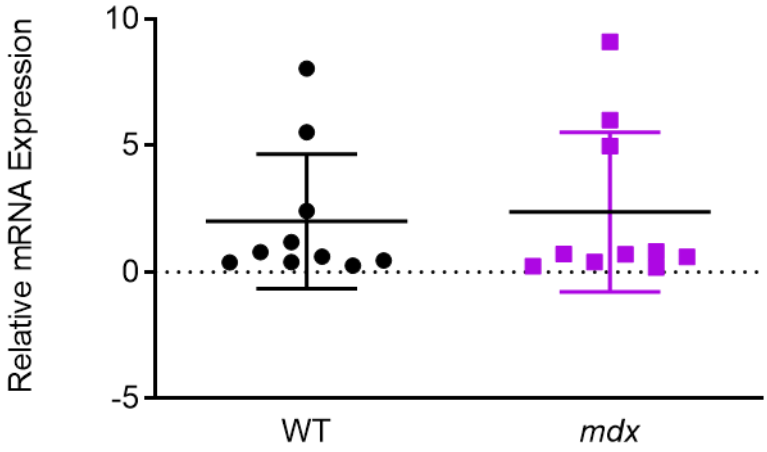


Figure 4.3: Hippocampal IL-6 gene expression is not different in mdx mice.

The data plot indicates that no difference in the relative mRNA expression of IL-6 was detected between mdx and WT mice (n=10, p>0.9999). Unpaired t test, p>0.05

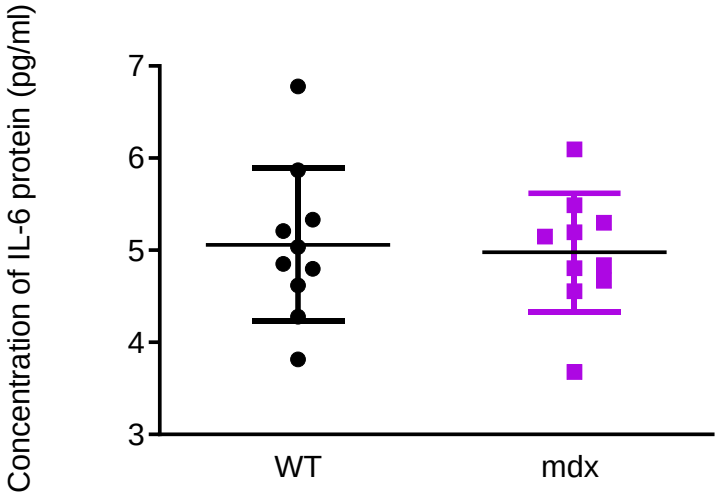


Figure 4.4: Hippocampal protein expression of IL-6 did not differ significantly between WT and mdx mice.

The dot plot illustrates the concentration of IL-6 protein (pg/ml) in WT and mdx hippocampal homogenates (n=10, p=0.8070). Unpaired t test, p>0.05

4.5. Hippocampal IL-6 receptor expression and intracellular signalling is not altered in the absence of dystrophin.

Although IL-6 at the gene and protein level was not significantly altered in *mdx* hippocampal tissue compared to WT controls, the sensitivity to this cytokine could be altered by changes in receptor expression or modification of downstream signalling pathways. We therefore examined gene expression of IL-6 receptors (IL-6Rs). Using RT-qpCR we found that IL-6R gene expression was similar in WT *(n=10, 1.078±0.139614)* and *mdx (n=10, 1.077±0.1386)* mice *(p=0.9990, figure 4.5).*

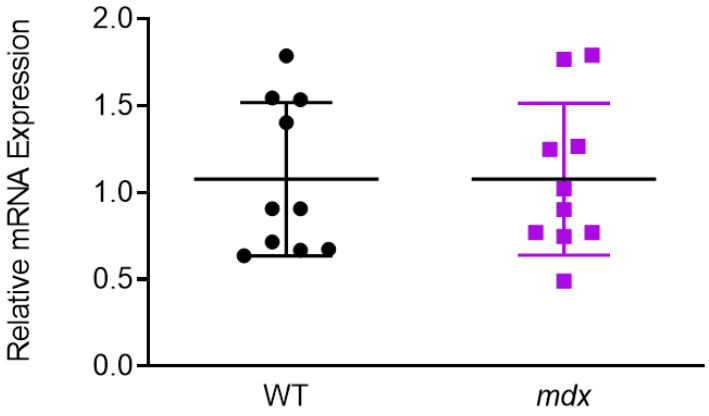


Figure 4.5: Hippocampal IL-6R gene expression is not different in mdx mice.

The data plot indicates that no difference in the relative mRNA expression of IL-6R was detected between mdx and WT mice (n=10, p=0.9990). Unpaired t test, p>0.05

As the IL-6/IL-6R complex subsequently binds to gp130, a membrane-bound signal transducer for IL-6, which leads to the downstream activation of the JAK/STAT pathway, and downstream cellular effects, we also measured gp130 expression in WT and *mdx* mice but, once again, we did not detect any significant differences *between WT (n=10, 1.155±0.6439) and mdx (n=10, 1.036±0.3121) mice (p=0.6048, figure 4.6).*

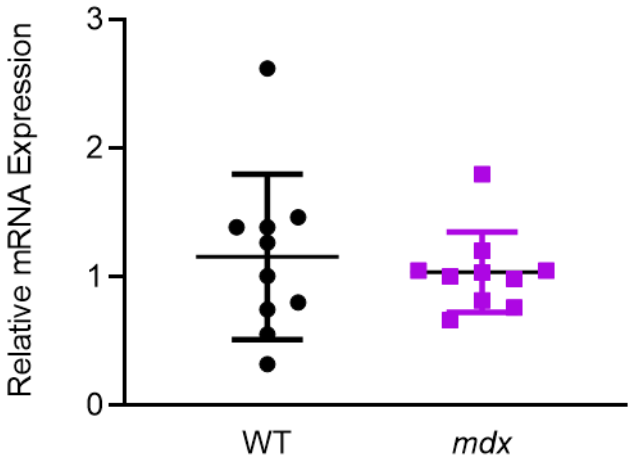


Figure 4.6: Hippocampal gp130 gene expression does not differ significantly in mdx mice.

The box plot illustrates that there is no difference in the relative mRNA expression of gp130 between mdx and WT mice (n=10, p=0.6048). Unpaired t test, p>0.05

Next, we examined the expression of STAT3, which is the main downstream target of IL-6 receptor activation. Its downstream actions include gene activation, cell growth and division, cell movement and apoptosis. At the gene level, in unstimulated tissue, no differences were detected in STAT3 gene expression between WT (n=10, 1.271± 0.2976) and *mdx* (n=10, 1.115 ± 0.1623, p=0.6502, figure 4.7) either.

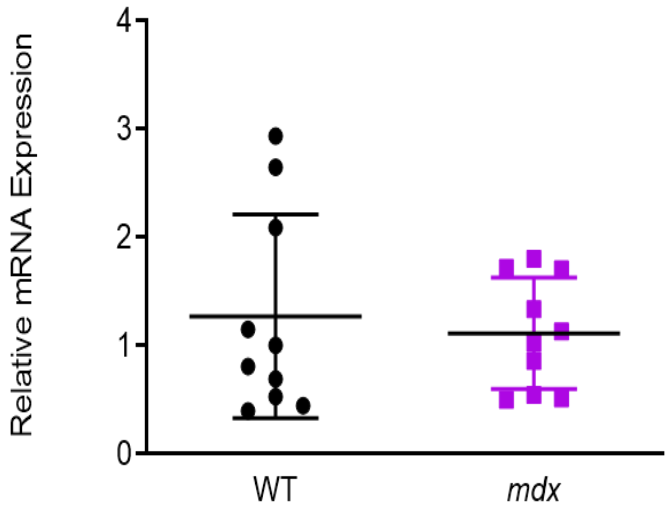


Figure 4.7: Hippocampal STAT3 gene expression is not different in mdx mice.

There is no significant difference in the relative mRNA expression of IL-6R between mdx and WT mice (n=10, p=0.6502). Unpaired t test, p>0.05

4.6. Regional differences in hippocampal IL-6 expression were detected in *mdx* mice.

Although useful for quantifying IL-6 expression, both qRT-PCR and ELISA use homogenised hippocampal tissue, therefore detection of region-specific changes in IL-6 or IL-6R was not possible with these techniques. However, immunofluorescence is a useful technique for identifying specific regions of protein expression. Using hippocampal slices, where the specific cell body layer remains intact, IL-6 expression was visualised in CA1, CA3 and the dentate gyrus (DG) regions using a monoclonal mouse antibody against IL-6. IL-6 expression was determined by analysing the mean fluorescent intensity in the pyramidal cell layer of the CA1 and CA3 regions and the granule cell layer in the DG. Confocal images were taken under identical conditions for laser and saturation between WT and *mdx* for IL-6 for accurate later comparison in each of the hippocampal regions.

The expression of IL-6 was increased in the CA1 region of *mdx* mice (% increase) compared to WT (*n=20 confocal images in this region from 5 WT and mdx animals, WT 1.610*±0.9609 *vs mdx* 2.601±1.741, p= 0.04). Further, there was also a significant increase in IL-6 expression observed in the DG region of *mdx* mice (36% increase) in comparison to WT (n= 17 confocal images in this region from 5 WT and *mdx* animals, WT 0.8728±0.3478 *vs mdx* 2.268±1.559, p= 0.0058). However, there was no difference detected between IL-6 expression in the CA3 region in *mdx* and WT mice (n=20 confocal images in this region from 5 WT and *mdx* animals, WT 1.346±0.8657 vs *mdx* 1.214±1.146, p=0.3506). This data can be seen in the data plot in figure 4.8 below.

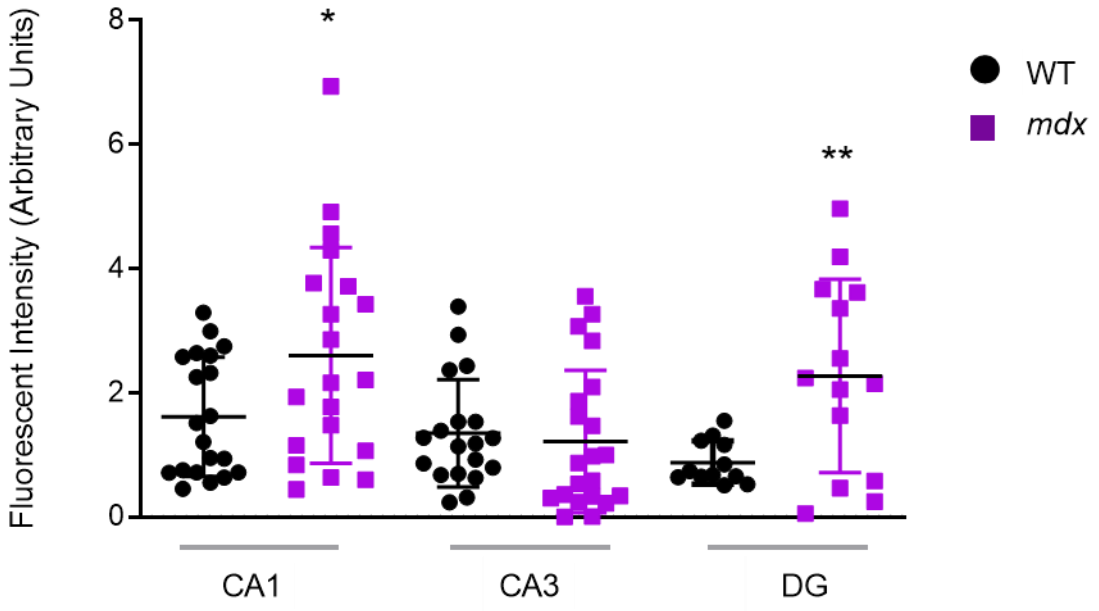


Figure 4.8: Regional hippocampal immunofluorescent expression of IL-6 is increased in dystrophin-deficient mdx mice.

The data plot illustrates a significant increase in IL-6 fluorescence in the CA1 and DG regions in mdx mice in comparison to WT mice and *DG: WT 0.8728±0.3478 vs mdx 2.268±1.559, p=0.0058). There is no significant difference in IL-6 fluorescence between CA3 regions in mdx and WT mice (CA3:* WT *1.346±0.8657 vs mdx 1.214±1.146, p=0.3506). Scale bars are 70µm. Unpaired t test, p<0.05* and p<0.01***

In the pyramidal cell layer of CA1 and CA3 and granule cell layer of DG, IL-6 expression is diffuse in the cytosol and localised to the cell membrane of both WT and *mdx* mice. Although, in CA1 and DG regions in *mdx* mice, IL-6 expression in the cell membrane of these cell layers is increased in comparison to WT which can be seen in the representative images in figure 4.9.

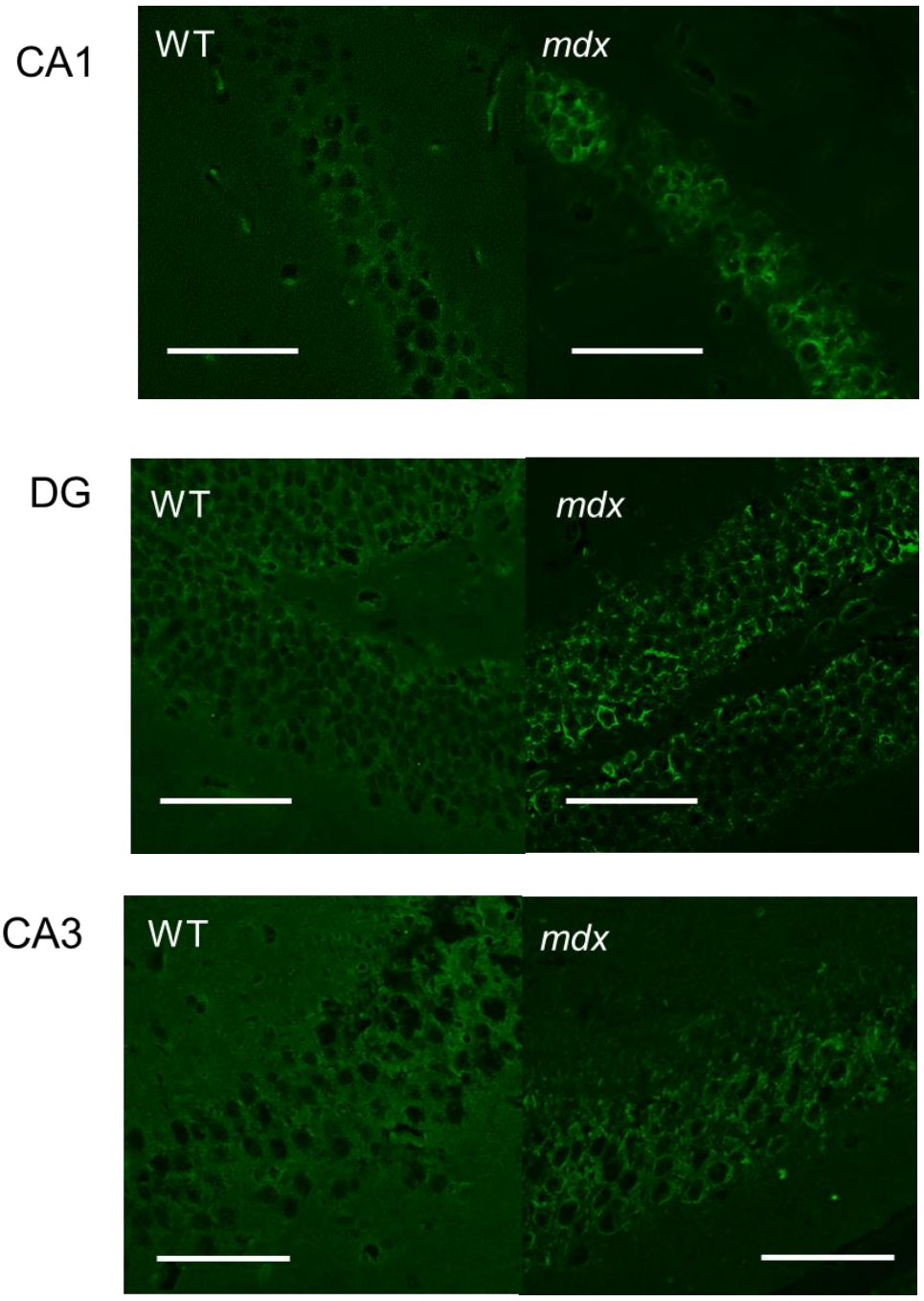


Figure 4.9: Representative images of regional hippocampal immunofluorescent illustrate that the expression of IL-6 is increased in dystrophin-deficient mdx mice.

In the pyramidal cell layer of CA1 and CA3 and granule cell layer of DG of both WT and mdx mice, IL-6 expression is diffuse in the cytosol, with IL-6 localised in the cell membrane. In mdx mice, this expression of IL-6 (fluorescence) in the cell membrane is increased in CA1 and DG in comparison to WT.

4.7. Regional differences in hippocampal IL-6 receptor expression were detected in *mdx* mice.

As IL-6 expression was shown to be increased in CA1 and DG, in the previous section, we next used a monoclonal mouse antibody against IL-6R. Similarly, IL-6R was determined by analysing the mean fluorescent intensity in the pyramidal cell layer of the CA1 and CA3 regions and the granule cell layer in the DG. With confocal images were taken under identical conditions for laser and saturation between WT and *mdx* for IL-6R for accurate later comparison in each of the hippocampal regions.

When immunofluorescence intensity was quantified, a significant increase in relative IL-6R protein expression was detected in both CA1 (63% increase, n=17 confocal images in this region from 5 WT and *mdx* animals, WT 7.072±3.764 vs *mdx* 11.61±4.543, p= 0.0126) and DG (52% increase, n=12 confocal images in this region from 5 WT and *mdx* animals, WT 2±0.9930 vs *mdx* 3.8±2.347, p=0.035) regions in *mdx* mice compared to WT (Figure 4.10). Lastly, and differing from IL-6, IL-6R expression in the CA3 region was significantly decreased in m*dx* and WT mice (n=12 confocal images in this region from 5 WT and *mdx* animals (56% decrease, WT 6.996±3.355 vs *mdx* 3.963±2.206, p=0.0242). This data can be seen in the data plot in figure 4.10 below.

Similarly, to IL-6, in the pyramidal cell layer of CA1 and CA3 and granule cell layer of DG, IL-6R expression is diffuse in the cytosol and localised to the cell membrane of both WT and *mdx* mice. Although, in CA1 and DG regions in *mdx* mice, IL-6R expression in the cell membrane is increased and for IL-6R, CA3 expression in the

cell membrane is decreased in these cell layers in comparison to WT which can be seen in the representative images in figure 4.11.

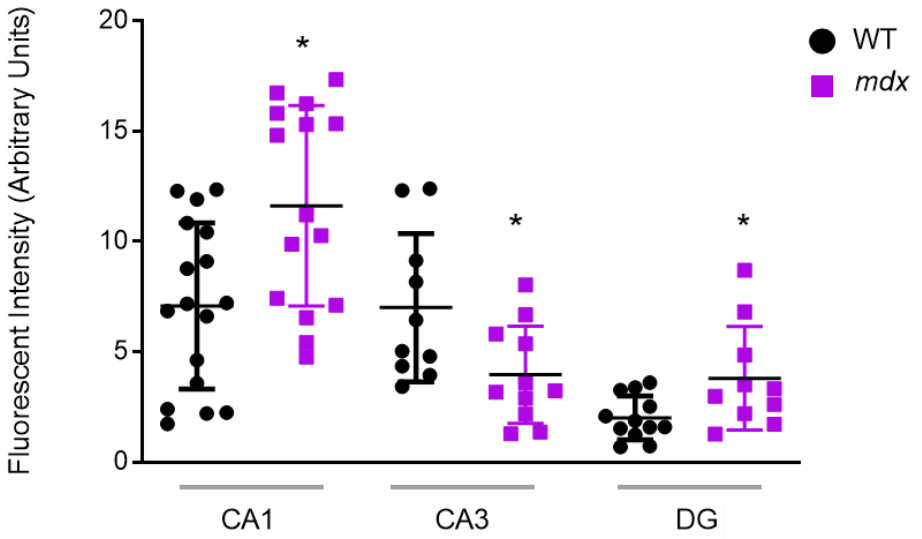


Figure 4.10: Regional hippocampal immunofluorescent expression of IL-6R is increased in dystrophin-deficient mdx mice.

The data plot illustrates a significant increase in IL-6R fluorescence in the CA1 and DG regions in mdx mice in comparison to WT mice (CA1: WT *7.072±3.764 vs mdx 11.61±4.543, p= 0.0126 and DG:* WT *2±0.9930 vs mdx 3.8±2.347, p=0.035). There is a significant decrease in IL-6R fluorescence between CA3 regions in mdx and WT mice (CA3: WT 6.996±3.355 vs mdx 3.963±2.206, p=0.0242). Scale bars are 70µm. Unpaired t test, p<0.05*.*

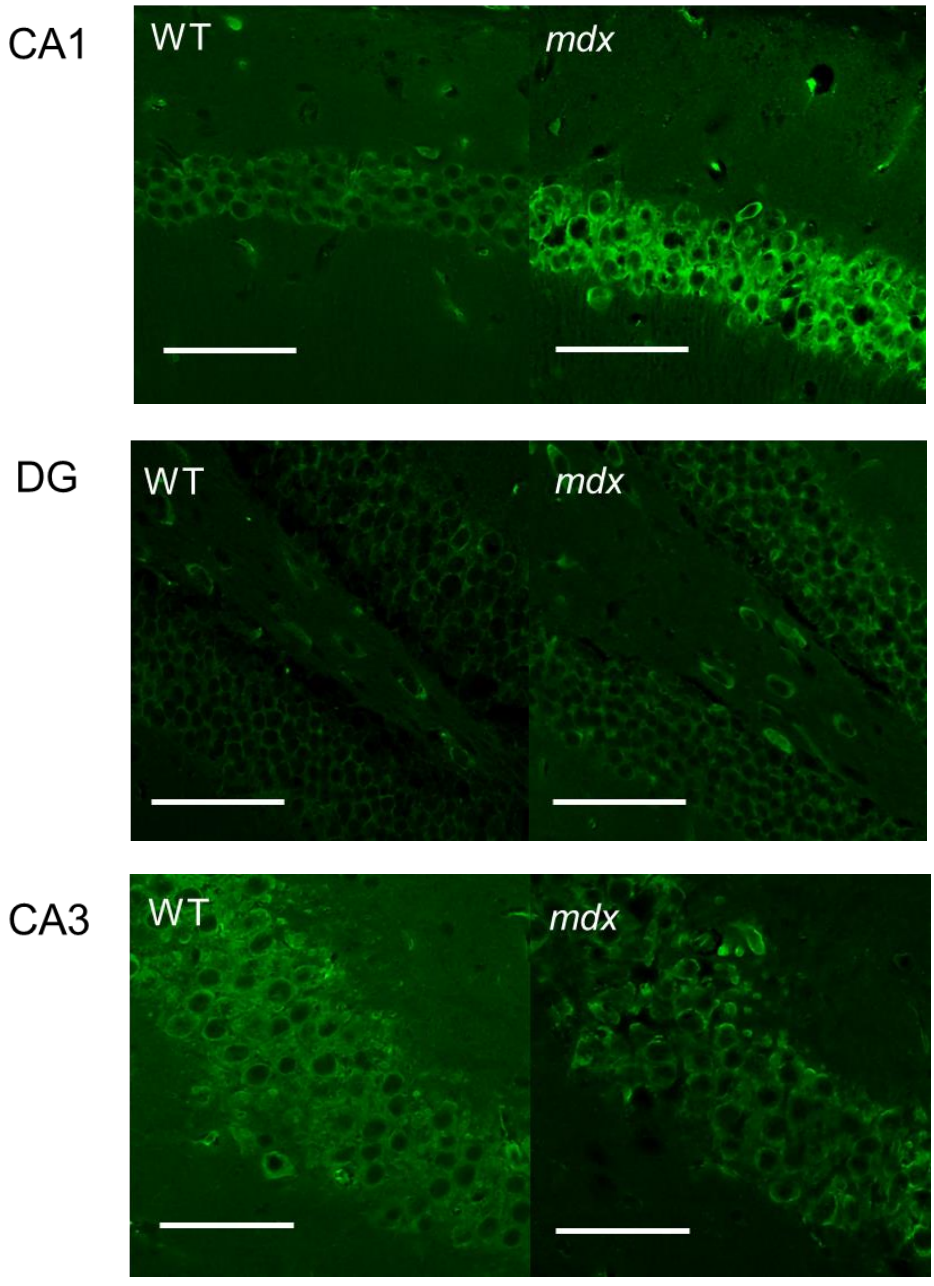


Figure 4.11: Representative images of regional hippocampal immunofluorescence illustrate that the expression of IL-6R is increased in dystrophin-deficient mdx mice.

In the pyramidal cell layer of CA1 and CA3 and granule cell layer of DG of both WT and mdx mice, IL-6R expression is diffuse in the cytosol, with IL-6R localised in the cell membrane. In mdx mice, this expression of IL-6R (fluorescence) in the cell membrane is increased in CA1 and DG in comparison to WT.

4.8. IL-6 supresses spontaneous calcium activity in dystrophin-deficient hippocampal neurons.

* *Experiments completed by Kimberley Stephenson and Michael Vaughan and data analysed by Claire Denley.*

As presented in chapter 3.4, under basal conditions spontaneous intracellular activity was increased in cultured *mdx* neurons in comparison to WT mice. To determine if the neuromodulatory cytokine, IL-6, modified this activity, the cultured neurons were exposed to exogenous recombinant IL-6 (1nM).

The pooled data and representative traces show that the elevated frequency of calcium peaks was unaffected by IL-6 in dystrophic *mdx* neurons (n= 29 neurons from 3 cultures and IL-6 did not modify activity in WT neurons (n=31 neurons from 3 cultures) either ($F(1,1027) = 0.25$, $p = 0.62$, two-way ANOVA). However, the strain difference was highly significant ($F(1, 1027) = 86.5$, $p<0.0001$) and an interaction between treatment and strain was detected ($F(1, 1027) = 6.7$, $p = 0.01$).

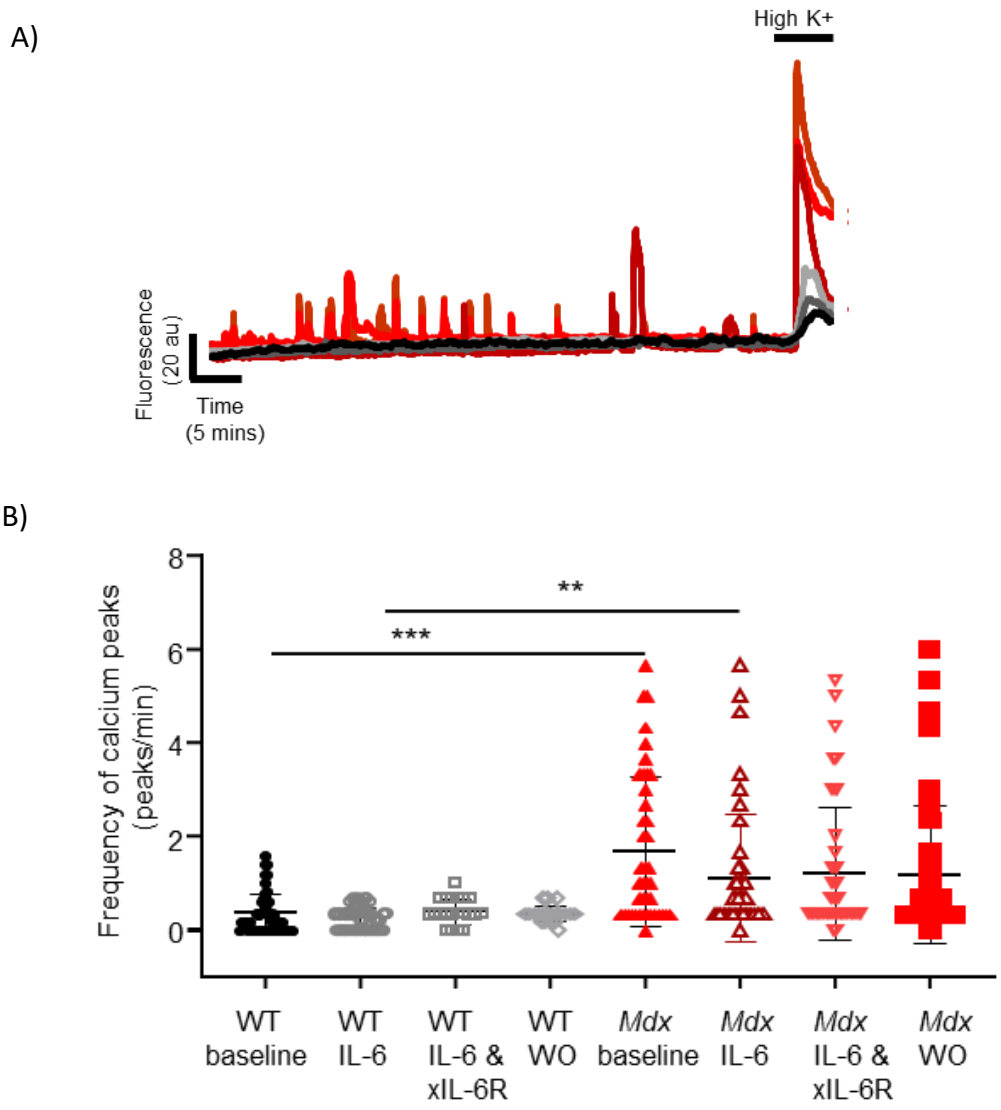


Figure 4.12: Spontaneous calcium activity in mdx hippocampal neurons is not changed by exogenous IL-6.

*The representative traces in A) show the effect of IL-6 WT neurons (grey) and mdx neurons (red) and B) The data plot illustrates the frequency of calcium peaks in WT and mdx mice following addition of IL-6 (1nM, 5 mins). Two-way ANOVA, p<0.01****

4.9. Exposure to IL-6 modifies LTP in WT but not *mdx* hippocampal slices.

While the previous experiments demonstrated that IL-6 has an impact on neuronal excitability in individual neurons, we next used extracellular electrophysiology to determine if IL-6 modified signalling pathways underpinning the formation and consolidation of new memories. Additionally, as detailed in the previous chapter (section 3.6), LTP could be generated in the Schaffer collaterals which span the CA3 to CA1 regions by applying high frequency stimulation (HFS – 4 x 100 pulses, 100Hz for 1s/60s) resulting in a long-lasting increase in the fEPSP slope, we found in control experiments, hippocampal LTP in *mdx* mice was reduced in comparison to LTP in WT mice (Chapter 3, section 3.3, pg. 77) And as IL-6 has shown to disrupt LTP with addition of exogenous IL-6 (Tancredi *et al.*, 2000), we wanted to investigate whether IL-6 has the same effect in *mdx* mice.

Hippocampal slices were perfused with aCSF containing recombinant IL-6 (1nM) for 1-hour prior to recording, as well as throughout the LTP protocol. LTP was induced as described in the previous chapter (as well as methods section 2.8, pg.58).

As in previous experiments, fEPSP baseline recordings were conducted for 20 minutes, with stimulation occurring every 30 seconds, using a current that induced fEPSPs that were 50% of the maximal size that could be generated. This recording period was followed by the application of four trains of high-frequency stimuli (HFS – 4 x 100 pulses, 100Hz for 1s/60s), with a current that induced fEPSPs that were 30% of the maximal size that could be generated.

In these experiments, immediately following the HFS, we saw the magnitude of potentiation of the fEPSP slope, was significantly decreased in WT slices perfused with exogenous IL-6 in comparison to WT controls (WT 231±35% *vs* WT + IL-6 177±25%; *p*= 0.01, unpaired t test, figure 4.13b). Importantly, this was only different in the early phase of LTP. Early LTP depends primarily on short-term kinase activity and is important in increasing synapse sensitivity but not *de novo* protein synthesis. Further, IL-6 seems to have stabilised fEPSP slopes over time in WT slices perfused with exogenous IL-6 in comparison to WT controls, which have a natural decay (figure 4.13a).

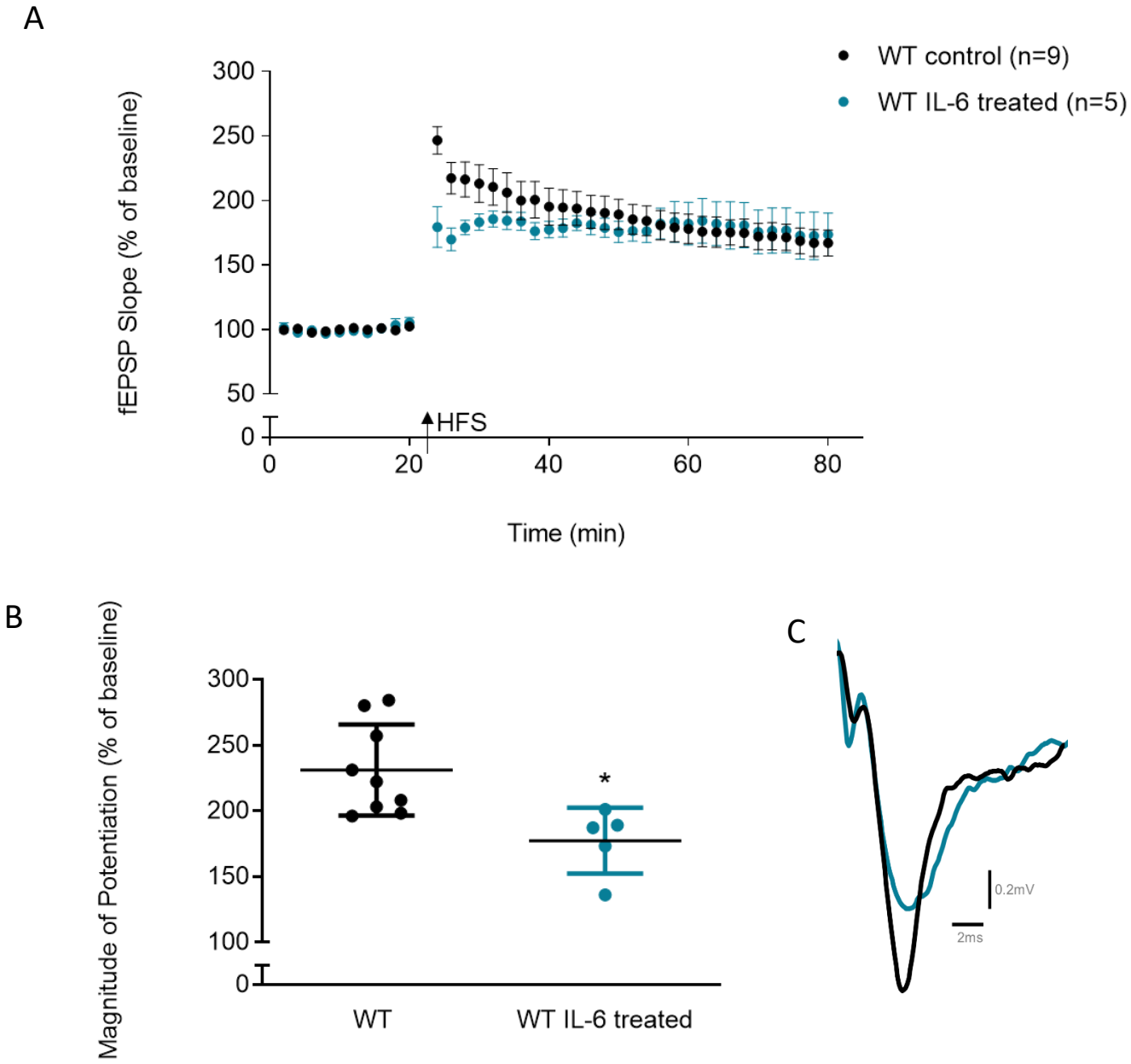


Figure 4.13: Early LTP in WT hippocampal Schaeffer collaterals-CA1 synapses was suppressed by IL-6.

- *A) Graph showing averaged time course of Schaffer collateral-evoked synaptic responses from WT controls (black circles) and WT slices perfused with IL-6 (blue circles) in the hippocampal region using extracellular field potential recordings in CA1 stratum radiatum (WT n=9; WT+IL-6 n=5). LTP was induced by high frequency stimulation (HFS) at the point indicated by the arrow.*
- *B) Immediately after LTP induction by HFS (5 minutes after LTP) the magnitude of the potentiation in in WT slices treated with IL-6 is significantly reduced in comparison to control WT slices. Unpaired t test, $p<0.05$**
- *C) Representative traces show fEPSP traces from WT controls (black line) and WT IL-6 treated (teal line).*

Following HFS in *mdx* slices perfused with exogenous IL-6, we did not see the same effect as we did in WT. Interestingly, there was no difference between *mdx* slices perfused with exogenous IL-6 and *mdx* control slices (*mdx* 168±38% vs *mdx* + IL-6 181±20%; p=0.5, unpaired t test, figure 4.14b). Also, the fEPSP slope over time in *mdx* slices perfused with exogenous IL-6 look nearly identical to *mdx* controls (figure 4.14b).

In fact, the fEPSP slope in WT slices perfused with exogenous IL-6 mirrored the fEPSP slope over time of control *mdx* mice (WT+IL-6, 177±25% *vs mdx* 168±38%, p=0.65, unpaired t test, figure 4.15b). This similarity was seen in the fEPSP slope for 50 minutes (figure 4.15a), after which WT slices perfused with exogenous IL-6 remain stable, whereas there is the decay in *mdx* controls that we also saw in WT controls. As expected, given that exposure to IL-6 reduced early LTP in WT mice but did not modify this LTP in *mdx* mice, the fEPSP slopes were also similar in WT and *mdx* hippocampal slices exposed to IL-6 (WT+IL-6, 177±25% vs *mdx* + IL-6 181±20%; p=0.81, unpaired t test, figure 4.16b). In the fEPSP slope over time (figure 4.16a), early 'stabilisation' of both WT and *mdx* by exogenous IL-6 was apparent.

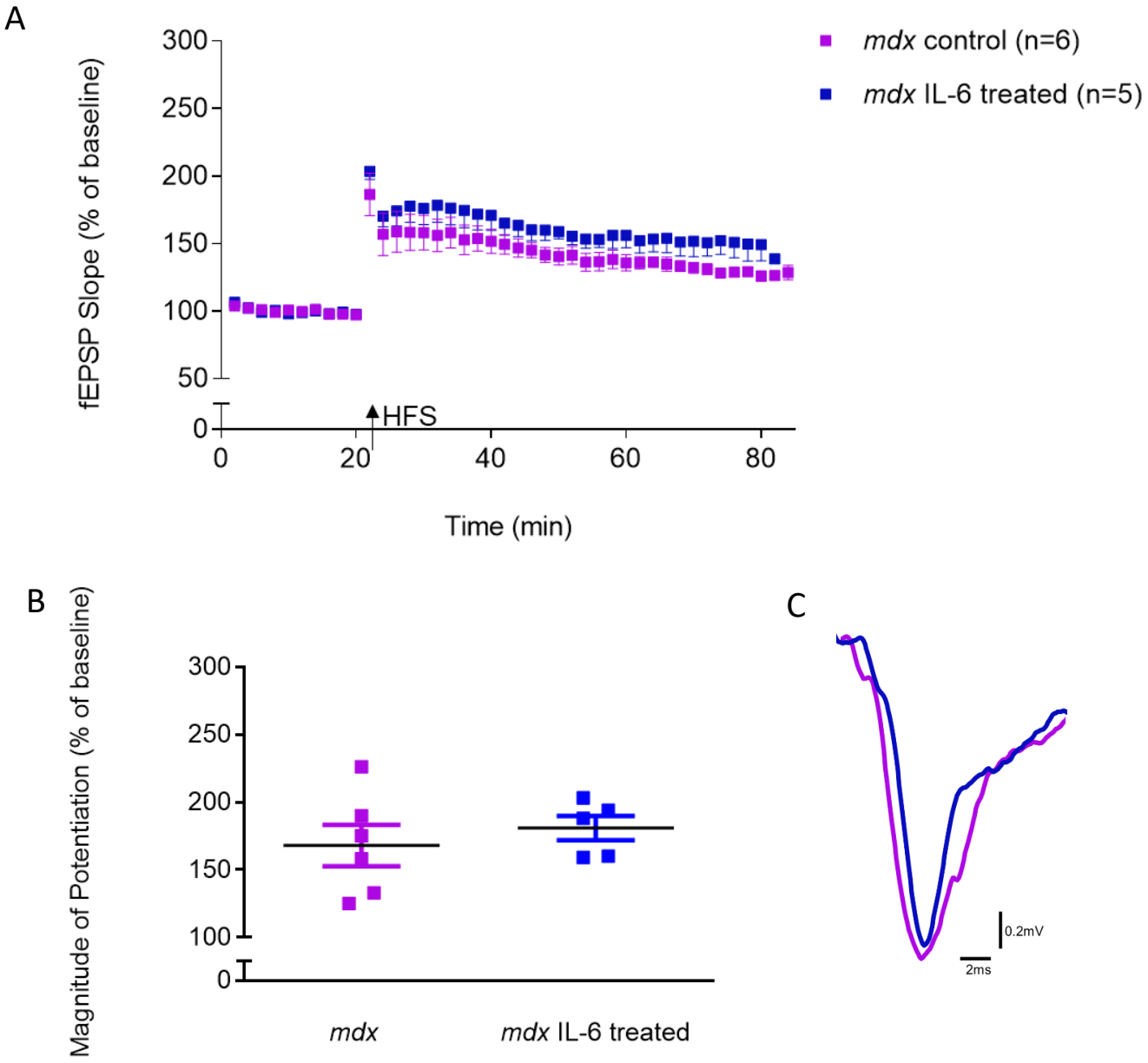
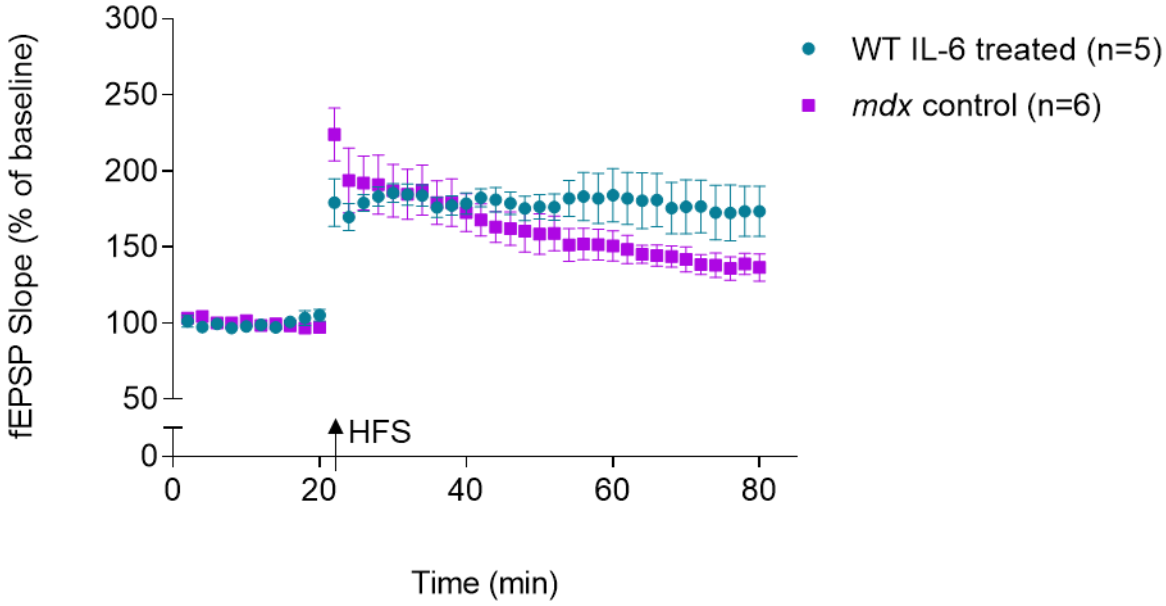


Figure 4.14: LTP in mdx hippocampal Schaeffer collaterals-CA1 synapses was not changed by IL-6.

- *A) Graph showing averaged time course of Schaffer collateral-evoked synaptic responses from mdx controls (purple squares) and mdx slices perfused with IL-6 (blue squares) in the hippocampal region using extracellular field potential recordings in CA1 stratum radiatum (mdx n=6; mdx+IL-6 n=5). Exposure to IL-6 (1nM) for 60 minutes prior to recording and for the duration of experiments.*
- *B) Immediately after LTP induction by HFS (5 minutes after LTP) the magnitude of the potentiation in mdx slices treated with IL-6 is similar to control mdx slices. Unpaired t test, p>0.05*
- *C) Representative fEPSP traces from mdx control (purple line) and mdx IL-6 treated (dark blue line) immediately after HFS.*

A



B

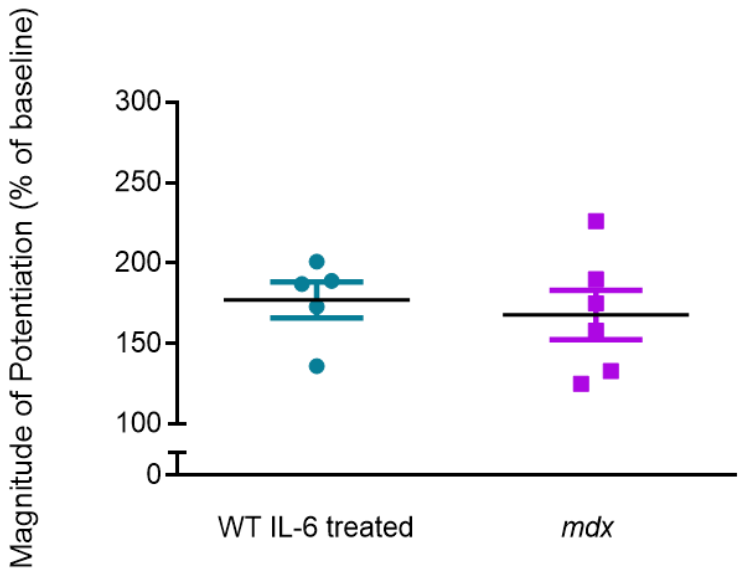


Figure 4.15: LTP generated in WT hippocampal Schaeffer collateral-CA1 synapses exposed to IL-6 is similar to untreated mdx LTP

A) Graph showing averaged time course of Schaffer collateral-evoked synaptic responses from mdx controls (purple squares) and WT slices perfused with IL-6 (blue circles) in the hippocampal region using extracellular field potential recordings in CA1 stratum radiatum (mdx n=5; mdx+IL-6 n=5). Exposure to IL-6 (1nM) for 60 minutes prior to recording and for the duration of experiments.

B) Immediately after LTP induction by HFS (5 minutes after LTP), the magnitude of the potentiation slope in WT slices treated with IL-6 is similar to control mdx slices. Unpaired t test, p>0.05

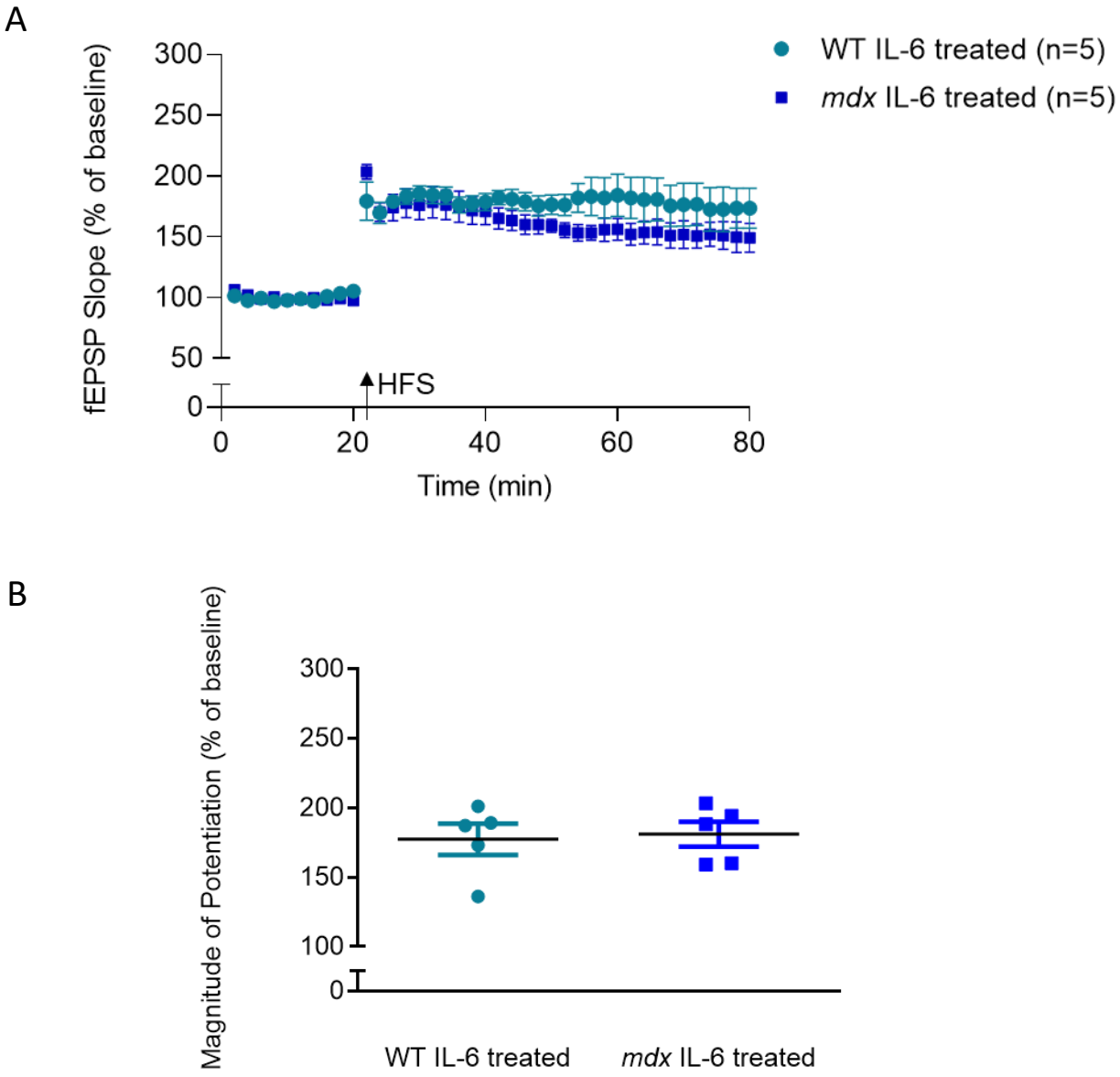


Figure 4.16: LTP generated in WT hippocampal Schaeffer collateral-CA1 synapses exposed to IL-6 is similar to LTP generated in mdx exposed to IL-6.

A) Graph showing averaged time course of Schaffer collateral-evoked synaptic responses from mdx perfused with IL-6 (blue squares) and WT slices perfused with IL-6 (blue circles) in the hippocampal region using extracellular field potential recordings in CA1 stratum radiatum (WT+IL-6 n=5; mdx+IL-6 n=5). Exposure to IL-6 (1nM) for 60 minutes prior to recording and for the duration of experiments.

B) Immediately after LTP induction by HFS (5 minutes after LTP), the magnitude of the potentiation in WT slices treated with IL-6 is similar to mdx slices treated with IL-6. Unpaired t test, $p>0.05$

4.10. Discussion

As brain dysfunction associated with loss of full-length dystrophin, Dp427, is reported to be due to dysfunctional synaptic inhibition (Perronnet & Vaillend, 2010), and neuronal dystrophin is normally expressed at PSDs, it is likely that dystrophin plays a role in synapse structure and function (Blake & Kroger, 2000). Indeed, we found that dystrophin was expressed in clusters along neuronal processes that co-localised with synaptophysin, a biomarker of synapses. We also found that IL-6R is expressed in similar way to dystrophin in that it also clusters along neuronal processes at synapses, as such the effects of IL-6R activation on synapses may be modified if dystrophin is absent from this region.

Given the elevated levels of peripheral IL-6 that is characteristic of DMD, we investigated whether IL-6 in the CNS was also elevated in the absence of dystrophin. Gene and protein expression of IL-6 in whole homogenised hippocampal tissue was not different to WT control tissue. Similarly, gene expression of IL-6R, gp130, the transmembrane protein which initiates the downstream signalling cascade, and STAT3, a signalling molecule activated by IL-6 were unchanged. However, the caveat of this experimental design is that regional differences, which are critical to the function of the hippocampus, cannot be elucidated. Further investigation, using immunofluorescent localisation demonstrated region-specific changes in IL-6 and IL-6R expression in dystrophin-deficient *mdx* tissue. There was an increase in IL-6 and IL-6R expression in the CA1 and DG region of the hippocampus of *mdx* mice in comparison to WT with a surprising decrease in IL-6R in the CA3 region in *mdx* mice compared to WT. The

CA1 and CA3 region of the hippocampus is important in LTP, the proposed correlate of learning and memory, as LTP can be induced along the Schaeffer-collateral (emanating in CA3)– CA1 pathway. Further, the DG, in the hippocampus, is of importance as it is one of the few brain regions where neurogenesis occurs and adult-born neurons are integrated into pre-existing neuronal circuits (Gage, 2000). In fact, IL-6 has been shown to influence neural stem cells in hippocampal adult neurogenesis (Islam *et al.*, 2009), with proliferation, survival and differentiation of hippocampal progenitor cells being compromised in the dentate gyrus when IL-6 concentrations are elevated (Vallieres *et al.*, 2002). Thus, an increase in IL-6 in *mdx* mice in these regions, could in part, explain deficits in neurogenesis and LTP. As well as a possible impact of IL-6 on neurogenesis and LTP, LTP itself can impact on neurogenesis (Bruel-Jungerman, 2006). A study by Bruel-Jungerman (2006) found that electrically induced LTP in the dentate gyrus in vivo provides a cellular/molecular environment that favours both proliferation and survival of adult-generated neurons, thus there likely may be a sort of coupling between synaptic plasticity and neurogenesis. Further, LTP can be induced more easily in newly born cells such as granule cells in the dentate gyrus (Schmidt-Hieber et al., 2004), thus an increase of neurogenesis in *mdx* DG that has previously been reported (Deng *et al.*, 2009) may underlie changes in LTP and associated cognitive deficits seen in DMD.

Our results showed that exposure to IL-6 reduced early-phase LTP induction in WT slices and this finding supports previous work which has also shown that IL-6 can modify LTP (Li *et al.*, 1997; Tancredi *et al.*, 2000; Stampanoni Bassi *et al.*, 2019). However, this difference was only seen in early LTP. At a molecular level, early LTP

includes activation of AMPA receptors, calcium influx through activated NMDA receptors which subsequently activates CaMKII, which eventually potentiates synaptic transmission. Later (> 1 hour following the high frequency stimulation) stimulation of gene transcription leads to *de novo* protein synthesis. However, if early LTP is disrupted or modified, that might impact on later cellular events. Importantly, IL-6 can serve as a negative regulator of both early and late LTP in the hippocampus (Bellinger et al., 1995; Li et al., 1997; Tancredi et al., 2000; Balschun et al., 2004) through multiple signalling pathways including p42/44 mitogen-activated protein kinase (MAPK) (Engberink et al., 2017). Interestingly though, after endogenous addition of IL-6 to *mdx* slices, there was no effect on LTP induction.

Although, the exact mechanism through which IL-6 could modify LTP is not yet known, this could be due to decreased IL-6R expression in the CA3 region of *mdx* mice, where the Schaffer collaterals are stimulated. Thus, chronic exposure to elevated IL-6 could have resulted in receptor internalisation or it is possible that reduced LTP observed in *mdx* mice could be due to a complex interplay between local IL-6 levels paired with abnormal neuron functioning due to a loss of synaptic dystrophin. As was noted with aberrant $GABA_AR$ clustering in *mdx* hippocampal neurons (Knuesel *et al.*, 1999; Knuesel *et al.*, 2001), it is possible that hippocampal IL-6Rs may not be appropriately expressed on the neuronal cell membrane, or, perhaps down-stream signalling is dysfunctional resulting in insensitivity to IL-6. While further research is needed to reveal the precise signalling mechanisms, these studies suggest that while overall IL-6 levels or IL-6R levels in the brain are not changed in dystrophic mice, there may be local changes in expression that could modify hippocampal LTP. Increases in IL-6 expression could be due to increases in

circulatory IL-6 that has been transported from the periphery across the BBB (Banks *et al.*, 1994) or IL-6 could be released locally in the brain from astrocytes and microglia during pathophysiological events such as inflammation (Gruol & Nelson, 1997), both of which could occur in DMD due to increased peripheral IL-6 (Rufo *et al.*, 2011; Pelosi *et al.*, 2015) and inflammation caused by a loss of dystrophin.

We also investigated the effect of exogenous IL-6 on calcium homeostasis in cultured hippocampal neurons. Though, exogenous IL-6 had no effect on neuronal activity in the *mdx* mouse. This aligned with our findings that the addition of IL-6 does not alter hippocampal LTP in *mdx* mice. Importantly, the experiments on neuronal activity were completed on cultured hippocampal neurons whereas, LTP experiments were done on intact hippocampal slices which could imply that there are other complex mechanisms at play on a physiological level, not just at a cellular level.

4.11. Conclusions

Although we did not detect changes in mRNA expression of components of the IL-6 pathway, namely IL-6, IL-6R, gp130 and STAT3, in whole hippocampi of *mdx* mice, we did see regions specific increases in both IL-6 and IL-6R in the CA1 and DG region of the hippocampus. This increase in IL-6 could possibly be due to the elevation of IL-6 in the periphery of *mdx* mice (Pelosi *et al.*, 2015) as IL-6 has been shown to cross the BBB *via* saturable transport mechanisms (Banks *et al.*, 1994) or local production of IL-6 from astrocytes and microglia, which are activated during inflammation.

Consistent with the findings of others (Li *et al.*, 1997; Tancredi *et al.*, 2000; Stampanoni Bassi *et al.*, 2019) and our own experiments, addition of exogenous IL-6 suppressed early-phase LTP in dystrophin-expressing WT mice. Following tetanic stimulation, changes in post-synaptic expression and activation of AMPA and NMDA receptors lead to depolarisation of the post-synaptic neuron and influx of calcium. This in turn results in activation of intracellular CaMKII and other protein kinases and are the key first steps in creating new memories. Elevated IL-6 suppresses this activity under normal circumstances, however, *mdx* mice were resistant to this effect. This could be due to altered expression of IL-6Rs in *mdx* hippocampal tissue. While increased IL-6R expression was observed in the CA1 and DG regions, IL-6R expression was specifically decreased in the CA3 region, the site where the tetanic stimulus is applied to generate LTP. While further work is needed to elucidate why these changes in IL-6R expression have occurred in specific dystrophic hippocampal regions, it does appear that these changes have had functional consequences in the cellular and molecular processes that underpin learning and the consolidation of memories

Chapter 5

Intervention study: Neutralisation of IL-6 receptor-mediated signalling improves cellular correlates of learning and memory.

5.1. Introduction

As demonstrated in the previous chapter, IL-6 could modulate the cellular processes underpinning learning and memory (figure 4.14, pg. 76). Research has shown that circulating levels of IL-6 are higher in severe neurological pathologies such as Alzheimer's and dementia (Campbell *et al.*, 1993) and similarly, transgenic mice over-expressing IL-6 exhibit broad memory impairment (Heyser *et al.*, 1997; Wei *et al.*, 2012; Wei *et al.*, 2013). Other studies have shown that transgenic mice deficient in IL-6 possess enhanced spatial learning capabilities in the radial arm maze (Braida *et al.*, 2004) and the Morris water maze (Bialuk & Winnicka, 2018) behavioural task-learning assessments, further emphasising the pleiotropic actions of this cytokine in the CNS. Consistent with these findings, IL-6 has also been shown to inhibit LTP (Li *et al.*, 1997; Tancredi *et al.*, 2000; Stampanoni Bassi *et al.*, 2019)as well as a blockade of endogenous IL-6 with a neutralizing IL-6 antibody, resulted in a remarkable prolongation of LTP, as well as improved performance in spatial memory tests (Balschun *et al.*, 2004).

In the *mdx* mouse model of DMD, inhibition of IL-6 signalling with the monoclonal anti-IL-6 receptor antibody (xIL-6R) improves the muscular physiology of DMD such as increasing diaphragm muscle force (Manning *et al.*, 2017) and overall respiratory function (Burns *et al.*, 2018) in *mdx* mice. Skeletal muscle regeneration is also improved by xIL-6R treatment (Wada *et al.*, 2017). It is also notable that another recombinant (humanized) monoclonal IL-6R antagonist (tocilizumab), which has been approved as an anti-inflammatory drug for inflammatory diseases such as rheumatoid arthritis, Castleman's disease, and systemic juvenile idiopathic arthritis,

has also shown promise in alleviating the muscular symptoms of DMD (Wada *et al.*, 2017). Tocilizumab blocks IL-6-mediated signalling via an inhibition of the binding of IL-6 to both soluble and transmembrane IL-6Rs in the same way as xIL-6R.

DMD patients have an increased incidence of mild-to-moderate cognitive impairment (Bresolin *et al.*, 1994; Anderson *et al.*, 2002) and exhibit impaired verbal, short-term and working memory (Snow *et al.*, 2013). Similarly, *mdx* mice display behaviours that are consistent with dysfunctions of the hippocampus and amygdala, such as a poor capacity to learn new tasks and deficits in spatial learning tasks, relative to controls (Vaillend *et al.*, 1995; Vaillend *et al.*, 2004; Chaussenot *et al.*, 2015). They also display deficits in associative learning and in the general processes involved in memory formation and consolidation which are both dependent upon optimal functioning of the hippocampus and amygdala (Chaussenot *et al.*, 2015). Along with cognitive impairment, DMD is also associated with a number of behavioural issues, such as anxiety, depression and Attention-Deficit / Hyperactivity Disorder (ADHD) (Rubinsztein *et al.*, 1998; Hendriksen & Vles, 2008). Behavioural abnormalities have also been observed in the *mdx* mouse model, with increases in both depressive behaviour and anxiety and fearfulness observed relative to controls (Manning *et al.*, 2014), sometimes independently of any skeletal muscle impairment (Sekiguchi *et al.*, 2009). Interestingly, increased levels of IL-6 in the blood have been associated with major depressive disorder (Dowlati *et al.*, 2010; Haapakoski *et al.*, 2015). Similarly, IL-6 knockout mice (IL-6 KO) show alterations in anxiety-like and depression-like behaviours (Armario *et al.*, 1998; Butterweck *et al.*, 2003; Chourbaji *et al.*, 2006; Aniszewska *et al.*, 2015).

Given that inhibition of IL-6-mediated signalling in the brain appears to enhance learning and memory, we hypothesised that central administration of neutralising xIL-6R antibodies to block IL-6 signalling, would have beneficial effects on hippocampal function in dystrophic animals.

5.1.1. Study objectives

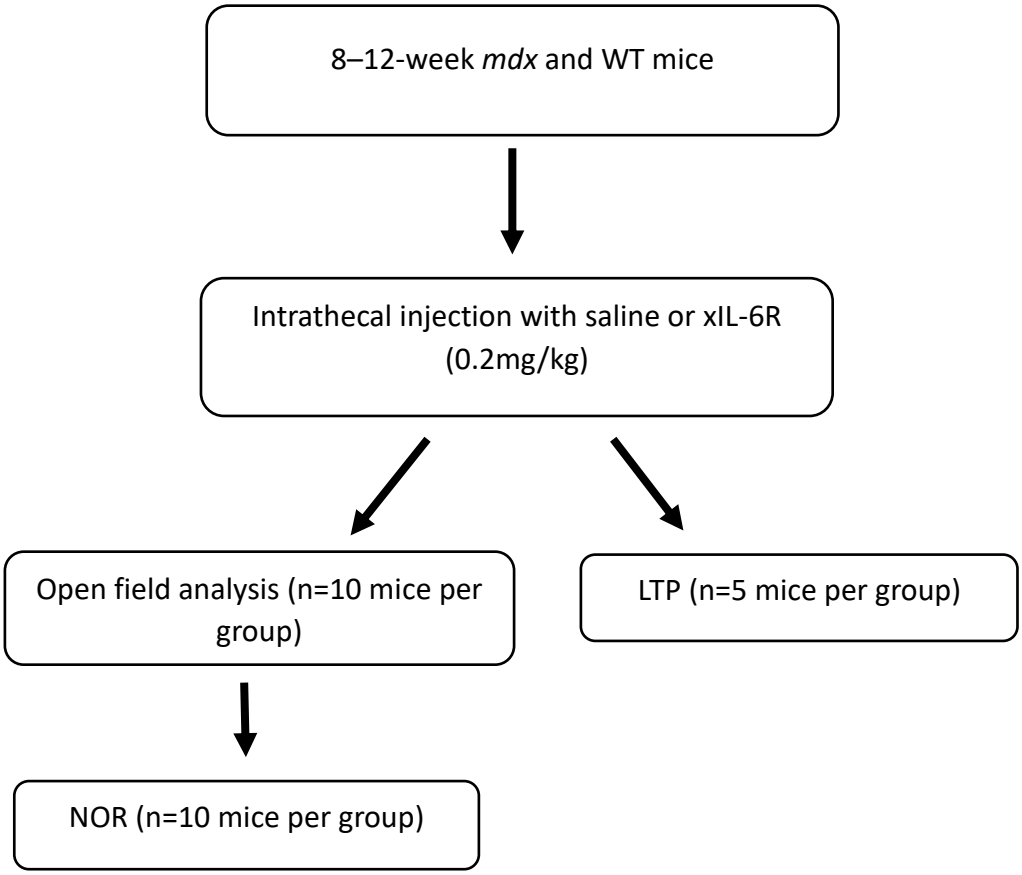
- To investigate if intrathecal delivery of monoclonal anti-IL-6 receptor antibodies modifies hippocampal long-term potentiation in dystrophin-deficient *mdx* mice.
- To determine if behavioural patterns are modified by the administration of monoclonal anti-IL-6 receptor antibodies.

5.1.2. Techniques used

- Intrathecal injection (see methods section 2.9, pg. 65).
- Extracellular electrophysiology (see methods section 2.8, pg. 59).
- Open field behavioural test (see methods section 2.7.3, pg. 58).

5.2. Study design for intervention

WT and *mdx* mice aged 8-12 weeks were intrathecally injected with a monoclonal anti-IL-6 receptor (xIL-6R) antibody between the L5 and L6 region of the spine (see methods section 2.9, pg. 64). Mice were allowed to recover for 24 hours and then underwent behavioural studies and electrophysiological studies.



5.3. Intrathecal administration of xIL-6R antibodies normalises hippocampal LTP in *mdx* mice.

In chapter 3, we reported that LTP was significantly reduced in *mdx* mice in comparison to WT (Figure 3.4, pg. 76) thus, we sought to determine if *in vivo* neutralisation of central IL-6 signalling modified this.

Following all LTP experiments in this thesis, monopolar stimulation of the Schäffer collaterals was performed through an electrode located on the border between areas CA1 and CA3. Baseline stimulations were recorded for 20 minutes following input/output curves at the intensity (mA) required to obtain 50% of the maximum output. High-frequency stimulation (HFS – 4 x 100 pulses, 100Hz for 1s/60s) followed the baseline, with stimulation intensity at 30% required for maximum output.

In *mdx* mice administered with intrathecal xIL-6R, immediately after HFS, the magnitude of LTP was significantly increased compared to saline treated *mdx* animals (saline treated 199.5±32% vs xIL-6R 282.3±6.11%, p=0.0074, n=3 animals, unpaired students t test, figure 5.1b, c). Furthermore, this potentiation was observed for the remaining 80 minutes of each experiment following HFS, such that LTP was significantly increased in *mdx* mice treated with xIL-6R (n=3) hippocampal slices as compared to saline treated *mdx* animals (n=3, Genotype factor, F (1, 3) = 10,51, p= 0.0478, two-way repeated-measures ANOVA starting at 1 min after stimulation, figure 5.1a).

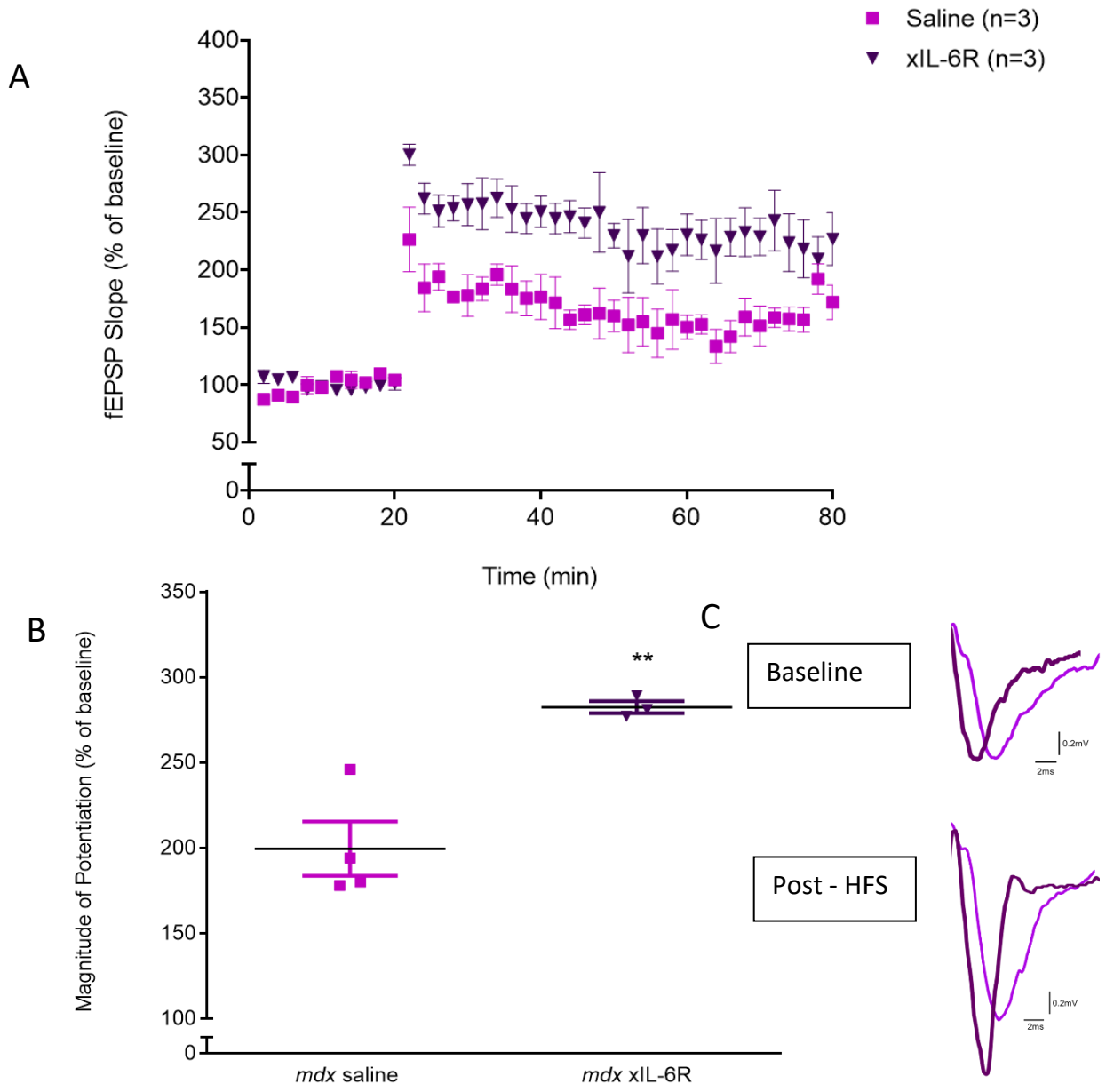


Figure 5.1: Long-term potentiation in the SC-CA1 pathway of the hippocampus in mdx mice intrathecally-injected with xIL-6R is enhanced compared to saline treated mdx controls.

- *A) Graph showing averaged time course of Schaffer collateral-evoked synaptic responses from saline treated mdx (purple squares) and xIL-6R-treated mdx (dark purple triangles) in the hippocampal region using extracellular field potential recordings in CA1 stratum radiatum (mdx n=3; xIL-6R-treated mdx n=3). Two-way ANOVA, p<0.001****
- *B) Immediately after LTP induction by HFS, the magnitude of potentiation in mdx mice intrathecally injected with xIL-6R is enhanced in comparison to saline treated controls (n=3, p= 0.0074**). Unpaired t test, p<0.01***
- *C) Representative traces show fEPSPs before and after high frequency stimulation to induce LTP in saline treated and xIL-6R treated mdx mice. At baseline, untreated (light purple) and treated (dark purple) fEPSP slopes (mV/ms) are similar, whereas, post-HFS, fEPSP slopes are significantly increased in treated mdx mice.*

Unlike its restorative effects on LTP in *mdx* mice, *in vivo* treatment of WT mice with xIL-6R did not have the same effect. Immediately following HFS, there was no significant difference between the magnitude of potentiation of the fEPSP for the first 5 minutes in WT mice treated with xIL-6R and saline treated WT controls (saline 192± 24% vs xIL-6R 209± 41.9%, p=0.3835, n=3-4 animals, unpaired students t test; Figure 5.2b, c). Furthermore, this potentiation was observed for the remaining 80 minutes of each experiment following HFS, with no change in LTP magnitude between slices from WT mice treated with xIL-6R (n=4) hippocampal slices compared to saline treated WT controls (n=3, Genotype factor, F (1, 4) = 0,1953, p= 0.6813, two-way repeated-measures ANOVA starting 1 min after stimulation, figure 5.2a).

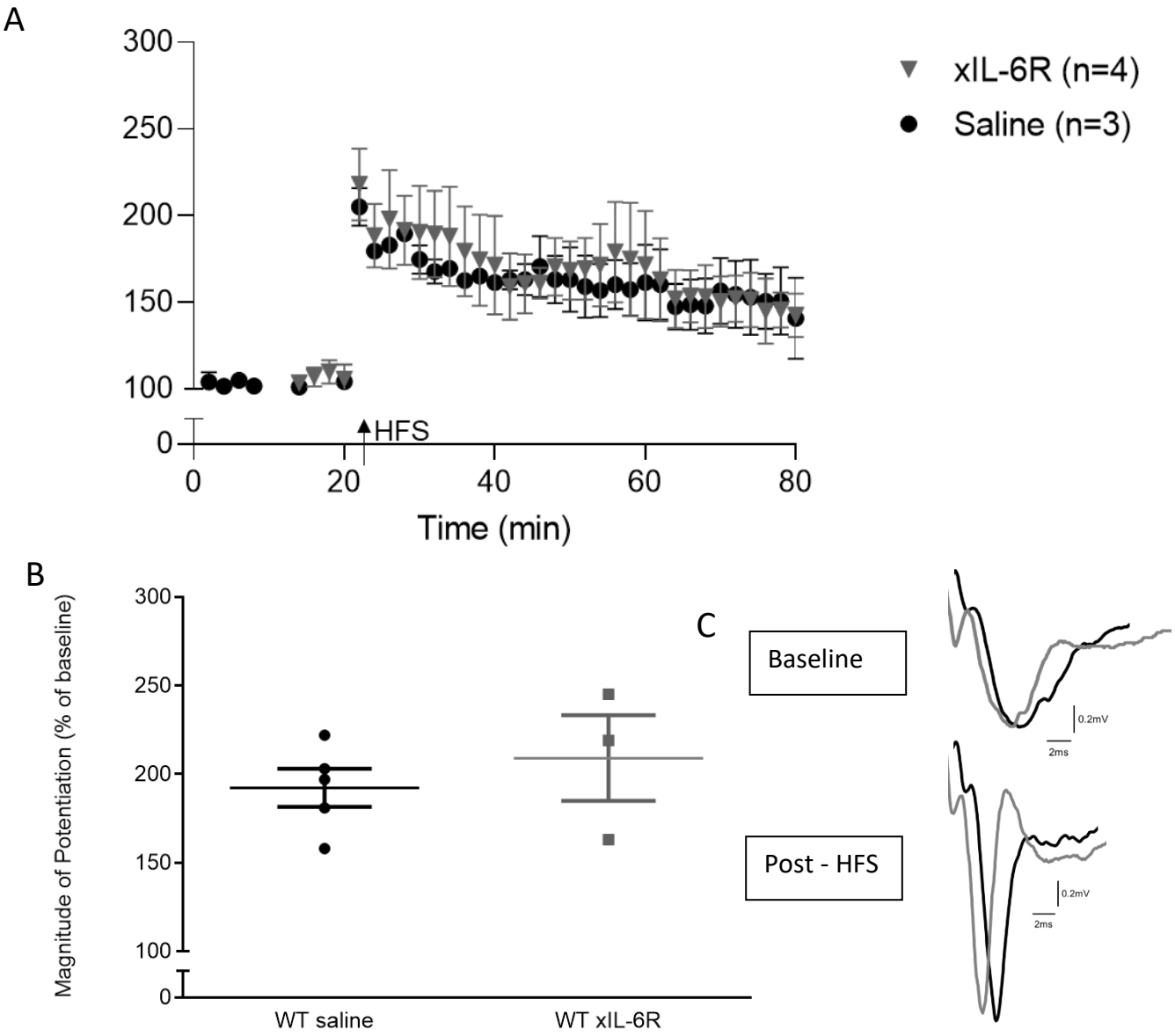


Figure 5.2: Long-term potentiation in the SC-CA1 pathway of the hippocampus in WT mice intrathecally-injected with xIL-6R is similar compared to untreated WT controls.

- *A) Graph showing averaged time course of Schaffer collateral-evoked synaptic responses from saline treated WT (black circles) and xIL-6R-treated WT (grey triangles) in the hippocampal region using extracellular field potential recordings in CA1 stratum radiatum (saline treated WT n=3; xIL-6R-treated WT n=3). Two-way ANOVA, p>0.05*
- *B) Immediately after LTP induction by HFS, the magnitude of potentiation in WT mice intrathecally injected with xIL-6R is similar to saline treated controls (n=3-4, p=0.4885). Unpaired t test, p>0.05*
- *C) Representative traces show fEPSPs before and after high frequency stimulation to induce LTP in saline treated and xIL-6R treated WT mice. At baseline and post-HFS, untreated (black) and treated (grey) fEPSP slopes (mV/ms) are similar.*

As a control for the injection procedure itself, the effects of intrathecal administration of saline on LTP induction and maintenance were examined and compared to those from the original, untreated WT animals and untreated *mdx* animals.

In WT mice, LTP magnitude was not significantly different between saline-injected and untreated WT mice, suggesting that the injection procedure itself had no effect on either LTP induction and/or maintenance. The initial magnitude of potentiation following HFS did not differ significantly between untreated and saline-injected WT animals (untreated WT, 216.4± 22 vs saline 200.8± 16.9, p= 0.1308; unpaired student t test, n=4-9 animals, figure 5.3b). Furthermore, this potentiation was observed for the remaining 80 minutes of each experiment following HFS, with no change in LTP between WT mice injected with saline (n=4) as compared to untreated controls (n=9, factor genotype, Genotype factor, F (1, 11) = 0.8061, p= 0.3885, two-way repeated-measures ANOVA starting at 1 min after stimulation, figure 5.3a).

The injection procedure had a similar lack of significant effect on LTP induction and/or maintenance in slices from *mdx* mice. The initial magnitude of potentiation following HFS did not differ significantly between untreated and saline-injected *mdx* animals (untreated *mdx* 174.8± 37.5 vs saline, vs 199.5± 31.8, p= 0.33; unpaired student t test, n= 4-5 animals, figure 5.4b). Furthermore, this potentiation was observed for the remaining 80 minutes of each experiment following HFS, with no change in LTP between *mdx* mice injected with saline (n=4) as compared to untreated controls (n=5, factor genotype, Genotype factor, F (1, 7) = 0.1513,

p=0.71, two-way repeated-measures ANOVA starting at 1 min after stimulation, figure 5.4a). This provided us with confidence that the restoration of LTP in *mdx* mice was due to central neutralisation of IL-6Rs.

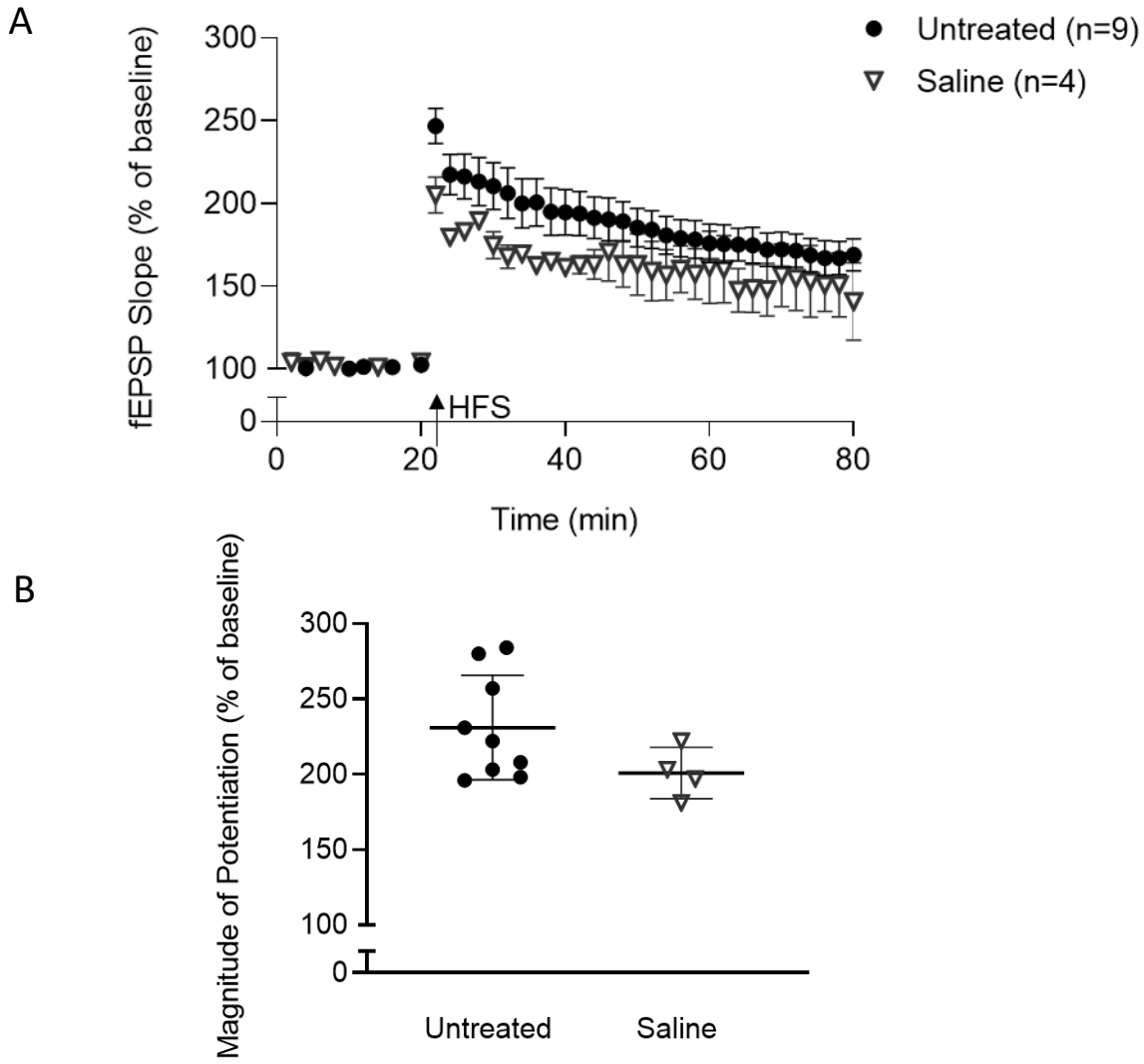
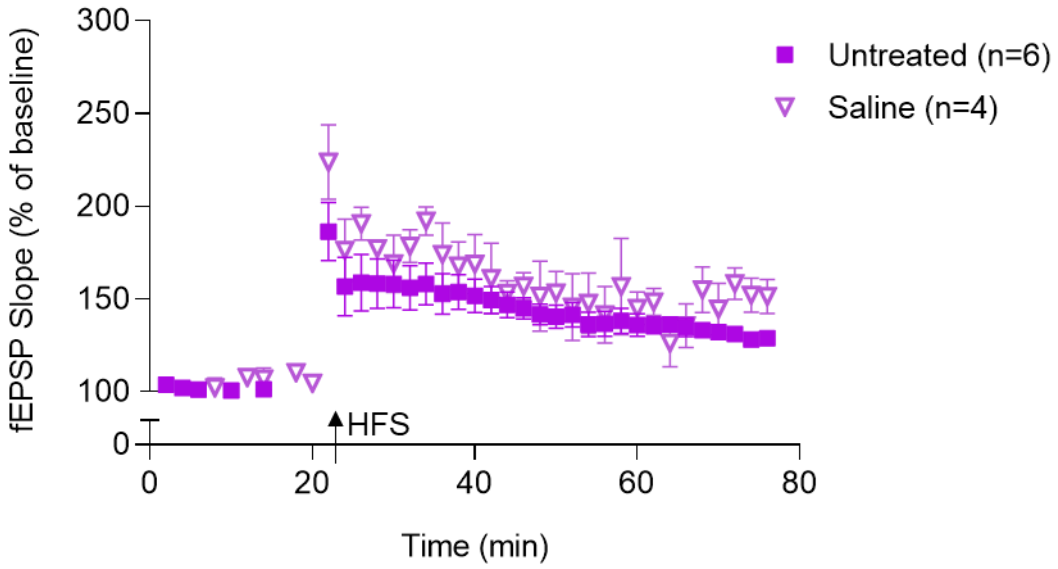


Figure 5.3: Intrathecal injection of saline had no impact on LTP induction and/or maintenance in WT mice.

A) *Graph showing averaged time course of Schaffer collateral-evoked synaptic responses from untreated WT (black circles) and saline-treated WT (grey triangles) in the hippocampal region using extracellular field potential recordings in CA1 stratum radiatum (WT n=9; saline treated WT n=4). Two-way ANOVA, p>0.05*
B) *Immediately after LTP induction by HFS, the magnitude of the potentiation in WT mice intrathecally injected with saline is similar to untreated WT mice (n=4-9, p=0.252). Unpaired t test, p>0.05*

A



B

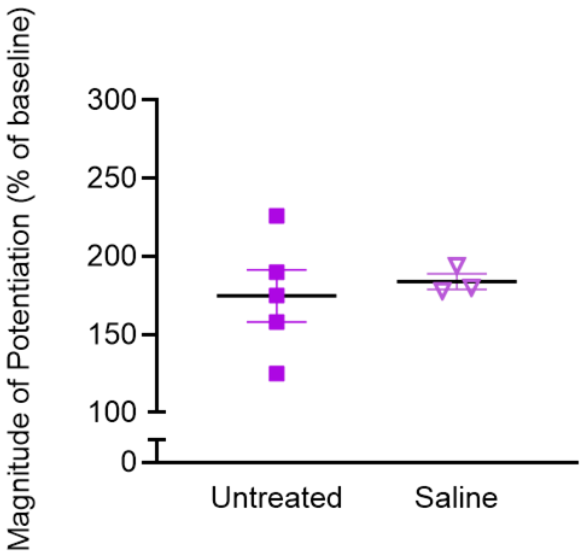


Figure 5.4: Intrathecal injection of saline had no impact on LTP induction and/or maintenance in mdx mice.

- *A) Graph showing averaged time course of Schaffer collateral-evoked synaptic responses from untreated mdx (purple squares) and saline-treated mdx (open purple triangles) in the hippocampal region using extracellular field potential recordings in CA1 stratum radiatum (mdx n=6; saline treated mdx n=4). Two-way ANOVA, p>0.05*
- *B) Immediately after LTP induction by HFS, the magnitude of potentiation in mdx mice intrathecally injected with saline is similar to untreated mdx mice (n=4-6, p=0. 33). Unpaired t test, p>0.05*

5.4. xIL-6R administration did not modify NOR recognition memory in WT or *mdx* mice.

Having observed such a dramatic restoration of the cellular correlate of learning and memory in *mdx* mouse hippocampal slices intrathecally injected with xIL-6R, we next investigated whether or not this potentiation of LTP in *mdx* mice translated into functional changes in behaviour, by repeating the NOR test in these mice.

As described in chapter 3, NOR uses two similar objects on a first testing day, and the mouse is left to explore for 10 minutes. 24 hours later, one of the similar objects is replaced with a novel object and once again the mouse is left to explore the area for 10 minutes. A percent of time spent exploring the novel object relative to the total time spent exploring both objects can be a measure of novel object recognition (Benice *et al.*, 2006; Sarkisyan & Hedlund, 2009; Broadbent *et al.*, 2010; Oliveira *et al.*, 2010). This concept can be represented by *Recognition Index* (RI), i.e., the time spent investigating the novel object relative to the novel object and the familiar object investigation [RI = T_N/ (T_N + T_F)], and it is the main index of retention (Mumby *et al.*, 2002; Piterkin *et al.*, 2008; Botton *et al.*, 2010; Gaskin *et al.*, 2010; Schindler *et al.*, 2010).

Despite its clear effects on LTP, intrathecal injection of xIL-6R did not appear to have any effect on recognition memory. No significant differences were seen in the time spent investigating the novel object relative to the novel object and the familiar object investigation (RI) between WT and *mdx* mice treated with either saline or xIL-6R (WT saline 0.76±0.04 vs xIL-6R 0.77±0.027, p=0.7088 and *mdx* saline 0.79±0.036 vs *mdx* xIL-6R 0.8±0.02, p=0.7601, unpaired t test, Figure 5.6).

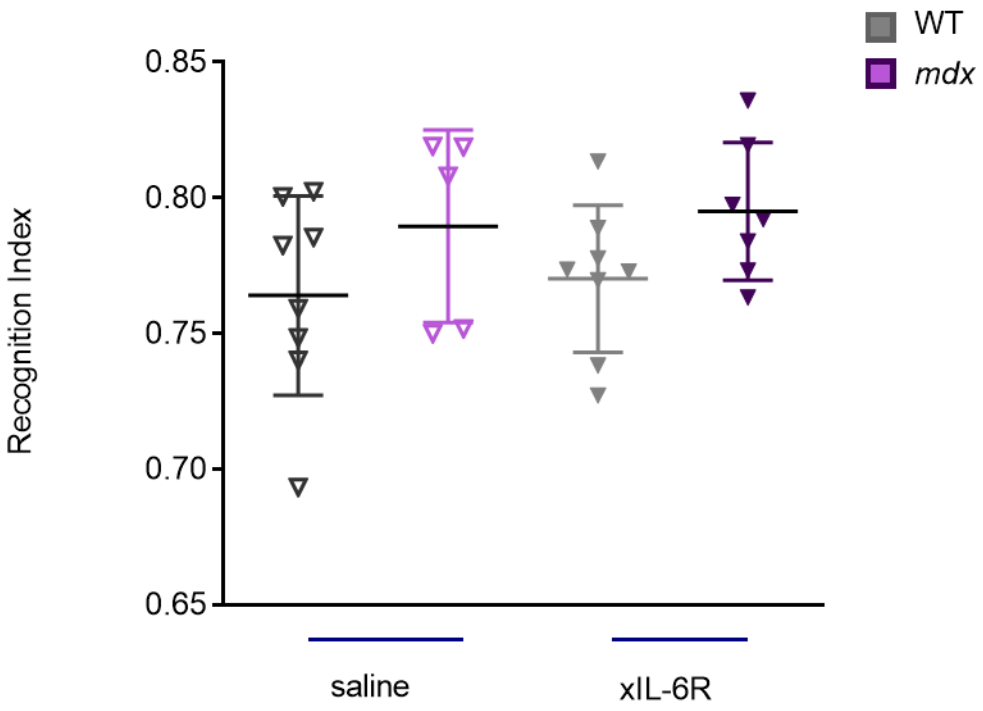


Figure 5.5: The NOR recognition index values for mdx and WT mice injected intrathecally injected with either saline or xIL-6R did not differ significantly from each other. Unpaired t test, p>0.05

5.5. Anxiety-like behaviours in *mdx* mice.

We showed in chapter 3 that freezing behaviours, which are associated with a fear response in mice (Sekiguchi *et al.*, 2009), are significantly increased in untreated *mdx* mice in comparison to untreated to WT mice. Therefore, we wanted to next investigate the effects of intrathecal administration of xIL-6R on freezing and anxiety-like behaviours (methods section 2.7.3, pg. 58).

These experiments showed that *mdx* mice administered with saline alone (n=7) were significantly more reluctant to enter the centre of the open field arena in comparison to saline-treated WT mice (n=10, two-way ANOVA, Strain, F (1, 29) =

9.063, p=0.005, Figure 5.6a) which is a behaviour consistent with increased anxiety (Hölter *et al.*, 2015) in this strain. Intrathecal injection of xIL-6R had no impact on this anxiety-like phenotype in the *mdx* mice (n=7, Intervention, F (1, 29) = 0.14, p=0.71).

Increased freezing, a recognised fear response in mice (Sekiguchi *et al.*, 2009) did not significantly differ between WT (n=9) and *mdx* mice (n=7) injected with either saline (two-way ANOVA, Strain, F (1, 29) = 2.0, p= 0.17, figure 5.6b) or xIL-6R (two-way ANOVA, intervention, F (1, 29) = 0.1, p=0.75).

Grooming frequency also did not differ significantly between WT (n=9) and *mdx* mice (n=7) treated with either saline (two-way ANOVA, Strain, F (1, 27) = 0.006, p=0.9, figure 5.6c) or xIL-6R (two-way ANOVA, Intervention, F (1, 27) = 0,1538, p= 0.7).

Escape behaviours were also assessed and showed that rearing frequency increased significantly in saline-treated *mdx* mice (n=6) in comparison to saline-treated WT mice (n=10, two-way ANOVA, Strain, F (1, 28) = 6.054, p=0.02, figure 5.6d). However, xIL-6R administration had no significant effect on the rearing frequency observed in the WT (n=9) and *mdx* mice (n=7, two-way ANOVA, Intervention, F (1, 28) = 0.006, p=0.94).

When we next counted the number of faecal boli excreted over 10 minutes as a measure of anxiety, we found that the number excreted by saline-treated *mdx* mice (n=7) did not differ significantly to that excreted by the saline-treated WT mice (n=9, two-way ANOVA, Strain, F (1, 27) = 1.76, p= 0.2, figure 5.6e). Further, administration of xIL-6R had no significant effect on the number of faecal boli

excreted by WT (n=8) or *mdx* mice relative to the saline-treated animals (n=7, two-way ANOVA, Intervention, $F(1, 27) = 0.65$, $p = 0.4$).

Finally, we found no significant difference in the frequency of jumping in the saline-treated *mdx* mice (n=7) relative to the saline-treated WT mice (n=10, two-way ANOVA, Strain, $F(1, 24) = 0.77$, $p = 0.4$, figure 5.6f). Further, administration of xIL-6R also had no significant effect on the frequency of jumping observed in either the WT (n=9) or *mdx* mice relative to the saline-treated animals (n=7, two-way ANOVA, Intervention, $F(1, 24) = 0.03$, $p = 0.9$).

Overall, the intrathecal administration of xIL-6R had no effect on these behavioural outputs.

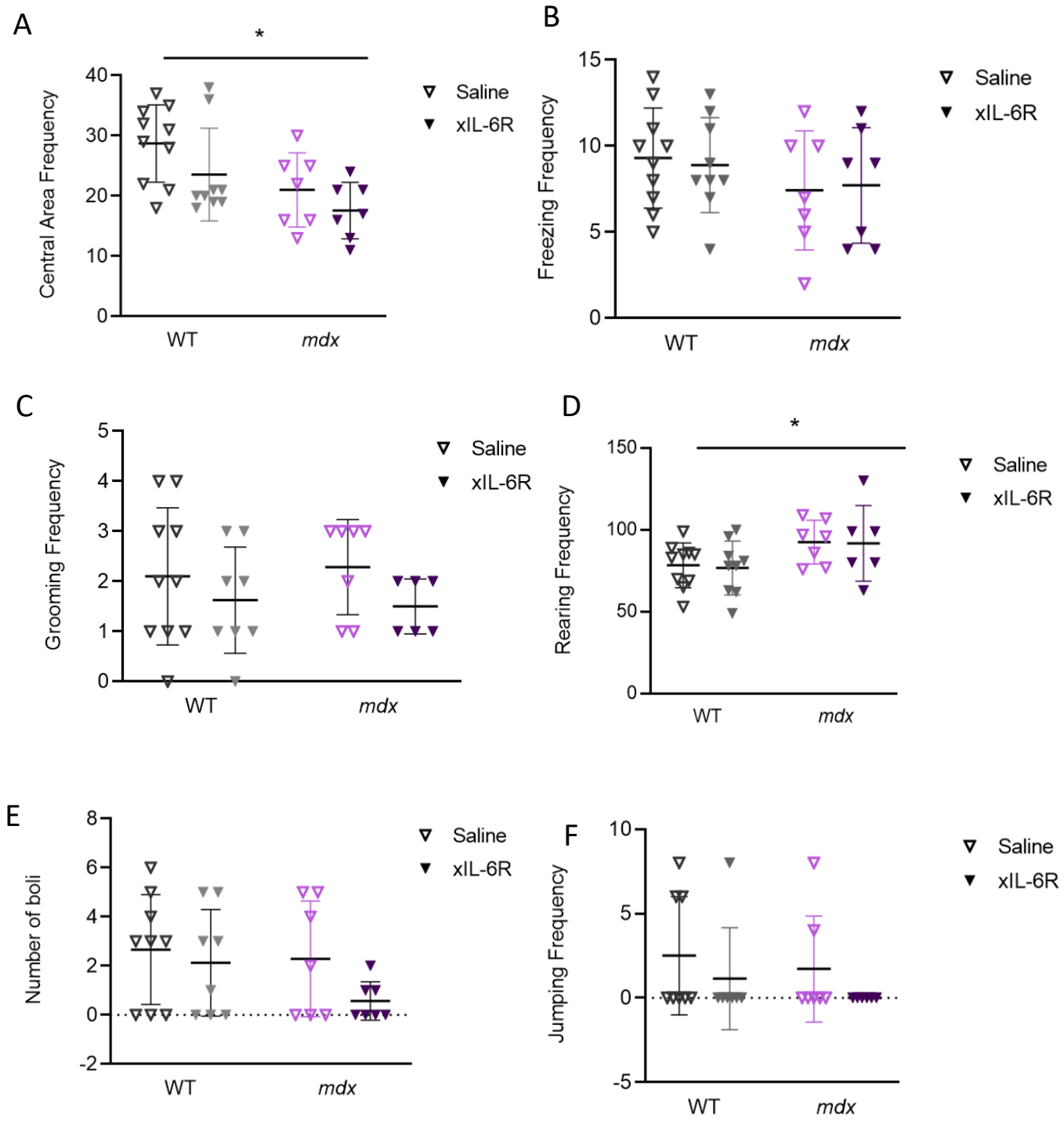


Figure 5.6: Behaviours of saline-treated and xIL-6R treated mdx and WT mice in an open field.

*The data plots illustrate that the central area frequency A) and rearing frequency D) is increased in saline-treated mdx mice but with no significant change observed in xIL-6R-treated mice. Freezing frequency B), grooming frequency C), faecal output (number of boli) E) and jumping frequency F) did not differ significantly between saline-treated mdx and WT mice, with no additional changes observed in either WT or mdx xIL-6R-treated mice. Open triangles indicate saline treated mice, closed triangles indicate xIL-6R treated mice. Two-way ANOVA, $p<0.05$**

5.6. Discussion

Given the deleterious effects of IL-6 on cognitive function (Campbell *et al.*, 1993; Heyser *et al.*, 1997; Wada-Isoe *et al.*, 2004; Wei *et al.*, 2012; Wei *et al.*, 2013; Lyra *et al.*, 2021), we set out to determine if intrathecal injection of xIL-6R monoclonal antibodies, which bind to IL-6 receptors and block IL-6-mediated signalling, modified hippocampal function and associated behaviours.

Compared to wildtype mice, *mdx* mice exhibit reduced hippocampal LTP as shown in Chapter 3. However, this could be reversed by intrathecal injection of xIL-6R in *mdx* mice. Not only was the initial magnitude of potentiation enhanced immediately after high frequency stimulation, this potentiation was maintained for at least 80 minutes. In fact, the enhanced LTP in *mdx* mice treated with xIL-6R surpassed the magnitude of the LTP evoked in untreated WT controls. Importantly however, neutralisation of central IL-6 receptors with xIL-6R did not modify LTP in WT mice, suggesting that the importance of IL-6 signalling in modulating LTP only becomes evident and significant in the context of dystrophin loss.

As we have already described region-specific changes in the expression of IL-6 and IL-6 receptors in *mdx* hippocampi (chapter 3), in cells present in the pyramidal cell layer of the CA1 region and granule cell layer of the DG. Our findings suggest that normal LTP induction may be disrupted by aberrant signalling caused by this neuroimmune molecule in dystrophic *mdx* mice.

Despite restoring LTP to control levels *ex vivo*, at the behavioural level, xIL-6R had no effect on recognition memory in *mdx* mice. Had time permitted, we would also

have liked to have investigated if spatial memory was altered in *mdx* mice relative to WT, by using behavioural tests such as the Morris water maze or Barnes maze. Although the use of the Morris water maze to measure hippocampal-dependent spatial navigation and reference memory is supported by numerous studies (Vorhees & Williams, 2006), the Barnes maze may be more valuable in this context as it does not involve forcing animals to swim, which is associated with increased levels of stress in mice (Harrison *et al.*, 2009). Furthermore, swimming may also reduce animals' core body temperature which could affect performance (Iivonen *et al.*, 2003).

In addition to the Novel Object Recognition test which was used to investigate recognition memory, we also looked at several behaviours in an open field. Behavioural issues linked to Autism, depression, anxiety and ADHD have been reported in DMD patients (Rubinsztein *et al.*, 1998; Hendriksen & Vles, 2008; Latimer *et al.*, 2017). Importantly, behavioural issues have also been observed in the *mdx* mouse model (Perronnet *et al.*, 2012) such as increased depressive behaviour, and increased anxiety and fearfulness (Sekiguchi *et al.*, 2009; Manning *et al.*, 2014). In mice, behaviours such as a reluctance to enter the centre of an open field arena, and escape behaviours such as rearing and jumping (Kraeuter *et al.*, 2019), are postulated to be a measure of animals' anxiety (Hölter *et al.*, 2015). Interestingly, we observed a significant increase in reluctance of the *mdx* mice to enter the centre of the open field compared to WT mice, suggesting a higher level of anxiety in these mice. Faecal output is yet another proposed measure of anxiety (Deacon & Rawlins, 2005). However, no alterations were noted in faecal output over the 10-minute study period in either control or xIL-6R-treated WT or *mdx*

mice. For jumping and freezing behaviours, we did not find any significant differences between *mdx* and WT mice in either saline- or xIL-6R-treated groups. Thus, the intrathecal injection itself, of xIL-6R did not affect these behaviours.

Grooming frequency and repetitive jumping in mice has been associated with other centrally-regulated behaviours such as autism-spectrum disorder and OCD (Kalueff et al., 2016). Our results showed that there were no significant differences in these behaviours between WT and *mdx* mice.

However, the lack of effect of the dystrophin-deficient phenotype on these behaviours may be due to the relatively young age of the *mdx* mice used in this study. Thus, memory and cognitive deficits we were investigating may not have fully developed in the 8–12-week-old *mdx* mice we studied here. This suggestion is supported by a recent study showing that cognitive deficits in *mdx* mice were progressive and developed from 4 months of age (7), a finding which also parallels with the fact that the severity of loss of dystrophin in skeletal muscle is also age-dependent in *mdx* mice (Moens *et al.*, 1993). Although *mdx* mice do show progressive muscle weakness and deterioration with age, this deterioration is most evident after 52 weeks of age (Pastoret & Sebille, 1995). This slowing of deterioration is primarily due to the compensatory upregulation of utrophin, which is able to perform the same function(s) as dystrophin does (Keep, 2000), resulting in the regeneration of sarcolemmal and plasma membrane integrity, thus saving muscle from deterioration, resulting in a less severe DMD phenotype with regard to skeletal muscle function (Gilbert *et al.*, 1999). Under normal circumstances, utrophin is down-regulated in muscle in the presence of dystrophin (Blake *et al.*,

1996). It has been suggested that similar compensatory mechanisms may also occur in the dystrophic *mdx* brain. However, upregulation of brain utrophin fails to rescue behavioural alterations such as exploration, emotional reactivity and spatial and fear memories in dystrophin-deficient *mdx* mice (Perronnet *et al.*, 2012) suggesting that that either utrophin-dependent or -independent mechanisms have no significant impact on cognitive and behavioural functions (Perronnet *et al.*, 2012). It remains possible however that other, currently unidentified, dystrophin-compensating mechanisms/proteins may exist within the brain to slow down the progression of cognitive deficits in *mdx* mice or other pre-clinical models of DMD. Whether or not the cognitive deficits in people with DMD are progressive in nature has not, to the best of our knowledge, been studied, probably due to the fact that patients with DMD have a relatively short life expectancy of 28.1 years (Landfeldt *et al.*, 2020; Broomfield *et al.*, 2021).

5.7. Conclusions

Having observed that hippocampal LTP was suppressed in untreated *mdx* mice, which would be consistent with dysfunctional learning and memory consolidation processes, we investigated whether or not an intervention procedure could improve these cognitive deficits. As elevated IL-6 is associated with memory impairment (Heyser *et al.*, 1997; Wei *et al.*, 2012; Wei *et al.*, 2013), and we and others (Li *et al.*, 1997; Tancredi *et al.*, 2000) have shown not only that exogenous IL-6 negatively impacts upon LTP in WT mice (Chapter 4), but also that suppression of IL-6 signalling restores normal LTP in *mdx* mice without impacting on LTP in

dystrophin-expressing WT mice, we examined whether centrally-administered, neutralising xIL-6R could improve cognitive outcomes in *mdx* mice. Our results showed that whilst the beneficial effect of xIL-6R on the molecular processes underlying hippocampal learning and memory was convincing at a cellular level, it did not translate into whole animal behavioural changes, with no deficits in recognition memory being observed. However, we hypothesise that this may be due, at least in part, to the relatively young age of the mice used for our study. Some anxiety-like behaviours were displayed by our *mdx* mice; however, these are largely likely to be regulated by other brain regions and were not modified by administration of xIL-6R.

Restoration of hippocampal LTP in *mdx* mice is an important finding and treatment with monoclonal neutralising IL-6R antibodies may be important in preventing future cognitive decline caused by loss of dystrophin.

Chapter 6:

Summary and Conclusions

6.1. Overview of research findings

In this research program, the possible contribution of the neuroimmune molecule, IL-6 in cognitive impairment associated with loss of the structural protein, dystrophin, was investigated. The main cognitive abnormalities seen in DMD patients involve specific deficits in verbal, short-term and working memory (Hinton et al., 2000, 2001; Snow et al., 2013). Using the *mdx* mice model of DMD, which lacks dystrophin, we focused on the hippocampus, as this brain region is critical for learning and the acquisition of new memories.

Little is known about the functional role of dystrophin in non-contracting cells such as neurons. Thus, we started by investigating the localisation of dystrophin in dystrophin-expressing mice. Full-length dystrophin (Dp427) was detected in the cell body and processes of cultured hippocampal neurons. Puncta at the synapses labelled strongly for dystrophin, implicating dystrophin in synapse structure and function. Indeed, others have reported a role for dystrophin in regulating $GABA_AR$ clustering at synapses (Knuesel *et al.*, 1999; Knuesel *et al.*, 2001), thus, a loss dystrophin could be associated with synaptic dysfunction.

Long-term potentiation (LTP), the proposed molecular correlate underpinning the formation and consolidation of new memories, results in structural and molecular changes in hippocampal synapses. This includes activation of NMDA receptors, increased expression and activation of AMPA receptors, calcium-induced activation of downstream signalling molecules and structural changes, such as the formation of new synapses and synaptic remodelling. Given that dystrophin is a structural

protein, it could be involved in both processes. Consistent with this role, *ex vivo* hippocampal slices from dystrophic *mdx* mice displayed reduced LTP in comparison to WT controls. This finding, although different to previous reports (Sesay *et al.*, 1996; Vaillend *et al.*, 2004) is consistent with the cognitive deficits reported in individuals with DMD (Hinton *et al.*, 2000, 2001; Snow *et al.*, 2013). That said, we did not observe differences between *mdx* and WT mice in terms of their recognition memory. However, this may have been due to the age of the mice used, as deficits have been observed in older *mdx* mice (Bagdatlioglu *et al.*, 2020). It is possible that compensatory mechanisms preserve learning behaviours despite pathophysiological changes at the cellular level. Other behavioural issues such as autism, depression, anxiety and ADHD, have been reported in DMD patients and in *mdx* mice (Hendriksen & Vles, 2008; Sekiguchi *et al.*, 2009; Perronnet *et al.*, 2012; Manning *et al.*, 2014). Although behavioural outputs for these were not different in *mdx* mice, we did observe increased freezing behaviours, that are associated with a fear response (Hendriksen & Vles, 2008; Pane *et al.*, 2013a; Banihani *et al.*, 2015). In humans, emotional disturbances have also been directly associated with this loss of dystrophin (Ricotti *et al.*, 2016).

A body of work has examined the progressive nature of DMD in skeletal muscle, where compensatory mechanisms allow near-normal development early in life. However, eventually, when these mechanisms fail, loss of mechanical function is inevitable. Adverse effects of dystrophin loss may progress similarly in cells of the CNS. Indeed, cellular changes were apparent in hippocampi from dystrophic *mdx* mice. We saw a decrease in the density of astrocytes in *mdx* mice in the DG region. This is relevant to hippocampal function as astrocytes release and regulate several

neuroactive molecules that can affect neuronal activity and modulate plasticity and LTP (Bains & Oliet, 2007; Theodosis *et al.*, 2008). Additionally, adult neural stem cells in the subgranular zone of the dentate gyrus are both positively and negatively regulated by contact with astrocytes (Cassé et al., 2018), which is consistent with our observed changes in hippocampal adult neurogenesis, as indicated by decreased doublecortin immunolabelling in *mdx* hippocampi. Neurogenesis plays a critical role in neural plasticity, brain homeostasis and is crucial in preserving the cognitive function and repair of damaged brain cells. Consistent with this function, we also observed an overall decrease in the density of mature neurons in the DG of aged *mdx* mice (8 months old). Obvious deterioration in hippocampal structure was also evident in these aged mice. Fluid-filled structures were present in the granule cell layer of aged *mdx* mice but not in age-matched WT animals. These fluid-filled structures disrupted the cellular morphology of the granule cell layer which, is likely to impact on the neurocircuitry that underpins learning and memory formation.

Although others have linked $GABA_A$ receptor clustering with dystrophin (Knuesel *et al.*, 1999; Knuesel *et al.*, 2001) we did not observe any notable differences in the number of neurons expressing $GABA_A$ receptors in the dentate gyrus of the hippocampus in *mdx* mice relative to controls. Normally, $GABA_A$ R inhibits activity in the postsynaptic cell by functioning as ligand-gated chloride channels, where binding of GABA to the receptor results in an influx of Cl^- ions, hyperpolarising the cell. However, that is not to say that $GABA_A$ receptor function is intact in *mdx* mice. Indeed, increases in spontaneous cellular excitability, manifested as increased intracellular calcium activity in neuronal cultures of *mdx* mice, could be due to dysfunction in the regulatory actions of inhibitory GABAergic interneurons. Indeed,

others in the lab have demonstrated that the $GABA_A$ receptor agonist, muscimol, can suppress neuronal hyperexcitability in *mdx* hippocampal cultures.

Figure 6.1. below summarises our observations, combined with other reports (Bagdatlioglu *et al.*, 2020) of the consequences of loss of dystrophin from hippocampal neurons in young, adult and aged *mdx* mice.

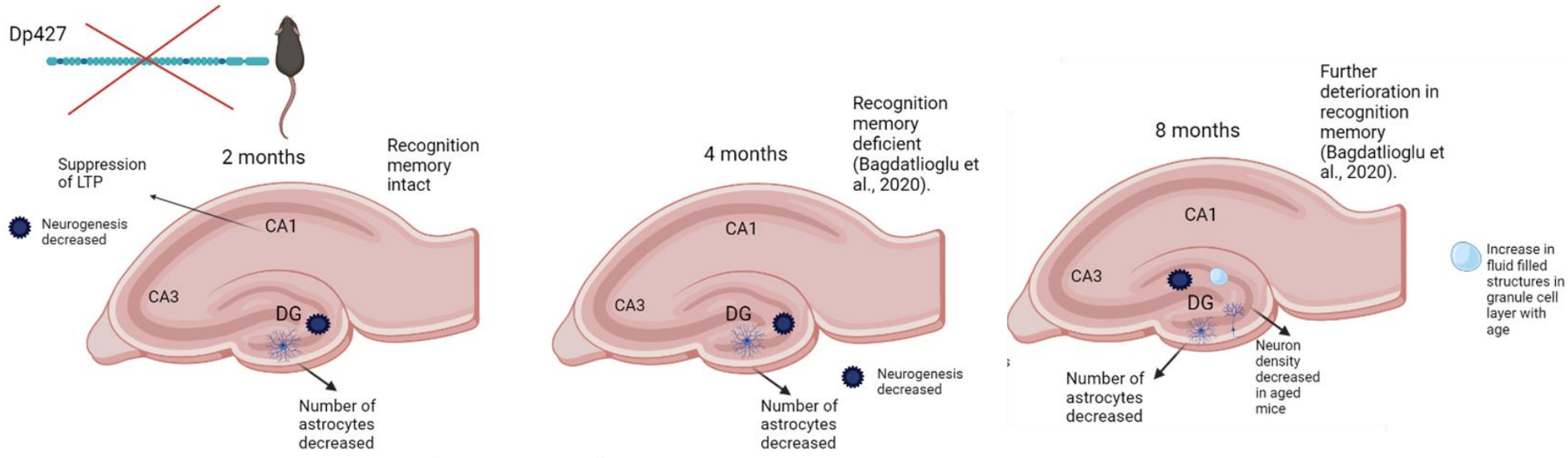


Figure 6.1. Loss of hippocampal dystrophin results in progressive pathophysiological changes.

The schematic illustrates the progressive consequences of the absence of dystrophin in the hippocampus, a brain region key to learning through the formation and consolidation of memories.

A. *Young mdx mice (2 months) exhibit intact recognition memory with suppressed LTP and reduced astrocytes.*
B. *Mature adult mdx mice (4 months) exhibit with deficits in recognition memory, decreased astrocytes as well as decreased neurogenesis.*
C. *Aged mdx mice (8 months) exhibit further deterioration in memory (Bagdatlioglu et al., 2020), decreased neurogenesis, decreased astrocytes and alterations to the cellular layer in the DG due to the presence of fluid-filled structures that result in decrease in neuronal density.*

Having established the morphological and cellular changes associated with the loss of dystrophin in *mdx* hippocampi, we went on to investigate the potential role of the pleiotropic cytokine, IL-6, in the pathophysiological changes occurring in dystrophic hippocampal tissue.

Our interest in IL-6 was piqued by the observed increase in circulating IL-6 both in DMD patients (Rufo *et al.*, 2011) and *mdx* mice (Pelosi *et al.*, 2015), likely reflecting chronic inflammation associated with this disease. This cytokine has been shown to influence LTP (Li *et al.*, 1997; Tancredi *et al.*, 2000; Stampanoni Bassi *et al.*, 2019), neurogenesis (Islam *et al.*, 2009) and astrogliogenesis (Nakanishi *et al.*, 2007), however, IL-6 in the specific context of the brain of *mdx* mice and patients with DMD has not been studied until now.

Somewhat surprisingly, we did not detect any changes in hippocampal IL-6 or IL-6Rs at the gene or protein level. Similarly, expression of the transmembrane protein gp130, which facilitates transcellular signalling by soluble IL-6 receptors, and STAT3, the downstream signalling molecule activated by IL-6Rs was unchanged in *mdx* mice. However, IL-6 can be transported from the periphery across the BBB (Banks *et al.*, 1994) and IL-6 can be released locally in the brain from astrocytes and microglia during pathophysiological events such as inflammation (Gruol & Nelson, 1997) and during physiological processes such as LTP (Balschun *et al.*, 2004) so a lack of global hippocampal differences between WT and *mdx* mice does not necessarily reflect possible local effects. It is also important to note that these results reflect expression levels in the whole hippocampus and are not region-

specific. As described above, the inter-regional neural circuitry is critical to hippocampal function and when we explored regional expression of IL-6 and IL-6Rs using immunofluorescence, regional differences were apparent as there was an increase in IL-6 and IL-6R expression in both the CA1 and DG region of the hippocampus of *mdx* mice, relative to WT. In the CA3 regions, IL-6 expression was similar to WT, whereas IL-6R expression was decreased in the CA3 regions of *mdx* mice. Additionally, we noted in dystrophin-expressing mice, that IL-6Rs were clustered at synapses, similarly to dystrophin on hippocampal processes. Interestingly, exposure to elevated extracellular IL-6 resulted in an increased density of IL-6R-expressing clusters on hippocampal processes. It is not clear if this effect is beneficial or otherwise in terms of cognitive function, or if it is dependent upon the expression of dystrophin, however, it may be important in the observed effects of IL-6 on the generation of LTP in WT and *mdx* mice.

As circulating IL-6 is elevated in the absence of dystrophin and we explored whether elevated levels of IL-6 could affect LTP in dystrophin-expressing hippocampi. Exposure to exogenous IL-6 reduced early LTP in WT animals, although this reduction was not seen in LTP maintenance. This suggested that IL-6 mechanisms could underlie the suppression of the initial kinase activity in LTP. Indeed, this is consistent with broad memory impairment characteristic of transgenic mice overexpressing IL-6 (Heyser *et al.*, 1997; Wei *et al.*, 2012; Wei *et al.*, 2013). In the same transgenic mouse model, a significant reduction in overall neurogenesis in the dentate gyrus of the hippocampus was also found with neural progenitor cells also reduced in the granule cell layer (Vallieres *et al.*, 2002). This is

consistent with our observations that hippocampal adult neurogenesis and the density of mature neurons is decreased the dentate gyrus of *mdx* hippocampi.

However, *mdx* hippocampal slices appeared to be insensitive to the suppressive effect of IL-6 observed in WT mice. This could be due to decreased IL-6R expression in the CA3 region, where the Schaffer collaterals are stimulated. Chronic exposure to elevated IL-6 could have resulted in receptor internalisation or it is possible that reduced LTP observed in *mdx* mice could be due to a complex interplay between local IL-6 levels paired with abnormal neuron functioning due to a loss of synaptic dystrophin. As was noted with aberrant $GABA_AR$ clustering in *mdx* neurons (Knuesel *et al.*, 1999; Knuesel *et al.*, 2001) it is possible that hippocampal IL-6Rs may not be appropriately expressed on the neuronal cell membrane, or, perhaps down-stream signalling is dysfunctional resulting in insensitivity to IL-6. While further research is needed to reveal the precise signalling mechanisms, these studies suggest that while overall IL-6 or receptor levels in the brain are not changed in dystrophic mice, there may be local changes in expression that could modify hippocampal LTP. Increases in IL-6 expression could be due to increases in circulatory IL-6 that has been transported from the periphery across the BBB (Banks *et al.*, 1994) or IL-6 could be released locally in the brain from astrocytes and microglia during pathophysiological events such as inflammation (Gruol & Nelson, 1997), both of which could occur in DMD due to increased peripheral IL-6 (Rufo *et al.*, 2011; Pelosi *et al.*, 2015) and inflammation caused by a loss of dystrophin.

Further support for this suggestion was generated by administering a monoclonal antibody against the IL-6 receptor (xIL-6R) *in vivo* to block IL-6R-evoked signalling in the CNS. Intrathecal administration of xIL-6R resulted in restoration of the suppressed LTP recorded from Shaffer collaterals in treated *mdx* mice. Our results showed that whilst the beneficial effect of xIL-6R on the molecular processes underlying hippocampal learning and memory was convincing at a cellular level, it did not translate into whole animal behavioural changes, with no deficits in recognition memory being observed. However, as discussed above, cognitive deficits were not apparent in this age category (8-12 weeks). It would however, be very interesting to study the effects of xIL-6R in aged mice, where behavioural deficits are apparent (Bagdatlioglu *et al.*, 2020). That said, the progressive loss of hippocampal neurons and glia may mean that the beneficial effects of xIL-6R on LTP in young animals is not effective at later disease stages. Indeed, as is the case with other neurodegenerative diseases when the behavioural deficits become apparent, neuronal deficits are already advanced and resistant to treatment. One small virtue of a DMD diagnosis early in life is that preventative treatments could be employed before cognitive deficits become advanced. Some anxiety-like behaviours were displayed by young *mdx* mice; however, these are largely likely to be regulated by brain regions other than the hippocampus and were not modified by administration of xIL-6R.

We proposed that dysfunctional GABAergic regulation of hippocampal networks could underpin the observed hyperexcitability in hippocampal neurons. It was therefore interesting to observe that acute exposure of *mdx* hippocampal neurons, which had been cultured in IL-6-free media for >7 days, to IL-6 resulted in

suppression, although not abolition, of the spontaneous calcium activity. Given that unregulated calcium can result in neuronal cytotoxicity and cell death (Orrenius & Nicotera, 1994) in this scenario, brief exposure to IL-6 appears to have a beneficial effect.

Figure 6.2 below summarises the findings from this study as well as others work on IL-6 in the brain.

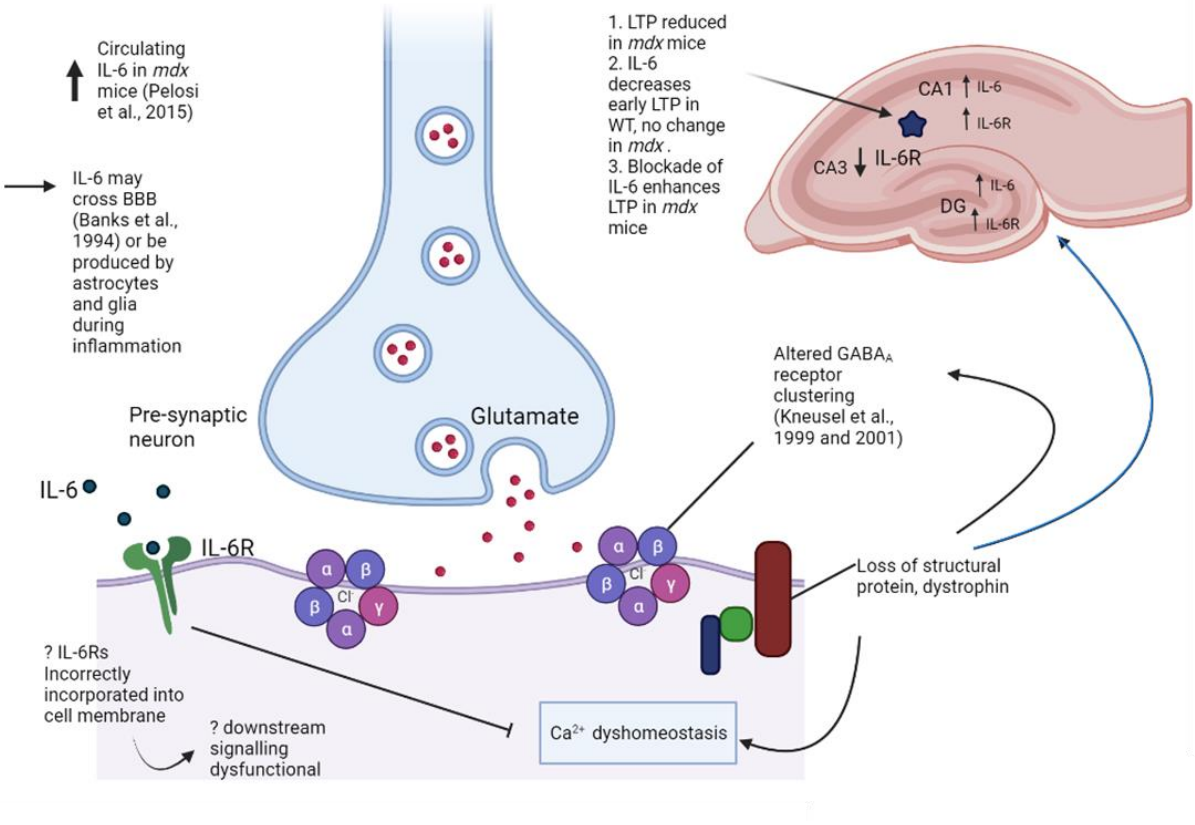


Figure 6.2. The figure illustrates the potential mechanisms of how IL-6Rs could be involved in hippocampal dysfunction associated with a loss of dystrophin.

6.2. Conclusion

This program of work has investigated the importance of dystrophin in hippocampal function and its interaction with the neuroimmune molecule IL-6. Suppression of LTP in *mdx* mice indicates the importance of dystrophin to the molecular corelate of learning and memory. However, in young adult mice this does not yet result in behavioural deficits in learning and memory. We hypothesised that chronically elevated levels of the pro-inflammatory cytokine, IL-6 contributed to dysfunctional LTP, and, indeed, blocking central IL-6 signalling resulted in recovery of LTP, even though baseline levels of IL-6 were not different in dystrophic hippocampal tissue. Impaired hippocampal adult neurogenesis and altered hippocampal cellularity were also observed in *mdx* mice. Others have shown that IL-6 can have similar detrimental effects, however, further studies are needed to determine if IL-6 is fundamental to these changes in the context of dystrophic tissue. Finally, and somewhat counterintuitively, IL-6 exhibited neuroprotective effects when it was applied acutely to cultured hippocampal neurons, where it suppressed neuronal hyperexcitability. However, in the context of physiological homeostasis, this may not be unusual. Acute stimuli often evoke a physiological response to restore baseline function. Generally, detrimental effects are observed when a stimulus is not inhibited through negative feedback, as would be the case with elevated IL-6 caused by chronic inflammation associated with the loss of dystrophin.

In conclusion, loss of dystrophin underlies early cellular and molecular deficits in the hippocampus leading to progressive deterioration in the structure and function of this brain region. However, altered hippocampal sensitivity to chronically

elevated IL-6 also appears to be a contributory factor in the pathophysiological consequences of dystrophin loss, as noted by the restoration of LTP when central IL-6 receptor mediated signalling was inhibited. It is likely that any therapeutic strategies to target IL-6 as a signalling intermediary would need to be applied prior to the presentation of cognitive decline, when neurocircuits may be irreversibly damaged. However, in contrast to other neurodegenerative conditions, DMD is diagnosed early in life. With significant advances in treatment of this disorder and prolongation of the duration and quality of life of individuals with DMD, increased attention should be focussed on understanding the cognitive aspects of the disease.

6.3. Limitations

In this thesis, there were a few limitations that need to be mentioned. Some data-sets were missing in hippocampal adult neurogenesis due to a lack of tissue availability. Further, deficits were not observed in learning at the age we studied (8-12 weeks), and differences could possibly only be seen at an older age, which would be interesting to look at. With regards to LTP, additional experiments on more animals as well as older animals could be beneficial as well. Importantly, where IL-6 was present in LTP experiments, the effect was only seen in the early phase of LTP. After 1 hour, LTP was similar between groups. This could possibly display that IL-6 is only effecting early changes and processes in LTP and further studies would be needed to confirm and explain this.

6.4. Future directions

Given our findings that dystrophin impacts on hippocampal morphology and function, which appears to involve the direct effects of dystrophin loss from neurons, in addition to the indirect actions of the pro-inflammatory cytokine, IL-6, which is elevated in *mdx* mice, there is a possibility that different cell types are having an effect on the hippocampus and the deficits we have seen in the *mdx* mouse with regards to IL-6 and LTP as well as hippocampal adult neurogenesis. One cell type of interest is microglia. Microglia are of particular interest as they are involved in the release of IL-6 as well as involved in the modulation of hippocampal plasticity processes. Thus, there is a necessity to extend LTP and behavioural test analysis to later time points such as 4-8 months and possibly older than a year. More analysis regarding hippocampal adult neurogenesis at older ages would be beneficial as well. With regards to hippocampal adult neurogenesis specifically, as neurogenesis occurs in the dentate gyrus, it could be beneficial to record neuronal plasticity in this region and to perform behavioural tests related with this particular hippocampal region in order to determine if any deficits seen are adding to the cognitive deficits in DMD. Further, GABAergic function in the CA1 could be analysed. Although we did not observe changes in the absolute number of GABA-expressing hippocampal interneurons in dystrophic tissue in the dentate gyrus, aberrant $GABA_A$ receptor clustering could nonetheless have an impact on the neuroregulatory actions of GABAergic neurons. Interestingly, we found that a loss of dystrophin increases neuronal excitability in cultured hippocampal neurons and thus, other regions of the hippocampus, such as CA1 could have altered GABAergic

function. There are a few future directions that this study could take and thus, this work is continuing in the lab and will all be pivotal to establishing a thorough understanding of the functional role of dystrophin in non-contracting neurons and how that feeds through to altered cognitive function in DMD.

Chapter 7: References

Abdel-Salam E, Abdel-Meguid I & Korraa SS. (2009). Markers of degeneration and regeneration in Duchenne muscular dystrophy. *Acta Myol* **28,** 94-100.

Ahn AH & Kunkel LM. (1993). The structural and functional diversity of dystrophin. *Nat Genet* **3,** 283-291.

Akira S, Taga T & Kishimoto T. (1993). Interleukin-6 in biology and medicine. *Adv Immunol* **54,** 1-78.

Amiri M, Bahrami F & Janahmadi M. (2012). Functional contributions of astrocytes in synchronization of a neuronal network model. *J Theor Biol* **292,** 60-70.

Amiri M, Hosseinmardi N, Bahrami F & Janahmadi M. (2013). Astrocyte- neuron interaction as a mechanism responsible for generation of neural synchrony: a study based on modeling and experiments. *J Comput Neurosci* **34,** 489-504.

Anand KS & Dhikav V. (2012). Hippocampus in health and disease: An overview. *Ann Indian Acad Neurol* **15,** 239-246.

Anderson JE, Ovalle WK & Bressler BH. (1987). Electron microscopic and autoradiographic characterization of hindlimb muscle regeneration in the mdx mouse. *Anat Rec* **219,** 243-257.

Anderson JL, Head SI, Rae C & Morley JW. (2002). Brain function in Duchenne muscular dystrophy. *Brain : a journal of neurology* **125,** 4-13.

Angulo MC, Kozlov AS, Charpak S & Audinat E. (2004). Glutamate released from glial cells synchronizes neuronal activity in the hippocampus. *J Neurosci* **24,** 6920-6927.

Aniszewska A, Chłodzińska N, Bartkowska K, Winnicka MM, Turlejski K & Djavadian RL. (2015). The expression of interleukin-6 and its receptor in various brain regions and their roles in exploratory behavior and stress responses. *J Neuroimmunol* **284,** 1-9.

Araque A, Carmignoto G, Haydon PG, Oliet SH, Robitaille R & Volterra A. (2014). Gliotransmitters travel in time and space. *Neuron* **81,** 728-739.

Arechavala-Gomeza V, Kinali M, Feng L, Guglieri M, Edge G, Main M, Hunt D, Lehovsky J, Straub V, Bushby K, Sewry CA, Morgan JE & Muntoni F. (2010).

Revertant fibres and dystrophin traces in Duchenne muscular dystrophy: implication for clinical trials. *Neuromuscul Disord* **20,** 295-301.

Armario A, Hernández J, Bluethmann H & Hidalgo J. (1998). IL-6 deficiency leads to increased emotionality in mice: evidence in transgenic mice carrying a null mutation for IL-6. *J Neuroimmunol* **92,** 160-169.

Artola A, Brocher S & Singer W. (1990). Different voltage-dependent thresholds for inducing long-term depression and long-term potentiation in slices of rat visual cortex. *Nature* **347,** 69-72.

Ascher P & Nowak L. (1988). The role of divalent cations in the N-methyl-D-aspartate responses of mouse central neurones in culture. *J Physiol* **399,** 247-266.

Bagdatlioglu E, Porcari P, Greally E, Blamire AM & Straub VW. (2020). Cognitive impairment appears progressive in the mdx mouse. *Neuromuscul Disord* **30,** 368-388.

Baier PC, May U, Scheller J, Rose-John S & Schiffelholz T. (2009). Impaired hippocampus-dependent and -independent learning in IL-6 deficient mice. *Behav Brain Res* **200,** 192-196.

Bains JS & Oliet SH. (2007). Glia: they make your memories stick! *Trends Neurosci* **30,** 417-424.

Balschun D, Wetzel W, Del Rey A, Pitossi F, Schneider H, Zuschratter W & Besedovsky HO. (2004). Interleukin-6: a cytokine to forget. *FASEB J* **18,** 1788-1790.

Bannerman DM, Grubb M, Deacon RMJ, Yee BK, Feldon J & Rawlins JNP (2003). Ventral hippocampal lesions affect anxiety but not spatial learning. Behavioural Brain Research 139, 197–213.

Bannerman DM, Rawlins JNP, McHugh SB, Deacon RMJ, Yee BK, Bast T, Zhang W-N, Pothuizen HHJ & Feldon J (2004). Regional dissociations within the hippocampus—memory and anxiety. Neuroscience & Biobehavioral Reviews 28, 273–283.

Bannerman DM, Sprengel R, Sanderson DJ, McHugh SB, Rawlins JN, Monyer H & Seeburg PH (2014). Hippocampal synaptic plasticity, spatial memory and anxiety. Nature Reviews Neuroscience 15, 181–192.

Banihani R, Smile S, Yoon G, Dupuis A, Mosleh M, Snider A & McAdam L. (2015). Cognitive and Neurobehavioral Profile in Boys With Duchenne Muscular Dystrophy. *J Child Neurol* **30,** 1472-1482.

Banks WA, Kastin AJ & Gutierrez EG. (1994). Penetration of interleukin-6 across the murine blood-brain barrier. *Neurosci Lett* **179,** 53-56.

Bellinger FP, Madamba SG, Campbell IL & Siggins GR. (1995). Reduced long-term potentiation in the dentate gyrus of transgenic mice with cerebral overexpression of interleukin-6. *Neurosci Lett* **198,** 95-98.

Benice TS, Rizk A, Kohama S, Pfankuch T & Raber J. (2006). Sex-differences in age-related cognitive decline in C57BL/6J mice associated with increased brain microtubule-associated protein 2 and synaptophysin immunoreactivity. *Neuroscience* **137,** 413-423.

Bialuk I & Winnicka MM. (2018). Facilitatory Effect of IL-6 Deficiency on Long-Term Spatial Memory in Young Adult Mice. *Behav Genet* **48,** 236-246.

Bies RD, Phelps SF, Cortez MD, Roberts R, Caskey CT & Chamberlain JS. (1992). Human and murine dystrophin mRNA transcripts are differentially expressed during skeletal muscle, heart, and brain development. *Nucleic Acids Res* **20,** 1725-1731.

Biggar WD, Harris VA, Eliasoph L & Alman B. (2006). Long-term benefits of deflazacort treatment for boys with Duchenne muscular dystrophy in their second decade. *Neuromuscul Disord* **16,** 249-255.

Billard C, Gillet P, Signoret JL, Uicaut E, Bertrand P, Fardeau M, Barthez-Carpentier MA & Santini JJ. (1992). Cognitive functions in Duchenne muscular dystrophy: a reappraisal and comparison with spinal muscular atrophy. *Neuromuscul Disord* **2,** 371-378.

Blake DJ, Hawkes R, Benson MA & Beesley PW. (1999). Different dystrophin-like complexes are expressed in neurons and glia. *J Cell Biol* **147,** 645-658.

Blake DJ & Kroger S. (2000). The neurobiology of duchenne muscular dystrophy: learning lessons from muscle? *Trends Neurosci* **23,** 92-99.

Blake DJ, Tinsley JM & Davies KE. (1996). Utrophin: a structural and functional comparison to dystrophin. *Brain Pathol* **6,** 37-47.

Blake DJ, Weir A, Newey SE & Davies KE. (2002). Function and genetics of dystrophin and dystrophin-related proteins in muscle. *Physiol Rev* **82,** 291-329.

Blanchard DC & Blanchard RJ. (1988). Ethoexperimental approaches to the biology of emotion. *Annu Rev Psychol* **39,** 43-68.

Bliss TV & Collingridge GL. (1993). A synaptic model of memory: long-term potentiation in the hippocampus. *Nature* **361,** 31-39.

Bliss TV & Lomo T. (1973). Long-lasting potentiation of synaptic transmission in the dentate area of the anaesthetized rabbit following stimulation of the perforant path. *J Physiol* **232,** 331-356.

Botton PH, Costa MS, Ardais AP, Mioranzza S, Souza DO, da Rocha JB & Porciúncula LO. (2010). Caffeine prevents disruption of memory consolidation in the inhibitory avoidance and novel object recognition tasks by scopolamine in adult mice. *Behav Brain Res* **214,** 254-259.

Braida D, Sacerdote P, Panerai AE, Bianchi M, Aloisi AM, Iosue S & Sala M. (2004). Cognitive function in young and adult IL (interleukin)-6 deficient mice. *Behav Brain Res* **153,** 423-429.

Bresolin N, Castelli E, Comi GP, Felisari G, Bardoni A, Perani D, Grassi F, Turconi A, Mazzucchelli F, Gallotti D & et al. (1994). Cognitive impairment in Duchenne muscular dystrophy. *Neuromuscul Disord* **4,** 359-369.

Brewer GJ. (1997). Isolation and culture of adult rat hippocampal neurons. *J Neurosci Methods* **71,** 143-155.

Brini M, Cali T, Ottolini D & Carafoli E. (2014). Neuronal calcium signaling: function and dysfunction. *Cell Mol Life Sci* **71,** 2787-2814.

Broadbent NJ, Gaskin S, Squire LR & Clark RE. (2010). Object recognition memory and the rodent hippocampus. *Learn Mem* **17,** 5-11.

Broomfield J, Hill M, Guglieri M, Crowther M & Abrams K. (2021). Life Expectancy in Duchenne Muscular Dystrophy: Reproduced Individual Patient Data Meta-analysis. *Neurology* **97,** e2304-e2314.

Brown JP, Couillard-Després S, Cooper-Kuhn CM, Winkler J, Aigner L & Kuhn HG. (2003). Transient expression of doublecortin during adult neurogenesis. *J Comp Neurol* **467,** 1-10.

Brunig I, Suter A, Knuesel I, Luscher B & Fritschy JM. (2002). GABAergic terminals are required for postsynaptic clustering of dystrophin but not of GABA(A) receptors and gephyrin. *J Neurosci* **22,** 4805-4813.

Bulfield G, Siller WG, Wight PA & Moore KJ. (1984). X chromosome-linked muscular dystrophy (mdx) in the mouse. *Proc Natl Acad Sci U S A* **81,** 1189-1192.

Burnashev N & Rozov A. (2005). Presynaptic Ca2+ dynamics, Ca2+ buffers and synaptic efficacy. *Cell Calcium* **37,** 489-495.

Bruel-Jungerman E (2006). Long-term potentiation enhances neurogenesis in the adult dentate gyrus. Journal of Neuroscience 26, 5888–5893.

Burns DP, Canavan L, Rowland J, O'Flaherty R, Brannock M, Drummond SE, O'Malley D, Edge D & O'Halloran KD. (2018). Recovery of respiratory function in mdx mice co-treated with neutralizing interleukin-6 receptor antibodies and urocortin-2. *J Physiol* **596,** 5175-5197.

Butterweck V, Prinz S & Schwaninger M. (2003). The role of interleukin-6 in stress-induced hyperthermia and emotional behaviour in mice. *Behav Brain Res* **144,** 49-56.

Byers TJ, Lidov HG & Kunkel LM. (1993). An alternative dystrophin transcript specific to peripheral nerve. *Nat Genet* **4,** 77-81.

Campbell IL, Abraham CR, Masliah E, Kemper P, Inglis JD, Oldstone MB & Mucke L. (1993). Neurologic disease induced in transgenic mice by cerebral overexpression of interleukin 6. *Proc Natl Acad Sci U S A* **90,** 10061-10065.

Campbell IL, Erta M, Lim SL, Frausto R, May U, Rose-John S, Scheller J & Hidalgo J. (2014). Trans-signaling is a dominant mechanism for the pathogenic actions of interleukin-6 in the brain. *J Neurosci* **34,** 2503-2513.

Carretta D, Santarelli M, Sbriccoli A, Pinto F, Catini C & Minciacchi D. (2004). Spatial analysis reveals alterations of parvalbumin- and calbindin-positive local circuit neurons in the cerebral cortex of mutant mdx mice. *Brain Res* **1016,** 1-11.

Carretta D, Santarelli M, Vanni D, Carrai R, Sbriccoli A, Pinto F & Minciacchi D. (2001). The organisation of spinal projecting brainstem neurons in an animal model of muscular dystrophy. A retrograde tracing study on mdx mutant mice. *Brain Res* **895,** 213-222.

Carretta D, Santarelli M, Vanni D, Ciabatti S, Sbriccoli A, Pinto F & Minciacchi D. (2003). Cortical and brainstem neurons containing calcium-binding proteins in a murine model of Duchenne's muscular dystrophy: selective changes in the sensorimotor cortex. *J Comp Neurol* **456,** 48-59.

Castles A & Coltheart M. (1993). Varieties of developmental dyslexia. *Cognition* **47,** 149-180.

Chamova T, Guergueltcheva V, Raycheva M, Todorov T, Genova J, Bichev S, Bojinova V, Mitev V, Tournev I & Todorova A. (2013). Association between loss of dp140 and cognitive impairment in duchenne and becker dystrophies. *Balkan J Med Genet* **16,** 21-30.

Chang L, Cloak CC & Ernst T. (2003). Magnetic resonance spectroscopy studies of GABA in neuropsychiatric disorders. *J Clin Psychiatry* **64 Suppl 3,** 7-14.

Chaussenot R, Edeline JM, Le Bec B, El Massioui N, Laroche S & Vaillend C. (2015). Cognitive dysfunction in the dystrophin-deficient mouse model of Duchenne muscular dystrophy: A reappraisal from sensory to executive processes. *Neurobiology of learning and memory* **124,** 111-122.

Chourbaji S, Urani A, Inta I, Sanchis-Segura C, Brandwein C, Zink M, Schwaninger M & Gass P. (2006). IL-6 knockout mice exhibit resistance to stress-induced development of depression-like behaviors. *Neurobiol Dis* **23,** 587-594.

Collingridge GL, Kehl SJ & McLennan H. (1983). Excitatory amino acids in synaptic transmission in the Schaffer collateral-commissural pathway of the rat hippocampus. *J Physiol* **334,** 33-46.

Constantin B. (2014). Dystrophin complex functions as a scaffold for signalling proteins. *Biochim Biophys Acta* **1838,** 635-642.

Cotton SM, Voudouris NJ & Greenwood KM. (2005). Association between intellectual functioning and age in children and young adults with Duchenne muscular dystrophy: further results from a meta-analysis. *Dev Med Child Neurol* **47,** 257-265.

Couillard-Despres S, Winner B, Schaubeck S, Aigner R, Vroemen M, Weidner N, Bogdahn U, Winkler J, Kuhn HG & Aigner L. (2005). Doublecortin expression levels in adult brain reflect neurogenesis. *Eur J Neurosci* **21,** 1-14.

D'Souza VN, Nguyen TM, Morris GE, Karges W, Pillers DA & Ray PN. (1995). A novel dystrophin isoform is required for normal retinal electrophysiology. *Hum Mol Genet* **4,** 837-842.

Dallerac G, Perronnet C, Chagneau C, Leblanc-Veyrac P, Samson-Desvignes N, Peltekian E, Danos O, Garcia L, Laroche S, Billard JM & Vaillend C. (2011). Rescue of a dystrophin-like protein by exon skipping normalizes synaptic plasticity in the hippocampus of the mdx mouse. *Neurobiol Dis* **43,** 635-641.

Darnell JE, Jr., Kerr IM & Stark GR. (1994). Jak-STAT pathways and transcriptional activation in response to IFNs and other extracellular signaling proteins. *Science* **264,** 1415-1421.

Davies KE & Nowak KJ. (2006). Molecular mechanisms of muscular dystrophies: old and new players. *Nat Rev Mol Cell Biol* **7,** 762-773.

De Paepe B & De Bleecker JL. (2013). Cytokines and chemokines as regulators of skeletal muscle inflammation: presenting the case of Duchenne muscular dystrophy. *Mediators Inflamm* **2013,** 540370.

De Sarro G, Russo E, Ferreri G, Giuseppe B, Flocco MA, Di Paola ED & De Sarro A. (2004). Seizure susceptibility to various convulsant stimuli of knockout interleukin-6 mice. *Pharmacol Biochem Behav* **77,** 761-766.

Deng B, Glanzman D & Tidball JG. (2009). Nitric oxide generated by muscle corrects defects in hippocampal neurogenesis and neural differentiation caused by muscular dystrophy. *J Physiol* **587,** 1769-1778.

Dong Y & Benveniste EN. (2001). Immune function of astrocytes. *Glia* **36,** 180-190.

Doorenweerd N, Mahfouz A, van Putten M, Kaliyaperumal R, PAC TH, Hendriksen JGM, Aartsma-Rus AM, Verschuuren J, Niks EH, Reinders MJT, Kan HE & Lelieveldt BPF. (2018). Author Correction: Timing and localization of human

dystrophin isoform expression provide insights into the cognitive phenotype of Duchenne muscular dystrophy. In *Sci Rep*, pp. 4058. England.

Dorman C, Hurley AD & D'Avignon J. (1988). Language and learning disorders of older boys with Duchenne muscular dystrophy. *Dev Med Child Neurol* **30,** 316-327.

Dowlati Y, Herrmann N, Swardfager W, Liu H, Sham L, Reim EK & Lanctôt KL. (2010). A meta-analysis of cytokines in major depression. *Biol Psychiatry* **67,** 446-457.

Eagle M, Baudouin SV, Chandler C, Giddings DR, Bullock R & Bushby K. (2002). Survival in Duchenne muscular dystrophy: improvements in life expectancy since 1967 and the impact of home nocturnal ventilation. *Neuromuscul Disord* **12,** 926-929.

Emery AE. (1991). Population frequencies of inherited neuromuscular diseases--a world survey. *Neuromuscul Disord* **1,** 19-29.

Eng LF, Ghirnikar RS & Lee YL. (2000). Glial fibrillary acidic protein: GFAP-thirty-one years (1969-2000). *Neurochem Res* **25,** 1439-1451.

Ennaceur A & Delacour J. (1988). A new one-trial test for neurobiological studies of memory in rats. 1: Behavioral data. *Behav Brain Res* **31,** 47-59.

Ernst M & Jenkins BJ. (2004). Acquiring signalling specificity from the cytokine receptor gp130. *Trends Genet* **20,** 23-32.

Erta M, Quintana A & Hidalgo J. (2012). Interleukin-6, a major cytokine in the central nervous system. *Int J Biol Sci* **8,** 1254-1266.

Ervasti JM & Campbell KP. (1993). A role for the dystrophin-glycoprotein complex as a transmembrane linker between laminin and actin. *J Cell Biol* **122,** 809-823.

Eulenfeld R, Dittrich A, Khouri C, Müller PJ, Mütze B, Wolf A & Schaper F. (2012). Interleukin-6 signalling: more than Jaks and STATs. *Eur J Cell Biol* **91,** 486-495.

Evans NP, Misyak SA, Robertson JL, Bassaganya-Riera J & Grange RW. (2009). Immune-mediated mechanisms potentially regulate the disease time-course

of duchenne muscular dystrophy and provide targets for therapeutic intervention. *PM R* **1,** 755-768.

Fairclough RJ, Wood MJ & Davies KE. (2013). Therapy for Duchenne muscular dystrophy: renewed optimism from genetic approaches. In *Nat Rev Genet*, pp. 373-378. England.

Farina C, Aloisi F & Meinl E. (2007). Astrocytes are active players in cerebral innate immunity. *Trends Immunol* **28,** 138-145.

Felisari G, Martinelli Boneschi F, Bardoni A, Sironi M, Comi GP, Robotti M, Turconi AC, Lai M, Corrao G & Bresolin N. (2000). Loss of Dp140 dystrophin isoform and intellectual impairment in Duchenne dystrophy. *Neurology* **55,** 559-564.

Feno S, Butera G, Vecellio Reane D, Rizzuto R & Raffaello A. (2019). Crosstalk between Calcium and ROS in Pathophysiological Conditions. *Oxid Med Cell Longev* **2019,** 9324018.

Frey U & Morris RG (1997). Synaptic tagging and long-term potentiation. Nature 385, 533–536.

Fujimoto T, Itoh K, Yaoi T & Fushiki S. (2014). Somatodendritic and excitatory postsynaptic distribution of neuron-type dystrophin isoform, Dp40, in hippocampal neurons. *Biochem Biophys Res Commun* **452,** 79-84.

Gage FH. (2000). Mammalian neural stem cells. *Science* **287,** 1433-1438.

Garbers C, Aparicio-Siegmund S & Rose-John S. (2015). The IL-6/gp130/STAT3 signaling axis: recent advances towards specific inhibition. *Curr Opin Immunol* **34,** 75-82.

Gareau MG, Wine E, Rodrigues DM, Cho JH, Whary MT, Philpott DJ, Macqueen G & Sherman PM. (2011). Bacterial infection causes stress-induced memory dysfunction in mice. *Gut* **60,** 307-317.

Gaskin S, Tardif M, Cole E, Piterkin P, Kayello L & Mumby DG. (2010). Object familiarization and novel-object preference in rats. *Behav Processes* **83,** 61-71.

Ge S, Goh EL, Sailor KA, Kitabatake Y, Ming GL & Song H. (2006). GABA regulates synaptic integration of newly generated neurons in the adult brain. *Nature* **439,** 589-593.

Gibertini M. (1998). Cytokines and cognitive behavior. *Neuroimmunomodulation* **5,** 160-165.

Gilbert R, Nalbantoglu J, Petrof BJ, Ebihara S, Guibinga GH, Tinsley JM, Kamen A, Massie B, Davies KE & Karpati G. (1999). Adenovirus-mediated utrophin gene transfer mitigates the dystrophic phenotype of mdx mouse muscles. *Hum Gene Ther* **10,** 1299-1310.

Gold BI, Bowers MB, Jr., Roth RH & Sweeney DW. (1980). GABA levels in CSF of patients with psychiatric disorders. *Am J Psychiatry* **137,** 362-364.

Gorecki DC, Monaco AP, Derry JM, Walker AP, Barnard EA & Barnard PJ. (1992). Expression of four alternative dystrophin transcripts in brain regions regulated by different promoters. *Hum Mol Genet* **1,** 505-510.

Gould E, Tanapat P, Rydel T & Hastings N. (2000). Regulation of hippocampal neurogenesis in adulthood. *Biol Psychiatry* **48,** 715-720.

Goussakov I, Synowiec S, Yarnykh V & Drobyshevsky A. (2019). Immediate and delayed decrease of long term potentiation and memory deficits after neonatal intermittent hypoxia. *Int J Dev Neurosci* **74,** 27-37.

Gruol DL & Nelson TE. (1997). Physiological and pathological roles of interleukin-6 in the central nervous system. *Mol Neurobiol* **15,** 307-339.

Haapakoski R, Mathieu J, Ebmeier KP, Alenius H & Kivimäki M. (2015). Cumulative meta-analysis of interleukins 6 and 1β, tumour necrosis factor α and C-reactive protein in patients with major depressive disorder. *Brain Behav Immun* **49,** 206-215.

Hall CS. (1934). Emotional behavior in the rat. I. Defecation and urination as measures of individual differences in emotionality. *Journal of Comparative Psychology* **18,** 385-403.

Harrison FE, Hosseini AH & McDonald MP. (2009). Endogenous anxiety and stress responses in water maze and Barnes maze spatial memory tasks. *Behav Brain Res* **198,** 247-251.

Hartmann J & Konnerth A. (2005). Determinants of postsynaptic Ca2+ signaling in Purkinje neurons. *Cell Calcium* **37,** 459-466.

Hasler G, Nugent AC, Carlson PJ, Carson RE, Geraci M & Drevets WC. (2008). Altered cerebral gamma-aminobutyric acid type A-benzodiazepine receptor binding in panic disorder determined by [11C]flumazenil positron emission tomography. *Arch Gen Psychiatry* **65,** 1166-1175.

Hatten ME & Mason CA. (1990). Mechanisms of glial-guided neuronal migration in vitro and in vivo. *Experientia* **46,** 907-916.

Haws CM & Lansman JB. (1991). Calcium-permeable ion channels in cerebellar neurons from mdx mice. *Proc Biol Sci* **244,** 185-189.

Hendriksen JG & Vles JS. (2008). Neuropsychiatric disorders in males with duchenne muscular dystrophy: frequency rate of attention-deficit hyperactivity disorder (ADHD), autism spectrum disorder, and obsessive--compulsive disorder. *J Child Neurol* **23,** 477-481.

Henneberger C, Papouin T, Oliet SH & Rusakov DA. (2010). Long-term potentiation depends on release of D-serine from astrocytes. *Nature* **463,** 232-236.

Heyser CJ, Masliah E, Samimi A, Campbell IL & Gold LH. (1997). Progressive decline in avoidance learning paralleled by inflammatory neurodegeneration in transgenic mice expressing interleukin 6 in the brain. *Proc Natl Acad Sci U S A* **94,** 1500-1505.

Hinton VJ, De Vivo DC, Nereo NE, Goldstein E & Stern Y. (2000). Poor verbal working memory across intellectual level in boys with Duchenne dystrophy. *Neurology* **54,** 2127-2132.

Hinton VJ, De Vivo DC, Nereo NE, Goldstein E & Stern Y. (2001). Selective deficits in verbal working memory associated with a known genetic etiology: the neuropsychological profile of duchenne muscular dystrophy. *J Int Neuropsychol Soc* **7,** 45-54.

Hinton VJ, Fee RJ, De Vivo DC & Goldstein E. (2007). Poor facial affect recognition among boys with duchenne muscular dystrophy. *J Autism Dev Disord* **37,** 1925-1933.

Hinton VJ, Nereo NE, Fee RJ & Cyrulnik SE. (2006). Social behavior problems in boys with Duchenne muscular dystrophy. *J Dev Behav Pediatr* **27,** 470-476.

Hirano T, Taga T, Nakano N, Yasukawa K, Kashiwamura S, Shimizu K, Nakajima K, Pyun KH & Kishimoto T. (1985). Purification to homogeneity and characterization of human B-cell differentiation factor (BCDF or BSFp-2). *Proc Natl Acad Sci U S A* **82,** 5490-5494.

Hitti FL & Siegelbaum SA. (2014). The hippocampal CA2 region is essential for social memory. *Nature* **508,** 88-92.

Hoffman EP & Kunkel LM. (1989). Dystrophin abnormalities in Duchenne/Becker muscular dystrophy. *Neuron* **2,** 1019-1029.

Holmes A, Kinney JW, Wrenn CC, Li Q, Yang RJ, Ma L, Vishwanath J, Saavedra MC, Innerfield CE, Jacoby AS, Shine J, Iismaa TP & Crawley JN. (2003). Galanin GAL-R1 receptor null mutant mice display increased anxiety-like behavior specific to the elevated plus-maze. *Neuropsychopharmacology* **28,** 1031-1044.

Howard PL, Dally GY, Ditta SD, Austin RC, Worton RG, Klamut HJ & Ray PN. (1999). Dystrophin isoforms DP71 and DP427 have distinct roles in myogenic cells. *Muscle Nerve* **22,** 16-27.

Hugnot JP, Gilgenkrantz H, Vincent N, Chafey P, Morris GE, Monaco AP, Berwald-Netter Y, Koulakoff A, Kaplan JC, Kahn A & et al. (1992). Distal transcript of the dystrophin gene initiated from an alternative first exon and encoding a 75-kDa protein widely distributed in nonmuscle tissues. *Proc Natl Acad Sci U S A* **89,** 7506-7510.

Hölter SM, Einicke J, Sperling B, Zimprich A, Garrett L, Fuchs H, Gailus-Durner V, Hrabé de Angelis M & Wurst W. (2015). Tests for Anxiety-Related Behavior in Mice. *Curr Protoc Mouse Biol* **5,** 291-309.

Iivonen H, Nurminen L, Harri M, Tanila H & Puoliväli J. (2003). Hypothermia in mice tested in Morris water maze. *Behav Brain Res* **141,** 207-213.

Islam O, Gong X, Rose-John S & Heese K. (2009). Interleukin-6 and neural stem cells: more than gliogenesis. *Mol Biol Cell* **20,** 188-199.

Izquierdo LA, Barros DM, da Costa JC, Furini C, Zinn C, Cammarota M, Bevilaqua LR & Izquierdo I. (2007). A link between role of two prefrontal areas in immediate memory and in long-term memory consolidation. *Neurobiol Learn Mem* **88,** 160-166.

Jagadha V & Becker LE. (1988). Brain morphology in Duchenne muscular dystrophy: a Golgi study. *Pediatr Neurol* **4,** 87-92.

Jankowsky JL, Derrick BE & Patterson PH. (2000). Cytokine responses to LTP induction in the rat hippocampus: a comparison of in vitro and in vivo techniques. *Learn Mem* **7,** 400-412.

Jones SA. (2005). Directing transition from innate to acquired immunity: defining a role for IL-6. *J Immunol* **175,** 3463-3468.

Jourdain P, Bergersen LH, Bhaukaurally K, Bezzi P, Santello M, Domercq M, Matute C, Tonello F, Gundersen V & Volterra A. (2007). Glutamate exocytosis from astrocytes controls synaptic strength. *Nat Neurosci* **10,** 331-339.

Jung D, Filliol D, Metz-Boutigue MH & Rendon A. (1993). Characterization and subcellular localization of the dystrophin-protein 71 (Dp71) from brain. *Neuromuscul Disord* **3,** 515-518.

Kaar A, Morley SJ & Rae MG. (2017). An efficient and cost-effective method of generating postnatal (P2-5) mouse primary hippocampal neuronal cultures. *J Neurosci Methods* **286,** 69-77.

Keep NH. (2000). Structural comparison of actin binding in utrophin and dystrophin. *Neurol Sci* **21,** S929-937.

Khachaturian ZS. (1987). Hypothesis on the regulation of cytosol calcium concentration and the aging brain. *Neurobiol Aging* **8,** 345-346.

Kheirbek MA, Drew LJ, Burghardt NS, Costantini DO, Tannenholz L, Ahmari SE, Zeng H, Fenton AA & Hen R. (2013). Differential control of learning and anxiety along the dorsoventral axis of the dentate gyrus. *Neuron* **77,** 955-968.

Kim TW, Wu K, Xu JL & Black IB. (1992). Detection of dystrophin in the postsynaptic density of rat brain and deficiency in a mouse model of Duchenne muscular dystrophy. *Proc Natl Acad Sci U S A* **89,** 11642-11644.

Kirchhoff F, Dringen R & Giaume C. (2001). Pathways of neuron-astrocyte interactions and their possible role in neuroprotection. *Eur Arch Psychiatry Clin Neurosci* **251,** 159-169.

Knuesel I, Bornhauser BC, Zuellig RA, Heller F, Schaub MC & Fritschy JM. (2000). Differential expression of utrophin and dystrophin in CNS neurons: an in situ hybridization and immunohistochemical study. *J Comp Neurol* **422,** 594-611.

Knuesel I, Mastrocola M, Zuellig RA, Bornhauser B, Schaub MC & Fritschy JM. (1999). Short communication: altered synaptic clustering of GABAA receptors in mice lacking dystrophin (mdx mice). *Eur J Neurosci* **11,** 4457-4462.

Knuesel I, Zuellig RA, Schaub MC & Fritschy JM. (2001). Alterations in dystrophin and utrophin expression parallel the reorganization of GABAergic synapses in a mouse model of temporal lobe epilepsy. *Eur J Neurosci* **13,** 1113-1124.

Kong X, Gong Z, Zhang L, Sun X, Ou Z, Xu B, Huang J, Long D, He X, Lin X, Li Q, Xu L & Xuan A. (2019). JAK2/STAT3 signaling mediates IL-6-inhibited neurogenesis of neural stem cells through DNA demethylation/methylation. *Brain Behav Immun*.

Kraeuter AK, Guest PC & Sarnyai Z. (2019). The Open Field Test for Measuring Locomotor Activity and Anxiety-Like Behavior. *Methods Mol Biol* **1916,** 99-103.

Krystal JH, Sanacora G, Blumberg H, Anand A, Charney DS, Marek G, Epperson CN, Goddard A & Mason GF. (2002). Glutamate and GABA systems as targets for novel antidepressant and mood-stabilizing treatments. *Mol Psychiatry* **7 Suppl 1,** S71-80.

Kueh SL, Head SI & Morley JW. (2008). GABA(A) receptor expression and inhibitory post-synaptic currents in cerebellar Purkinje cells in dystrophin-deficient mdx mice. *Clin Exp Pharmacol Physiol* **35,** 207-210.

Kuhn HG, Dickinson-Anson H & Gage FH. (1996). Neurogenesis in the dentate gyrus of the adult rat: age-related decrease of neuronal progenitor proliferation. *J Neurosci* **16,** 2027-2033.

Landfeldt E, Thompson R, Sejersen T, McMillan HJ, Kirschner J & Lochmüller H. (2020). Life expectancy at birth in Duchenne muscular dystrophy: a systematic review and meta-analysis. *Eur J Epidemiol* **35,** 643-653.

Landfield PW. (1987). 'Increased calcium-current' hypothesis of brain aging. *Neurobiol Aging* **8,** 346-347.

Lapidos KA, Kakkar R & McNally EM. (2004). The dystrophin glycoprotein complex: signaling strength and integrity for the sarcolemma. *Circ Res* **94,** 1023-1031.

Larson J, Wong D & Lynch G. (1986). Patterned stimulation at the theta frequency is optimal for the induction of hippocampal long-term potentiation. *Brain Res* **368,** 347-350.

Latimer R, Street N, Conway KC, James K, Cunniff C, Oleszek J, Fox D, Ciafaloni E, Westfield C & Paramsothy P. (2017). Secondary Conditions Among Males With Duchenne or Becker Muscular Dystrophy. *J Child Neurol* **32,** 663-670.

Lederfein D, Levy Z, Augier N, Mornet D, Morris G, Fuchs O, Yaffe D & Nudel U. (1992). A 71-kilodalton protein is a major product of the Duchenne muscular dystrophy gene in brain and other nonmuscle tissues. *Proc Natl Acad Sci U S A* **89,** 5346-5350.

LeDoux JE, Iwata J, Cicchetti P & Reis DJ. (1988). Different projections of the central amygdaloid nucleus mediate autonomic and behavioral correlates of conditioned fear. *J Neurosci* **8,** 2517-2529.

Li AJ, Katafuchi T, Oda S, Hori T & Oomura Y. (1997). Interleukin-6 inhibits long-term potentiation in rat hippocampal slices. *Brain Res* **748,** 30-38.

Lidov HG, Byers TJ & Kunkel LM. (1993). The distribution of dystrophin in the murine central nervous system: an immunocytochemical study. *Neuroscience* **54,** 167-187.

Lidov HG, Byers TJ, Watkins SC & Kunkel LM. (1990). Localization of dystrophin to postsynaptic regions of central nervous system cortical neurons. *Nature* **348,** 725-728.

Lisman J, Schulman H & Cline H. (2002). The molecular basis of CaMKII function in synaptic and behavioural memory. *Nat Rev Neurosci* **3,** 175-190.

Liu Y, Beyer A & Aebersold R. (2016). On the Dependency of Cellular Protein Levels on mRNA Abundance. *Cell* **165,** 535-550.

Lopez JR, Kolster J, Uryash A, Esteve E, Altamirano F & Adams JA. (2018). Dysregulation of Intracellular Ca(2+) in Dystrophic Cortical and Hippocampal Neurons. *Mol Neurobiol* **55,** 603-618.

Love DR, Hill DF, Dickson G, Spurr NK, Byth BC, Marsden RF, Walsh FS, Edwards YH & Davies KE. (1989). An autosomal transcript in skeletal muscle with homology to dystrophin. *Nature* **339,** 55-58.

Lueptow LM (2017). Novel object recognition test for the investigation of learning and memory in mice. Journal of Visualized Experiments; DOI: 10.3791/55718.

Lust JA, Donovan KA, Kline MP, Greipp PR, Kyle RA & Maihle NJ. (1992). Isolation of an mRNA encoding a soluble form of the human interleukin-6 receptor. *Cytokine* **4,** 96-100.

Lv SY, Zou QH, Cui JL, Zhao N, Hu J, Long XY, Sun YC, He J, Zhu CZ, He Y & Zang YF. (2011). Decreased gray matter concentration and local synchronization of spontaneous activity in the motor cortex in Duchenne muscular dystrophy. *AJNR Am J Neuroradiol* **32,** 2196-2200.

Lydiard RB. (2003). The role of GABA in anxiety disorders. *J Clin Psychiatry* **64 Suppl 3,** 21-27.

Lyra ESNM, Gonçalves RA, Pascoal TA, Lima-Filho RAS, Resende EPF, Vieira ELM, Teixeira AL, de Souza LC, Peny JA, Fortuna JTS, Furigo IC, Hashiguchi D, Miya-Coreixas VS, Clarke JR, Abisambra JF, Longo BM, Donato J, Jr., Fraser PE, Rosa-Neto P, Caramelli P, Ferreira ST & De Felice FG. (2021). Pro-inflammatory interleukin-6 signaling links cognitive impairments and peripheral metabolic alterations in Alzheimer's disease. *Transl Psychiatry* **11,** 251.

Malenka RC & Nicoll RA. (1999). Long-term potentiation--a decade of progress? *Science* **285,** 1870-1874.

Manning J, Buckley MM, O'Halloran KD & O'Malley D. (2017). Combined XIL-6R and urocortin-2 treatment restores MDX diaphragm muscle force. *Muscle Nerve* **56,** E134-e140.

Manning J, Kulbida R, Rai P, Jensen L, Bouma J, Singh SP, O'Malley D & Yilmazer-Hanke D. (2014). Amitriptyline is efficacious in ameliorating muscle inflammation and depressive symptoms in the mdx mouse model of Duchenne muscular dystrophy. *Exp Physiol* **99,** 1370-1386.

Martin SJ, Grimwood PD & Morris RG. (2000). Synaptic plasticity and memory: an evaluation of the hypothesis. *Annu Rev Neurosci* **23,** 649-711.

Marz P, Cheng JG, Gadient RA, Patterson PH, Stoyan T, Otten U & Rose-John S. (1998). Sympathetic neurons can produce and respond to interleukin 6. *Proc Natl Acad Sci U S A* **95,** 3251-3256.

Matsumura CY, Taniguti AP, Pertille A, Santo Neto H & Marques MJ. (2011). Stretch-activated calcium channel protein TRPC1 is correlated with the different degrees of the dystrophic phenotype in mdx mice. *Am J Physiol Cell Physiol* **301,** C1344-1350.

Mattson MP. (2007). Calcium and neurodegeneration. *Aging Cell* **6,** 337-350.

McCormick DA & Contreras D. (2001). On the cellular and network bases of epileptic seizures. *Annu Rev Physiol* **63,** 815-846.

McDouall RM, Dunn MJ & Dubowitz V. (1990). Nature of the mononuclear infiltrate and the mechanism of muscle damage in juvenile dermatomyositis and Duchenne muscular dystrophy. *J Neurol Sci* **99,** 199-217.

Mendell JR & Rodino-Klapac LR. (2016). Duchenne muscular dystrophy: CRISPR/Cas9 treatment. *Cell Res* **26,** 513-514.

Messina S, Vita GL, Aguennouz M, Sframeli M, Romeo S, Rodolico C & Vita G. (2011). Activation of NF-kappaB pathway in Duchenne muscular dystrophy: relation to age. *Acta Myol* **30,** 16-23.

Ming GL & Song H. (2011). Adult neurogenesis in the mammalian brain: significant answers and significant questions. *Neuron* **70,** 687-702.

Miranda R, Laroche S & Vaillend C. (2016). Reduced neuronal density in the CA1 anterodorsal hippocampus of the mdx mouse. *Neuromuscul Disord* **26,** 775-781.

Miranda R, Sebrie C, Degrouard J, Gillet B, Jaillard D, Laroche S & Vaillend C. (2009). Reorganization of inhibitory synapses and increased PSD length of perforated excitatory synapses in hippocampal area CA1 of dystrophin-deficient mdx mice. *Cerebral cortex* **19,** 876-888.

Missiaen L, Robberecht W, van den Bosch L, Callewaert G, Parys JB, Wuytack F, Raeymaekers L, Nilius B, Eggermont J & De Smedt H. (2000). Abnormal intracellular ca(2+)homeostasis and disease. *Cell Calcium* **28,** 1-21.

Moens P, Baatsen PH & Marechal G. (1993). Increased susceptibility of EDL muscles from mdx mice to damage induced by contractions with stretch. *J Muscle Res Cell Motil* **14,** 446-451.

Morgan JE, Prola A, Mariot V, Pini V, Meng J, Hourde C, Dumonceaux J, Conti F, Relaix F, Authier FJ, Tiret L, Muntoni F & Bencze M. (2018). Publisher Correction: Necroptosis mediates myofibre death in dystrophin-deficient mice. *Nat Commun* **9,** 4107.

Morris RG, Anderson E, Lynch GS & Baudry M. (1986). Selective impairment of learning and blockade of long-term potentiation by an N-methyl-D-aspartate receptor antagonist, AP5. *Nature* **319,** 774-776.

Morris RG, Moser EI, Riedel G, Martin SJ, Sandin J, Day M & O'Carroll C. (2003). Elements of a neurobiological theory of the hippocampus: the role of activity-dependent synaptic plasticity in memory. *Philos Trans R Soc Lond B Biol Sci* **358,** 773-786.

Moser M-B & Moser EI (1998). Distributed encoding and retrieval of spatial memory in the hippocampus. The Journal of Neuroscience 18, 7535–7542.

Moukhles H & Carbonetto S. (2001). Dystroglycan contributes to the formation of multiple dystrophin-like complexes in brain. *J Neurochem* **78,** 824-834.

Muller D, Joly M & Lynch G. (1988). Contributions of quisqualate and NMDA receptors to the induction and expression of LTP. *Science* **242,** 1694-1697.

Mumby DG, Glenn MJ, Nesbitt C & Kyriazis DA. (2002). Dissociation in retrograde memory for object discriminations and object recognition in rats with perirhinal cortex damage. *Behav Brain Res* **132,** 215-226.

Muntoni F, Mateddu A & Serra G. (1991). Passive avoidance behaviour deficit in the mdx mouse. *Neuromuscul Disord* **1,** 121-123.

Müllberg J, Schooltink H, Stoyan T, Günther M, Graeve L, Buse G, Mackiewicz A, Heinrich PC & Rose-John S. (1993). The soluble interleukin-6 receptor is generated by shedding. *Eur J Immunol* **23,** 473-480.

Nakanishi M, Niidome T, Matsuda S, Akaike A, Kihara T & Sugimoto H. (2007). Microglia-derived interleukin-6 and leukaemia inhibitory factor promote

astrocytic differentiation of neural stem/progenitor cells. *Eur J Neurosci* **25,** 649-658.

Nardes F, Araujo AP & Ribeiro MG. (2012). Mental retardation in Duchenne muscular dystrophy. *J Pediatr (Rio J)* **88,** 6-16.

National Research Council Committee for the Update of the Guide for the Care and Use of Laboratory A. (2011). The National Academies Collection: Reports funded by National Institutes of Health. In *Guide for the Care and Use of Laboratory Animals*. National Academies Press (US)

Copyright © 2011, National Academy of Sciences., Washington (DC).

Nichols B, Takeda S & Yokota T. (2015). Nonmechanical Roles of Dystrophin and Associated Proteins in Exercise, Neuromuscular Junctions, and Brains. *Brain Sci* **5,** 275-298.

Nudel U, Zuk D, Einat P, Zeelon E, Levy Z, Neuman S & Yaffe D. (1989). Duchenne muscular dystrophy gene product is not identical in muscle and brain. *Nature* **337,** 76-78.

Nutt DJ & Malizia AL. (2001). New insights into the role of the GABA(A)-benzodiazepine receptor in psychiatric disorder. *Br J Psychiatry* **179,** 390-396.

Oliveira AM, Hawk JD, Abel T & Havekes R. (2010). Post-training reversible inactivation of the hippocampus enhances novel object recognition memory. *Learn Mem* **17,** 155-160.

Orrenius S & Nicotera P. (1994). The calcium ion and cell death. *J Neural Transm Suppl* **43,** 1-11.

Osten P, Valsamis L, Harris A & Sacktor TC (1996). Protein synthesis-dependent formation of protein kinase Mzeta in long- term potentiation. The Journal of Neuroscience 16, 2444–2451.

Pane M, Messina S, Bruno C, D'Amico A, Villanova M, Brancalion B, Sivo S, Bianco F, Striano P, Battaglia D, Lettori D, Vita GL, Bertini E, Gualandi F, Ricotti V, Ferlini A & Mercuri E. (2013a). Duchenne muscular dystrophy and epilepsy. *Neuromuscul Disord* **23,** 313-315.

Pane M, Scalise R, Berardinelli A, D'Angelo G, Ricotti V, Alfieri P, Moroni I, Hartley L, Pera MC, Baranello G, Catteruccia M, Casalino T, Romeo DM, Graziano A,

Gandioli C, Bianco F, Mazzone ES, Lombardo ME, Scoto M, Sivo S, Palermo C, Gualandi F, Sormani MP, Ferlini A, Bertini E, Muntoni F & Mercuri E. (2013b). Early neurodevelopmental assessment in Duchenne muscular dystrophy. *Neuromuscul Disord* **23,** 451-455.

Pastoret C & Sebille A. (1995). mdx mice show progressive weakness and muscle deterioration with age. *J Neurol Sci* **129,** 97-105.

Pelosi L, Berardinelli MG, Forcina L, Spelta E, Rizzuto E, Nicoletti C, Camilli C, Testa E, Catizone A, De Benedetti F & Musaro A. (2015). Increased levels of interleukin-6 exacerbate the dystrophic phenotype in mdx mice. *Hum Mol Genet* **24,** 6041-6053.

Penkowa M, Molinero A, Carrasco J & Hidalgo J. (2001). Interleukin-6 deficiency reduces the brain inflammatory response and increases oxidative stress and neurodegeneration after kainic acid-induced seizures. *Neuroscience* **102,** 805-818.

Perloff JK. (1984). Cardiac rhythm and conduction in Duchenne's muscular dystrophy: a prospective study of 20 patients. *J Am Coll Cardiol* **3,** 1263-1268.

Perronnet C, Chagneau C, Le Blanc P, Samson-Desvignes N, Mornet D, Laroche S, De La Porte S & Vaillend C. (2012). Upregulation of brain utrophin does not rescue behavioral alterations in dystrophin-deficient mice. *Hum Mol Genet* **21,** 2263-2276.

Perronnet C & Vaillend C. (2010). Dystrophins, utrophins, and associated scaffolding complexes: role in mammalian brain and implications for therapeutic strategies. *J Biomed Biotechnol* **2010,** 849426.

Piterkin P, Cole E, Cossette MP, Gaskin S & Mumby DG. (2008). A limited role for the hippocampus in the modulation of novel-object preference by contextual cues. *Learn Mem* **15,** 785-791.

Pramparo T, Youn YH, Yingling J, Hirotsune S & Wynshaw-Boris A. (2010). Novel embryonic neuronal migration and proliferation defects in Dcx mutant mice are exacerbated by Lis1 reduction. *J Neurosci* **30,** 3002-3012.

Rando TA. (2001). The dystrophin-glycoprotein complex, cellular signaling, and the regulation of cell survival in the muscular dystrophies. *Muscle Nerve* **24,** 1575-1594.

Rao MS, Hattiangady B, Abdel-Rahman A, Stanley DP & Shetty AK. (2005). Newly born cells in the ageing dentate gyrus display normal migration, survival and neuronal fate choice but endure retarded early maturation. *Eur J Neurosci* **21,** 464-476.

Rapaport D, Fuchs O, Nudel U & Yaffe D. (1992). Expression of the Duchenne muscular dystrophy gene products in embryonic stem cells and their differentiated derivatives. *J Biol Chem* **267,** 21289-21292.

Reinig AM, Mirzaei S & Berlau DJ. (2017). Advances in the Treatment of Duchenne Muscular Dystrophy: New and Emerging Pharmacotherapies. *Pharmacotherapy* **37,** 492-499.

Ricotti V, Mandy WP, Scoto M, Pane M, Deconinck N, Messina S, Mercuri E, Skuse DH & Muntoni F. (2016). Neurodevelopmental, emotional, and behavioural problems in Duchenne muscular dystrophy in relation to underlying dystrophin gene mutations. *Dev Med Child Neurol* **58,** 77-84.

Rose-John S. (2012). IL-6 trans-signaling via the soluble IL-6 receptor: importance for the pro-inflammatory activities of IL-6. *Int J Biol Sci* **8,** 1237-1247.

Rose-John S & Heinrich PC. (1994). Soluble receptors for cytokines and growth factors: generation and biological function. *Biochem J* **300 (Pt 2),** 281-290.

Rosman NP. (1970). The cerebral defect and myopathy in Duchenne muscular dystrophy. A comparative clinicopathological study. *Neurology* **20,** 329-335.

Rothaug M, Becker-Pauly C & Rose-John S. (2016). The role of interleukin-6 signaling in nervous tissue. *Biochim Biophys Acta* **1863,** 1218-1227.

Rubinsztein JS, Rubinsztein DC, Goodburn S & Holland AJ. (1998). Apathy and hypersomnia are common features of myotonic dystrophy. *J Neurol Neurosurg Psychiatry* **64,** 510-515.

Rufo A, Del Fattore A, Capulli M, Carvello F, De Pasquale L, Ferrari S, Pierroz D, Morandi L, De Simone M, Rucci N, Bertini E, Bianchi ML, De Benedetti F & Teti A. (2011). Mechanisms inducing low bone density in Duchenne muscular dystrophy in mice and humans. *J Bone Miner Res* **26,** 1891-1903.

Sarkisyan G & Hedlund PB. (2009). The 5-HT7 receptor is involved in allocentric spatial memory information processing. *Behav Brain Res* **202,** 26-31.

Saxena S & Caroni P. (2011). Selective neuronal vulnerability in neurodegenerative diseases: from stressor thresholds to degeneration. *Neuron* **71,** 35-48.

Sbriccoli A, Santarelli M, Carretta D, Pinto F, Granato A & Minciacchi D. (1995). Architectural changes of the cortico-spinal system in the dystrophin defective mdx mouse. *Neurosci Lett* **200,** 53-56.

Schaper F & Rose-John S. (2015). Interleukin-6: Biology, signaling and strategies of blockade. *Cytokine Growth Factor Rev* **26,** 475-487.

Scheller J, Chalaris A, Garbers C & Rose-John S. (2011a). ADAM17: a molecular switch to control inflammation and tissue regeneration. *Trends Immunol* **32,** 380-387.

Scheller J, Chalaris A, Schmidt-Arras D & Rose-John S. (2011b). The pro- and anti-inflammatory properties of the cytokine interleukin-6. *Biochim Biophys Acta* **1813,** 878-888.

Schindler AG, Li S & Chavkin C. (2010). Behavioral stress may increase the rewarding valence of cocaine-associated cues through a dynorphin/kappa-opioid receptor-mediated mechanism without affecting associative learning or memory retrieval mechanisms. *Neuropsychopharmacology* **35,** 1932-1942.

Schmidt-Hieber C, Jonas P & Bischofberger J (2004). Enhanced synaptic plasticity in newly generated granule cells of the adult hippocampus. Nature 429, 184–187.

Sekiguchi M, Zushida K, Yoshida M, Maekawa M, Kamichi S, Sahara Y, Yuasa S, Takeda S & Wada K. (2009). A deficit of brain dystrophin impairs specific amygdala GABAergic transmission and enhances defensive behaviour in mice. *Brain* **132,** 124-135.

Sesay AK, Errington ML, Levita L & Bliss TV. (1996). Spatial learning and hippocampal long-term potentiation are not impaired in mdx mice. *Neuroscience letters* **211,** 207-210.

Silverman JL, Tolu SS, Barkan CL & Crawley JN. (2010). Repetitive self-grooming behavior in the BTBR mouse model of autism is blocked by the mGluR5 antagonist MPEP. *Neuropsychopharmacology* **35,** 976-989.

Simpson DM, Hallett M, Ashman EJ, Comella CL, Green MW, Gronseth GS, Armstrong MJ, Gloss D, Potrebic S, Jankovic J, Karp BP, Naumann M, So YT &

Yablon SA. (2016). Practice guideline update summary: Botulinum neurotoxin for the treatment of blepharospasm, cervical dystonia, adult spasticity, and headache: Report of the Guideline Development Subcommittee of the American Academy of Neurology. *Neurology* **86,** 1818-1826.

Snow WM, Anderson JE & Jakobson LS. (2013). Neuropsychological and neurobehavioral functioning in Duchenne muscular dystrophy: a review. *Neurosci Biobehav Rev* **37,** 743-752.

Sogos V, Ennas MG, Mussini I & Gremo F. (1997). Effect of dystrophin antisense oligonucleotides on cultured human neurons. *Neurochem Int* **31,** 447-457.

Sparkman NL, Buchanan JB, Heyen JR, Chen J, Beverly JL & Johnson RW. (2006). Interleukin-6 facilitates lipopolysaccharide-induced disruption in working memory and expression of other proinflammatory cytokines in hippocampal neuronal cell layers. *J Neurosci* **26,** 10709-10716.

Stampanoni Bassi M, Iezzi E, Mori F, Simonelli I, Gilio L, Buttari F, Sica F, De Paolis N, Mandolesi G, Musella A, De Vito F, Dolcetti E, Bruno A, Furlan R, Finardi A, Marfia GA, Centonze D & Rizzo FR. (2019). Interleukin-6 Disrupts Synaptic Plasticity and Impairs Tissue Damage Compensation in Multiple Sclerosis. *Neurorehabil Neural Repair* **33,** 825-835.

Stedman HH, Sweeney HL, Shrager JB, Maguire HC, Panettieri RA, Petrof B, Narusawa M, Leferovich JM, Sladky JT & Kelly AM. (1991). The mdx mouse diaphragm reproduces the degenerative changes of Duchenne muscular dystrophy. *Nature* **352,** 536-539.

Suchyna TM, Johnson JH, Hamer K, Leykam JF, Gage DA, Clemo HF, Baumgarten CM & Sachs F. (2000). Identification of a peptide toxin from Grammostola spatulata spider venom that blocks cation-selective stretch-activated channels. *J Gen Physiol* **115,** 583-598.

Suzuki Y, Higuchi S, Aida I, Nakajima T & Nakada T. (2017). Abnormal distribution of GABA(A) receptors in brain of duchenne muscular dystrophy patients. *Muscle Nerve* **55,** 591-595.

Tancredi V, D'Antuono M, Cafe C, Giovedi S, Bue MC, D'Arcangelo G, Onofri F & Benfenati F. (2000). The inhibitory effects of interleukin-6 on synaptic plasticity in the rat hippocampus are associated with an inhibition of mitogen-activated protein kinase ERK. *J Neurochem* **75,** 634-643.

Teyler TJ & DiScenna P. (1987). Long-term potentiation. *Annu Rev Neurosci* **10,** 131-161.

Theodosis DT, Poulain DA & Oliet SH. (2008). Activity-dependent structural and functional plasticity of astrocyte-neuron interactions. *Physiol Rev* **88,** 983-1008.

Toescu EC & Verkhratsky A. (2007). The importance of being subtle: small changes in calcium homeostasis control cognitive decline in normal aging. *Aging Cell* **6,** 267-273.

Tozawa T, Itoh K, Yaoi T, Tando S, Umekage M, Dai H, Hosoi H & Fushiki S. (2012). The shortest isoform of dystrophin (Dp40) interacts with a group of presynaptic proteins to form a presumptive novel complex in the mouse brain. *Mol Neurobiol* **45,** 287-297.

Tracey I, Scott RB, Thompson CH, Dunn JF, Barnes PR, Styles P, Kemp GJ, Rae CD, Pike M & Radda GK. (1995). Brain abnormalities in Duchenne muscular dystrophy: phosphorus-31 magnetic resonance spectroscopy and neuropsychological study. *Lancet* **345,** 1260-1264.

Treves A & Rolls ET. (1994). Computational analysis of the role of the hippocampus in memory. *Hippocampus* **4,** 374-391.

Tulving E & Markowitsch HJ. (1998). Episodic and declarative memory: role of the hippocampus. *Hippocampus* **8,** 198-204.

Unglaub Silverthorn D. (2013). Human Physiology, An Integrated Approach, ed. Johnson BR, Ober, William C., Garrison, Claire W., Silverthorn, Andrew C. Pearson Education, Boston.

Vaillend C & Billard JM. (2002). Facilitated CA1 hippocampal synaptic plasticity in dystrophin-deficient mice: role for GABAA receptors? *Hippocampus* **12,** 713-717.

Vaillend C, Billard JM & Laroche S. (2004). Impaired long-term spatial and recognition memory and enhanced CA1 hippocampal LTP in the dystrophin-deficient Dmd(mdx) mouse. *Neurobiol Dis* **17,** 10-20.

Vaillend C, Perronnet C, Ros C, Gruszczynski C, Goyenvalle A, Laroche S, Danos O, Garcia L & Peltekian E. (2010). Rescue of a dystrophin-like protein by exon

skipping in vivo restores GABAA-receptor clustering in the hippocampus of the mdx mouse. *Mol Ther* **18,** 1683-1688.

Vaillend C, Rendon A, Misslin R & Ungerer A. (1995). Influence of dystrophin-gene mutation on mdx mouse behavior. I. Retention deficits at long delays in spontaneous alternation and bar-pressing tasks. *Behavior genetics* **25,** 569-579.

Vallieres L, Campbell IL, Gage FH & Sawchenko PE. (2002). Reduced hippocampal neurogenesis in adult transgenic mice with chronic astrocytic production of interleukin-6. *J Neurosci* **22,** 486-492.

van Praag H, Schinder AF, Christie BR, Toni N, Palmer TD & Gage FH. (2002). Functional neurogenesis in the adult hippocampus. *Nature* **415,** 1030-1034.

Vargha-Khadem F, Gadian DG, Watkins KE, Connelly A, Van Paesschen W & Mishkin M. (1997). Differential effects of early hippocampal pathology on episodic and semantic memory. *Science* **277,** 376-380.

Vorhees CV & Williams MT. (2006). Morris water maze: procedures for assessing spatial and related forms of learning and memory. *Nat Protoc* **1,** 848-858.

Wada E, Tanihata J, Iwamura A, Takeda S, Hayashi YK & Matsuda R. (2017). Treatment with the anti-IL-6 receptor antibody attenuates muscular dystrophy via promoting skeletal muscle regeneration in dystrophin-/utrophin-deficient mice. *Skelet Muscle* **7,** 23.

Wada-Isoe K, Wakutani Y, Urakami K & Nakashima K. (2004). Elevated interleukin-6 levels in cerebrospinal fluid of vascular dementia patients. *Acta Neurol Scand* **110,** 124-127.

Wagner KR. (2008). Approaching a new age in Duchenne muscular dystrophy treatment. *Neurotherapeutics* **5,** 583-591.

Waite A, Brown SC & Blake DJ. (2012). The dystrophin-glycoprotein complex in brain development and disease. *Trends Neurosci* **35,** 487-496.

Waite A, Tinsley CL, Locke M & Blake DJ. (2009). The neurobiology of the dystrophin-associated glycoprotein complex. *Ann Med* **41,** 344-359.

Watanabe D, Yoshimura R, Khalil M, Yoshida K, Kishimoto T, Taga T & Kiyama H. (1996). Characteristic localization of gp130 (the signal-transducing receptor component used in common for IL-6/IL-11/CNTF/LIF/OSM) in the rat brain. *Eur J Neurosci* **8,** 1630-1640.

Wei H, Alberts I & Li X. (2013). Brain IL-6 and autism. *Neuroscience* **252,** 320-325.

Wei H, Chadman KK, McCloskey DP, Sheikh AM, Malik M, Brown WT & Li X. (2012). Brain IL-6 elevation causes neuronal circuitry imbalances and mediates autism-like behaviors. *Biochim Biophys Acta* **1822,** 831-842.

Wu MV & Hen R. (2014). Functional dissociation of adult-born neurons along the dorsoventral axis of the dentate gyrus. *Hippocampus* **24,** 751-761.

Yang Z & Wang KK. (2015). Glial fibrillary acidic protein: from intermediate filament assembly and gliosis to neurobiomarker. *Trends Neurosci* **38,** 364-374.

Ye SM & Johnson RW. (1999). Increased interleukin-6 expression by microglia from brain of aged mice. *J Neuroimmunol* **93,** 139-148.

Yoshioka M, Okuno T, Honda Y & Nakano Y. (1980). Central nervous system involvement in progressive muscular dystrophy. *Arch Dis Child* **55,** 589-594.

Yuste R, Majewska A & Holthoff K. (2000). From form to function: calcium compartmentalization in dendritic spines. *Nat Neurosci* **3,** 653-659.

Zhou L & Lu H. (2010). Targeting fibrosis in Duchenne muscular dystrophy. *J Neuropathol Exp Neurol* **69,** 771-776.

Zubrzycka-Gaarn EE, Bulman DE, Karpati G, Burghes AH, Belfall B, Klamut HJ, Talbot J, Hodges RS, Ray PN & Worton RG. (1988). The Duchenne muscular dystrophy gene product is localized in sarcolemma of human skeletal muscle. *Nature* **333,** 466-469.

Appendix

Cytokine 133 (2020) 15513 4

Contents lists available at ScienceDirect

Cytokine

journal homepage: www.elsevier.com/locate/cytokine

Review article

Interleukin-6: A neuro-active cytokine contributing to cognitive impairment in Duchenne muscular dystrophy?

Kimberley A. Stephenson[a], Mark G. Rae[a], Dervla O'Malley[a,b,*]

[a] Department of Physiology, School of Medicine, University College Cork, Western Road, Cork, Ireland [b] APC Microbiome Ireland, University College Cork, Western Road, Cork, Ireland

ARTICLEINFO

Keywords:
Duchenne Muscular Dystrophy
Dystrophin
Hippocampus
Learning
Memory

ABSTRACT

Interleukin-6 (IL-6) is a pro-inflammatory cytokine, classically associated with orchestrating an immune respons pathogens. However, IL-6 can also directly or indirectly modify central nervous system function, and thereby alte functions, such as learning and the consolidation of memories. IL-6 is chronically elevated in Duchenne Muscul (DMD), a neuromuscular disorder arising when a mutation causes the loss of the structural protein, dystrophi dystrophin leads to progressive immobility, chronic inflammation and premature death. However, the role of dy mechano-transducing signalling molecule is unnecessary in non-contracting cells such as neurons, where it may synapse formation. Specific brain regions, including the hippocampus, which is the site of memory acquisiti dystrophin and therefore, loss of this protein may underlie variable deficits in cognitive function that are common with DMD. This review will evaluate the potential role of IL-6 in cognitive dysfunction in dystrophin-deficient D

1. Introduction

Dystrophin is expressed in skeletal, cardiac and smooth muscle and in endocrine and neuronal tissue. Thus, loss of this protein, which underlies the progressive symptoms of Duchenne Muscular Dystrophy (DMD), results in deficiencies in multiple physiological systems. In the central nervous system (CNS), high levels of dystrophin have been detected in neurons of the cerebellum, cerebral cortex and also, the hippocampus [1], which is a region important for learning, and in memory formation. In contrast to its function as a sarcolemma-spanning structural protein, which provides stability to contracting peripheral myocytes, neuronal dystrophin is thought to play a role in the formation of new synaptic connections [2]. Individuals with DMD often exhibit nonprogressive cognitive deficiencies, which vary in severity [3], in addition to difficulties in communication and poor facial affect recognition [4,5]. Deficits in verbal, short-term and working memory, functions that are likely to be facilitated by the hippocampus, have also been observed in individuals with DMD [6–8]. Elevated levels of proinflammatory cytokines, including TNFα, IL-1β and IL-6 [9–13] have been detected in DMD muscle biopsies, which is likely to be due to degeneration and regeneration of myofibres. In addition to their well characterized role in the immune response, cytokines can also modify neuronal function, both directly by binding to receptors expressed on neurons [14,15] and indirectly, by stimulating secretion of neuromodulatory molecules from glia or endothelial cells [16,17]. Cross-talk between immune and neuronal cells are key to maintaining normal homeostasis of the nervous system [18]. Thus, chronic inflammation, which is prevalent in individuals with dystrophin-deficient DMD, in addition to structural changes at synapses, could contribute to dysfunctional synaptic transmission (Fig. 1) leading to deficits in cognitive function.

2. Interleukin-6, a pleiotropic cytokine with modulatory actionsin the central nervous system (CNS)

Cytokines are molecules of the immune system that are critical for

Abbreviations: AMPA, α-amino-3-hydroxy-5-methyl-4-isoxazolepropionic acid; CNS, central nervous system; DAPC, dystrophin-associated protein complex; DMD, Duchenne Muscular Dystrophy; ERK, extracellular-signal-regulated kinase; EPSPs, excitatory post-synaptic potentials; GABA, gamma-aminobutyric acid; IP_3R, inositol − 1,4,5-trisphosphate receptor; IQs, intelligence quotients; IL-6, interleukin-6; IL-6R, IL-6 receptor; JAK/STAT, Janus kinase/signal transducer and activator of transcription; LTP, long-term potentiation; nAChRs, nicotinic acetylcholine receptors; NMDA, N-methyl-D-aspartate; PI 3-kinase, phosphoinositide 3-kinase; (RyR), ryanodine receptor

* Corresponding author at: Department of Physiology, Western Gateway Building, University College Cork, Cork, Ireland. E-mail address: d.omalley@ucc.ie (D. O'Malley).

https://doi.org/10.1016/j.cyto.2020.155134
Received 3 April 2020; Received in revised form 13 May 2020; Accepted 14 May 2020
1043-4666/ © 2020 Elsevier Ltd. All rights reserved.

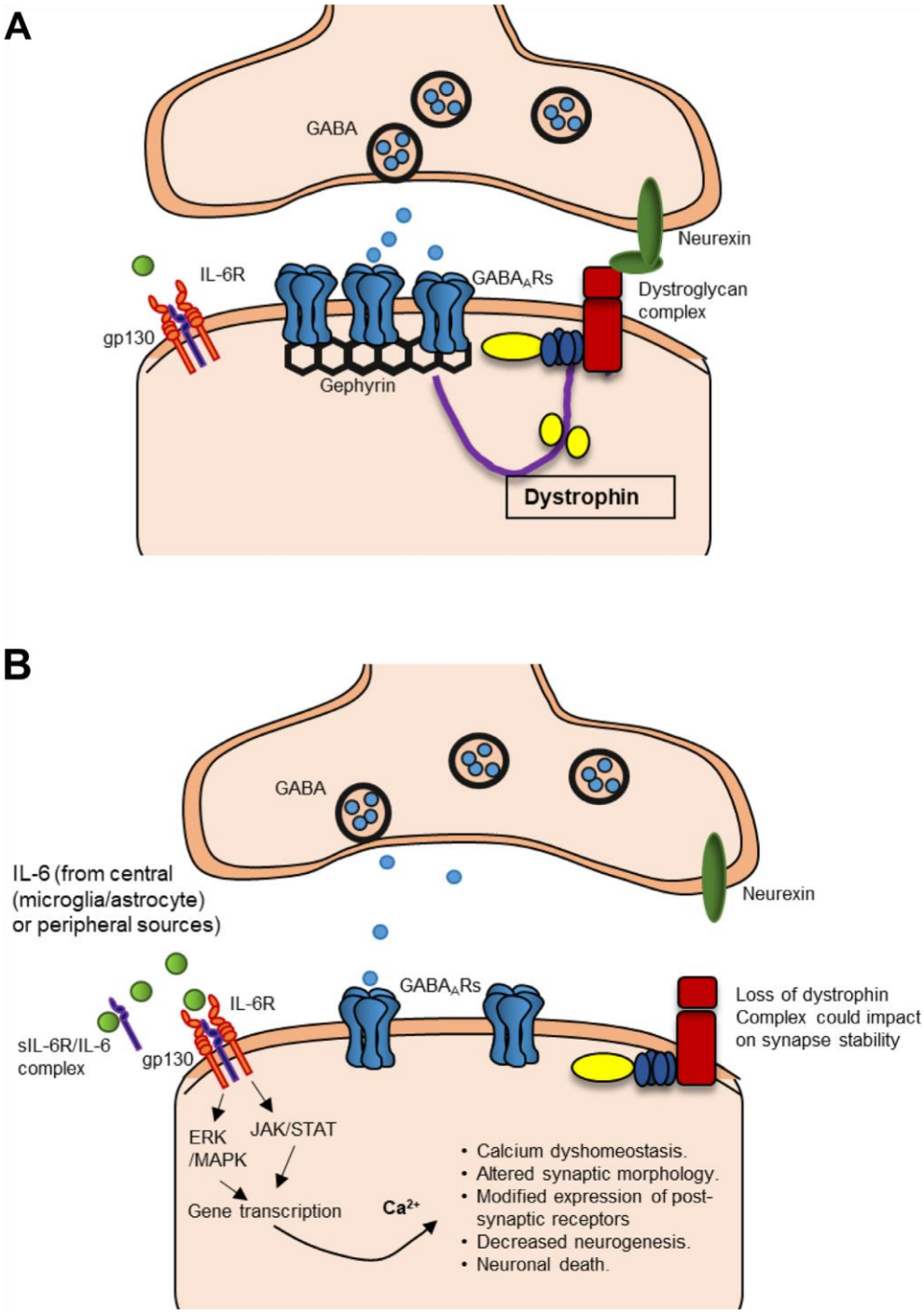


Fig. 1. Mechanisms by which IL-6 could contribute to dysfunction hippocampal neurotransmission in the absence of dystrophin. The schematic compares inhibitory synapses in hippocampal neurons from A: healthy individuals and B: individuals with dystrophin-deficient Duchenne Muscular Dystrophy. Extracellularsignal-regulated kinase/Mitogen-activated protein kinase: ERK/MAPK; gamma-aminobutyric acid receptors: $GABA_AR$s; interleukin-6: IL-6; IL-6 receptor: IL-6R; Janus kinase/signal transducer and activator of transcription: JAK/STAT; sIL-6R soluble IL-6R.

pro- or anti-inflammatory signalling. One such pleiotropic cytokine, interleukin-6 (IL-6) is secreted by both immune and non-immune cells [19], and has diverse effects on many different cell types. In health, plasma levels of IL-6 vary between ~ 1–10 pg/ml [20]. However, this can rise to the lower nanogram/ml range during infection or inflammation [21]. IL-6 has a key role in regulating immune cell function [22], although this 26 kDa protein can also modify function in other cells, including neurons [23]. This cytokine evokes its biological effects by binding to IL-6 receptors, which can either be membrane bound or soluble. Membrane-bound IL-6 receptors (IL-6Rα) are only expressed in a restricted subset of cells [24], but this does include many neurons in the brain [25]. Although IL-6Rα lacks intrinsic signal transduction capacity, binding of IL-6 to membrane-bound IL-6Rα and glycoprotein 130 kDa (gp130) complex results in a plethora of downstream cellular responses. Dimerization of gp130 and subsequent phosphorylation of Janus kinase/signal transducer and activator of transcription (JAK/ STAT), extracellular-signal-regulated kinase (ERK) and Phosphoinositide 3-kinase (PI 3-kinase) signal transduction molecules represents the classical signalling pathways for this cytokine. IL-6 can, however, also trigger signalling in cells which do not express IL-6Rα via soluble IL-6 receptors (sIL-6R).

sIL-6Rα uses a trans-signalling mechanism where sIL-6Rα forms a complex with IL-6 which then binds to gp130 [26,27]. Gp130 is expressed in most cell types including neural cells in the CNS [28]. Although expression of gp130 is not changed by inflammation, the concentrations of sIL-6R can increase between two and five-fold [29,30], thereby increasing trans-membrane signalling. In fact, many cells that respond to IL-6 during inflammation do not express membrane-bound IL-6Rs, but are activated by IL-6/sIL-6R complexes. Furthermore, downstream activation of JAK/STAT, ERK or PI 3-kinase proceeds in a similar manner in cells that don't express membrane-bound IL-6Rα as cells that do express IL-6Rα [31,32].

Differences in the evoked cellular response between classic receptormediated IL-6 signalling and trans-signalling can however, be detected. IL-6 evokes anti-inflammatory signals using classical signalling, which contrasts with the pro-inflammatory, and potentially deleterious actions of IL-6/sIL-6R-evoked trans-signalling [33]. Furthermore, the kinetics of how these two IL-6 receptor systems signal, also differ, which can lead to the generation of fundamentally different cellular responses [24]. For example, within the CNS, neuronal degeneration evoked by IL-6 is mediated by trans-signalling, whereas membrane receptormediated IL-6 signalling facilitates neural tissue regeneration [34] and neuronal protection [35]. Thus, understanding the specific signalling mechanisms of this and other cytokines is particularly pertinent when therapeutically targeting this signalling pathway for the treatment of neurological disorders.

3. Neuromodulatory actions of IL-6 in the hippocampus.

The hippocampus, a structure within the medial temporal lobe upon which the acquisition of new declarative/spatial memories is contingent, has abundant expression of IL-6Rα [15] and indeed, IL-6 induces multiple effects in this brain region. An initial clue to the role that IL-6 may play in modulating cognitive function came from investigating 'sickness behaviour', which describes behavioural symptoms during infection and inflammation. High levels of pro-inflammatory cytokines, including IL-6 and IL-1β [36], are associated with a deterioration of cognitive function during infection. IL-6 has also been implicated in lipopolysaccharide-evoked cognitive dysfunction [37]. Moreover, transgenic mice over-expressing IL-6 also exhibit broad memory impairment [38–40] and severe neurological pathologies [34]. Further support for the suggestion that IL-6 negatively impacts learning and memory function comes from the finding that transgenic IL-6-deficent mice possess enhanced spatial learning capabilities in the radial arm [41] and Morris water mazes [42] as well as behavioural task-learning assessments. However, it is notable that various forms of learning were also deficient in IL-6 knock-out mice [43], suggesting that basal levels of IL-6 are essential for normal cognitive function.

4. IL-6 modifies synaptic transmission

Ex vivo hippocampal slices retain the hippocampal architecture and intact neural circuitry between the dentate gyrus, CA1 and CA3 areas [44] and as such, can be utilised to study the proposed molecular correlate of memory formation, long-term potentiation (LTP). LTP induction in the hippocampus recapitulates the molecular mechanisms underlying the coding of new memories by modifying the strength of synaptic transmission [45–47]. Using this experimental procedure, a high frequency electrical stimulus induces a long-lasting potentiation of glutamatergic excitatory post-synaptic potentials (EPSPs).

Interestingly, IL-6 gene expression in the CA1 region of the hippocampus is increased after induction of N-methyl-D-aspartate (NMDA) receptor-dependent LTP via stimulation of the Schaffer collateral-CA1 pathway, although it is important to note that expression of IL-6 mRNA was specific to nearby astrocytes, not neurons [48]. Significant increases in the levels of IL-6 mRNA one hour post stimulation were also noted in ex vivo experiments, but only when LTP had been successfully induced [49]. Intriguingly, blockade of endogenous IL-6 using a neutralizing antibody resulted in a remarkable prolongation of LTP, as well as improved performance in spatial memory tests, further emphasising the pleiotropic actions of this cytokine in the CNS [49]. However, it appears that a delicate balance between too little or too much IL-6 is required to maintain optimal memory function, as IL-6 knock-out mice performed less well in hippocampus-dependent memory tests [43] and were more susceptible to hippocampal damage following induced convulsions [50,51], whereas transgenic mice with cerebral overexpression of IL-6 were characterised by suppressed LTP in the perforant pathway dentate gyrus synapses [52].

Although it is recognised that exogenous application of IL-6 may not mimic endogenously released IL-6 during LTP [49], ex vivo application of IL-6 inhibited hippocampal LTP using a mechanism that was dependent upon IL-6R activation and stimulation of the JAK/STAT pathway [53,54]. Moreover, inhibition of LTP by IL-6 was attenuated by administration of monoclonal antibodies, used to block IL-6 receptors [55]. Thus, IL-6 may fine-tune memory consolidation by acting as a molecular filter that

limits the long-term storage of some types of information. Although the mechanistic connections between IL-6mediated JAK/STAT pathway activation and LTP inhibition remain unclear, work conducted in rat hippocampal neurons suggests that at least one component may be due to an alteration in intracellular neuronal homeostasis of calcium, which is a critical mediator of synaptic plasticity, by increasing its influx through NMDA receptors [54]. This mirrors, to a certain extent, earlier work conducted in rat cerebellar and Purkinje cells which also showed that IL-6 not only raised basal cytosolic calcium concentrations, but also increased flux through NMDA receptors and voltage-gated calcium channels in cerebellar granule cells [56,57], and also enhanced the magnitude of group 1 metabotropic glutamate receptor-mediated responses in Purkinje neurons [58,59].

Neuroinflammatory molecules, including IL-6, also have the capacity to modify synaptic transmission [60] and hippocampal synaptic network activity [61] by modulating γ-aminobutyric acid (GABA)mediated signalling. GABA is the key inhibitory neurotransmitter in the adult CNS. It can be synthesised and secreted by both neurons and astrocytes and binds to GABA receptors on nearby neurons. Altered distribution of GABA receptors, abnormal subunit composition and aberrant $GABA_A$ receptor-mediated signalling have been detected in disorders such as Huntington's disease, which are characterised by neuroinflammation [62].

5. Cytokines modify neurogenesis

The posterior or dorsal portion of the hippocampus participates in contextual learning, declarative memory and spatial navigation [63]. Within this region, the "input zone" of the classical, tri-synaptic hippocampal circuit, the dentate gyrus region of the hippocampus, which may serve to facilitate translation of cortical signals into coding patterns suitable for memory encoding [64], is one of only two brain regions where neurogenesis occurs and adult-born neurons are integrated into pre-existing neuronal circuits [65]. Indeed, it is this integration of new cells into existing neuronal circuits that is proposed to contribute to hippocampal-dependent learning and memory processes [66]. However,

IL-6 can directly influence neural stem cells during neurogenesis [67], with proliferation, survival and differentiation of hippocampal progenitor cells being compromised in the dentate gyrus when IL-6 concentrations are elevated [68]. Indeed, IL-6 dose-dependently reduces proliferation of neural stem cells, decreases neuronal differentiation and ultimately impacts upon neurogenesis through activation of the JAK2/STAT3 signalling pathway. The importance of JAK2/ STAT3 signalling in memory consolidation is highlighted by the fact that cognitive deficits can be rescued in a mouse model of neuroinflammation (APP/PS1) by inhibiting this signalling cascade [69].

Microglia are macrophage-like cells which reside in the CNS and coordinate the brain's inflammatory response. Interestingly, microglia form a particularly dense populations in the subventricular zone [70], which, in addition to the dentate gyrus, is the other brain region where neurogenesis occurs. Activated microglia enhance neurogenesis and oligodendrogenesis in the subventricular zone through their release of cytokines, which include IL-6, IL-1β, TNF-α and IFN-γ [71]. Others have specifically described the potential role of astrocyte-derived IL-6 in hippocampal neurogenesis [72]. As the number of hippocampal neural stem cells correlates inversely with microglial density, it was proposed that they inhibited adult hippocampal neurogenesis [73]. Indeed, although the contribution of microglia to neurogenesis remains complex, more recent studies have demonstrated that homeostasis of the adult hippocampal neurogenic cascade is dependent upon microglial phagocytosis (Diaz-Aparicio et al., preprint 2019). The prevailing conditions appear to modify both cytokine profile and quantity secreted by microglia, with different cytokines having varying effects on neural stems cells at different concentrations [74].

It is understood that neuro-immune interactions are critical to the maintenance of homeostasis in the nervous system [18], and therefore it is interesting to note that elevated levels of pro-inflammatory cytokines, including IL-6 have been detected in cognitive diseases characterised by neuroinflammation, including Alzheimer's disease [75], Multiple Sclerosis [76], Parkinson's disease [77] and Huntington's disease [78]. The remainder of this review will consider the evidence for IL-6 as a contributory factor in cognitive dysfunction in individuals with DMD.

6. DMD, a multi-system disorder.

DMD is a heritable X chromosome-linked recessive disorder which affects approximately 1 in 3500 live male births, thus ranking it as one of the most prevalent inherited disorders worldwide [79]. Symptoms of DMD are evident in many physiological systems, however, progressive tissue inflammation and loss of function in cardiac and skeletal muscles leading to immobility and eventual cardio-respiratory failure [80] and premature death, have justifiably taken priority in terms of research. The manifestation of the aforementioned symptoms is due to mutations in the DMD gene leading to loss of the structural protein dystrophin [81]. In muscle, dystrophin forms part of the dystrophin-associated protein complex (DAPC) that functions as an essential link in connecting the sarcolemmal cytoskeletal actin to the extracellular matrix [82–84]. As dystrophin stabilises the sarcolemma, myofibres lacking this protein are more susceptible to contraction-induced damage [85]. Repair mechanisms are eventually exhausted and skeletal myofibres are replaced by connective and adipose tissue, which underlies loss of ambulation and respiratory complications [86]. Absence of dystrophin also contributes to cardiac muscle dysfunction, resulting in cardiac myopathies [87] and arrhythmias [88]. Furthermore, expression of dystrophin in smooth muscle underscores symptoms of bowel dysfunction [89] and urologic diagnoses [90] in DMD patients.

Due to improvement in the efficacy of therapeutic interventions [91] including nocturnal ventilation, routine influenza vaccinations, early delivery of antibiotics and physiotherapy [92], life-expectancy for individuals with DMD has increased considerably [93]. Moreover, new gene-editing technologies have made progress in restoring dystrophin to dystrophin-deficient mdx mice [94–97] and human induced pluripotent stem cells [98]. In individuals with DMD, eteplirsen, an oligonucleotide that

facilitates skipping of exon 51 mutations in the dystrophin gene, slows but does not halt disease progression [99]. Given this progress in treating the peripheral symptoms of DMD, it is becoming increasingly important to consider less researched aspects of the disorder, including DMD-associated cognitive impairment [100,101].

7. Cognitive dysfunction in individuals with DMD

Varying degrees of non-progressive intellectual impairment, including lower intelligence quotients (IQs) [3,102], cognitive impairment [103,104], communication difficulties, poor affect recognition [4,5] and specific deficits in verbal, short-term and working memory [6–8], are exhibited by individuals with DMD. Changes in neuronal function in the hippocampus, cerebral cortex, amygdala and cerebellum, where the full length isoform of dystrophin is normally expressed [1,105–108], are likely to contribute to the aetiology of the cognitive impairment and memory deficits seen in patients with DMD. Neuronal loss, neurofibrillary tangles, alterations in dendritic branching, cortical atrophy and metabolic abnormalities have all been reported in the brains of DMD individuals [109–113]. However, not all individuals with DMD exhibit brain abnormalities and such pathological changes do not correlate well with the degree of IQ impairment [103].

8. Cognitive dysfunction in a rodent model of DMD

Understanding the functions of specific proteins in the CNS has been facilitated enormously by the generation of transgenic rodent models where the expression of individual proteins has been selectively deleted or suppressed. Thus, the fortuitous discovery of the dystrophin-deficient mdx mouse [81], which has a nonsense mutation within exon 23 of the dystrophin gene [114], similar to the mutation found in human DMD, has provided an opportunity to understand the mechanistic underpinnings of this disease. As such, mdx mice do indeed recapitulate striated muscle dysfunction and inflammation [115], although the severity of fibrosis and limb muscle dysfunction is substantially less than the human disease [116–118]. Nonetheless, similar to studies of humans with DMD [104,119–121], studies in mdx mice [81,122,123] did not detect gross abnormalities in brain structures. However, ultrastructural architectural changes, as well as reduced dendritic branching and condensed spinal density in corticospinal neurons have been reported in mdx mice [124–126]. The density of hippocampal neurons is decreased in mdx mice [127] and lateral ventricles are enlarged, possibly due to grey matter atrophy [128]. Similar to DMD patients, muscle levels of IL-6, TNFα and IL-1β are elevated in mdx mice [129–131]. However, changes in circulating or CNS levels of inflammatory mediators in this mouse model have not yet been determined.

Behaviours consistent with hippocampal dysfunction, such as deficits in associative learning and storage of spatial memories and an inability to learn new tasks, have been observed in mdx mice [132–134]. Interestingly, no variance in spatial learning, or the magnitude of LTP stimulated in the dentate gyrus and CA1 regions of the hippocampus, was detected by Sesay and colleagues [135]. In contrast, Vaillend et al. (2004) reported an enhanced LTP magnitude in mdx mice compared to that in wild type mice [132]. Given the known structural function of dystrophin in muscle cells, loss of this protein could lead to disruptions in normal neuronal physiology which could, in turn, alter cellular processes underlying learning and memory. In this vein, it is noteworthy that mdx cortical and hippocampal neurons display significant intracellular calcium dyshomeostasis relative to controls due to both excessive plasmalemmal cation influx and intracellular release through the endoplasmic reticulum-located calcium-release channels, inositol − 1,4,5 −trisphosphate receptors (IP_3Rs) and ryanodine receptors (RyRs) [136]. Significantly, a spatial learning deficit in the mdx mice could be significantly improved using a compound which inhibited the extracellular calcium influx [136]. Changes in long- and short-term memory formation linked to a loss of dystrophin have been associated with altered synapse morphology and plasticity [122,132,133].

9. Altered synaptic receptor clustering in dystrophin-deficient neurons.

The density and expression of several types of receptor is changed in hippocampal neurons from mdx mice. The full-length form of dystrophin is exclusively expressed in dense puncta on the post-synaptic cell membranes of inhibitory neurons [106,137–141], where it is believed to anchor GABA [for review see 142] and other neurotransmitter receptors [143]. Significantly, this clustering is absent in dystrophic membranes, which has implications for the regulation of synaptic excitability. It is notable, however, that normal clustering of $GABA_A$ receptors can be restored by administering specific antisense oligonucleotides, designed to restore functional dystrophin [144]. Moreover, NMDA-dependent LTP can be normalised using the same treatment, thus providing strong support for the suggestion that dystrophin-dependent clustering of GABAergic neurotransmitter receptors at inhibitory synapses is essential for the regulation of normal neuronal excitability and synaptic transmission [145].

A muted response to nicotine in passive avoidance memory tasks, indicated that mdx mice have either altered expression or responsivity of nicotinic acetylcholine receptors (nAChRs) [146]. Indeed, there are lower levels of hippocampal α3 nAChR mRNA [147] and α7 nAChR binding sites in mdx brains [148]. However, such changes, which should result in decreased nicotinic cholinergic synaptic signalling, appear to be mitigated by an upregulation of nAChR-mediated cholinergic transmission in dystrophic animals [149]. Intriguingly, the fact that there is no change in expression of hippocampal muscarinic receptors in dystrophic mice [123] indicates that dystrophin does not exert a generalised effect on the expression of all cholinergic receptor subtypes. However, dystrophic hippocampal neurons did express lower densities of kainic acid / α-amino-3-hydroxy-5-methyl-4-isoxazolepropionic acid (AMPA) receptors, although this could reflect a compensatory response to increased glutamatergic input [122,150]. Combined, these studies demonstrate that a loss of dystrophin from post-synaptic neurons is linked to modified expression of post-synaptic receptors [122,139,150–152], which will inevitably impact upon the neuronal response to afferent stimuli [153] and will also inevitably affect their efferent output .The exact and synchronised neural network activity critical for normal hippocampal function will thereby be disrupted [for review see 154].

10. Pro-inflammatory cytokines could contribute to cognitive dysfunction linked to loss of dystrophin.

The pro-inflammatory characteristics of DMD is due, in part, to the secretion of cytokines from damaged dystrophin-deficient muscle fibres [155,156]. Given that plasma levels of IL-6 are consistently raised in both individuals with DMD [13], and mdx mice [157], and peripheral IL-6 can cross the blood brain barrier using a saturable transport system [158], inflammatory cytokines originating in the periphery could potentially impact upon brain function. As cytokines can modify channels and receptors at both pre- and post-synaptic membranes [159], this could facilitate deficits in cognition linked to a loss of dystrophin. For example, over-expression of IL-6 not only promotes abnormal dendritic spine formation at both inhibitory and excitatory synapses, which mimics the abnormal spines formed by neurons lacking dystrophin, but it is also, as previously discussed, associated with impaired cognitive abilities and deficits in learning [38,40,160–162]. Prenatal exposure to IL-6 in rats leads to elevated hippocampal levels of IL-6, altered expression of NMDA and $GABA_A$ receptors and deficits in spatial learning [163]. Furthermore, as previously mentioned, IL-6 can modify synaptic transmission [60] and hippocampal synaptic network activity [61] by modulating GABA-mediated signalling. Thus, IL-6 is a multifaceted neuroinflammatory molecule which can modify neural function by modulating synaptic transmission and synaptic plasticity, promoting neurite outgrowth, neurogenesis and/or neuronal survival [18,25,164,165].

11. Conclusions

The emergence of treatments, which have extended both the life expectancy and the life quality of individuals with DMD, have highlighted the unmet need to investigate and understand the deficits in cognition, that are common in this dystrophin-deficient neuromuscular disorder. In healthy individuals, dystrophin expression is restricted to specific brain regions, including the hippocampus, a region which is critical for learning and acquisition of declarative memory. Loss of dystrophin from this region is thereby implicated it in the presentation of deficiencies in verbal, short-term and working memory, which vary in severity in boys with DMD. Altered density and clustering of postsynaptic receptors, in addition to malformed and malfunctional hippocampal synapses, have been linked to the loss of dystrophin. These pathological changes are likely to impair the precise and coordinated activation of neural networks underlying learning. As DMD patients and the mdx dystrophin-deficient animal model of DMD both exhibit elevated circulating levels of the pro-inflammatory cytokine, IL-6, we evaluated the potential role that IL-6 plays in the deficits in hippocampal function in dystrophin-deficient individuals. IL-6 has neuromodulatory effects in the CNS, and elevated levels of IL-6 have been linked to cognitive dysfunction and memory impairment. IL-6 has the capacity to modify expression of post-synaptic receptors, a feature which has been described in dystrophin-deficient neurons. Moreover, intracellular calcium homeostasis, a critical mediator of synaptic plasticity, is also modulated by IL-6 and could underlie neuronal dysfunction in the absence of dystrophin. Neurogenesis, where adult-born neurons are incorporated into pre-existing neuronal circuits, is impaired when levels of IL-6 are elevated. In parallel, the density of hippocampal neurons is decreased in mdx mice, which lack dystrophin and have elevated levels of circulating IL-6 [127]. This review has focussed on the possible role of IL-6 in cognitive dysfunction (Fig. 1) associated with the loss of dystrophin. The evidence supports a possible role for this neuromodulatory immune molecule in the pathophysiological deficits in cognition exhibited by individuals with DMD. However, further studies are needed to pin down the precise role IL-6 plays in synaptic transmission in hippocampal neurons that lack dystrophin.

Author contributions

K.A.S. drafted manuscript; M.G.R. and D.OM. edited and revised the manuscript and approved final version of manuscript.

Funding

This work was supported by the Health Research Board Ireland, Investigator Led Project (ILP-POR-2017-040).

Declaration of Competing Interest

The authors declare that they have no known competing financial interests or personal relationships that could have appeared to influence the work reported in this paper.

References

[1] H.G. Lidov, T.J. Byers, S.C. Watkins, L.M. Kunkel, Localization of dystrophin to postsynaptic regions of central nervous system cortical neurons, Nature 348 (6303) (1990) 725–728.

[2] F. Rodius, T. Claudepierre, H. Rosas-Vargas, B. Cisneros, C. Montanez, H. Dreyfus, D. Mornet, A. Rendon, Dystrophins in developing retina: Dp260 expression correlates with synaptic maturation, NeuroReport 8 (9–10) (1997) 2383–2387.

[3] G. Felisari, F. Martinelli Boneschi, A. Bardoni, M. Sironi, G.P. Comi, M. Robotti, A.C. Turconi, M. Lai, G. Corrao, N. Bresolin, Loss of Dp140 dystrophin isoform and intellectual impairment in Duchenne dystrophy, Neurology 55 (4) (2000) 559–564.

[4] V.J. Hinton, R.J. Fee, D.C. De Vivo, E. Goldstein, Poor facial affect recognition among boys with duchenne muscular dystrophy, J. Autism Dev. Disord. 37 (10) (2007) 1925–1933.

[5] V.J. Hinton, N.E. Nereo, R.J. Fee, S.E. Cyrulnik, Social behavior problems in boys with Duchenne muscular dystrophy, J. Dev. Behav. Pediatr. 27 (6) (2006) 470–476.

[6] W.M. Snow, J.E. Anderson, L.S. Jakobson, Neuropsychological and neurobehavioral functioning in Duchenne muscular dystrophy: a review, Neurosci. Biobehav. Rev. 37 (5) (2013) 743–752.

[7] V.J. Hinton, D.C. De Vivo, N.E. Nereo, E. Goldstein, Y. Stern, Poor verbal working memory across intellectual level in boys with Duchenne dystrophy, Neurology 54 (11) (2000) 2127–2132.

[8] V.J. Hinton, D.C. De Vivo, N.E. Nereo, E. Goldstein, Y. Stern, Selective deficits in verbal working memory associated with a known genetic etiology: the neuropsychological profile of duchenne muscular dystrophy, J. Int. Neuropsychol. Soc. 7 (1) (2001) 45–54.

[9] E. Porreca, M.D. Guglielmi, A. Uncini, P. Di Gregorio, A. Angelini, C. Di Febbo, S.D. Pierdomenico, G. Baccante, F. Cuccurullo, Haemostatic abnormalities, cardiac involvement and serum tumor necrosis factor levels in X-linked dystrophic patients, Thromb. Haemost. 81 (4) (1999) 543–546.

[10] S. Kuru, A. Inukai, T. Kato, Y. Liang, S. Kimura, G. Sobue, Expression of tumor necrosis factor-alpha in regenerating muscle fibers in inflammatory and non-inflammatory myopathies, Acta Neuropathol. 105 (3) (2003) 217–224.

[11] N.P. Evans, S.A. Misyak, J.L. Robertson, J. Bassaganya-Riera, R.W. Grange, Immune-mediated mechanisms potentially regulate the disease time-course of duchenne muscular dystrophy and provide targets for therapeutic intervention, PM R 1 (8) (2009) 755–768.

[12] S. Messina, G.L. Vita, M. Aguennouz, M. Sframeli, S. Romeo, C. Rodolico, G. Vita, Activation of NF-kappaB pathway in Duchenne muscular dystrophy: relation to age, Acta Myol 30 (1) (2011) 16–23.

[13] A. Rufo, A. Del Fattore, M. Capulli, F. Carvello, L. De Pasquale, S. Ferrari, D. Pierroz, L. Morandi, M. De Simone, N. Rucci, E. Bertini, M.L. Bianchi, F. De Benedetti, A. Teti, Mechanisms inducing low bone density in Duchenne muscular dystrophy in mice and humans, J. Bone Miner. Res. 26 (8) (2011) 1891–1903. [14] F. Gardoni, M. Boraso, E. Zianni, E. Corsini, C.L. Galli, F. Cattabeni, M. Marinovich, M. Di Luca, B. Viviani, Distribution of interleukin-1 receptor complex at the synaptic membrane driven by interleukin-1beta and NMDA stimulation, J. Neuroinflammation 8 (1) (2011) 14.

[15] B. Schobitz, E.R. de Kloet, W. Sutanto, F. Holsboer, Cellular localization of interleukin 6 mRNA and interleukin 6 receptor mRNA in rat brain, Eur. J. Neurosci. 5 (11) (1993) 1426–1435.

[16] S.L. Montgomery, W.J. Bowers, Tumor necrosis factor-alpha and the roles it plays in homeostatic and degenerative processes within the central nervous system, J. Neuroimmune Pharmacol. 7 (1) (2012) 42–59.

[17] S.M. Allan, N.J. Rothwell, Cytokines and acute neurodegeneration, Nat. Rev. Neurosci. 2 (10) (2001) 734–744.

[18] I. Marin, J. Kipnis, Learning and memory and the immune system, Learn Mem 20 (10) (2013) 601–606.

[19] P. Marz, J.G. Cheng, R.A. Gadient, P.H. Patterson, T. Stoyan, U. Otten, S. RoseJohn, Sympathetic neurons can produce and respond to interleukin 6, Proc. Natl. Acad Sci. U S A 95 (6) (1998) 3251–3256.

[20] S. Akira, T. Taga, T. Kishimoto, Interleukin-6 in biology and medicine, Adv. Immunol. 54 (1993) 1–78.

[21] S.A. Jones, Directing transition from innate to acquired immunity: defining a role for IL-6, J. Immunol. 175 (6) (2005) 3463–3468.

[22] T. Hirano, T. Taga, N. Nakano, K. Yasukawa, S. Kashiwamura, K. Shimizu, K. Nakajima, K.H. Pyun, T. Kishimoto, Purification to homogeneity and characterization of human B-cell differentiation factor (BCDF or BSFp-2), Proc. Natl. Acad. Sci. U S A 82 (16) (1985) 5490–5494.

[23] G.M. Arisi, Nervous and immune systems signals and connections: cytokines in hippocampus physiology and pathology, Epilepsy Behav. 38 (2014) 43–47.

[24] M. Rothaug, C. Becker-Pauly, S. Rose-John, The role of interleukin-6 signaling in nervous tissue, Biochim Biophys Acta 1863(6 Pt A) (2016) 1218–1227.

[25] M. Erta, A. Quintana, J. Hidalgo, Interleukin-6, a major cytokine in the central nervous system, Int. J. Biol. Sci.. 8 (9) (2012) 1254–1266.

[26] S. Rose-John, P.C. Heinrich, Soluble receptors for cytokines and growth factors: generation and biological function, Biochem. J. 300 (Pt 2) (1994) 281–290.

[27] J. Scheller, A. Chalaris, D. Schmidt-Arras, S. Rose-John, The pro- and anti-inflammatory properties of the cytokine interleukin-6, BBA 1813 (5) (2011) 878–888.

[28] D. Watanabe, R. Yoshimura, M. Khalil, K. Yoshida, T. Kishimoto, T. Taga, H. Kiyama, Characteristic localization of gp130 (the signal-transducing receptor component used in common for IL-6/IL-11/CNTF/LIF/OSM) in the rat brain, Eur. J. Neurosci. 8 (8) (1996) 1630–1640.

[29] S. Rose-John, IL-6 trans-signaling via the soluble IL-6 receptor: importance for the pro-inflammatory activities of IL-6, Int. J. Biol. Sci. 8 (9) (2012) 1237–1247.

[30] F. Schaper, S. Rose-John, Interleukin-6: Biology, signaling and strategies of blockade, Cytokine Growth Factor Rev. 26 (5) (2015) 475–487.

[31] M. Ernst, B.J. Jenkins, Acquiring signalling specificity from the cytokine receptor gp130, Trends Genet. 20 (1) (2004) 23–32.

[32] I.L. Campbell, M. Erta, S.L. Lim, R. Frausto, U. May, S. Rose-John, J. Scheller, J. Hidalgo, Trans-signaling is a dominant mechanism for the pathogenic actions of interleukin-6 in the brain, J. Neurosci. 34 (7) (2014) 2503–2513.

[33] C. Garbers, S. Aparicio-Siegmund, S. Rose-John, The IL-6/gp130/STAT3 signaling axis: recent advances towards specific inhibition, Curr. Opin. Immunol. 34 (2015) 75–82.

[34] I.L. Campbell, C.R. Abraham, E. Masliah, P. Kemper, J.D. Inglis, M.B. Oldstone, L. Mucke, Neurologic disease induced in transgenic mice by cerebral overexpression of interleukin 6, Proc. Natl. Acad. Sci. U S A 90 (21) (1993) 10061–10065.

[35] A.J. Chucair-Elliott, C. Conrady, M. Zheng, C.M. Kroll, T.E. Lane, D.J. Carr, Microglia-induced IL-6 protects against neuronal loss following HSV-1 infection of neural progenitor cells, Glia 62 (9) (2014) 1418–1434.

[36] M. Gibertini, Cytokines and cognitive behavior, NeuroImmunoModulation 5 (3–4) (1998) 160–165.

[37] N.L. Sparkman, J.B. Buchanan, J.R. Heyen, J. Chen, J.L. Beverly, R.W. Johnson, Interleukin-6 facilitates lipopolysaccharide-induced disruption in working memory and expression of other proinflammatory cytokines in hippocampal neuronal cell layers, J. Neurosci. 26 (42) (2006) 10709–10716.

[38] C.J. Heyser, E. Masliah, A. Samimi, I.L. Campbell, L.H. Gold, Progressive decline in avoidance learning paralleled by inflammatory neurodegeneration in transgenic mice expressing interleukin 6 in the brain, Proc. Natl. Acad. Sci. U S A 94 (4) (1997) 1500–1505.

[39] H. Wei, I. Alberts, X. Li, Brain IL-6 and autism, Neuroscience 252 (2013) 320–325.

[40] H. Wei, K.K. Chadman, D.P. McCloskey, A.M. Sheikh, M. Malik, W.T. Brown, X. Li, Brain IL-6 elevation causes neuronal circuitry imbalances and mediates autismlike behaviors, BBA 1822 (6) (2012) 831–842.

[41] D. Braida, P. Sacerdote, A.E. Panerai, M. Bianchi, A.M. Aloisi, S. Iosue, M. Sala, Cognitive function in young and adult IL (interleukin)-6 deficient mice, Behav. Brain Res. 153 (2) (2004) 423–429.

[42] I. Bialuk, M.M. Winnicka, Facilitatory Effect of IL-6 Deficiency on Long-Term Spatial Memory in Young Adult Mice, Behav. Genet. 48 (3) (2018) 236–246.

[43] P.C. Baier, U. May, J. Scheller, S. Rose-John, T. Schiffelholz, Impaired hippocampus-dependent and -independent learning in IL-6 deficient mice, Behav. Brain Res. 200 (1) (2009) 192–196.

[44] R.C. Malenka, R.A. Nicoll, Long-term potentiation–a decade of progress? Science 285 (5435) (1999) 1870–1874.

[45] T.V. Bliss, G.L. Collingridge, A synaptic model of memory: long-term potentiation in the hippocampus, Nature 361 (6407) (1993) 31–39.

[46] D. Muller, M. Joly, G. Lynch, Contributions of quisqualate and NMDA receptors to the induction and expression of LTP, Science 242 (4886) (1988) 1694–1697.
[47] G.L. Collingridge, S.J. Kehl, H. McLennan, Excitatory amino acids in synaptic transmission in the Schaffer collateral-commissural pathway of the rat hippocampus, J. Physiol. 334 (1983) 33–46.
[48] J.L. Jankowsky, B.E. Derrick, P.H. Patterson, Cytokine responses to LTP induction in the rat hippocampus: a comparison of in vitro and in vivo techniques, Learn Mem 7 (6) (2000) 400–412.
[49] D. Balschun, W. Wetzel, A. Del Rey, F. Pitossi, H. Schneider, W. Zuschratter, H.O. Besedovsky, Interleukin-6: a cytokine to forget, FASEB J. 18 (14) (2004) 1788–1790.
[50] G. De Sarro, E. Russo, G. Ferreri, B. Giuseppe, M.A. Flocco, E.D. Di Paola, A. De Sarro, Seizure susceptibility to various convulsant stimuli of knockout interleukin6 mice, Pharmacol. Biochem. Behav. 77 (4) (2004) 761–766.
[51] M. Penkowa, A. Molinero, J. Carrasco, J. Hidalgo, Interleukin-6 deficiency reduces the brain inflammatory response and increases oxidative stress and neurodegeneration after kainic acid-induced seizures, Neuroscience 102 (4) (2001) 805–818.
[52] F.P. Bellinger, S.G. Madamba, I.L. Campbell, G.R. Siggins, Reduced long-term potentiation in the dentate gyrus of transgenic mice with cerebral overexpression of interleukin-6, Neurosci. Lett. 198 (2) (1995) 95–98.
[53] V. Tancredi, M. D'Antuono, C. Cafe, S. Giovedi, M.C. Bue, G. D'Arcangelo, F. Onofri, F. Benfenati, The inhibitory effects of interleukin-6 on synaptic plasticity in the rat hippocampus are associated with an inhibition of mitogen-activated protein kinase ERK, J. Neurochem. 75 (2) (2000) 634–643.
[54] D.I. Orellana, R.A. Quintanilla, C. Gonzalez-Billault, R.B. Maccioni, Role of the JAKs/STATs pathway in the intracellular calcium changes induced by interleukin6 in hippocampal neurons, Neurotox. Res. 8 (3–4) (2005) 295–304.
[55] A.J. Li, T. Katafuchi, S. Oda, T. Hori, Y. Oomura, Interleukin-6 inhibits long-term potentiation in rat hippocampal slices, Brain Res. 748 (1–2) (1997) 30–38.
[56] Z. Qiu, K.L. Parsons, D.L. Gruol, Interleukin-6 selectively enhances the intracellular calcium response to NMDA in developing CNS neurons, J. Neurosci. 15 (10) (1995) 6688–6699.
[57] Z. Qiu, D.D. Sweeney, J.G. Netzeband, D.L. Gruol, Chronic interleukin-6 alters NMDA receptor-mediated membrane responses and enhances neurotoxicity in developing CNS neurons, J. Neurosci. 18 (24) (1998) 10445–10456.
[58] T.E. Nelson, J.G. Netzeband, D.L. Gruol, Chronic interleukin-6 exposure alters metabotropic glutamate receptor-activated calcium signalling in cerebellar Purkinje neurons, Eur. J. Neurosci. 20 (9) (2004) 2387–2400.
[59] T.E. Nelson, C.L. Ur, D.L. Gruol, Chronic interleukin-6 exposure alters electrophysiological properties and calcium signaling in developing cerebellar purkinje neurons in culture, J. Neurophysiol. 88 (1) (2002) 475–486.
[60] F. Garcia-Oscos, H. Salgado, S. Hall, F. Thomas, G.E. Farmer, J. Bermeo, L.C. Galindo, R.D. Ramirez, S. D'Mello, S. Rose-John, M. Atzori, The stress-induced cytokine interleukin-6 decreases the inhibition/excitation ratio in the rat temporal cortex via trans-signaling, Biol. Psychiatry 71 (7) (2012) 574–582.
[61] E.J. Vereyken, H. Bajova, S. Chow, P.N. de Graan, D.L. Gruol, Chronic interleukin6 alters the level of synaptic proteins in hippocampus in culture and in vivo, Eur. J.
Neurosci. 25 (12) (2007) 3605–3616.
[62] Y.T. Hsu, Y.G. Chang, Y. Chern, Insights into GABAAergic system alteration in Huntington's disease, Open Biol 8 (12) (2018).
[63] M.A. Kheirbek, L.J. Drew, N.S. Burghardt, D.O. Costantini, L. Tannenholz, S.E. Ahmari, H. Zeng, A.A. Fenton, R. Hen, Differential control of learning and anxiety along the dorsoventral axis of the dentate gyrus, Neuron 77 (5) (2013) 955–968.
[64] A. Treves, E.T. Rolls, Computational analysis of the role of the hippocampus in memory, Hippocampus 4 (3) (1994) 374–391.
[65] F.H. Gage, Mammalian neural stem cells, Science 287 (5457) (2000) 1433–1438.
[66] M.V. Wu, R. Hen, Functional dissociation of adult-born neurons along the dorsoventral axis of the dentate gyrus, Hippocampus 24 (7) (2014) 751–761.
[67] O. Islam, X. Gong, S. Rose-John, K. Heese, Interleukin-6 and neural stem cells: more than gliogenesis, Mol. Biol. Cell 20 (1) (2009) 188–199.
[68] L. Vallieres, I.L. Campbell, F.H. Gage, P.E. Sawchenko, Reduced hippocampal neurogenesis in adult transgenic mice with chronic astrocytic production of interleukin-6, J. Neurosci. 22 (2) (2002) 486–492.
[69] X. Kong, Z. Gong, L. Zhang, X. Sun, Z. Ou, B. Xu, J. Huang, D. Long, X. He, X. Lin, Q. Li, L. Xu, A. Xuan, JAK2/STAT3 signaling mediates IL-6-inhibited neurogenesis of neural stem cells through DNA demethylation/methylation, Brain Behav.
Immun. (2019).
[70] K.I. Mosher, R.H. Andres, T. Fukuhara, G. Bieri, M. Hasegawa-Moriyama, Y. He, R. Guzman, T. Wyss-Coray, Neural progenitor cells regulate microglia functions and activity, Nat. Neurosci. 15 (11) (2012) 1485–1487.
[71] Y. Shigemoto-Mogami, K. Hoshikawa, J.E. Goldman, Y. Sekino, K. Sato, Microglia enhance neurogenesis and oligodendrogenesis in the early postnatal subventricular zone, J. Neurosci. 34 (6) (2014) 2231–2243.
[72] J. Oh, M.A. McCloskey, C.C. Blong, L. Bendickson, M. Nilsen-Hamilton, D.S. Sakaguchi, Astrocyte-derived interleukin-6 promotes specific neuronal differentiation of neural progenitor cells from adult hippocampus, J. Neurosci. Res. 88 (13) (2010) 2798–2809.
[73] E. Gebara, S. Sultan, J. Kocher-Braissant, N. Toni, Adult hippocampal neurogenesis inversely correlates with microglia in conditions of voluntary running and aging, Front. Neurosci. 7 (2013) 145.
[74] I. Russo, S. Barlati, F. Bosetti, Effects of neuroinflammation on the regenerative capacity of brain stem cells, J. Neurochem. 116 (6) (2011) 947–956.
[75] H. Hampel, A. Haslinger, M. Scheloske, F. Padberg, P. Fischer, J. Unger,
S.J. Teipel, M. Neumann, C. Rosenberg, R. Oshida, C. Hulette, D. Pongratz, M. Ewers, H.A. Kretzschmar, H.J. Moller, Pattern of interleukin-6 receptor complex immunoreactivity between cortical regions of rapid autopsy normal and Alzheimer's disease brain, Eur. Arch. Psychiatry Clin. Neurosci. 255 (4) (2005) 269–278.
[76] D. Maimone, G.C. Guazzi, P. Annunziata, IL-6 detection in multiple sclerosis brain, J. Neurol. Sci. 146 (1) (1997) 59–65.
[77] M. Mogi, M. Harada, T. Kondo, P. Riederer, H. Inagaki, M. Minami, T. Nagatsu, Interleukin-1 beta, interleukin-6, epidermal growth factor and transforming growth factor-alpha are elevated in the brain from parkinsonian patients, Neurosci. Lett. 180 (2) (1994) 147–150.
[78] M. Bjorkqvist, E.J. Wild, J. Thiele, A. Silvestroni, R. Andre, N. Lahiri, E. Raibon,
R.V. Lee, C.L. Benn, D. Soulet, A. Magnusson, B. Woodman, C. Landles,
M.A. Pouladi, M.R. Hayden, A. Khalili-Shirazi, M.W. Lowdell, P. Brundin, G.P. Bates, B.R. Leavitt, T. Moller, S.J. Tabrizi, A novel pathogenic pathway of immune activation detectable before clinical onset in Huntington's disease, J. Exp. Med. 205 (8) (2008) 1869–1877.
[79] A.E. Emery, Population frequencies of inherited neuromuscular diseases–a world survey, Neuromuscul. Disord. 1 (1) (1991) 19–29.
[80] K.R. Wagner, N. Lechtzin, D.P. Judge, Current treatment of adult Duchenne muscular dystrophy, BBA 1772 (2) (2007) 229–237.
[81] G. Bulfield, W.G. Siller, P.A. Wight, K.J. Moore, X chromosome-linked muscular dystrophy (mdx) in the mouse, Proc. Natl. Acad Sci. U S A 81 (4) (1984) 1189–1192.
[82] J.M. Ervasti, K.P. Campbell, A role for the dystrophin-glycoprotein complex as a transmembrane linker between laminin and actin, J. Cell Biol. 122 (4) (1993) 809–823.
[83] D.J. Blake, A. Weir, S.E. Newey, K.E. Davies, Function and genetics of dystrophin and dystrophin-related proteins in muscle, Physiol. Rev. 82 (2) (2002) 291–329.
[84] K.E. Davies, K.J. Nowak, Molecular mechanisms of muscular dystrophies: old and new players, Nat. Rev. Mol. Cell Biol. 7 (10) (2006) 762–773.

[85] E.E. Zubrzycka-Gaarn, D.E. Bulman, G. Karpati, A.H. Burghes, B. Belfall, H.J. Klamut, J. Talbot, R.S. Hodges, P.N. Ray, R.G. Worton, The Duchenne muscular dystrophy gene product is localized in sarcolemma of human skeletal muscle, Nature 333 (6172) (1988) 466–469.

[86] J.O. Benditt, L. Boitano, Respiratory support of individuals with Duchenne muscular dystrophy: toward a standard of care, Phys. Med. Rehabil. Clin. N Am. 16 (4) (2005) pp. 1125–39, xii.

[87] G. Nigro, L.I. Comi, L. Politano, R.J. Bain, The incidence and evolution of cardiomyopathy in Duchenne muscular dystrophy, Int. J. Cardiol. 26 (3) (1990) 271–277.

[88] S.I. Mavrogeni, G. Markousis-Mavrogenis, A. Papavasiliou, G. Papadopoulos, G. Kolovou, Cardiac Involvement in Duchenne Muscular Dystrophy and Related Dystrophinopathies, Methods Mol. Biol. 1687 (2018) 31–42.

[89] L.A. Bertrand, E.J. Askeland, K.D. Mathews, B.A. Erickson, C.S. Cooper, Prevalence and bother of patient-reported lower urinary tract symptoms in the muscular dystrophies, J. Pediatr. Urol. 12 (6) (2016) 398 e1-398 e4.

[90] M. MacLeod, R. Kelly, S.A. Robb, M. Borzyskowski, Bladder dysfunction in Duchenne muscular dystrophy, Arch. Dis. Child. 88 (4) (2003) 347–349.

[91] A.M. Reinig, S. Mirzaei, D.J. Berlau, Advances in the Treatment of Duchenne Muscular Dystrophy: New and Emerging Pharmacotherapies, Pharmacotherapy 37 (4) (2017) 492–499.

[92] M. Eagle, S.V. Baudouin, C. Chandler, D.R. Giddings, R. Bullock, K. Bushby, Survival in Duchenne muscular dystrophy: improvements in life expectancy since 1967 and the impact of home nocturnal ventilation, Neuromuscul. Disord. 12 (10) (2002) 926–929.

[93] W.D. Biggar, V.A. Harris, L. Eliasoph, B. Alman, Long-term benefits of deflazacort treatment for boys with Duchenne muscular dystrophy in their second decade, Neuromuscul. Disord. 16 (4) (2006) 249–255.

[94] M.G. Dunckley, M. Manoharan, P. Villiet, I.C. Eperon, G. Dickson, Modification of splicing in the dystrophin gene in cultured Mdx muscle cells by antisense oligoribonucleotides, Hum. Mol. Genet. 7 (7) (1998) 1083–1090.

[95] C. Long, J.R. McAnally, J.M. Shelton, A.A. Mireault, R. Bassel-Duby, E.N. Olson, Prevention of muscular dystrophy in mice by CRISPR/Cas9-mediated editing of germline DNA, Science 345 (6201) (2014) 1184–1188.

[96] C. Long, L. Amoasii, A.A. Mireault, J.R. McAnally, H. Li, E. Sanchez-Ortiz, S. Bhattacharyya, J.M. Shelton, R. Bassel-Duby, E.N. Olson, Postnatal genome editing partially restores dystrophin expression in a mouse model of muscular dystrophy, Science 351 (6271) (2016) 400–403.

[97] C.E. Nelson, C.H. Hakim, D.G. Ousterout, P.I. Thakore, E.A. Moreb, R.M. Castellanos Rivera, S. Madhavan, X. Pan, F.A. Ran, W.X. Yan, A. Asokan, F. Zhang, D. Duan, C.A. Gersbach, In vivo genome editing improves muscle function in a mouse model of Duchenne muscular dystrophy, Science 351 (6271) (2016) 403–407.

[98] C.S. Young, M.R. Hicks, N.V. Ermolova, H. Nakano, M. Jan, S. Younesi, S. Karumbayaram, C. Kumagai-Cresse, D. Wang, J.A. Zack, D.B. Kohn, A. Nakano, S.F. Nelson, M.C. Miceli, M.J. Spencer, A.D. Pyle, A Single CRISPR-Cas9 Deletion Strategy that Targets the Majority of DMD Patients Restores Dystrophin Function in hiPSC-Derived Muscle Cells, Cell Stem Cell 18 (4) (2016) 533–540.

[99] J.R. Mendell, L.R. Rodino-Klapac, Duchenne muscular dystrophy: CRISPR/Cas9 treatment, Cell Res. 26 (5) (2016) 513–514.

[100] L. Passamano, A. Taglia, A. Palladino, E. Viggiano, P. D'Ambrosio, M. Scutifero, M. Rosaria Cecio, V. Torre, D.E.L. F, E. Picillo, O. Paciello, G. Piluso, G. Nigro, L. Politano, Improvement of survival in Duchenne Muscular Dystrophy: retrospective analysis of 835 patients, Acta Myol 31(2) (2012) 121-5.

[101] M.G. Rae, D. O'Malley, Cognitive dysfunction in Duchenne muscular dystrophy: a possible role for neuromodulatory immune molecules, J. Neurophysiol. 116 (3) (2016) 1304–1315.

[102] F. Nardes, A.P. Araujo, M.G. Ribeiro, Mental retardation in Duchenne muscular dystrophy, J Pediatr (Rio J) 88 (1) (2012) 6–16.

[103] J.L. Anderson, S.I. Head, C. Rae, J.W. Morley, Brain function in Duchenne muscular dystrophy, Brain 125 (Pt 1) (2002) 4–13.

[104] N. Bresolin, E. Castelli, G.P. Comi, G. Felisari, A. Bardoni, D. Perani, F. Grassi, A. Turconi, F. Mazzucchelli, D. Gallotti, et al., Cognitive impairment in Duchenne muscular dystrophy, Neuromuscul. Disord. 4 (4) (1994) 359–369.

[105] H.G. Lidov, T.J. Byers, L.M. Kunkel, The distribution of dystrophin in the murine central nervous system: an immunocytochemical study, Neuroscience 54 (1) (1993) 167–187.

[106] I. Knuesel, B.C. Bornhauser, R.A. Zuellig, F. Heller, M.C. Schaub, J.M. Fritschy, Differential expression of utrophin and dystrophin in CNS neurons: an in situ hybridization and immunohistochemical study, J. Comp. Neurol. 422 (4) (2000) 594–611.

[107] M. Sekiguchi, K. Zushida, M. Yoshida, M. Maekawa, S. Kamichi, M. Yoshida, Y. Sahara, S. Yuasa, S. Takeda, K. Wada, A deficit of brain dystrophin impairs specific amygdala GABAergic transmission and enhances defensive behaviour in mice, Brain 132 (Pt 1) (2009) 124–135.

[108] R.D. Bies, S.F. Phelps, M.D. Cortez, R. Roberts, C.T. Caskey, J.S. Chamberlain, Human and murine dystrophin mRNA transcripts are differentially expressed during skeletal muscle, heart, and brain development, Nucleic Acids Res. 20 (7) (1992) 1725–1731.

[109] S.Y. Lv, Q.H. Zou, J.L. Cui, N. Zhao, J. Hu, X.Y. Long, Y.C. Sun, J. He, C.Z. Zhu, Y. He, Y.F. Zang, Decreased gray matter concentration and local synchronization of spontaneous activity in the motor cortex in Duchenne muscular dystrophy, AJNR Am. J. Neuroradiol. 32 (11) (2011) 2196–2200.

[110] V. Jagadha, L.E. Becker, Brain morphology in Duchenne muscular dystrophy: a Golgi study, Pediatr. Neurol. 4 (2) (1988) 87–92.

[111] N.P. Rosman, The cerebral defect and myopathy in Duchenne muscular dystrophy. A comparative clinicopathological study, Neurology 20 (4) (1970) 329–335.

[112] I. Tracey, R.B. Scott, C.H. Thompson, J.F. Dunn, P.R. Barnes, P. Styles, G.J. Kemp, C.D. Rae, M. Pike, G.K. Radda, Brain abnormalities in Duchenne muscular dystrophy: phosphorus-31 magnetic resonance spectroscopy and neuropsychological study, Lancet 345 (8960) (1995) 1260–1264.

[113] M. Yoshioka, T. Okuno, Y. Honda, Y. Nakano, Central nervous system involvement in progressive muscular dystrophy, Arch. Dis. Child. 55 (8) (1980) 589–594.

[114] V. Arechavala-Gomeza, M. Kinali, L. Feng, M. Guglieri, G. Edge, M. Main, D. Hunt, J. Lehovsky, V. Straub, K. Bushby, C.A. Sewry, J.E. Morgan, F. Muntoni, Revertant fibres and dystrophin traces in Duchenne muscular dystrophy: implication for clinical trials, Neuromuscul. Disord. 20 (5) (2010) 295–301.

[115] M.D. Grounds, H.G. Radley, G.S. Lynch, K. Nagaraju, A. De Luca, Towards developing standard operating procedures for pre-clinical testing in the mdx mouse model of Duchenne muscular dystrophy, Neurobiol. Dis. 31 (1) (2008) 1–19.

[116] J. Dangain, G. Vrbova, Muscle development in mdx mutant mice, Muscle Nerve 7 (9) (1984) 700–704.

[117] G.R. Coulton, N.A. Curtin, J.E. Morgan, T.A. Partridge, The mdx mouse skeletal muscle myopathy: II. Contractile properties, Neuropathol. Appl. Neurobiol. 14 (4) (1988) 299–314.

[118] J. Manning, D. O'Malley, What has the mdx mouse model of Duchenne muscular dystrophy contributed to our understanding of this disease? J. Muscle Res. Cell Motil. 36 (2) (2015) 155–167.

[119] A.A. al-Qudah, J. Kobayashi, S. Chuang, M. Dennis, P. Ray, Etiology of intellectual impairment in Duchenne muscular dystrophy, Pediatr Neurol 6(1) (1990) 57-9.

[120] V. Dubowitz, Intellectual Impairment in Muscular Dystrophy, Arch. Dis. Child. 40 (211) (1965) 296–301.

[121] C. Rae, R.B. Scott, C.H. Thompson, R.M. Dixon, I. Dumughn, G.J. Kemp, A. Male, M. Pike, P. Styles, G.K. Radda, Brain biochemistry in Duchenne muscular dystrophy: a 1H magnetic resonance and neuropsychological study, J. Neurol. Sci. 160 (2) (1998) 148–157.

[122] R. Miranda, C. Sebrie, J. Degrouard, B. Gillet, D. Jaillard, S. Laroche, C. Vaillend, Reorganization of inhibitory synapses and increased PSD length of perforated excitatory synapses in hippocampal area CA1 of dystrophin-deficient mdx mice, Cereb. Cortex 19 (4) (2009) 876–888.

[123] Y. Yoshihara, H. Onodera, K. Iinuma, Y. itoyama, Abnormal kainic acid receptor density and reduced seizure susceptibility in dystrophin-deficient mdx mice, Neuroscience 117(2) (2003) 391-5.
[124] A. Sbriccoli, M. Santarelli, D. Carretta, F. Pinto, A. Granato, D. Minciacchi, Architectural changes of the cortico-spinal system in the dystrophin defective mdx mouse, Neurosci. Lett. 200 (1) (1995) 53–56.
[125] D. Carretta, M. Santarelli, A. Sbriccoli, F. Pinto, C. Catini, D. Minciacchi, Spatial analysis reveals alterations of parvalbumin- and calbindin-positive local circuit neurons in the cerebral cortex of mutant mdx mice, Brain Res. 1016 (1) (2004) 1–11.
[126] D. Carretta, M. Santarelli, D. Vanni, S. Ciabatti, A. Sbriccoli, F. Pinto, D. Minciacchi, Cortical and brainstem neurons containing calcium-binding proteins in a murine model of Duchenne's muscular dystrophy: selective changes in the sensorimotor cortex, J. Comp. Neurol. 456 (1) (2003) 48–59.
[127] R. Miranda, S. Laroche, C. Vaillend, Reduced neuronal density in the CA1 anterodorsal hippocampus of the mdx mouse, Neuromuscul. Disord. 26 (11) (2016) 775–781.
[128] S. Xu, D. Shi, S.J.P. Pratt, W. Zhu, A. Marshall, R.M. Lovering, Abnormalities in brain structure and biochemistry associated with mdx mice measured by in vivo MRI and high resolution localized (1)H MRS, Neuromuscul. Disord. 25 (10) (2015) 764–772.
[129] P. Huang, X.S. Zhao, M. Fields, R.M. Ransohoff, L. Zhou, Imatinib attenuates skeletal muscle dystrophy in mdx mice, FASEB J. 23 (8) (2009) 2539–2548.
[130] T. Huynh, K. Uaesoontrachoon, J.L. Quinn, K.S. Tatem, C.R. Heier, J.H. Van Der Meulen, Q. Yu, M. Harris, C.J. Nolan, G. Haegeman, M.D. Grounds, K. Nagaraju, Selective modulation through the glucocorticoid receptor ameliorates muscle pathology in mdx mice, J. Pathol. 231 (2) (2013) 223–235.
[131] J. Kurek, J. Bower, M. Romanella, L. Austin, Leukaemia inhibitory factor treatment stimulates muscle regeneration in the mdx mouse, Neurosci. Lett. 212 (3) (1996) 167–170.
[132] C. Vaillend, J.M. Billard, S. Laroche, Impaired long-term spatial and recognition memory and enhanced CA1 hippocampal LTP in the dystrophin-deficient Dmd (mdx) mouse, Neurobiol. Dis. 17 (1) (2004) 10–20.
[133] C. Vaillend, A. Rendon, R. Misslin, A. Ungerer, Influence of dystrophin-gene mutation on mdx mouse behavior. I. Retention deficits at long delays in spontaneous alternation and bar-pressing tasks, Behav. Genet. 25 (6) (1995) 569–579.
[134] R. Chaussenot, J.M. Edeline, B. Le Bec, N. El Massioui, S. Laroche, C. Vaillend, Cognitive dysfunction in the dystrophin-deficient mouse model of Duchenne muscular dystrophy: A reappraisal from sensory to executive processes, Neurobiol. Learn. Mem. 124 (2015) 111–122.
[135] A.K. Sesay, M.L. Errington, L. Levita, T.V. Bliss, Spatial learning and hippocampal long-term potentiation are not impaired in mdx mice, Neurosci. Lett. 211 (3) (1996) 207–210.
[136] J.R. Lopez, J. Kolster, A. Uryash, E. Estève, F. Altamirano, J.A. Adams, Dysregulation of Intracellular Ca(2+) in Dystrophic Cortical and Hippocampal Neurons, Mol. Neurobiol. 55 (1) (2018) 603–618.
[137] S. Levi, R.M. Grady, M.D. Henry, K.P. Campbell, J.R. Sanes, A.M. Craig, Dystroglycan is selectively associated with inhibitory GABAergic synapses but is dispensable for their differentiation, J. Neurosci. 22 (11) (2002) 4274–4285.
[138] I. Brunig, A. Suter, I. Knuesel, B. Luscher, J.M. Fritschy, GABAergic terminals are required for postsynaptic clustering of dystrophin but not of GABA(A) receptors and gephyrin, J. Neurosci. 22 (12) (2002) 4805–4813.
[139] I. Knuesel, M. Mastrocola, R.A. Zuellig, B. Bornhauser, M.C. Schaub, J.M. Fritschy, Altered synaptic clustering of GABAA receptors in mice lacking dystrophin (mdx mice), Europ. J. Neurosci. 11 (12) (1999) 4457–4462.
[140] T.W. Kim, K. Wu, J.L. Xu, I.B. Black, Detection of dystrophin in the postsynaptic density of rat brain and deficiency in a mouse model of Duchenne muscular dystrophy, Proc. Natl. Acad Sci. U S A 89 (23) (1992) 11642–11644.
[141] T. Sakamoto, T. Arima, M. Ishizaki, R. Kawano, T. Koide, Y. Uchida, S. Yamashita, E. Kimura, T. Hirano, Y. Maeda, M. Uchino, Regions downstream from the WW domain of dystrophin are important for binding to postsynaptic densities in the brain, Neuromuscul. Disord. 18 (5) (2008) 382–388.
[142] J.M. Fritschy, P. Panzanelli, S.K. Tyagarajan, Molecular and functional heterogeneity of GABAergic synapses, Cell. Mol. Life Sci. 69 (15) (2012) 2485–2499.
[143] E. Krasowska, K. Zablocki, D.C. Gorecki, J.D. Swinny, Aberrant location of inhibitory synaptic marker proteins in the hippocampus of dystrophin-deficient
mice: implications for cognitive impairment in duchenne muscular dystrophy, PLoS ONE 9 (9) (2014) e108364.
[144] C. Vaillend, C. Perronnet, C. Ros, C. Gruszczynski, A. Goyenvalle, S. Laroche, O. Danos, L. Garcia, E. Peltekian, Rescue of a dystrophin-like protein by exon skipping in vivo restores GABAA-receptor clustering in the hippocampus of the mdx mouse, Molecul. Therapy : J. Am. Soc. Gene Therapy 18 (9) (2010) 1683–1688.
[145] G. Dallerac, C. Perronnet, C. Chagneau, P. Leblanc-Veyrac, N. Samson-Desvignes, E. Peltekian, O. Danos, L. Garcia, S. Laroche, J.M. Billard, C. Vaillend, Rescue of a dystrophin-like protein by exon skipping normalizes synaptic plasticity in the hippocampus of the mdx mouse, Neurobiol. Dis. 43 (3) (2011) 635–641.
[146] R. Coccurello, C. Castellano, P. Paggi, A. Mele, A. Oliverio, Genetically dystrophic mdx/mdx mice exhibit decreased response to nicotine in passive avoidance, NeuroReport 13 (9) (2002) 1219–1222.
[147] T. Wallis, W.A. Bubb, J.A. McQuillan, V.J. Balcar, C. Rae, For want of a nail. ramifications of a single gene deletion, dystrophin, in the brain of the mouse, Frontiers in bioscience : a journal and virtual library 9 (2004) 74-84.
[148] P.C. Ghedini, M.C. Avellar, T.C. De Lima, M.T. Lima-Landman, A.J. Lapa, C. Souccar, Quantitative changes of nicotinic receptors in the hippocampus of dystrophin-deficient mice, Brain Res. 1483 (2012) 96–104.
[149] S.F. Parames, E.D. Coletta-Yudice, F.M. Nogueira, M.B. Nering de Sousa, M.A. Hayashi, M.T. Lima-Landman, A.J. Lapa, C. Souccar, Altered acetylcholine release in the hippocampus of dystrophin-deficient mice, Neuroscience 269 (2014) 173–183.
[150] R. Miranda, U. Nudel, S. Laroche, C. Vaillend, Altered presynaptic ultrastructure in excitatory hippocampal synapses of mice lacking dystrophins Dp427 or Dp71, Neurobiol. Dis. 43 (1) (2011) 134–141.
[151] I. Knuesel, R.A. Zuellig, M.C. Schaub, J.M. Fritschy, Alterations in dystrophin and utrophin expression parallel the reorganization of GABAergic synapses in a mouse model of temporal lobe epilepsy, Europ. J. Neurosci. 13 (6) (2001) 1113–1124.
[152] S.L. Kueh, S.I. Head, J.W. Morley, GABA(A) receptor expression and inhibitory post-synaptic currents in cerebellar Purkinje cells in dystrophin-deficient mdx mice, Clin. Exp. Pharmacol. Physiol. 35 (2) (2008) 207–210.
[153] L. Graciotti, A. Minelli, D. Minciacchi, A. Procopio, G. Fulgenzi, GABAergic miniature spontaneous activity is increased in the CA1 hippocampal region of dystrophic mdx mice, Neuromuscul. Disord. 18 (3) (2008) 220–226.
[154] E.J. Cohen, E. Quarta, G. Fulgenzi, D. Minciacchi, Acetylcholine, GABA and neuronal networks: A working hypothesis for compensations in the dystrophic brain, Brain Res. Bull. 110 (2015) 1–13.
[155] J.D. Porter, S. Khanna, H.J. Kaminski, J.S. Rao, A.P. Merriam, C.R. Richmonds, P. Leahy, J. Li, W. Guo, F.H. Andrade, A chronic inflammatory response dominates the skeletal muscle molecular signature in dystrophin-deficient mdx mice, Hum.
Mol. Genet. 11 (3) (2002) 263–272.
[156] B. De Paepe, J.L. De Bleecker, Cytokines and chemokines as regulators of skeletal muscle inflammation: presenting the case of Duchenne muscular dystrophy, Mediators Inflamm. 2013 (2013) 540370.
[157] L. Pelosi, M.G. Berardinelli, L. Forcina, E. Spelta, E. Rizzuto, C. Nicoletti, C. Camilli, E. Testa, A. Catizone, F. De Benedetti, A. Musaro, Increased levels of interleukin-6 exacerbate the dystrophic phenotype in mdx mice, Hum. Mol. Genet.
24 (21) (2015) 6041–6053.
[158] W.A. Banks, A.J. Kastin, E.G. Gutierrez, Penetration of interleukin-6 across the murine blood-brain barrier, Neurosci. Lett. 179 (1–2) (1994) 53–56.
[159] A. Vezzani, B. Viviani, Neuromodulatory properties of inflammatory cytokines and their impact on neuronal excitability, Neuropharmacology 96 (Pt A) (2015) 70–82.

[160] A.L. Marsland, K.L. Petersen, R. Sathanoori, M.F. Muldoon, S.A. Neumann, C. Ryan, J.D. Flory, S.B. Manuck, Interleukin-6 covaries inversely with cognitive performance among middle-aged community volunteers, Psychosom. Med. 68 (6) (2006) 895–903.

[161] C.B. Wright, R.L. Sacco, T. Rundek, J. Delman, L. Rabbani, M. Elkind, Interleukin6 is associated with cognitive function: the Northern Manhattan Study, J Stroke Cerebrovasc Dis 15 (1) (2006) 34–38.

[162] T.C. Ma, X.Z. Zhu, Effects of intrahippocampal infusion of interleukin-6 on passive avoidance and nitrite and prostaglandin levels in the hippocampus in rats, Arzneimittelforschung 50 (3) (2000) 227–231.

[163] A.M. Samuelsson, E. Jennische, H.A. Hansson, A. Holmang, Prenatal exposure to interleukin-6 results in inflammatory neurodegeneration in hippocampus with NMDA/GABA(A) dysregulation and impaired spatial learning, Am. J. Physiol. Regul. Integr. Comp. Physiol. 290 (5) (2006) R1345–R1356.

[164] D.L. Gruol, IL-6 regulation of synaptic function in the CNS, Neuropharmacology 96 (Pt A) (2015) 42–54.

[165] H.O. Besedovsky, A. del Rey, I. Klusman, H. Furukawa, G. Monge Arditi, A. Kabiersch, Cytokines as modulators of the hypothalamus-pituitary-adrenal axis, J. Steroid Biochem. Mol. Biol. 40 (4–6) (1991) 613–618.